METHOD VALIDATION FOR THE QUANTIFICATION OF IMPURITIES IN ZIRCONIUM METAL AND OTHER RELEVANT Zr COMPOUNDS

A thesis submitted to meet the requirements for the degree of

Magister Scientiae

in the

FACULTY OF NATURAL AND AGRICULTURAL SCIENCES
DEPARTMENT OF CHEMISTRY

at the

UNIVERSITY OF THE FREE STATE
BLOEMFONTEIN

by

LITHEKO LEGAPA NKABITI

Internal Supervisor
Prof. W. Purcell

External Supervisor
Dr. J.T. Nel

External Co-supervisor
Dr. E. Snyders

November 2012

UFS Chemistry

Acknowledgements

My deepest sense of gratitude is extended to the following individuals who have contributed in various ways to make this research a success

Lord GOD Jesus Christ (Creator), for all the blessings and spiritual courage bestowed on me to the completion of this study. For HIS divine guidance of the following individuals mentioned hereunder to instil the sense of purpose in me for the completing of this study

Prof. W. Purcell (Internal Supervisor), for his patient guidance through the course of this research. He has extended his great moral support and help in molding me to be a capable student in science. There are no words of acknowledgement which would adequately express my gratitude and I shall eternally remain indebted to him.

Dr. J.T. Nel (External Supervisor), for his great knowledge in the field of this study and the reviews of each chapter with insightful recommendations that assisted in enhancing the content of my thesis.

Dr. E. Snyders (External Co-Supervisor), for his valuable contribution and notable encouragement in the initial stages of the experimental part of this study.

Analytical Group (M. Nete, T. Chiweshe, S. Lötter and F. Koko), for their sincere suggestions and assistance with the carrying out of my experiments using the equipment in the laboratory in order to obtain the best results.

Family (Mr. I.C. Nkabiti, Mrs. M.S. Nkabiti, M. Litheko, K.D. Litheko, M.P. Baiocco, L. Nkabiti, N.L. Mokoena and Mojaboswa Nkabiti), without them there is no reason for existence and I thank them for believing in me and constantly motivating me with prayers and words of encouragement. May the great Almighty Jesus Christ bless you all!!!

Litheko Legapa Nkabiti

Declaration by Candidate

To my knowledge this dissertation for the *Magister Scientiae* degree in Chemistry, at the University of the Free State

- is my own original project and has not been submitted as part of any thesis at another institution of higher education in the Republic of South Africa or abroad
- has clearly quoted all sources in the comprehensive list of references, and
- any views expressed in the dissertation are those of the author and in no way represent those of the University of the Free State

I therefore submit this dissertation being conscious of the fact that the breach of these rules, in part or as a whole, will be considered an academic misconduct.

Signature: _____ Date: _____

Litheko Legapa Nkabiti

Table of Contents

List of Tables vi

List of Figures xii

List of Abbreviations xvi

Keywords xviii

Summary xix

Opsomming xxii

1 HISTORY, MOTIVATION and OBJECTIVES 1

1.1 HISTORICAL BACKGROUND 1

1.1.1 EXTRACTION OF ZIRCONIUM FROM MINERALS 5

1.1.2 THE PRESENCE OF HAFNIUM IN ZIRCONIUM 10

1.2 GEOGRAPHICAL DISTRIBUTION AND ECONOMICAL SIGNIFICANCE 12

1.2.1 GEOGRAPHICAL DISTRIBUTION 12

1.2.2 COMMERCIAL BENEFITS 14

1.3 CHEMICAL AND PHYSICAL PROPERTIES OF ZIRCONIUM 16

1.3.1 AN OVERVIEW OF THE ZIRCONIUM HALIDES 19

1.3.2 CHEMICAL AND PHYSICAL PROPERTIES OF ZIRCONIUM TETRAFLUORIDE (ZrF_4) 19

1.4 MOTIVATION OF THIS STUDY 21

1.4.1 THE GLOBAL NEED FOR ALTERNATIVE ENERGY SOURCE 21

1.4.2 ZIRCONIUM IN THE NUCLEAR INDUSTRY 30

1.4.3 IMPORTANCE OF ZIRCONIUM TECHNOLOGY IN SOUTH AFRICA 32

1.5 OBJECTIVES 35

2 LITERATURE REVIEW ON METHODS OF ANALYSIS FOR ZIRCONIUM AND ITS ASSOCIATED IMPURITIES 36

2.1 INTRODUCTION 36

2.2 METHODS OF DIGESTION 37

2.2.1 DIGESTION BY BORAX 37

2.2.2 DIGESTION BY PEROXIDE 38

4.2.2 MICROWAVE EQUIPMENT 103
4.2.3 ICP-OES SPECTROMETER 105
4.2.4 ATOMIC ABSORPTION (AA) SPECTROPHOTOMETER 106
4.2.5 WATER DISTILLATION EQUIPMENT 106
4.2.6 WEIGHING EQUIPMENT 107
4.2.7 GLASSWARE 107
4.2.8 PIPETTES 107
4.2.9 REAGENTS 107
4.3 QUANTIFICATION OF ZIRCONIUM IN HIGH PURITY PRODUCTS BY ICP-OES 108
4.3.1 GENERAL EXPERIMENTAL PROCEDURE 108
4.3.2 PREPARATION OF ICP CALIBRATION STANDARDS 108
4.3.3 DETECTION LIMITS 108
4.3.4 DISSOLUTION OF THE ZIRCONIUM ROD 110
4.3.5 DISSOLUTION OF THE ZIRCONIUM FOIL 113
4.3.6 PREPARATION AND QUANTIFICATION OF ZIRCONIUM REFERENCE MATERIALS (RM) 116
4.4 DISCUSSION, VALIDATION AND CONCLUSION 123
4.4.1 DISCUSSION OF RESULTS 123
4.4.2 VALIDATION OF RESULTS 127
4.4.3 CONCLUSION 143

5 QUANTITATIVE DETERMINATIONS OF IMPURITIES IN ULTRA PURE ZIRCONIUM METAL SAMPLES 144

5.1 INTRODUCTION 144
5.2 EQUIPMENT, REAGENTS AND GENERAL EXPERIMENTAL PROCEDURE 145
5.2.1 ICP-OES SPECTROMETER AND OTHER EQUIPMENT 145
5.2.2 REAGENTS 146
5.3 PREPARATION OF THE ZIRCONIUM AND THE IMPURITY STOCK SOLUTIONS 147
5.3.1 PREPRATION OF THE ALUMINIUM STOCK SOLUTION 147
5.3.2 PREPARATION OF THE BORON STOCK SOLUTION 147
5.3.3 PREPARATION OF THE CADMIUM STOCK SOLUTION 147

4.2.2 MICROWAVE EQUIPMENT 103
4.2.3 ICP-OES SPECTROMETER 105
4.2.4 ATOMIC ABSORPTION (AA) SPECTROPHOTOMETER 106
4.2.5 WATER DISTILLATION EQUIPMENT 106
4.2.6 WEIGHING EQUIPMENT 107
4.2.7 GLASSWARE 107
4.2.8 PIPETTES 107
4.2.9 REAGENTS 107
4.3 QUANTIFICATION OF ZIRCONIUM IN HIGH PURITY PRODUCTS BY ICP-OES 108
4.3.1 GENERAL EXPERIMENTAL PROCEDURE 108
4.3.2 PREPARATION OF ICP CALIBRATION STANDARDS 108
4.3.3 DETECTION LIMITS 108
4.3.4 DISSOLUTION OF THE ZIRCONIUM ROD 110
4.3.5 DISSOLUTION OF THE ZIRCONIUM FOIL 113
4.3.6 PREPARATION AND QUANTIFICATION OF ZIRCONIUM REFERENCE MATERIALS (RM) 116
4.4 DISCUSSION, VALIDATION AND CONCLUSION 123
4.4.1 DISCUSSION OF RESULTS 123
4.4.2 VALIDATION OF RESULTS 127
4.4.3 CONCLUSION 143

5 QUANTITATIVE DETERMINATIONS OF IMPURITIES IN ULTRA PURE ZIRCONIUM METAL SAMPLES 144

5.1 INTRODUCTION 144
5.2 EQUIPMENT, REAGENTS AND GENERAL EXPERIMENTAL PROCEDURE 145
5.2.1 ICP-OES SPECTROMETER AND OTHER EQUIPMENT 145
5.2.2 REAGENTS 146
5.3 PREPARATION OF THE ZIRCONIUM AND THE IMPURITY STOCK SOLUTIONS 147
5.3.1 PREPRATION OF THE ALUMINIUM STOCK SOLUTION 147
5.3.2 PREPARATION OF THE BORON STOCK SOLUTION 147
5.3.3 PREPARATION OF THE CADMIUM STOCK SOLUTION 147

5.3.4 PREPARATION OF THE CHROMIUM STOCK SOLUTION 147
5.3.5 PREPARATION OF THE COBALT STOCK SOLUTION 147
5.3.6 PREPARATION OF THE COPPER STOCK SOLUTION 148
5.3.7 PREPARATION OF THE IRON STOCK SOLUTION 148
5.3.8 PREPARATION OF THE HAFNIUM STOCK SOLUTION 148
5.3.9 PREPARATION OF THE MANGANESE STOCK SOLUTION 148
5.3.10 PREPARATION OF THE MOLYBDENUM STOCK SOLUTION 148
5.3.11 PREPARATION OF THE NICKEL STOCK SOLUTION 149
5.3.12 PREPARATION OF THE SILICON STOCK SOLUTION 149
5.3.13 PREPARATION OF THE TITANIUM STOCK SOLUTION 149
5.3.14 PREPARATION OF THE TUNGSTEN STOCK SOLUTION 149
5.3.15 PREPARATION OF THE URANIUM STOCK SOLUTION 149
5.3.16 PREPARATION OF THE ZIRCONIUM STOCK SOLUTION 149
5.4 QUANTIFICATION OF THE SPECIFIED IMPURITIES IN THE ZIRCONIUM FOIL BY ICP-OES 150
5.4.1 GENERAL EXPERIMENTAL PROCEDURE 150
5.4.2 PREPARATION OF THE ICP CALIBRATION STANDARDS 150
5.4.3 DETECTION AND QUANTIFICATION LIMITS OF THE IMPURITIES ASSOCIATED WITH THE NUCLEAR GRADE ZIRCONIUM 152
5.4.4 QUANTIFICATION OF INDIVIDUALLY ADDED IMPURITIES IN THE ULTRA PURE ZIRCONIUM FOIL 153
5.4.5 QUANTIFICATION OF GROUPS OF IMPURITIES ADDED IN THE ULTRA PURE ZIRCONIUM FOIL 162
5.4.6 QUANTIFICATION OF COMBINED GROUPS OF IMPURITIES ADDED TO THE PURE ZIRCONIUM FOIL 166
5.4.7 QUANTIFICATION OF ALL IMPURITIES ADDED TO PURE ZIRCONIUM SOLUTION 170
5.5 DISCUSSION, VALIDATION AND CONCLUSION 171
5.5.1 DISCUSSION OF RESULTS 171
5.5.2 VALIDATION OF RESULTS 175
5.5.3 CONCLUSION 207

6 EVALUATION OF THE STUDY AND FUTURE RESEARCH 208

6.1 INTRODUCTION 208
6.2 DEGREE OF SUCCESS OF STUDY WITH REGARD TO THE SET OBJECTIVES 208
6.3 FUTURE RESEARCH 210

7 Appendix ..... CD

List of Tables

Table 1.1: Atomic weight determinations of zirconium 11

Table 1.2: World Mine Production, Reserves and Reserve Bases..... 13

Table 1.3: Examples of the coordination number of zirconium 16

Table 1.4: Chemical requirements of zirconium sponge, reactor grade R60001..... 31

Table 1.5: Composition (weight %) of zirconium alloys..... 34

Table 2.1: Analyses of zirconium, titanium and rare earth metals in diorite rock..... 38

Table 2.2: Determination of zirconium in steel 39

Table 2.3: Fusions of zirconia using sodium carbonate flux..... 40

Table 2.4: Comparison of results for zirconium in six carbonate rock reference materials by different dissolution methods 41

Table 2.5: Comparison of results for zirconium in six carbonate rock reference materials by different analytical techniques 42

Table 2.6: Results of boron and zirconium determinations in ceramic materials..... 43

Table 2.7: Results of sodium hydroxide fusions of zirconia 43

Table 2.8: Results of potassium hydroxide fusions of zirconia..... 44

Table 2.9: Analytical results of microwave-assisted digestion of zircon samples..... 46

Table 2.10: Table showing microwave-assisted digestion results using various reagents.... 47

Table 2.11: Table showing the effect of varying amounts of ammonium sulphate on the % recovery of different elements 48

Table 2.12: Effect of common alloying elements on the analysis of zirconium 49

Table 2.13: Analysis of zirconium in synthetic metallic standards..... 50

Table 2.14: Analysis of zirconium in the presence of titanium 50

Table 2.15: Determination of zirconium in zirconia 51

Table 2.16: Determination of hafnium in hafnia..... 52

Table 2.17: Determination of zirconium with trimesic acid in the presence of diverse ions... 53

List of Tables

Table 2.18: Effect of known interferences on zirconium determination 55

Table 2.19: Analysis of zirconium samples after addition of known amounts of rare earths . 57

Table 2.20: Statistical study of reproducibility in solid zirconium day-to-day analyses 58

Table 2.21: Trace elements determined in the Zr SRMs from NIST 59

Table 2.22: Determination of zirconium in the presence of hafnium 61

Table 2.23: Effect of hydrofluoric acid on the absorbance of copper in the presence of $ZrOCl_2$ 63

Table 2.24: Quantification of copper in commercial zirconium samples 64

Table 2.25: Silicon contents determined in TiO2 and ZrO2 by slurry ETAAS and AES 64

Table 2.26: Zirconium and hafnium abundances in some standard rocks and related natural materials 65

Table 3.1: A summary of benefits and limitations of open and closed acid digestion systems 76

Table 3.2: Elements that are quantitatively analyzed using NAAS 86

Table 4.1: Microwave digestion conditions for the high purity zirconium metal 104

Table 4.2: Operating conditions of the ICP-OES analysis of zirconium content 105

Table 4.3: Operating conditions of the AA analysis of zirconium content 106

Table 4.4: Determination of the LOD and LOQ for zirconium 110

Table 4.5: ICP-OES analyses results for bench-top digestions of zirconium rods with different mineral acids (λ = 343.823 nm) 112

Table 4.6: ICP-OES analyses results for bench-top digestions of zirconium rods with different mineral acids (λ = 339.198 nm) 112

Table 4.7: ICP-OES analyses results for microwave-assisted digestions of zirconium rods with different mineral acids (λ = 343.823 nm) 113

Table 4.8: ICP-OES analyses results for microwave-assisted digestions of zirconium rods with different mineral acids (λ = 339.198 nm) 113

List of Tables

Table 4.9: ICP-OES analyses results for bench-top digestions of zirconium foils with different mineral acids (λ = 343.823 nm) 114

Table 4.10: ICP-OES analyses results for bench-top digestions of zirconium foils with different mineral acids (λ = 339.198 nm) 114

Table 4.11: ICP-OES analyses results for microwave-assisted digestions of zirconium foils with different mineral acids (λ = 343.823 nm) 115

Table 4.12: ICP-OES analyses results for microwave-assisted digestions of zirconium foils with different mineral acids (λ = 339.198 nm) 116

Table 4.13: ICP-OES analysis for bench-top diluted sulphuric acid digestion of ZrF_4 (λ = 343.823 nm) 117

Table 4.14: ICP-OES analysis for bench-top diluted sulphuric acid digestion of ZrF_4 (λ = 339.198 nm) 117

Table 4.15: Quantitative ICP-OES analyses of the impurities present in the bench-top diluted sulphuric acid digestion of ZrF_4 117

Table 4.16: ICP-OES analyses of K (λ = 766.491 nm) and Zr (λ = 343.823 nm) in K_2ZrF_6 . 121

Table 4.17: ICP-OES analyses of K (λ = 769.898 nm) and Zr (λ = 339.198 nm) in K_2ZrF_6 . 121

Table 4.18: AA determinations of the LOD and LOQ for potassium 122

Table 4.19: AA analyses of K (λ = 766.491 nm) in K_2ZrF_6 123

Table 4.20: AA analyses of K (λ = 769.898 nm) in K_2ZrF_6 123

Table 4.21: Validation criteria of the ICP-OES method for the analysis of zirconium in various materials 128

Table 4.22: Validation of ICP-OES analyses for sulphuric acid digestions of zirconium rod (λ = 343.823 nm) 129

Table 4.23: Validation of ICP-OES analyses for sulphuric acid digestions of zirconium rod (λ = 339.198 nm) 130

Table 4.24: Validation of ICP-OES analyses for phosphoric acid digestions of zirconium rod (λ = 343.823 nm) 131

Table 4.25: Validation of ICP-OES analyses for phosphoric acid digestions of zirconium rod (λ = 339.198 nm) 132

Table 4.26: Validation of ICP-OES analyses for *aqua regia* digestions of zirconium rod (λ = 343.823 nm) 133

Table 4.27: Validation of ICP-OES analyses for *aqua regia* digestions of zirconium rod (λ = 339.198 nm) 134

Table 4.28: Validation of ICP-OES analyses for sulphuric acid digestions of zirconium foil (λ = 343.823 nm) 135

Table 4.29: Validation of ICP-OES analyses for sulphuric acid digestions of zirconium foil (λ = 339.198 nm) 136

Table 4.30: Validation of ICP-OES analyses for phosphoric acid digestions of zirconium foil (λ = 343.823 nm) 137

Table 4.31: Validation of ICP-OES analyses for phosphoric acid digestions of zirconium foil (λ = 339.198 nm) 138

Table 4.32: Validation of ICP-OES analyses for *aqua regia* digestions of zirconium foil (λ = 343.823 nm) 139

Table 4.33: Validation of ICP-OES analyses for *aqua regia* digestions of zirconium foil (λ = 339.198 nm) 140

Table 4.34: Validation of ICP-OES analyses for sulphuric acid digestions of ZrF_4 141

Table 4.35: Validation of ICP-OES analyses for sulphuric acid digestions of K_2ZrF_6 at both wavelengths 142

Table 5.1: Selection and experimental grouping of the permissible impurities in zirconium 145

Table 5.2: Determination of the LOD and LOQ from their blank intensities for impurities associated with nuclear grade zirconium 152

Table 5.3: Determination of the LOD and LOQ from their blank intensities for impurities associated with nuclear grade zirconium 153

Table 5.4: ICP-OES analysis for the sulphuric acid digestion of zirconium foil (λ = 339.198 nm) 154

Table 5.5: ICP-OES analyses of individual impurities at their most sensitive wavelengths in Zr-solution (λ = 339.198 nm) 162

Table 5.6: ICP-OES analyses of Group 1 (Tenth of the threshold) in Zr-solution 163

Table 5.7: ICP-OES analyses of Group 1 (Threshold) in Zr-solution 163

Table 5.8: ICP-OES analyses of Group 2 (Tenth of the threshold) in Zr-solution 164

Table 5.9: ICP-OES analyses of Group 2 (Threshold) in Zr-solution 164

Table 5.10: ICP-OES analyses of Group 3 (Tenth of the threshold) in Zr-solution 165

Table 5.11: ICP-OES analyses of Group 3 (Threshold) in Zr-solution 165

Table 5.12: ICP-OES analyses of Group 1 and 2 (Tenth of the threshold) in Zr-solution 166

Table 5.13: ICP-OES analyses of Group 1 and 2 (Threshold) in Zr-solution 167

Table 5.14: ICP-OES analyses of Group 1 and 3 (Tenth of the threshold) in Zr-solution 168

Table 5.15: ICP-OES analyses of Group 1 and 3 (Threshold) in Zr-solution 168

Table 5.16: ICP-OES analyses of Group 2 and 3 (Tenth of the threshold) in Zr-solution 169

Table 5.17: ICP-OES analyses of Group 2 and 3 (Threshold) in Zr-solution 169

Table 5.18: ICP-OES analyses of all impurities (Tenth of the threshold) in Zr-solution 171

Table 5.19: ICP-OES analyses of all impurities (Threshold) in Zr-solution 171

Table 5.20: The overall average recovery of individual impurities in their respective zirconium solution 173

Table 5.21: Validation of ICP-OES analyses for aluminium in the pure zirconium solution. 176

Table 5.22: Validation of ICP-OES analyses for chromium in the pure zirconium solution . 177

Table 5.23: Validation of ICP-OES analyses for hafnium in the pure zirconium solution 178

Table 5.24: Validation of ICP-OES analyses for iron in the pure zirconium solution 179

Table 5.25: Validation of ICP-OES analyses for boron in the pure zirconium solution 180

Table 5.26: Validation of ICP-OES analyses for cadmium in the pure zirconium solution .. 181

Table 5.27: Validation of ICP-OES analyses for cobalt in the pure zirconium solution 182

Table 5.28: Validation of ICP-OES analyses for copper in the pure zirconium solution 183

Table 5.29: Validation of ICP-OES analyses for manganese in the pure zirconium solution 184

Table 5.30: Validation of ICP-OES analyses for molybdenum in the pure zirconium solution 185

Table 5.31: Validation of ICP-OES analyses for nickel in the pure zirconium solution 186

Table 5.32: Validation of ICP-OES analyses for silicon in the pure zirconium solution 187

Table 5.33: Validation of ICP-OES analyses for titanium in the pure zirconium solution 188

Table 5.34: Validation of ICP-OES analyses for tungsten in the pure zirconium solution ... 189

Table 5.35: Validation of ICP-OES analyses for uranium in the pure zirconium solution 190

Table 5.36: Validation of ICP-OES analyses for group 1 impurities (Tenth of the threshold) in the pure zirconium solution 191

Table 5.37: Validation of ICP-OES analyses for group 1 impurities (Threshold) in the pure zirconium solution 192

Table 5.38: Validation of ICP-OES analyses for group 2 impurities (Tenth of the threshold) in the pure zirconium solution 193

Table 5.39: Validation of ICP-OES analyses for group 2 impurities (Threshold) in the pure zirconium solution 194

Table 5.40: Validation of ICP-OES analyses for group 3 impurities (Tenth of the threshold) in the pure zirconium solution 195

Table 5.41: Validation of ICP-OES analyses for group 3 impurities (Threshold) in the pure zirconium solution 196

Table 5.42: Validation of ICP-OES analyses for groups 1 and 2 impurities (Tenth of the threshold) in the pure zirconium solution 197

Table 5.43: Validation of ICP-OES analyses for groups 1 and 2 impurities (Threshold) in the pure zirconium solution 198

Table 5.44: Validation of ICP-OES analyses for groups 1 and 3 impurities (Tenth of the threshold) in the pure zirconium solution 199

Table 5.45: Validation of ICP-OES analyses for groups 1 and 3 impurities (Threshold) in the pure zirconium solution 200

Table 5.46: Validation of ICP-OES analyses for groups 2 and 3 impurities (Tenth of the threshold) in the pure zirconium solution 201

Table 5.47: Validation of ICP-OES analyses for groups 2 and 3 impurities (Threshold) in the pure zirconium solution 202

Table 5.48: Validation of ICP-OES analyses for all the impurities (Tenth of the threshold) in the pure zirconium solution 203

Table 5.49: Validation of ICP-OES analyses for all the impurities (Threshold) in the pure zirconium solution 205

List of Figures

Figure 1.1: Zirconium-containing mineral ores 1

Figure 1.2: Martin Heinrich Klaproth (1743 - 1817) 2

Figure 1.3: A mining pit for different kinds of minerals, including baddeleyite in Kovdor, Russia 5

Figure 1.4: Flow diagram for Kroll process in the production of zirconium 9

Figure 1.5: Geographical distribution of zirconium in 2005 12

Figure 1.6: (a) Zirconium powder; (b) Zirconium sponge; (c) Zirconium crystal bar 14

Figure 1.7: Zirconium tubes and bars for nuclear fuel and cladding 15

Figure 1.8: Graph portraying the world economic trend of zircon supply, demand and pricing 15

Figure 1.9: Different crystal lattices to which zirconium can conform (axes = a and c) 17

Figure 1.10: Monoclinic crystal lattice structure of zirconium fluoride 20

Figure 1.11: A petrochemical refinery in Grangemouth, Scotland, UK 22

Figure 1.12: Carbon emissions annual trend in South Africa 23

Figure 1.13: General model for non-renewable resource with high demand and no substitute 24

Figure 1.14: Chart of the average spot price per barrel for crude oil over the past decade .. 26

Figure 1.15: Chart of the average quarterly prices for coking coal per short ton since 1996. 27

Figure 1.16: A graph of historical spot prices for uranium 29

Figure 1.17: A schematical diagram of a nuclear power plant 30

Figure 2.1: A graph depicting the effect of Zr^{4+} ion on the copper absorbance 63

Figure 3.1: Cross section of Parr plain calorimeter 69

Figure 3.2: (a) Tölg's stainless steel pressure digestion system with a 12-sample heating block and temperature regulator; (b) Scheme of Tölg's PTFE bomb for sample preparation 70

Figure 3.3: Scheme of Knapp's high-pressure Asher for sample preparation 71

Figure 3.4: The electromagnetic spectrum 72

Figure 3.5: The magnetron 72

Figure 3.6: The operating concept of a magnetron 73

Figure 3.7: The interaction of various electromagnetic radiations with matter 73

Figure 3.8: Components of an AA spectrometer 77

Figure 3.9: Graphite tubes 78

Figure 3.10: Hollow cathode lamps for AAS 79

Figure 3.11: (a) Components of an ICP torch; (b) Generation of plasma in an ICP torch 80

Figure 3.12: Energy transitions of electrons 81

Figure 3.13: Temperature regions of a typical ICP discharge 81

Figure 3.14: Schematic representation of the ICP components and the process of analysis 82

Figure 3.15: A sequential (single detector) type monochromator ICP-OES system 83

Figure 3.16: A multi-detector type monochromator ICP-OES system 83

Figure 3.17: Schematic representation of ICP-MS components and processes 84

Figure 3.18: ICP-MS quadrupole mass filter separating ions 85

Figure 3.19: Procedure of NAAS in analyzing trace elements 86

Figure 3.20: Principle of X-ray fluorescence 87

Figure 3.21: XRF component arrangement in a Bruker S8 Tiger WDXRF 88

Figure 3.22: Illustration of the concept of LOD and LOQ by showing the theoretical normal distributions associated with blank, LOD and LOQ level samples 91

Figure 3.23: A plot depicting different positions of validation parameters on a calibration curve 92

Figure 3.24: The normal distribution for the *z*-statistic at 95 % confidence interval 94

Figure 3.25: Illustration of accuracy and precision in relation to the reference value 97

Figure 3.26: Direct calibration method 98

Figure 3.27: Standard addition calibration curve 100

List of Figures

Figure 4.1: Anton Paar Perkin-Elmer Multiwave 3000 microwave equipment 104

Figure 4.2: Shimadzu ICPS-7510 radial-sequential plasma spectrometer 105

Figure 4.3: Shimadzu AA-6300 atomic absorption spectrophotometer..... 106

Figure 4.4: Calibration curve of zirconium at wavelength 339.198 nm 109

Figure 4.5: Calibration curve of zirconium at wavelength 343.823 nm 109

Figure 4.6: Infrared (IR) spectrum of ZrF_4..... 118

Figure 4.7: Spectrum of ZrF_4 magnified on the far IR 118

Figure 4.8: Spectrum of ZrF_4 magnified and stretched on the near IR 119

Figure 4.9: Infrared (IR) spectrum of K_2ZrF_6..... 119

Figure 4.10: Spectrum of K_2ZrF_6 magnified on the far IR 120

Figure 4.11: Spectrum of K_2ZrF_6 magnified and stretched on the near IR..... 120

List of Abbreviations

ANALYTICAL EQUIPMENT

AAS	Atomic absorption spectroscopy
ETAAS	Electrothermal atomic absorption spectroscopy
FAAS	Flame atomic absorption spectroscopy
GFAAS	Graphite furnace atomic absorption spectroscopy
ICP-MS	Inductively coupled plasma-mass spectroscopy
ICP-OES	Inductively coupled plasma-optical emission spectroscopy
NAAS	Neutron activation analysis spectroscopy
XRD	X-ray diffraction
XRF	X-ray fluorescence

CHEMISTRY TERMS

[ ] or Conc.	Concentration
HDPE	High-density polyethylene
m/z	Mass-to-charge ionization ratio
PTFE	Polytetrafluoroethylene
RM	Reference material

SI UNITS

nm	nanometer
ppt	parts per thousand
ppb	parts per billion
ppm	parts per million

STATISTICAL TERMS

C.L. or C.I.	Confidence level or confidence interval
H_0	Null hypothesis
LOD	Limit of detection
LOQ	Limit of quantification
m	Slope

SD	Standard deviation
RSD	Relative standard deviation
R^2	Correlation coefficient

Keywords

Detection limits

Digestion

Dissolution

High purity

ICP-OES

Impurities

Matrix/Matrices

Nuclear grade

Zirconium

Summary

Zirconium occurs in nature as a component of the lithosphere in various molecular fractions within a number of mineral ores. Since its discovery in 1789, many chemical processes have been developed to have zirconium in its pure and malleable form for different uses in various industries. These industries include the nuclear, jewellery, medicine and cosmetic industries. It is considered extremely important in the nuclear industry and is used, for example, in the aligning of nuclear arcs, its chemical and radiation resistance, metallurgical properties as well as its low thermal neutron capture cross section. For this purpose the metal has to be extremely pure (>99.9 %) and devoid of the elements which can render it unusable as fuel rod cladding material in the nuclear reactor.

The objectives of this study were to:

i) develop an alternative digestion method for zirconium to hydrofluoric acid,
ii) develop an effective and efficient analytical method for the multi-element quantification of zirconium and its associated impurities in ultra-pure metal (foil: >99.98 % and rod: >99 %) and zirconium(IV) tetrafluoride samples at threshold and one-tenth of threshold by using commercially available equipment such as ICP-OES,
iii) identify and compare the different analytical techniques and
iv) determine the LOD/LOQ of zirconium and its associated impurities and perform method validation on these analytical methods.

Various digestion techniques, including individual mineral acids and their combinations, as well as microwave-assisted digestion were investigated with varying degrees of success. These included bench-top and microwave digestions with sulphuric acid (98 %), phosphoric acid (80 %) and *aqua regia* (nitric acid (55 %):hydrochloric acid (32 %), 3:1). The bench-top digestions of the zirconium rod samples by mineral acids gave average zirconium recoveries of 100.6 % for the sulphuric acid, 57.6 % and 89.6 % for phosphoric acid and *aqua regia* respectively, while the average recoveries for the bench-top digestions of the zirconium foil were 101.9 % for the sulphuric acid, 100.8 % and 85.1 % for the phosphoric acid and *aqua regia*, respectively. Microwave-assisted digestions of the metal samples with these mineral acids gave an average of 88.2 % for the phosphoric acid digestion, 100.2 % and 100.3 % for the sulphuric acid and *aqua regia* respectively for the zirconium rod digestion. The zirconium recoveries for the metal rod gave average recoveries of 32.7 %, 5.6 % and 97.4 % for phosphoric acid, *aqua regia* and sulphuric acid, respectively. Excellent recoveries for the

zirconium(IV) tetrafluoride dissolutions were obtained at 99.5 % at the optical emission wavelengths of 343.823 nm and 101.7 % at 339.198 nm. Trace elements, which included aluminium, chromium and silicon, were quantified in this sample at 1.9 ppm, 0.1 ppm and 0.5 ppm, respectively. Potassium hexafluorozirconate was obtained by reacting KF and ZrF_4 and gave zirconium recoveries of 100.9 % at 343.823 nm and 100.5 % at 339.198 nm. The product was also characterized using IR and the quantification of K using AA. The LOD and LOQ for zirconium were determined to be about 4 ppb at the two most sensitive wavelengths (343.823 nm and 339.198 nm) for the zirconium quantification.

The elements were first quantified individually at one-tenth of the threshold and at the threshold of their permissible concentrations in the nuclear grade zirconium. The results obtained ranged from 98 % to 103 %. The elements were then batched into 3 groups which were quantified respectively, followed by their combinations and ultimately all the elements were quantified in a single batch at one-tenth of the threshold and at the threshold. The results obtained ranged from 99 % to 102 % for **Group 1** (Al, Cr, Hf and Fe), 98 % to 102 % for **Group 2** (B, Cd, Co, Cu and Mn) and 100 % to 102 % for **Group 3** (Mo, Ni, Si, Ti, W and U) at threshold recovery. Recoveries between 98 % and 103 % for **Group 1**, 99 % and 101 % for **Group 2** and 99 and 102 % for **Group 3** elements were obtained at one-tenth of the threshold. The quantification results obtained for the element combinations of **Groups 1** and **2** at the threshold concentrations ranged from 99 % to 102 %, which were similar also for **Groups 1** and **3** combinations while 98 % to 103.5 % were obtained for the **Groups 2** and **3** combinations. At one-tenth of the threshold the recoveries were obtained between 98 % and 102 % for **Groups 1** and **2**, 70 % and 103.5 % for **Groups 1** and **3** while 4 % and 102 % were achieved for **Groups 2** and **3**. In the quantitative analyses of all the elements combined, recoveries between 98.8 % and 102.3 % were obtained at threshold recovery while 97.8 % and 102 % were obtained at one-tenth of the threshold concentrations. Poor recoveries at one-tenth of the threshold for boron, cadmium and uranium were obtained in the quantifications of the element mixtures – this was due to these elements being quantitatively analyzed close to their LOQ's.

The experimental results obtained for the quantitative analyses of zirconium and its specified impurities for nuclear purposes were validated using the hypothesis test of the *t*-statistic value (t_{crit} of ±2.31 for the pooled results in the quantification of zirconium metal samples and t_{crit} of ±4.30 for the quantitative analyses of zirconium and its impurities) at 95 % confidence interval to determine the acceptability of the results as recommended by ISO17025. Other

statistical parameters, such as the accuracy, precision and specificity, were investigated and the results were shown to be reproducible for all the experimental measurements.

Opsomming

Sirkonium kom in die natuur voor as 'n komponent van die litosfeer. Dit is teenwoordig in verskeie molekulêre fraksies in seker minerale ertse. Sedert die ontdekking daarvan in 1789, is verskeie chemiese prosesse ontwikkel om sirkonium vir verskillende gebruike in verskeie industrieë in sy suiwerste en mees smeebare vorm te produseer. Hierdie nywerhede sluit in die kern-, juweliersware-, medisyne- en kosmetiese industrieë. Dit word as uiters belangrik in die kernindustrie beskou vir die rig van die kernboë, sy chemiese en radiologiese weerstand, metallurgiese eienskappe en 'n lae-termiese-neutron-opvangsdeursnit. Vir hierdie doel moet die metaal baie suiwer (>99 %) en vry van elemente wees wat dit onbruikbaar kan maak as brandstofstaaf-bekledingsmateriaal in die kernreaktor.

Die doel van hierdie studie was om:

i) die ontwikkeling van 'n alternatiewe verteringsmetode as fluoorsuur te ondersoek,
ii) die ontwikkeling van 'n effektiewe en doeltreffende analitiese metode te ontwikkel vir die multi-element kwantifisering van sirkonium en sy verwante onsuiwerhede in 'n ultra-suiwer metaal (foelie: >99.98 % en staaf: >99 %) en sirkoniumtetrafluoriedmonsters by drempel en 'n eentiende van die drempel deur die gebruik van kommersieel-beskikbare toerusting soos IGP-OES,
iii) verskillende analitiese tegnieke te identifiseer en te vergelyk en
iv) om uiteindelik die LOD/LOQ van sirkonium en sy geassosieerde onsuiwerhede te bepaal en gevolglik die validasie op hierdie analitiese metodes uit te voer.

Verskeie verteringstegnieke, insluitende individuele mineralesure en hul kombinasies, sowel as mikrogolfvertering, is met wisselende grade van sukses ondersoek. Dit sluit in laboratoriumskaal- en mikrogolfverterings met swawelsuur (98 %), fosforsuur (80 %) en *aqua regia* (salpetersuur (55 %):soutsuur (32 %), 3:1). Die laboratoriumskaalverterings van die sirkoniumbasis-monsters deur minerale sure, het gemiddelde opbrengs van 100.6 % vir die swawelsuur, 57.6 % en 89.6 % vir fosforsuur en *aqua regia*, onderskeidelik gelewer, terwyl die gemiddelde opbrengs vir die vertering van die sirkoniumfoelie 101.9 % vir die swawelsuur, 100.8 % en 85.1 % en vir die fosforsuur en *aqua regia*, onderskeidelik was. Mikrogolf-gesteunde verterings van die metaalmonsters met hierdie minerale sure het 'n gemiddeld van 88.2 % vir die fosforsuur-vertering, 100.2 % en 100.3 % vir die swawelsuur en *aqua regia* onderskeidelik vir die sirkoniumstaaf-vertering. Die sirkoniumopbrengs vir die metaalstaaf het 'n gemiddeld van 32.7 %, 5.6 % en 97.4 % vir fosforsuur, *aqua regia* en

swawelsuur, onderskeidelik behaal. Uitstekende opbrengs vir die sirkonium(IV)tetrafluoried-verbindings is verkry teen 99.5 % by optiese emissie golflengte van 343.823 nm en 101.7 % by 339.198 nm. Spoorelemente, wat aluminium, chroom en silikon insluit, is in hierdie steekproef gekwantifiseer op 1.9 dpm, 0.1 dpm en 0.5 dpm, onderskeidelik. Kaliumheksafluorosirkonaat is verkry deur die reaksie van KF met ZrF_4, en het sirkonium-opbrengste van 100.9 % by 343.823 nm en 100.5 % by 339.198 nm gelewer. Die produk is ook gekarakteriseer is met behulp van IR en kwantifisering van K met die gebruik van AA. Die LOD en LOQ vir sirkonium is bereken as opgeveer 4 dpb by die twee mees sensitiewe golflengtes (343.823 nm en 339.198 nm) vir die sirkonium-kwantifisering.

Die elemente is vir die eerste keer individueel gekwantifiseer teen eentiende van die drempel en op die drempel van hul toelaatbare konsentrasies in die kerngraad-sirkonium. Die resultate wat verkry is, het gewissel van 98 % tot 103 %. Daarna is die elemente in 3 groepe verdeel wat onderskeidelik gekwantifiseer is, gevolg deur hul kombinasies en uitendelik is al die elemente in 'n groep op eentiende van die drempel en op die drempel gekwantifiseer. Die resultate wat verkry is, het gewissel van 99 % tot 102 % vir **Groep 1** (Al, Cr, Hf en Fe), 98 % tot 102 % vir **Groep 2** (B, Cd, Co, Cu en Mn) en 100 % tot 102 % vir **Groep 3** (Mo, Ni, Si, Ti, W en U) op drempel. Opbrengs van tussen 98 % en 103 % vir **Groep 1**, 99 % en 101 % vir **Groep 2** en 99 % en 102 % vir **Groep 3** elemente is verkry op eentiende van die drempel. Die kwantifiseringsresultate wat verkry is vir die elementkombinasies van **Groepe 1** en **2** op die drempelkonsentrasies het gewissel van 99 % tot 102 %, wat dieselfde was vir **Groepe 1** en **3** kombinasies, terwyl 98 % tot 103.5 % verkry is vir die **Groepe 2** en **3** kombinasies. By eentiende van die drempel is die opbrengs verkry tussen 98 % en 102 % vir **Groepe 1** en **2**, 70 % en 103.5 % vir **Groepe 1** en **3** terwyl 4 % en 102 % verkry is vir **Groepe 2** en **3**. Tydens die kwantitatiewe analise van al die elemente gekombineer, is opbrengste van tussen 98.8 % en 102.3 % verkry by die drempelherwinning, terwyl 97.8 % en 102 % verkry is op eentiende van die drempelkonsentrasies. Swak opbrengs op eentiende van die drempel is vir die boor, kadmium en uraan verkry in die kwantifisering van die elementmengsels. Die rede hiervoor was dat hierdie elemente kwantitatief naby aan hul LOQ ontleed word.

Die eksperimentele resultate wat verkry is vir die kwantitatiewe analise van sirkonium en sy gespesifiseerde onsuiwerhede vir kerndoeleindes, is gevalideer met behulp van die hipotese toets van die *t*-statistiese waarde (t_{krit} van ± 2.31 vir die gesamentlike resultate in die kwantifisering van sirkonium en sy onsuiwerhede) by 95 % vertroue-interval om die aanvaarbaarheid van die resultate, soos aanbeveel deur die ISO17025, te bepaal. Ander

statistiese parameters, soos die akkuraatheid, presisie en spesifisiteit, is ondersoek en die resultate blyk herhaalbaar te wees vir al die eksperimentele bepalings.

1 History, Motivation and Objectives

1.1 HISTORICAL BACKGROUND

Zirconium (Zr) is widely distributed in nature as a component of the lithosphere (earth's crust) and is found in a number of different mineral ores[1,2,3], e.g. baddeleyite (zirconia – ZrO_2), chernobylite (zircon – $ZrSiO_4$), eudialyte (mineral containing small amounts of zirconium), painite ($CaZrAl_9O_{15}(BO_3)$), sabinaite ($Na_4Zr_2TiO_4(CO_3)_4$), vlasovite ($Na_2ZrSi_4O_{11}$), weloganite ($Na_2(Sr,Ca)_3Zr(CO_3)_6 \cdot 3H_2O$), zirconolite ($CaZrTi_2O_7$), zircophyllite (a complex zirconium-containing mineral) and zirkelite ($(Ca,Th,Ce)Zr(Ti,Nb)_2O_7$). Different zirconium-containing mineral ores are shown in **Figure 1.1**.

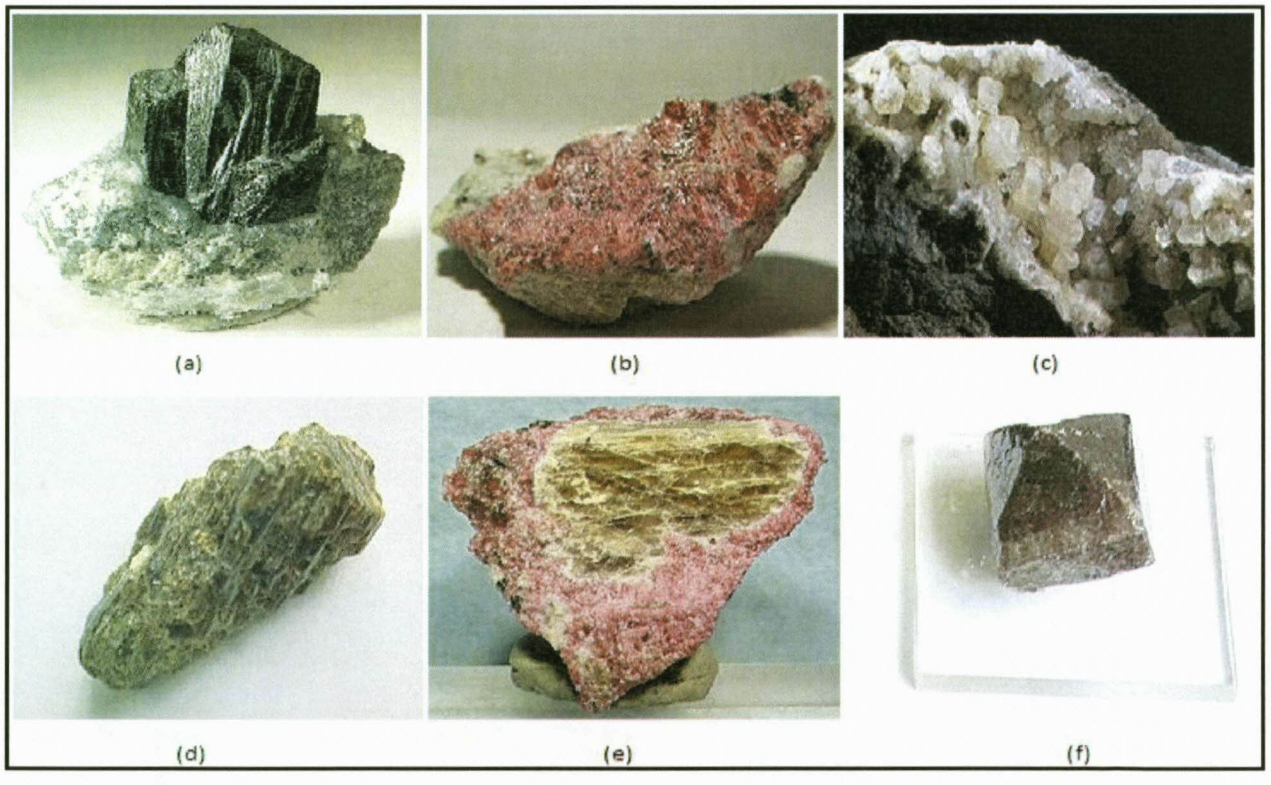

Figure 1.1: Zirconium-containing mineral ores: (a) baddeleyite, (b) eudialyte, (c) weloganite, (d) painite, (e) vlasovite, (f) zircon.[3]

[1] W.B. Blumenthal., *The Chemical Behavior of Zirconium*, D. Van Norstrand Co. Inc, New Jersey (1958)

[2] http://en.wikipedia.org/wiki/Zirconium (17 February 2010)

[3] http://en.wikipedia.org/wiki/Category:Zirconium_minerals (23 March 2011)

Precious stones containing zirconium, e.g. hyacinth and jacinth, have been known to mankind since antiquity as mentioned in some biblical writings. The book of Exodus refers to the different stones which were used to decorate the breastplates of ancient Israelite high priests that one of them was made of ligure[4], which is supposedly the same as jacinth.[5] In another example, Apostle John gave account of a vision where he was shown the foundations of the walls of New Jerusalem. In this vision he saw that the foundations were garnished with all kinds of precious stones, of which the eleventh was made of jacinth.[6] The Greek philosopher, Theophratus (*ca.* BC 300)[7], who also had interest in botany, zoology and physics, was the first person to classify rocks based on their behaviour when heated, which led to the grouping of minerals according to their common properties. He mentioned, in his findings, the mineral lyncurium, the presence of which for a while some researchers assumed it to be made of zircon. However, this assumption proved to be doubtful according to studies carried out by J.W. Mellor.[8] Pliny the Elder (AD 77 – 79)[9] described many different minerals and gemstones, building on works by Theophratus and other authors. The *hyacinthus* he listed with other minerals, was possibly the same as hyacinth which contains zircon. The presence of zirconium in some of these minerals was only confirmed in the 18th and 19th centuries.

Figure 1.2: Martin Heinrich Klaproth (1743 - 1817)[10]

[4] Exodus 39:12 (KJV)

[5] http://dictionary.reference.com/browse/ligure (23 March 2011)

[6] Revelation 21:20 (KJV)

[7] Theophratus., *Peri Dithon*

[8] J.W. Mellor., *A Comprehensive Treatise on Inorganic and Theoretical Chemistry*, Longmans, Green and Co., New York, Vol. VII (1927)

[9] Pliny. *Historia Naturalis*

[10] http://www.sil.si.edu/digitalcollections/hst/scientific-identity/explore.htm (reworked) (23 March 2011)

In 1789 M.H. Klaproth[11] discovered that jargon and hyacinth samples from the island of Sri Lanka in the Indian Ocean and France possessed a distinguishing oxide when he analyzed these samples. He fused the specimens with sodium hydroxide, then extracted the reaction product with hydrochloric acid and found the solution to contain an element of different chemical behaviour to others he had already discovered. He proposed the name *Zirkonerde* in German or the name *terra circonia* in Latin for this new oxide.

He wrote the following remark after his discovery[12]: "*Was ist dieses nun für eine Erde? Kann ich solche für eine bisher ungekannte, selbständige, einfache Erde halten? In so fern mir nicht bewußt ist, ob sich eine oder andere der bisher bekannten fünf einfachen Erden künstlich so umändern lasse, daß sie die nemlichen Erscheinungen und Verhältnisse, wie diese Erde aus dem Zirkon, gewährte, glaube ich mich dazu wohl berechtigt, und lege selbiger, bis dahin, daß man sie vielleicht in mehrern Steinarten antreffen, und anderweitige Eigenschaften, welche eine angemessenere Benennung veranlassen mögten, an ihr kennen lernen wird, den Namen Zirkonerde (Terra circonia) bey.*"

Rough translation:

What kind of earth is this? Can I assume that since it is thus far unknown, to be independent and simple earth? I am not aware, to some extent, that any of the five simple earths known so far can be artificially altered to show the appearance and behave as this earth from zircon that I then consider myself entitled to, until it is perhaps found in other types of rocks, with further properties as to render a more appropriate name for it, to give it the name zircon earth (zirconia).

The specimens he analyzed contained, on average, about 68 % zirconium. He also associated the identity of hyacinth and zirconite with zirconium.[13] Several attempts were made to isolate the new element some years after Klaproth discovery. J.B. Trommsdorff (1799)[14] unsuccessfully tried to reduce zirconia by chemical means. H. Davy (1808)[15] also reported his failure to isolate the new element using electrolytic methods.

[11] M.H. Klaproth., *Beobacht. Entdeck. Naturkunde*, **3**, p. 2 (1789)

[12] http://elements.vanderkrogt.net/element.php?sym=Zr (23 March 2011)

[13] M.H. Klaproth., *Ann. Chim. Phys.*, **8** (1789)

[14] J.B. Trommsdorff., *Trommsdorff's Jour.*, **6**, p. 116 (1799)

[15] H. Davy., *Phil. Mag.*, **32**, pp. 203 – 207 (1808)

Thirty-five years after the discovery of zirconium, J.J. Berzelius (1824)[16] succeeded in the isolation of the first impure form of zirconium metal. He achieved this by heating a mixture of potassium metal and potassium fluorozirconate in an iron tube placed inside a platinum crucible.

L. Troost (1865)[17] repeated the experiment of Berzelius and also obtained an impure zirconium metal by reducing the gaseous zirconium tetrachloride with magnesium. However, due to limited knowledge on the chemical properties of zirconium, both Berzelius and Troost did not use a completely sealed tube for conducting their reduction which resulted in an impure final product. It should be noted that if element zirconium is prepared at red heat or higher temperatures, it becomes so chemically reactive that it avidly absorbs trace amounts of carbon, oxygen and nitrogen from its surroundings and thus affecting the purity of the product.[1] Berzelius obtained at best an altered zirconium metal product while Troost obtained an amorphous zirconium mixed with zirconia. The presence of these impurities prevented the metal to be malleable.

In 1910 L. Weiss and E. Neumann[18] qualified the zirconium in Berzelius's procedure, which showed a metal content of up to 93.7 % purity. They improved the purity to 98 % by first treating it with absolute alcohol instead of water, and thereafter washed with dilute acid. D. Lely, Jr. and L. Hamburger (1914)[19] were the first researchers to report the preparation of malleable zirconium metal of nearly 100 % purity by heating the resublimed zirconium tetrachloride with sodium in a sealed bomb. About the same time, E. Podszus (1917)[20] reported to have obtained a product of 99.3 % purity by heating potassium fluorozirconate with sodium in a sealed bomb. A number of other methods to prepare zirconium metal with high purity were reported after the successful isolation of the pure product. J.W. Marden and M.N. Rich (1920 – 1921)[21,22] reported zirconium of 99.76 – 99.89 % purity by volatilizing the aluminium out of a zirconium-aluminium alloy in an arc furnace. Finally in 1925, A.E. van

[16] J.J. Berzelius., *Ann. Chim. Phys.*, **20**, p. 43 (1824)

[17] L. Troost., *Comptes Rendus.*, **61**, pp. 109 – 113 (1865)

[18] L. Weiss and E. Neumann., *Z. Anorg. Allgem. Chem.*, **65**, pp. 248 (1910)

[19] D. Lely, Jr., and L. Hamburger., *Z. Anorg. Allgem. Chem.*, **87**, pp. 209 (1914)

[20] E. Podszus., *Z. Anorg. Allgem. Chem.*, **99**, pp. 123 – 131 (1917)

[21] J.W. Marden and M.N. Rich., *Ind. Eng. Chem.*, **12**, pp. 651 – 656 (1920)

[22] J.W. Marden and M.N. Rich., *Investigation of Zirconium with Especial Reference to the Metal and Oxide*, US Bureau of Mines, **186** (1921)

Arkel and J.H. de Boer[23], working at the University of Leyden and the Philips Lamp Works at Eindhoven, Holland, developed the first practical method for producing extremely pure, grossly crystalline, ductile zirconium metal. Their method, commonly known as the iodide process, depends on the decomposition of zirconium iodide vapour on a hot tungsten filament.

1.1.1 EXTRACTION OF ZIRCONIUM FROM MINERALS

The extraction of zirconium from its mineral ores is rather a painstaking procedure. Much of the effort goes into obtaining the highest purity of the metal by ensuring that most of the impurities associated with its extraction are eliminated or kept at a minimum. An example of a mining operation, in Russia, for some of the zirconium-containing minerals is shown in **Figure 1.3**.

Figure 1.3: A mining pit for different kinds of minerals, including baddeleyite, in Kovdor, Russia[24]

Beneficiation of zirconium-containing ores and the conversion of zircon to other useful zirconium compounds is a highly developed science which has taken extensive advantage of

[23] A.E. van Arkel and J.H. de Boer., *Z. Anorg. Allgem. Chem.*, **148**, pp. 345 – 350 (1925)

[24] http://www.nhm.ac.uk/hosted_sites/eurocarb/pictures/finland/pages/fin1.html (23 March 2011)

the physical and chemical properties of zircon. Although zircon sand is the starting material for current large scale production of zirconium products, methods for treating zircon-containing rocks have also been described and used to a limited extent. Wet and dry techniques have been used to isolate the grains of zircon sand in high state of purity by industrial standards – commonly over 99 % pure zircon.[25] The most well-known extraction procedures for zirconium from its ores are i) chlorination extraction and ii) alkali extraction.

A. Extraction by carbochlorination

The major mineral ore, zircon – $ZrSiO_4$, is a very stable compound and resists attack by most mineral acids.[26] The most common approach to extracting the metal from the ore is by the conversion of zirconium content to the tetrachloride compound, $ZrCl_4$. This process, called carbochlorination of zircon, takes place in a fluidized bed at temperatures of about 1200 °C. Carbon acts as a reducing agent which is required in bringing the reaction to completion and its presence reduces the propensity of oxide formation and favours the formation of chlorides by providing a low oxygen potential atmosphere.[27]

$$ZrSiO_{4(s)} + 2C_{(s)} + 4Cl_{2(g)} \xrightarrow{1200^{o}C} ZrCl_{4\,(g)} + SiCl_{4\,(g)} + 2CO_2\uparrow \qquad (1.1)$$

The mixture of $ZrCl_4$ and $SiCl_4$ are separated according to their differences in boiling point (331 °C and 58 °C, respectively) by selective condensation.

Fluidized bed condensation has the advantage of close temperature control, which provides a means to prevent co-condensation of metal chloride impurities, such as silicon tetrachloride ($SiCl_4$), titanium tetrachloride ($TiCl_4$), ferric chloride ($FeCl_3$) and aluminium chloride ($AlCl_3$). The extraction and purification of zirconium from baddeleyite (ZrO_2) can be done also *via* carbochlorination.

$$ZrO_{2(s)} + 2C_{(s)} + 2Cl_{2(g)} \rightarrow ZrCl_{4\,(g)} + 2CO\uparrow \qquad (1.2)$$

[25] R.C. Gosbreau., *Eng. Min. J. Press.*, **119**, pp. 405 – 406 (1925)

[26] D.G. Franklin and R.B. Adamson., Eds. *Zirconium in the Nuclear Industry: Sixth International Symposium, ASTM STP 824*, American Society for Testing and Materials, pp. 5 – 36 (1984)

[27] A. Movahedian *et al.*, *Thermochimica Acta*, **512**, pp. 93 – 97 (2011)

Conversion of zirconium tetrachloride into pure zirconium metal, involves reduction with metal magnesium in a sealed furnace.[17]

$$ZrCl_{4\,(g)} + 2Mg_{(s)} \rightarrow Zr_{(s)} + 2MgCl_{2(s)} \quad (1.3)$$

After further purification, all of the above procedures can yield zirconium metal of > 99.99 % purity. Another way of separating zirconium and silicon from zircon is by high temperature fusion (> 3500 °C) to produce fused zirconia and fumed silica.

$$ZrSiO_4 + 2C \xrightarrow{3500^{o}C} ZrO_2 + SiO^{*}\uparrow + CO\uparrow \quad (1.4)$$

$$2SiO^{*} + O_{2\,(air)} \longrightarrow 2SiO_{2\,(fumed)} \quad (1.5)$$

B. *Extraction by alkali*

The second most common commercial method of converting the zircon to usable zirconium products is by alkali extraction. Different alkalis, such as caustic soda and sodium carbonate are used in these methods.

I. *Caustic fusion*

In the caustic fusion process the zircon is reacted with sodium hydroxide in steel pots at temperature ranges of 600 °C to 650 °C to form a fused product of sodium zirconate

$$ZrSiO_{4(s)} + 4NaOH_{(s)} \xrightarrow{600^{o}C-650^{o}C} Na_2ZrO_{3(s)} + Na_2SiO_{3(s)} + 2H_2O_{(g)} \quad (1.6)$$

II. *Soda ash fusion*

A variation to the caustic fusion is the soda ash fusion method at 1200 °C. When 1 mole of zircon is heated with 2 moles of soda ash, sodium zirconate and sodium silicate are formed

$$ZrSiO_{4(s)} + 2Na_2CO_{3(s)} \xrightarrow{1200^{o}C} Na_2ZrO_{3(s)} + Na_2SiO_{3(s)} + 2H_2O_{(g)} + CO_2\uparrow \quad (1.7)$$

This process is used when the zirconium-hafnium separation process calls for a feed solution other than the chloride.

Following any of the above fusion processes, the next step is to leach the soluble sodium silicate from the reaction product with water and the residue is centrifuged and washed, after which the sodium zirconate isdissolved in sulphuric acid (H_2SO_4), hydrochloric acid (HCl), or nitric acid (HNO_3) to provide a solution which is ready for further processing, e.g.

$$2Na_2ZrO_3 + 6H_2SO_4 \longrightarrow 2Zr(SO_4)_{2(s)} + 2Na_2SO_{4(aq)} + 6H_2O \quad (1.8)$$

$$Na_2ZrO_3 + 4HCl \longrightarrow ZrOCl_{2(s)} + 2NaCl_{(aq)} + 2H_2O \quad (1.9)$$

$$Na_2ZrO_3 + 6HNO_3 \longrightarrow Zr(NO_3)_{4(s)} + 2NaNO_{3\,(aq)} + 3H_2O \quad (1.10)$$

c. *Other methods for extraction and purification of zirconium*

Many processes of obtaining relatively pure zirconium metal were developed and applied over the years before and after the pyrolysis of zirconium iodide process was developed by van Arkel-de Boer process in 1925.[23] Research indicated that during the reduction process of the halogenide compounds of zirconium, all possible care should be taken to keep oxygen and oxygen-containing substances out of the reacting system.

The reduction of zirconium tetrachloride by magnesium was developed to a high state of perfection by W.J. Kroll and his associates (1946)[28], which followed the same method that was used to reduce titanium tetrachloride. They performed the reaction under argon or any other inert gas to protect the product from atmospheric contamination. An ingot of zirconium metal and magnesium chloride is obtained. This ingot is then further melted by high temperature arc furnaces and ore electron beam furnaces. The excess magnesium and magnesium chloride are then removed by volatilizing to produce a pure zirconium metal with "voids" in it, where magnesium chloride bubbles escaped. Thus, a typical sponge structure is yielded and it is known as the zirconium sponge. This process is generally known as the Kroll process (see **Figure 1.4**).

[28] W.J. Kroll, A.W. Schlechten and L.A. Yerkes., *Trans. Elec. Soc.*, **89**, pp. 365 – 376 (1946)

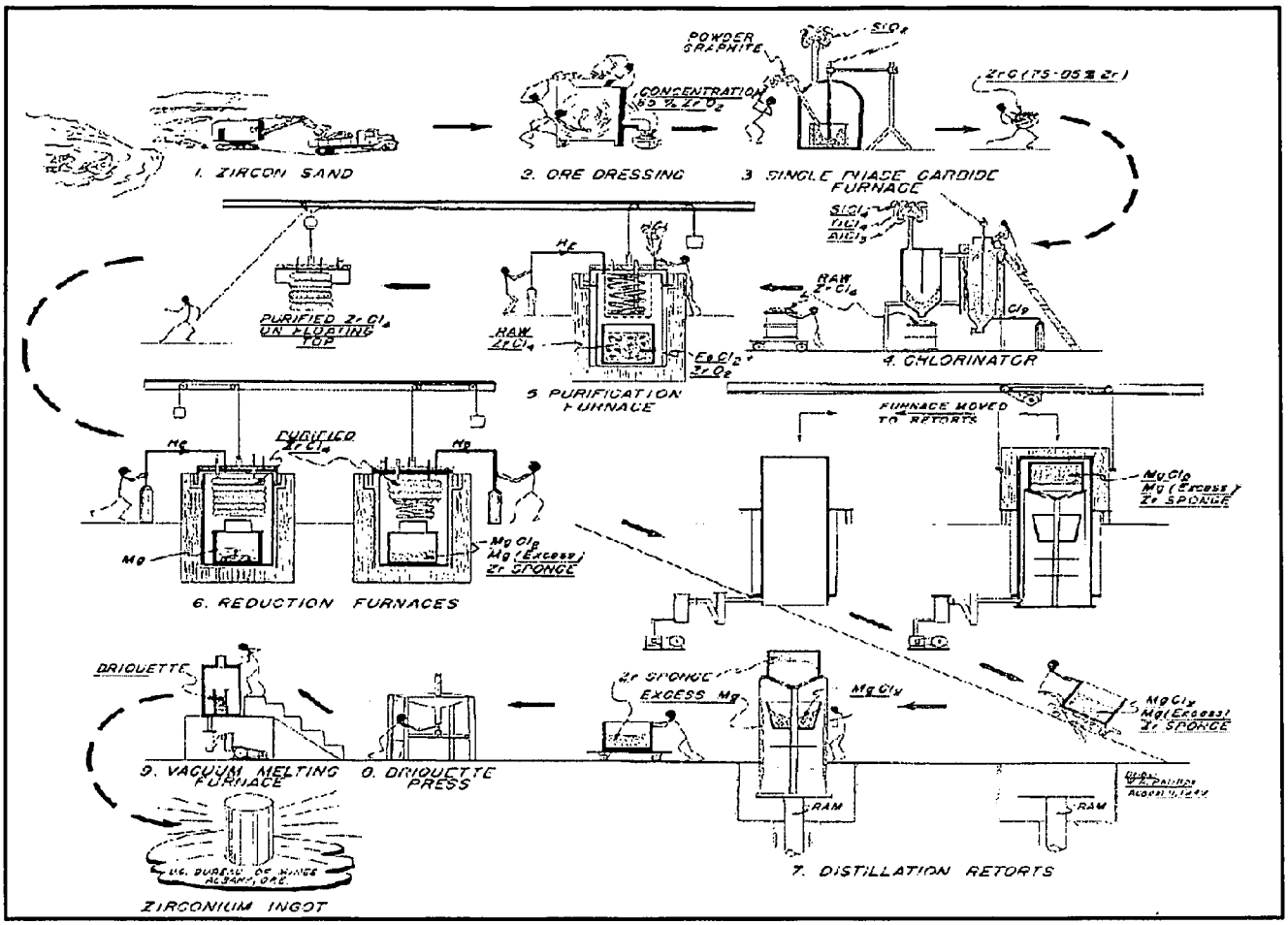

Figure 1.4: Flow diagram for Kroll process in the production of zirconium[29]

Another method for the production of pure zirconium metal makes use of the reduction of zirconium dioxide in the presence of oxygen. S.A. Tucker and H.R. Moody (1902) applied the thermite process (a pyrotechnic composition of a metal powder and metal oxide which produces an exothermic redox reaction). Initially the process, using aluminium, proved to be unsuccessful in the preparation of pure zirconium.[30] This process, also known as aluminothermic reaction, produced zirconium-aluminium alloys instead of the zirconium metal and the products were contaminated with aluminium and zirconium oxides, which is difficult to separate from the metal. Alterations to this process were carried out until a metal of 99.76 – 99.89 % purity was achieved by Marden and Rich in 1920.[21]

Calcium metal was also reported to react with oxide compounds of zirconium to achieve zirconium metal of up to 99 %. A. Burger (1907)[31] reported zirconium of 98.77 % purity by

[29] W.J. Kroll and W.W. Stephens., *Ind. Eng. Chem.*, **42**, pp. 395 – 398 (1950)

[30] S.A. Tucker and H.R. Moody., *J. Am. Chem. Soc.*, **81**, p. 14 (1902)

[31] A.Burger., *Reduktionen durch Calcium*, Basel, p. 30 (1907)

heating zirconia with excess calcium. W.J. Kroll (1937)[32] used calcium hydride in the presence of alkaline earth chlorides instead of calcium metal to reduce zirconium dioxide to the metal. He obtained a metal that was malleable, but it contained enough residual oxygen to render it brittle. In another method, W.C. Lilliendahl and E.D. Gregory (1947 and 1952)[33,34] purified zirconium metal by heating it with molten calcium or in contact with calcium vapour at 1000 – 1300 °C for five hours or longer to reduce the oxygen content from 0.5 % to about 0.02 %. The use of liquid calcium requires a nitrogen-free environment since the presence of nitrogen contaminates the metal. The calcium is purified by heating it with scrap zirconium prior to its use for removal of nitrogen to form high grade zirconium.

1.1.2 THE PRESENCE OF HAFNIUM IN ZIRCONIUM

All the zirconium occurring in the earth's crust has a small amount of the element hafnium. This element behaves very much like zirconium – they both possess the same number of valence electrons and belong to the same group – to the extent that no qualitative differences in chemical behaviour between the two elements have been sufficiently observed thus far. The element hafnium was discovered in 1923 by G. von Hevesy and D. Coster[35] after they conducted a careful study of zircon and the element was named *hafnium* after Hafnia, an ancient name of the city Copenhagen, where the two scientists discovered the element. They noted that the occurrence of element 72 with trivalent ytterbium was not in accord with the expected tetravalency for this element demanded by the quantum theory. Moreover, the indicated rarity of element 72 as a minor constituent of ytterbium concentrates did not agree with the general statistics of abundances of elements of even atomic numbers. They reasoned that element 72 was more likely to occur with zirconium than with the rare earths and undertook a careful X-ray study of zircon. They found two very distinct α_1 and α_2 lines situated exactly at the positions interpolated by means of Moseley's law and also identified the β_1, β_2, β_3 and γ_1 lines and found that the relative intensities were those anticipated by the theory.

[32] W.J. Kroll., *Z. Anorg. Allgem. Chem.*, **234**, pp. 42 – 50 (1937)

[33] W.C. Lilliendahl., E.D. Gregory and D.M. Wroughton, *J. Am. Electrochem. Soc.*, **99**, pp. 187 – 190 (1947)

[34] W.C. Lilliendahl and E.D. Gregory., U.S. Patent **2707679**, (1947)

[35] G. von Hevesy and D. Coster., *Chem. Rev.*, **2**, pp. 1 – 41 (1925)

Only after the discovery of hafnium and its subsequent separation from zirconium through a recrystallization procedure, was it possible to determine the accurate value of the atomic weight of zirconium. Historically significant determinations of the atomic weight of zirconium are summarized in **Table 1.1**. The value reported by Hönigschmid *et al.*[36] in 1924 has been proved to be accurate and is still the accepted value.

Table 1.1: Atomic weight determinations of zirconium[1]

Year	Analyst	Ratio Used	Atomic Weight Found
1825	J.J. Berzelius	$Zr(SO_4)_2$:ZrO_2	89.46
1844	R. Herman	$ZrCl_4$:ZrO_2	88.64
1844	R. Herman	$ZrOCl_2 \cdot 8H_2O$:ZrO_2	89.98
1860	J.C.G. Marignac	K_2ZrF_6:H_2SO_4	90.03
1860	J.C.G. Marignac	K_2ZrF_6: ZrO_2	91.54
1881	M. Weibull	$Zr(SO_4)_2$:ZrO_2	89.54
1881	M. Weibull	$Zr(SeO_4)_2$:ZrO_2	90.79
1889	G.H. Bailley	$Zr(SO_4)_2$:ZrO_2	90.45
1898	F.P. Venable	$ZrOCl_2 \cdot 8H_2O$:ZrO_2	90.81
1917	F.P. Venable and J.M. Bell	$ZrCl_4$:Ag	91.76
1924	O. Hönigschmid, E. Zintl, and F. Gonzalez	$ZrBr_4$:AgBr	91.22

Though both zirconium and hafnium chemically behave in a similar manner, these two elements have different nuclear properties. Their thermal neutron absorption cross sections are different, with hafnium having barns (neutron absorption cross sectional area) of 104 cm^{-2} and that of zirconium is 0.184 cm^{-2}. Thus zirconium is chemically inert in nuclear reactions as compared to hafnium. For the generation of nuclear energy, zirconium has to either be completely free of hafnium and any other element or comprise acceptable maximum contents of these elements which will render it non-viable, so as to be usable in aligning nuclear arcs.

[36] O. Hönigschmid, E. Zintl, and F. Gonzalez., *Z. Anorg. Allgem. Chem.* **139**, p. 293 (1924)

1.2 GEOGRAPHICAL DISTRIBUTION AND ECONOMICAL SIGNIFICANCE

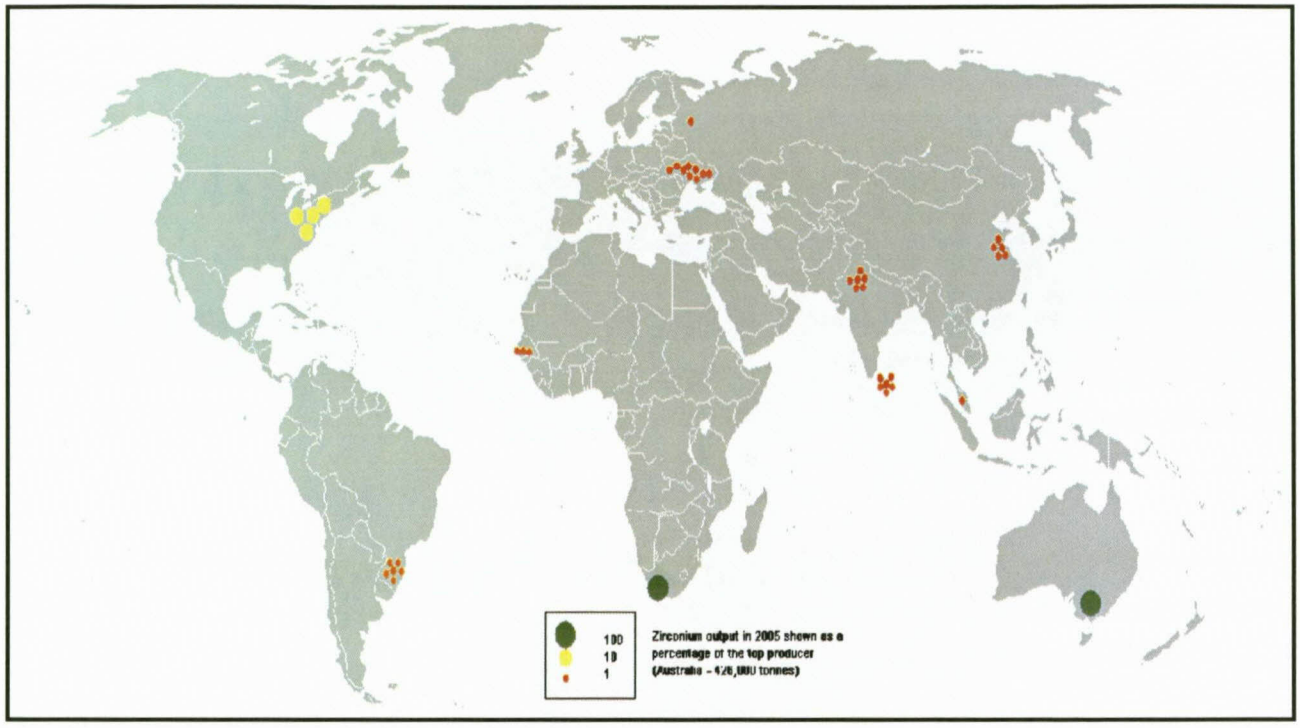

Figure 1.5: Geographical distribution of zirconium shown as a percentage of the top producers in 2005[2]

1.2.1 GEOGRAPHICAL DISTRIBUTION

Compounds of zirconium are widely and fairly abundantly distributed in the lithosphere as indicated by **Figure 1.5**. The two major sources of zirconium are minerals zircon, $ZrSiO_4$, and baddeleyite, ZrO_2. However, a variety of complex minerals – especially silicates – also contain zirconium. During the disintegration of rocks by climatic changes and hydrolytic action, the highly inert zircon crystals are often preserved while the parent rock crumbled, dissolved and ultimately became clay and soil.[1] On average, zirconium is estimated to comprise about 184 ppm (0.0184 %) of earth's crust.[37] F.W. Clarke and H.S. Washington[38,39] estimated that zirconium constitutes about 0.017 % of the lithosphere whereas

[37] http://en.wikipedia.org/wiki/Abundance_of_elements_in_Earth's_crust#cite_note-3 (03 Aug 2011)

[38] F.W. Clarke., *U.S. Geol. Survey Bull.*, **695**, p. 30 (1920)

[39] F.W. Clarke and H.S. Washington., *Proc. Nat. Acad. Sci.*, **8**, p. 108 (1922)

W. Vernadsky[40] estimated it to be in the range of 0.0019 – 0.1 %. J. Peterson *et al.*[41] deduced that zirconium is contained in the lithosphere at a concentration of about 130 ppm and its concentration in seawater is about 0.026 ppm. The major commercial source of zirconium is zircon ($ZrSiO_4$) and is mainly found in Australia, Brazil, India, Russia, South Africa, and the United States. Smaller deposits are located around the world. Australia and South Africa are the principal miners of zircon, and together they produce 80 % of the mineral annually (see **Table 1.2**).[42] Global zircon mineral deposits exceed 60 million metric tons and the annual worldwide zirconium production is approximately 1.2 million metric tons.[41,42]

Table 1.2: World Mine Production, Reserves and Reserve Bases[42]

	Zirconium			
	Mine production (thousand metric tons)		Reserves[a] (million metric tons, ZrO_2)	Reserve base[b] (million metric tons, ZrO_2)
	2006	2007[e]		
United States	W	W	3.4	5.7
Australia	491	550	9.1	30.0
Brazil	26	26	2.2	4.6
China	170	170	0.5	3.7
India	21	21	3.4	3.8
South Africa	398	405	14.0	14.0
Ukraine	35	35	4.0	6.0
Other countries	38	32	0.9	4.1
World total (rounded)	1180	1240	38	72

[e] – Estimated

W – Withheld to avoid disclosing company proprietary data

[a] – That part of the reserve base which could be economically extracted or produced at the time of determination

[b] – That part of an identified resource that meets specified minimum physical and chemical criteria related to current mining and production practices, including those for grade, quality, thickness, and depth.

[40] W. Vernadsky., *La Geochimie*, Alcan, Paris (1924)

[41] J. Peterson and M. MacDonell., *Radiological and Chemical Fact Sheets to Support Health Risk Analyses for Contaminated Areas*, Argonne National Laboratory, pp. 64–65 (2007)

[42] "Zirconium and Hafnium", *Mineral Commodity Summaries* (US Geological Survey), pp. 192–193 (2008)

1.2.2 COMMERCIAL BENEFITS

Zirconium metal is mainly found on the market in three forms—powder, sponge, and crystal bar (see **Figure 1.6**). Since 1930 powdered zirconium metal has been used primarily for its pyrophoric and alloying properties. Principal uses are for the preparation of ammunition primers, vacuum-tube getters, flash powder used in photography, as catalyst in organic reactions in the manufacturing of water repellent textiles, in dye pigments, ceramics and corrosion-resistant steel alloys. The development of the Kroll or magnesium-reduction process in the mid-1940's to produce the first zirconium metal sponge became commercially available in the early 1950's.[41]

Figure 1.6: (a) Zirconium powder; (b) Zirconium sponge; (c) Zirconium crystal bar[2]

The sponge is mainly used in the production of zirconium metal and its alloys, especially for their application in nuclear fuel cladding (see **Figure 1.7**), corrosion resistant pipes in chemical processing plants, and heat exchangers. Zirconium oxychloride has been used as an antiperspirant, while zirconium carbonate and oxide are used for dermatitis. Intravenous injection of zirconium has been advocated for prophylactic use to prevent skeletal deposition of certain radio elements especially plutonium.[43] Crystal bar is the ultra pure form of zirconium metal that is used mostly in research projects, such as developing methods for the analysis of nuclear grade zirconium.

[43] Y.K. Agrawal & S. Sudhakar., *Separation and Purification Technology*., **27**, pp. 111–119 (2002)

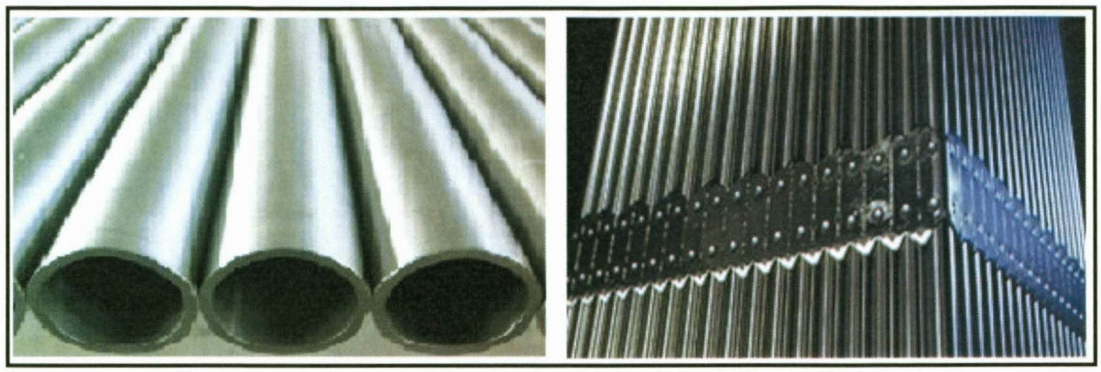

Figure 1.7: Zirconium tubes and bars for nuclear fuel and cladding[44]

The price of the mineral zircon has been somewhat dependent on the supply-demand relationship since 1997 up to 2010, as reported on Roskill's 13th Report on Zirconium (see **Figure 1.8**).[45]

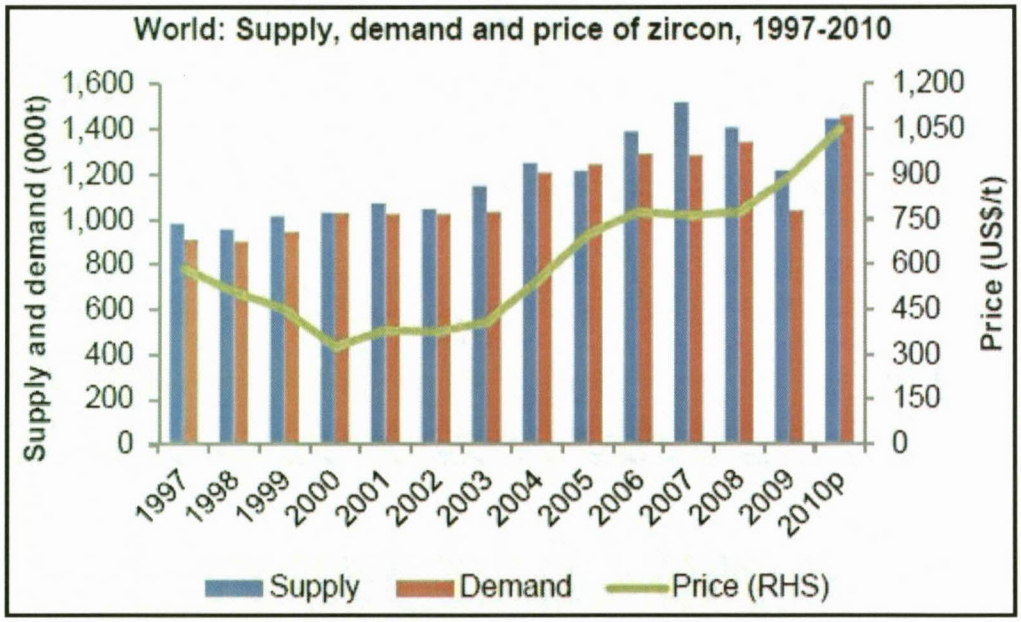

Figure 1.8: Graph portraying the world economic trend of zircon supply, demand and pricing[45]

The report states, as seen on the graph, that the zircon market contracted sharply towards the end of 2008 and the trend lasted for a year. The main cause of this contraction was due to the reduction of output by the producers in order to cut costs and stop the accumulation of stock as the market appetite for zircon subsided and supply outweighed the demand. However, consumption started to recover in the late 2009, accelerated in 2010 and continued

[44] http://www.product-category.com/p/zirconium (15 July 2010)

[45] www.roskill.com/zirconium (09 May 2011)

to grow in 2011. The tightness in the market, coupled with the drawdown in stocks, led to a series of rising prices that started in early 2009.

1.3 CHEMICAL AND PHYSICAL PROPERTIES OF ZIRCONIUM

Zirconium is a hard, malleable, silvery white metal with an atomic mass of 91.22 g/mol. It belongs together with titanium and hafnium to group 4 (IVb) of the transitional elements on the periodic table and its electron configuration is [Kr] $4d^2 5s^2$. In the oxidation process of the element, the four valence electrons are removed to different degrees to form zirconium compounds. The vacant and partially vacant d-orbitals of the metal play an important role in the formation of a large variety of compounds of zirconium. During the molecular formation, these d-orbitals split up into subsets due to ligand environments to form different types of orientation, e.g. octahedral and tetrahedral.[46] Research indicated that zirconium compounds exist in various coordination numbers ranging from coordination number of 4 to 8 (see **Table 1.3**).

Table 1.3: Examples of the coordination number of zirconium[47]

Coordination number	Examples
4	$ZrCl_4$; $Zr(SO_4)_2$
5	$NaZrCl_5$; $[(\eta^5\text{-}CpMe_4H)_2ZrH]_2(\mu^2, \eta^2, \eta^2\text{-}N_2H_2)$ where $CpMe_4H$ = Tetramethylcyclopentadienyl
6	K_2ZrF_6; $[(P_2N_2)Zr]_2(\mu^2, \eta^2, \eta^2\text{-}N_2)$ where $P_2N_2 = PhP(CH_2SiMe_2NSiMe_2CH_2)_2PPh)$
7	K_3ZrF_7; $[(P_2N_2)Zr]_2(\mu^2, \eta^2, \eta^2\text{-}N_2H)(\mu^2\text{-}H)$ where $P_2N_2 = PhP(CH_2SiMe_2NSiMe_2CH_2)_2PPh)$
8	Li_4ZrF_8; $Zr(acac)_4$

Research indicated that zirconium occurs in nature in five oxidation states, *viz.* Zr^0, Zr^{1+}, Zr^{2+}, Zr^{3+} and Zr^{4+} in different complexes. Most zirconium compounds contain the element at oxidation number of 4, *i.e.* Zr^{4+}, with the loss of 4d and 5s electrons to have [Kr].

[46] F.A. Cotton, G. Wilkinson and P.L. Gaus., *Basic Inorganic Chemistry*, 3rd ed., John Wiley and Sons, Inc, pp. 503 – 530 (1995)

The general oxidative behaviour of zirconium or its alloys is approximately the same, irrespective of the type of oxidant to which they are exposed.[48] In nature zirconium has five major isotopes, ^{90}Zr, ^{91}Zr, ^{92}Zr, ^{94}Zr and ^{96}Zr. The first four isotopes are said to be stable, whereas ^{96}Zr is the radioisotope of zirconium with half-life of 3.6×10^{17} years.[2] Of these natural isotopes, ^{90}Zr is the major isotope, constituting 51.45% of all zirconium and ^{96}Zr is the least, comprising only 2.76%.

There are two crystalline structures in which relatively pure zirconium exist (see **Figure 1.9**): namely i) as a hexagonal α-phase below 862 °C and ii) as a β-body-centred cubic phase above 862 °C. Research indicated that these crystalline phases are altered when some foreign elements are absorbed or included during its preparation. It is found, for example, that if sufficient amount of carbon or nitrogen are dissolved in the solid metal, it adopts a face-centred cubic symmetry, but should it be hydrogen or boron that is dissolved, other lattice types may form (see **Figure 1.9** (iii)).

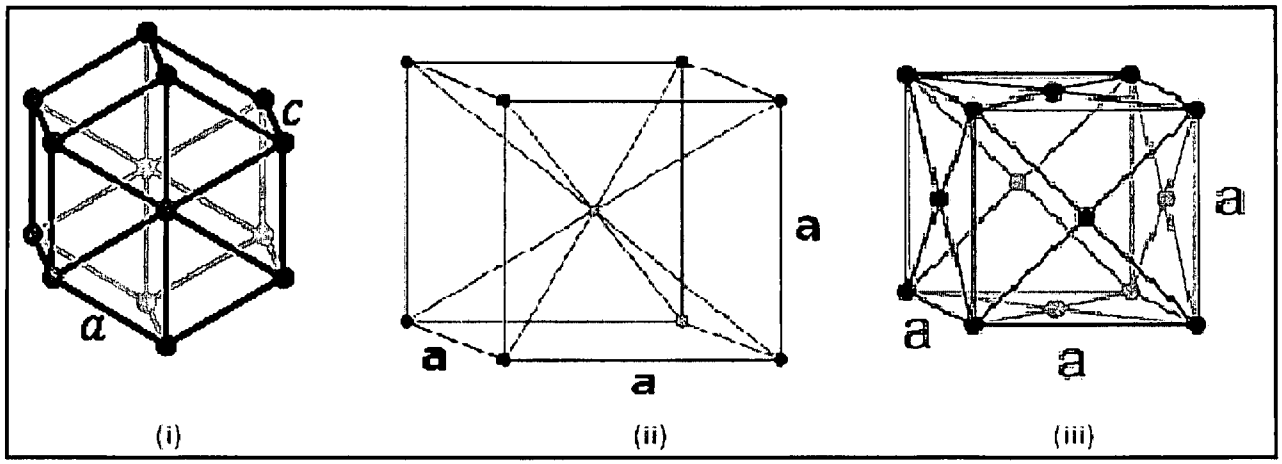

Figure 1.9: Different crystal lattices to which zirconium can conform (axes = a and c)[49,50,51]

Research also indicated that when oxygen is dissolved in significant proportions in both phases, it does not influence any alteration or the formation of other lattices of the element.

[47] T.E. Hanna., *Synthesis and Reactivity of Low-Valent Titanium and Zirconium Complexes: Dinitrogen Activation and Functionalization*, Ph.D. Dissertation at the Faculty of Graduate School of Cornell University, NY, USA (2007)

[48] R.A. Causey, D.F. Cowgill, and B.H. Nilson., *Review of the Oxidation Rate of Zirconium Alloys*, Engineered Materials Department and Nanoscale Science and Technology Department Sandia National Laboratories (2005)

[49] http://en.wikipedia.org/wiki/Hexagonal_crystal_system (23 March 2010)

[50] http://chemwiki.ucdavis.edu/Wikitexts/UCD_Chem_124A%3A_Kauzlarich/ChemWiki_Module_Topics/The_Unit_Cell (23 March 2010)

[51] http://www.threeplanes.net/images/Cubic-face-centered.png&imgrefurl (23 March 2010)

However, it considerably affects the physical and chemical properties of the element by decreasing its chemical activity and its malleability and increasing its hardness and melting point. These oxygen-induced properties may be regarded as quantitative rather than qualitative. It tends to stabilize the α-phase against the conversion to the β-phase. The initial zirconium metal prepared by Berzellius in 1824 contained about 6 – 7 % of oxygen.[16] This means that it would not have been ideal for working into shapes for structural use, but might have exhibited characteristic crystalline and chemical properties of zirconium, which would have subsequently qualified its acceptance for a preparation of the element in crude form. Zirconium slowly reacts with nitrogen compared to oxygen to form a layer of zirconium nitride at temperatures above 700 °C. The rate, with which the nitride layer is formed, is enhanced by the presence of oxygen in the nitrogen atmosphere or on the surface of the metal.

Zirconium metal is chemically inert and thus not easily digested by most mineral acids, organic acids orstrong alkalis. It is readily attacked by hydrofluoric acid or solutions containing fluoride ions, such as ammonium bifluoride, *etc.*[52] It is a very reactive metal at elevated temperatures, but due to the presence of its stable, cohesive and protective oxide layer in air or water at lower temperatures it acts as a very passive metal. In bulk, zirconium does not burn in air but it oxidizes rapidly at temperatures above 600 °C in air. In the presence of approximately 2 MPa oxygen pressure, clean zirconium metal ignites spontaneously but research indicated that the auto-ignition pressure lowers with the decreasing metal thickness. Zirconium powder readily ignites in an inert atmosphere during its preparation through the hydride-dehydride process when it gets in contact with air. Thus its surface has to be conditioned before its preparation by pre-oxidizing the powder with slow addition of air to the inert atmosphere.

Zirconium has a low capture for thermal neutrons making it less susceptible to react with other elements *via* nuclear collision. This means that the cross sectional area of its atom is not sufficient to capture neutrons during atomic collisions. In addition to its low thermal neutron absorption area, zirconium is quite resistant to damage by radiation and corrosion in pressurized water up to 350 °C.

[52] *Kirk-Othmer Enclopedia of Chemical Technology*, 3rd Ed., vol. 24, John Wiley and Sons, pp. 863 – 896 (1984)

1.3.1 AN OVERVIEW OF THE ZIRCONIUM HALIDES

Zirconium halides are used as the standard/certified reference materials (SRM/CRM) in the preparation or analysis of the zirconium metal and they are made up of numerous compounds of different types.[53] These include zirconium mono-, di-, tri-, and tetrahalides as well as their addition and substitution products in which some halogens are displaced or retained in the reaction medium. The chlorides, bromides and iodides of zirconium compounds chemically behave in a similar trend that they are usually treated as a group in their discussion; whereas the fluorides behave differently from the rest of the zirconium halides.[1] Therefore, when any of the three halogens (chlorine, bromine and iodine) is discussed, the other two are thus taken into consideration. Zirconium tetrachloride powder is quickly hydrolyzed in humid atmosphere and it dissolves completely and irreversibly in water. Thus in preparing zirconium and its alloys for cladding of fuel rods, the environment in which zirconium tetrachloride primary materials are reacted should be devoid of humidity and oxygen.

Several physico-chemical experiments have been carried out and applied to update and extend the knowledge of the thermodynamic properties of zirconium halides in various fields of science including chemical vapour deposition, nuclear engineering and metal refining. For instance, zirconium tetrachloride and tetrabromide are used as the primary reagents in preparing the chemical vapour deposited zirconium carbide layers of TRISO-coated fuel particles for High-Temperature Gas-cooled Reactors (HTGR).[53]

1.3.2 CHEMICAL AND PHYSICAL PROPERTIES OF ZIRCONIUM TETRAFLUORIDE (ZrF_4)

The chemistry of the fluorine compounds of zirconium is different from that of other halogen compounds (Cl, Br, I) primarily because of greater strength of the Zr-F bond and because of the smaller size of the fluorine atom, which permits a greater number of them to be bound to a zirconium atom.[1] This high Zr-F bond strength renders the compounds stable in water, whereas the other halogens are generally replaced from zirconium by water. In preparation of the metal from zirconium tetrafluoride, there is no need to have an inert atmosphere and humidity is not a factor to consider. Therefore, in developing methods of analysis for the

[53] M.G.M. van der Vis, E.H.P. Cordfunke and R.J.M. Konings., *Thermochimica Acta*, **302**, pp. 93 – 108 (1997)

zirconium metal, zirconium tetrafluoride is used as the most suitable standard material due to its similar characteristics to zirconium metal by being resistant to most mineral acids. The minute size of fluorine atom allow as many as 8 fluorine atoms to be bound to a single zirconium atom, and there are known compounds with 2, 3, 4, 5, 6, 7 and 8 fluorine atoms bound a zirconium atom, *e.g.* K_2ZrF_6 and Li_2ZrF_8.

Zirconium tetrafluoride is a colourless, crystalline solid. It has a monoclinic crystal lattice in which each zirconium atom is coordinated by 8 fluorine atoms in the form of a square Archimedean antiprism and each fluorine atom is coordinated by 2 zirconium atoms (see **Figure 1.10**).

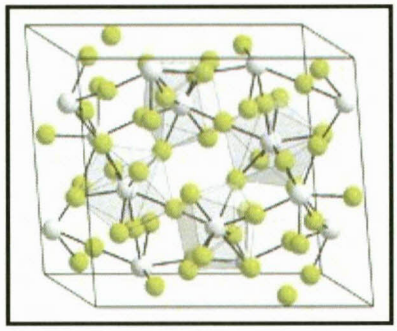

Figure 1.10: Monoclinic crystal lattice structure of zirconium tetrafluoride

When zirconium tetrafluoride is added to water, it is superficially hydrolyzed and only a small amount (~1.3 g/100 ml) goes into solution. The compound is readily dissolved by aqueous hydrofluoric acid and hot sulphuric acid.

A. *Methods for preparing zirconium tetrafluoride*

a) *Synthesis from the elements*[54]

$$Zr + 2F_2 \xrightarrow{>190^\circ C} ZrF_4 \qquad (1.6)$$

b) *Displacement of oxygen*[54]

$$ZrO_2 + 2F_2 \xrightarrow{525^\circ C} ZrF_4 + O_2 \qquad (1.7)$$

c) *Thermal decomposition of fluorozirconates*[55]

$$(NH_4)_2ZrF_6 \xrightarrow{<300^\circ C} ZrF_4 + 2NH_4F \qquad (1.8)$$

[54] H.M. Haendler *et al.*, *J. Am. Chem. Soc.*, **76**, pp. 2177 – 2178 (1954)

d) *Metathesis from the oxide*[54]

$$ZrO_2 + 4HF \xrightarrow{550^{o}C} ZrF_4 + 2H_2O \quad (1.9)$$

e) *Metathesis from zircon*[56]

$$ZrSiO_4 + 8HF \xrightarrow{\text{White heat}} ZrF_4 + 2H_2O + SiO_2 \quad (1.10)$$

f) *Metathesis from the tetrachloride*[56]

$$ZrCl_4 + 4HF \longrightarrow ZrF_4 + 4HCl \quad (1.11)$$

1.4 MOTIVATION OF THIS STUDY

1.4.1 THE GLOBAL NEED FOR ALTERNATIVE ENERGY SOURCE

The use of fossil fuel-based methods to produce energy has lately proved to be problematic to different societies, including governments and environmental-friendly organizations. The carbon-containing fossil fuels such as coal, crude oil (petroleum) and natural gas are converted into different end-products, which include refined oil (lubricants), petrol, diesel, paraffin, etc. These end-products are combusted daily to propel vehicles and used as energy to carry out various household chores, which in turn lead to the production of unwanted waste in the form of carbon dioxide, carbon monoxide, sulphur dioxide and nitrous oxide, among others. In other instances these natural resources are burned and the energy produced is used at power stations and converted into electricity.

The burning of fossil fuels globally produces around 21.3 billion metric ton of carbon dioxide per year, but it is estimated that natural processes can only absorb about half of that amount, so there is a net increase of 10.65 billion metric ton of atmospheric carbon dioxide per year.[57] **Figure 1.11** depicts a power plant in Scotland for the refining of petrochemicals, which contribute to greenhouse gas in the atmosphere.

[55] G. Von Hevesy and W. Dullenkopf., *Z. Anorg. Allgem. Chem.*, **221**, pp. 161 – 166 (1934)

[56] C. Woolf., US Patent **2,805,121**, (03 Sept. 1957)

[57] http://en.wikipedia.org/wiki/Fossil_fuel (20 May 2011)

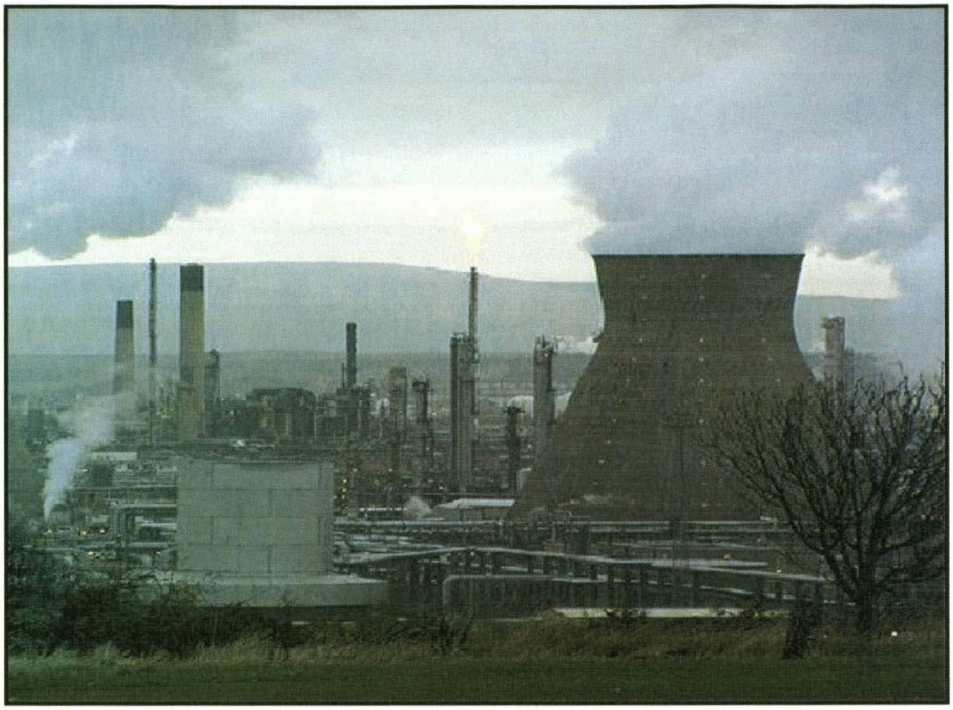

Figure 1.11: A petrochemical refinery in Grangemouth, Scotland, UK[58]

In 2007, South Africa was listed as the 13th largest carbon dioxide emitting country in the world and the largest in Africa.[59] This was mainly due to the burning of coal for electricity generation and on which the country had mainly relied since 1950. Consequently it has experienced a seven-fold increase in fossil fuel CO_2 emissions with 80 – 90 % emissions from coal. It is estimated that in 2007, 85% of South Africa's fossil-fuel CO_2 emissions of 118 million metric tons of carbon were from coal, another 11.5% were from oil consumption, and the remainder was from cement manufacture and natural gas and coke-oven gas consumption. Another factor that contributes to the search for alternative energy source is the steep rising of oil prices that led to many countries reducing their consumption of crude oil and thus lesser CO_2 emissions. Apparently it had little impact on South African fossil-fuel CO_2 emissions as indicated by the annual trend of carbon emissions in South Africa from various activities as shown in a graph in **Figure 1.12**.

[58] http://en.wikipedia.org/wiki/Image:Grangemouth04nov06.jpg (20 May 2011)

[59] T.A. Boden, G. Marland and R.J. Andres., *Global, Regional, and National Fossil-Fuel CO_2 Emissions.*, Carbon Dioxide Information Analysis Centre, Oak Ridge National Laboratory, U.S. Department of Energy, Oak Ridge, Tenn., U.S.A. (2010)

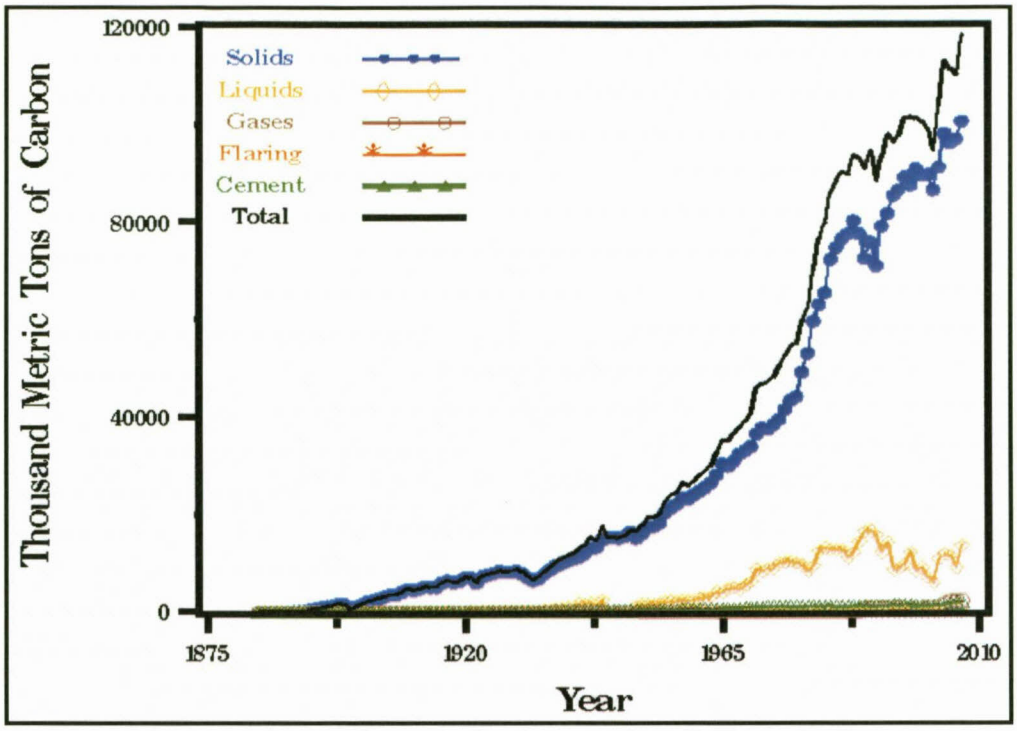

Figure 1.12: Carbon emissions annual trend in South Africa[59]

The increase in greenhouse emissions is partly due to anthropogenic pollution and this has been extrapolated by environmental groups to consequently affect the earth's climate changes. Assessment done by the National Research Council in 2001 concluded that the greenhouse gases emitted over the past century were as a result of human activity affecting the atmosphere, causing surface air temperatures and subsurface ocean temperatures to rise.[60]

Production of electricity by power plants is also one of the main reasons for the cause of carbon emissions. According to Environment Canada in 2007, the electricity sector is unique among the industrial sectors worldwide in its enormous contribution to emissions associated with nearly all atmospheric issues. Electricity generation produces a large share of Canadian nitrous oxides and sulphur dioxide emissions, which contribute to smog, acid rain and the formation of fine particulate matter. Electric power plants that are operating on fossil fuel also emit carbon dioxide, which may contribute to climate change. In addition, the sector has significantly impacted on land and water habitats and the living organisms found in them. In particular, hydro dams and transmission lines have significant effects, such as influencing the

[60] National Research Council, *Climate Change Science: An Analysis of Some Key Questions*. National Academy Press, p. 29 (2001)

quality of water and biodiversity.[61] Even though that is the case, power plants on a daily basis have to supply constant and alternative minimum amount of energy to their customers to meet minimum demands based on reasonable requirements of the customer.[62,63] This minimum alternative energy is known as base load electricity, which can be provided by nuclear energy, hydroelectric, bio-energy, *etc.*, in substitution of coal-fired electricity.

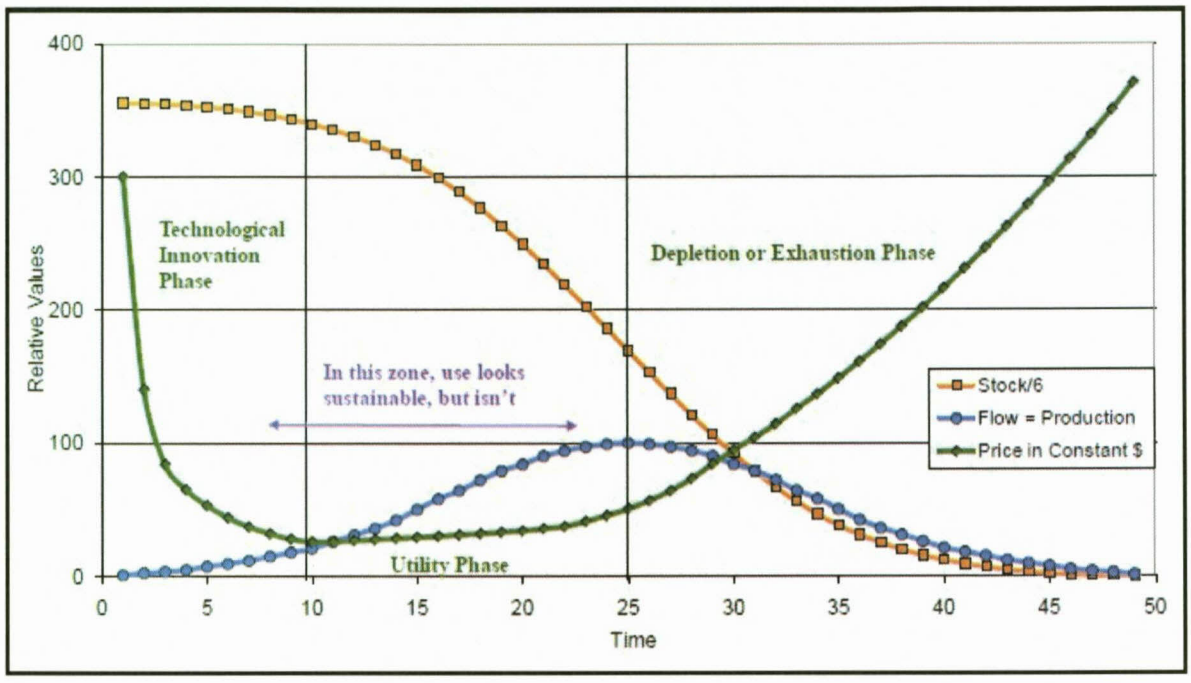

Figure 1.13: General model for non-renewable resource with high demand and no substitute[64]

In **Figure 1.13**, stock was divided by 6 so as to visually expand the scales of both production and price. As stocks are used and consistently depleted, the production rises to a peak and plateaus for a while before it drops. The price depicts the manner in which humans respond to the biophysical process. During technological innovations, newly developed methods are applied to manipulate a natural resource, leading to the rapid drop in price of a commodity. A period of perpetual low prices, known as the utility phase, follows and the use of a natural resource is seemingly sustainable. However, this sustainability is not conclusive because the documenting of resource stocks is difficult and done mainly by inference from estimated reserves.

[61] http://www.ec.gc.ca/ges-ghg/archives (10 May 2011)

[62] http://en.wikipedia.org/wiki/Base_load_power_plant (19 Aug 2011)

[63] http://www.energyscience.org.au/BP16%20BaseLoad.pdf (19 Aug 2011)

[64] http://snre.ufl.edu/pubsevents/humphrey.htm (06 June 2011)

Finally, the period of depletion or exhaustion is phased in, with prices surging high and presenting difficult challenges when the demand outweighs the supply for the commodity.

Fossil fuels are non-renewable energy resources which take long periods of time to form and the natural reserves are being depleted at a faster rate than the new ones are being formed. In 1956 Hubbert made predictions by using the peak theory on production rates based on prior discoveries and anticipated oil projections.[65] He presented his publication by explaining the long periods it took to produce fossils to be about 500 million years and the rate at which they are being depleted from the recent history. His research led to American Petroleum Institute (API) estimating, in 1999, the world's supply of oil to be depleted between 2062 and 2094.[66] The high demand of natural fossil fuels for the generation of energy led to their high prices and making them expensive, thus putting financial strains on the worldwide economic climate as well as on government fiscus to acquire them.

Crude oil prices have been steadily rising over the past decade (see **Figure 1.14**). This trend has been perpetuated by the demand for this commodity during the season of winter, when more electricity is needed to fend the cold temperatures. The main producers of this commodity are put under strain to supply the growing demand in the world, and therefore the volume required on the market becomes lesser than that supplied. In mid-2008, the spot price of crude oil underwent a significant increase to peak at the record high of US$145/barrel before it subsided to about US$30/barrel by the end of the same year.

Besides the high demand for crude oil, civil unrests in the oil-producing countries, e.g. Egypt, Tunisia, Yemen, Iraq etc., aggravated the situation in contributing to the rise of this commodity. Earlier in 2011, the spot price of crude oil hit US$100/barrel for the first time since October 2008.[67]

[65] M.K. Hubbert., *Nuclear Energy and Fossil Fuels,* American Petroleum Institute, Shell Development Co., Pub. 95 (1956)

[66] American Petroleum Institute, *Popular Science* (1999)

[67] http://www.bbc.co.uk/news/business-12328745 (06 June 2011)

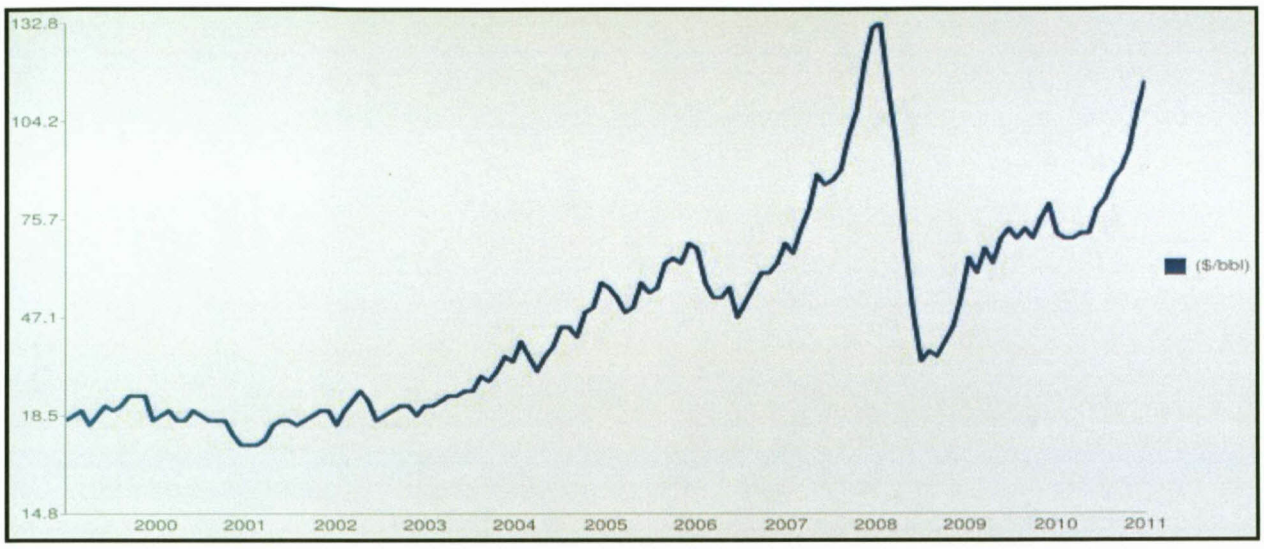

Figure 1.14: Chart of the average spot price per barrel for crude oil over the past decade[68]

About the same time – early 2011 – as the crude prices were on the rise, coking coal prices were also surging. The spot price for coking coal in Australia exceeded US$300/metric ton and the market experts predict it to hit US$400/metric ton later in the year. The reason behind this increase was primarily based on the flood in Australia that hampered the supply of coking coal to the global market.[69]

One other reason for the increase in spot prices of coking coal is the low stock levels available on the market. The production in the USA – considering the output from the state of West Virginia – stood below 119 million metric tons in the last quarter of 2010, whereas in 2009 the production was 120.5 million metric tons. For the historic price trend of the coking coal since 1996, see **Figure 1.15**. These high and unpredictably fluctuating prices of coal and crude oil, together with the polluting tendencies of these commodities, calls for the need to have alternative energy sources, which are affordable & highly effective than fossil-fuels.

[68] http://www.mongabay.com/images/commodities/charts/crude_oil.html (06 June 2011)

[69] http://paguntaka.org/2011/01/29/chinese-domestic-coal-prices-stable-and-coking-coal-prices-continue-to-rise/ (06 June 2011)

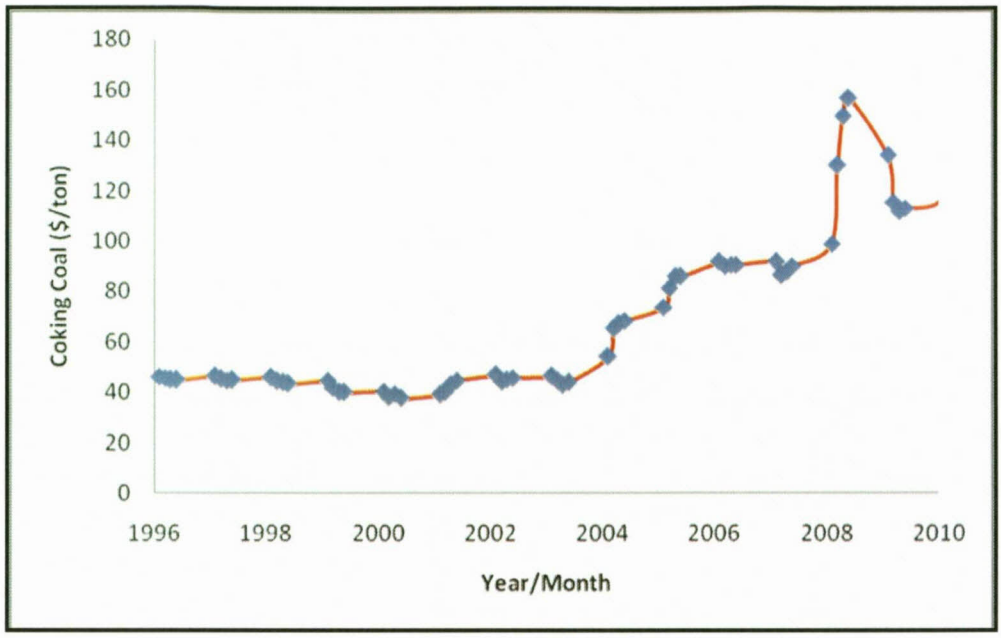

Figure 1.15: Chart of the average quarterly prices for coking coal per short ton since 1996 (adapted to a graph from the supplied data)[70]

The production and use of fossil fuels raise environmental concerns and there is a global movement toward the generation of alternative renewable energy sources to help meet increased needs for energy.

Before alternative energy becomes main-stream there are a few critical objectives that it must achieve: First there must be increased understanding of how alternative energies work and why they are beneficial; secondly the availability components for these systems must increase, as well as be relatively affordable to acquire on the market; and lastly the pay-off time must be decreased. Several methods for the generation of renewable energy have been used in South Africa as alternative sources to fossil fuels. These include – among others – solar, wind, tidal and nuclear powers as well as hydroelectricity and biomass energy.

Of all these alternative sources, the nuclear power generates the most energy, and it is has been described as the most viable alternative to fossil fuels. Nuclear power is favourable as it is much more efficient than coal in producing energy; 250 g of uranium produces 20000 times more electricity than 250 g of coal.[71] With so much energy produced by nuclear reactions, it is beneficial in that it does not result in any of the harmful gasses associated with

[70] http://www.steelonthenet.com/files/metallurgical_coal.html (06 June 2011)

[71] http://library.thinkquest.org (20 May 2011)

fossil fuels and consequently it does not lead to air pollution. Nuclear waste is small in quantity compared to that produced by fossil fuels, and it is disposed off to confined geological areas where it degenerates with time and does not affect the environment. Nuclear power is a very reliable source of energy since the nuclear reactors have life cycles of about 40 to 60 years.[72] One other advantage of the nuclear energy is that it is competitively available as compared to other energy sources like oil and gas since the nuclear fuel costs are lesser and the market fluctuations need not affect its price. The historical uranium spot prices are given in **Figure 1.16**.

The main disadvantage regarding the use of nuclear energy is safety. Nuclear power plants have to be built in a way which will render them indestructible and safe. Thus, they have to withstand different kinds of catastrophes, such as natural disasters – including earthquakes, hurricanes, flooding by water, etc. and human accidents – including arson, explosive reactions etc. The major nuclear energy disasters that are recorded so far are the human error that took place in Chernobyl, Ukraine in 1986 and the natural catastrophe in Fukushima, Japan in 2011. In Chernobyl, an explosion occurred during the testing of systems when an emergency shutdown was attempted after a sudden increase in power output, leading to a rupture of vessel reactor.[73] The Fukushima disaster was due to the earthquake, which was followed by the tsunami. The walls of the Daiichi nuclear plant were built to handle about 6 metres of a tsunami and therefore could not withstand the 14 metre tsunami wave that struck on the 11th day of March 2011.[74] A smaller scale nuclear disaster happened near Middletown, Pennsylvania (USA) in 1979 at the Three Miles Island Unit 2 (TMI-2) nuclear power station. The accident occurred when what is believed to either be an electrical or mechanical failure, prevented the heat from being removed by the steam generators.[75]

Regardless of all these misfortunes, nuclear energy seems to be supported by most environmental groups because no harmful gasses are emitted in the process and as long as the people are well informed about radiation and the accidents are minimized.[72] The effect of Pennsylvanian disaster was considered small because the authorities reacted quickly to

[72] http://www.benefitsofnuclearpower.com/ (10 June 2011)

[73] http://en.wikipedia.org/wiki/Chernobyl_disaster (10 June 2011)

[74] http://en.wikipedia.org/wiki/Fukushima_nuclear_accident (10 June 2011)

[75] http://www.nrc.gov/reading-rm/doc-collections/fact-sheets/3mile-isle.html (10 June 2011)

contain the small radiation released and the area about a radius of 5 miles from the point of the accident was affected, whereas the Chernobyl & Fukushima disasters were of a large scale because areas of more than 50 km radius were affected.

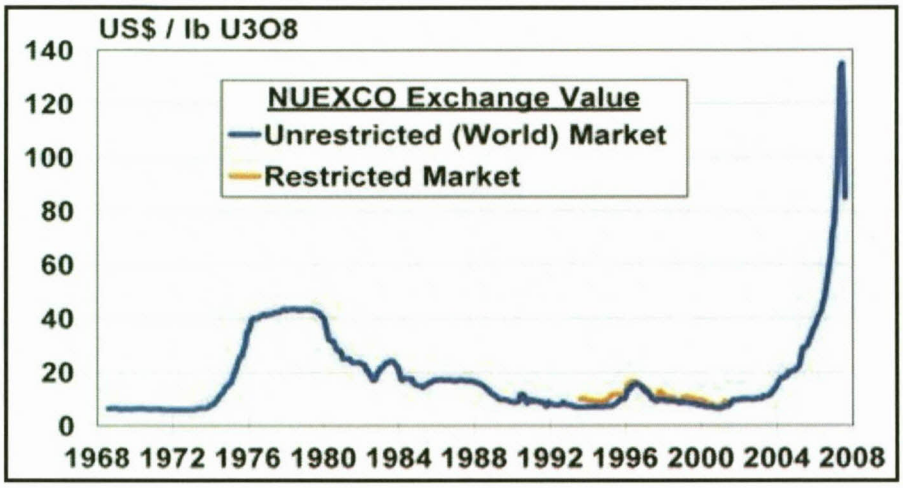

Figure 1.16: A graph of historical spot prices for uranium[76]

When the energy is generated during a nuclear reaction, much care is taken that there is little or no interference with the reaction from the surroundings , which may have undesired effects, such as explosions or neutron absorption, by also taking part in the reaction. The manufacturing of arcs and fuel rods for nuclear power stations necessitates that the components be utterly inert to the nuclear reactions in order to be the most efficient and effective industry. An example of a nuclear power plant is depicted in **Figure 1.17**.

[76] http://www.uranium-stocks.net/uranium-spot-price-85lb/ (10 June 2011)

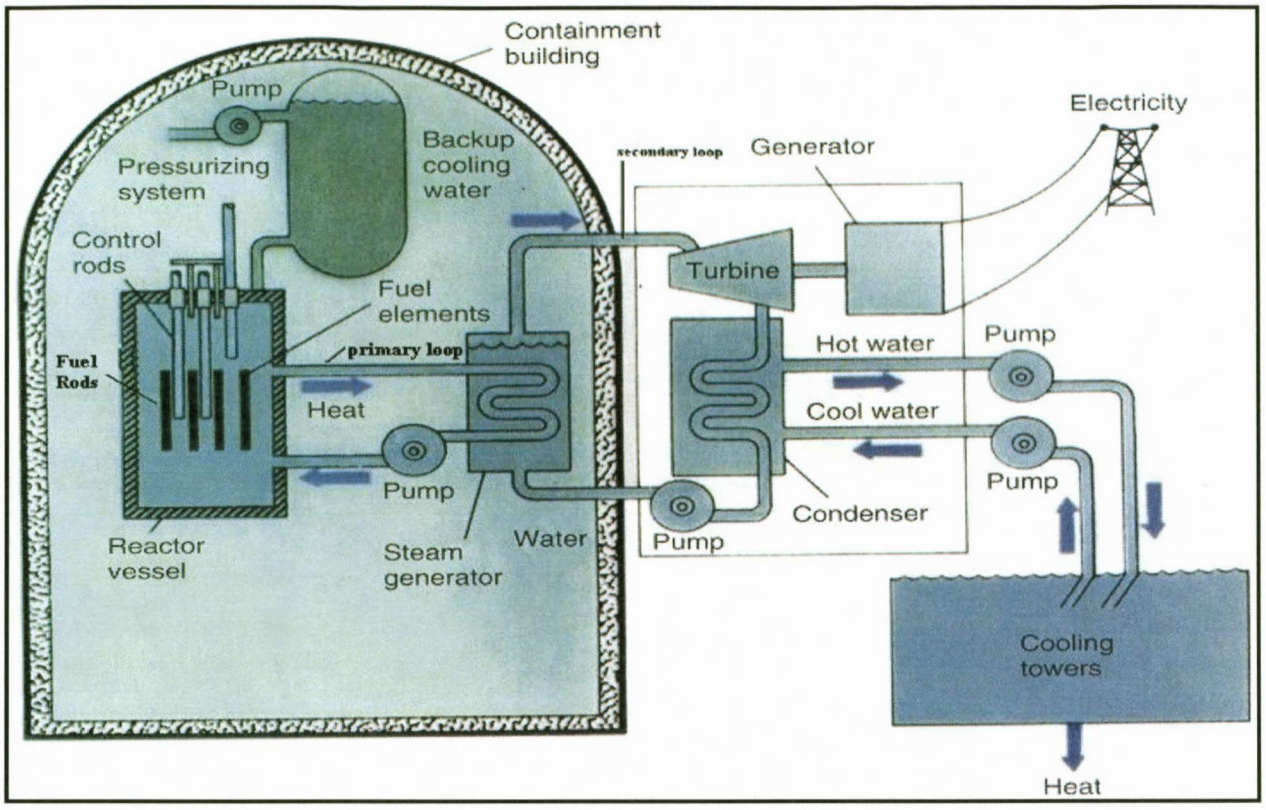

Figure 1.17: A schematical diagram of a nuclear power plant[77]

1.4.2 ZIRCONIUM IN THE NUCLEAR INDUSTRY

Zirconium as element or metal is considered to be extremely important in the nuclear industry for the aligning of nuclear arcs due to its chemical resistance, hardness and low thermal neutron capture cross section, which does not interfere in the nuclear reactions within these arcs and thus making it extremely effective to be used in this industry. It has to be extremely pure (>99 %) and devoid of the elements, such as boron, cadmium, hafnium, *etc.*, which render it unusable as cladding for fuel rods. The specifications for a nuclear grade zirconium are given in **Table 1.4**.

[77] http://electricalandelectronics.org/ (20 May 2011)

Table 1.4: Chemical requirements of zirconium sponge, reactor grade R60001[78]

Element	Thermal Neutron Capture (barns)	Permissible Impurities (ppm_{max})
Aluminium	0.232	75
Boron	767	0.5
Cadmium	2450	0.5
Carbon	0.0035	250
Chlorine	35.5	1300
Chromium	3.1	200
Cobalt	37.2	20
Copper	3.78	30
Hafnium	104	100
Iron	2.56	1500
Manganese	13.3	50
Molybdenum	2.6	50
Nickel	4.49	70
Nitrogen	1.91	50
Oxygen	0.00019	1400
Silicon	0.171	120
Titanium	6.09	50
Tungsten	18.3	50
Uranium	7.57	3.0

All the elements specified in the table above have negative effects – at concentrations above those permitted – on zirconium by making it hard and brittle at high temperatures associated

[78] *Standard Specification for Zirconium Sponge and Other Forms of Virgin Metal for Nuclear Application*, ASTM International, Designation: B 349/B 349M – 03

with the production of nuclear energy and due to their high thermal neutron absorption cross sections. A recommended method for calculating the equivalent boron content (EBC) values for natural elements is used to provide a measure of the macroscopic neutron absorption cross section of a nuclear material.[79] These values are determined from their atomic masses and barns (thermal neutron absorption cross sections). The most important of all these elements are boron, cadmium and uranium. Boron and cadmium (767 and 2450 barns, respectively) have the highest atomic absorption cross-sectional area for the neutron capture and therefore the requirement to be at the lowest impurity permitted in the nuclear grade zirconium. As discussed earlier in the last paragraph of **Section 1.4.1**, there should be no interference with nuclear reactions from the environment and therefore uranium must be kept at the specified level in the zirconium aligning the arcs so as not to take part in the reaction.

Several techniques have been developed and validated to investigate the quality of zirconium in the nuclear industry in order to determine the amount of these elements left in the purified zirconium. These techniques include, among others, absorptiometric, volumetric, gravimetric, conductimetric, amperometric procedures[80], atomic absorption (AA), ICP-OES and ICP-MS. All these analytical techniques require the zirconium metal to be in solution before being carried out in determining the trace elements. In the previous projects done to investigate the impurity elements within zirconium metal sample, hydrofluoric acid is the common mineral acid of choice to digest the metal and dissolve it into the solution. Other mineral acids including, among others, sulphuric, hydrochloric and nitric acids have been used in conjunction with hydrofluoric acid.

1.4.3 IMPORTANCE OF ZIRCONIUM TECHNOLOGY IN SOUTH AFRICA

Due to the increasing need for the electricity in the country, the South African government seems to be strongly committed to invest in the future of the nuclear energy.[81] In her budget speech in May 2011, energy minister Dipuo Peters supported and projected the use of nuclear energy in electricity production to 22.6 % by 2030 from the draft Integrated Electricity

[79] *Standard Practice for Determining Equivalent Boron Contents of Nuclear Materials*, ASTM International, Designation: C1233 - 09

[80] W.T. Elwell and D.F. Wood., *The Analysis of Titanium, Zirconium and Their Alloys*. John Wiley & Sons Ltd (1961)

[81] http://www.world-nuclear.org/info/inf88.html (01 July 2011)

Resource Plan (IRP2010).[82] This means that South Africa has to build 5 more 1200 MW nuclear reactors by 2030. The energy department allocated R586 million to Necsa in 2011 for research, development and innovation in nuclear energy. In developing the nuclear industry in the country to meet the demand for electricity, one of the projects Necsa is engaged in is to develop methods of producing the pure zirconium needed to clad the nuclear fuel reactors.[83] This project is funded *via* support from the Advanced Metals Initiative (AMI) from the Department of Science and Technology (DST). These methods have to be economical, environmentally friendly, *etc.* to suit the scope for the development of nuclear industry in South Africa.

Zirconium is mined as zircon ore from Namakwa Sands in the Western Cape and Richards Bay in Kwazulu-Natal, South Africa.[84] The ore is exported in bulk to the world *via* Saldanha Bay, Richards Bay and Cape Town after being certified by ISO 17025:2005-accreditted laboratories. The annual export turnover is valued atUS$ 400 million for 400 kilotons.[85] There are no refineries of zirconium in South Africa to produce a pure nuclear grade zirconium metal. Thus when the pure zirconium sponge is imported back into the country, the value is more than when the ore was exported.[86] In 2010 the value of zirconium sponge was US$ 20769.23 per metric ton, thus making the importing of the metal much more expensive than exporting the ore.[86] When the annual turnover is deduced to simple units, the zircon ore costs US$ 1000 per metric ton and then there would be left a difference of more than US$ 19000 when the pure zirconium is resold on the global market. If this remains the operational status in the financial markets in regards to zirconium, it would then be very expensive to run a nuclear industry in South Africa.

However, for South Africa to have a viable and independent nuclear industry, it is vital that it invests more money into research for the purification of zirconium metal within its borders. If zirconium can be produced and purified in the country, nuclear energy will be generated at a lower cost than if the metal was to be imported for nuclear purposes. The path used to refine

[82] http://www.polity.org.za/article/sa-peters-budget-speech-by-the-minister-of-energy-in-the-national-assembly-26052011-2011-05-26 (01 July 2011)

[83] http://firemailer.firewater.net/ami/pages/content.asp?PageID=4 (01 July 2011)

[84] http://www.westerncapebusiness.co.za/pls/cms/ti_company_search.company_display_province?p_c_id=1844&p_site_id=127 (01 July 2011)

[85] http://www.southafrica.info/business/investing/refinery-190210.htm (01 July 2011)

[86] http://www.metalnewsnet.com/Zirconium/76mCAr6h12592MM6.html (01 July 2011)

raw mineral materials to useful industrial components is known as mineral processing. In this process, four main steps are followed to purify zirconium from its ores. These steps involve characterization, liberation, separation and disposition.[87] In the characterization step the mineral is identified and the components are elucidated to determine their chemical makeup and physical properties. When this is accomplished, all the elemental components are released in the liberation step into their basic atoms. In the third separation step, zirconium is pre-concentrated and the metal is produced and isolated by purification for nuclear purposes. The final step of disposition is the removal of waste in an environmentally friendly manner and the sale of the products.

Pure zirconium metal is not used as such in a nuclear reactor. It is further alloyed as a component in different zirconium alloys (Zircaloy-2, Zircaloy-4, *etc.*) which are advantageous in the disposal of nuclear waste due to excellent radiation stability and resistance to corrosion. [88] See **Table 1.5** for composition of different zirconium alloys.

Table 1.5: Composition (weight %) of zirconium alloys[88]

Name	Zircaloy-2	Zircaloy-4	Zr-2.5Nb
UNS Grade	R60802	R60804	R60904
Tin	1.20 – 1.70	1.20 – 1.70	-
Iron	0.07 – 0.20	0.18 – 0.24	-
Chromium	0.05 – 0.15	0.07 – 0.13	-
Nickel	0.03 – 0.08	-	-
Niobium	-	-	2.40 – 2.80
Oxygen	Per P.O.	Per P.O.	Per P.O.
Iron + Chromium + Nickel	0.18 – 0.38	-	-
Iron + Chromium	-	0.28 – 0.37	-

P.O. – processed ore

[87] http://www.scribd.com/doc/29463079/Mineral-Processing (05 July 2011)

[88] http://www.wahchang.com/pages/products/data/pdf/Zr_Alloys (19 Aug 2011)

In this project, within the bigger scope of mineral processing, the main purpose is to develop analytical techniques to be able to accurately analyze locally produced zirconium and hopefully nuclear grade material for impurities in the characterization step to ensure its adherence to the strict specification as outlined in **Table 1.4**. It is therefore imperative to develop and validate an alternative method to that of hydrofluoric acid and employ it in digesting the zirconium metal samples and analyzing the impurity elements at the low level specification that is needed for the zirconium to be used in the nuclear industry.

1.5 OBJECTIVES

The purpose of this study is to:

a) Develop an alternative digestion method for zirconium metal and zirconium tetrafluoride samples for the analysis of their impurity elements; zirconium tetrafluoride is used as is or converted to zirconium hexafluoride to develop as the RM (reference material)

b) Develop effective and efficient analytical method for the multi-element quantification of zirconium and its impurities in ultra-pure nuclear grade metal samples at different levels of concentration (at threshold and a 1/10 of threshold) by using commercially available equipment such as ICP-OES

c) Identify and compare the different analytical techniques, with much emphasis on the recent and modern technique such as ICP-OES

d) Determine LOD/LOQ for zirconium and its associated impurities for nuclear purposes

e) Perform method validation on these analytical methods

f) The physical evaluation of the most relevant and promising analytical methods using pure standards in the mentioned technique

2 LITERATURE REVIEW ON METHODS OF ANALYSIS FOR ZIRCONIUM AND ITS ASSOCIATED IMPURITIES

2.1 INTRODUCTION

The importance of zirconium in the nuclear industry was first realized in 1947 when the then US Navy Captain H.G. Rickover saw the advantage of using enriched uranium reactors in ships.[89] He realized that zirconium would be ideal to be used as cladding in navy nuclear reactors since the metal does not absorb neutrons (low cross section). It was therefore necessary to obtain extremely pure zirconium metal with the most important object its separation from hafnium, which has a relatively high neutron cross section. His team began their work in 1949 at the US National Security Complex, Y-12, by attempting to separate zirconium from hafnium by using a calutron. A calutron, which is very similar to a cyclotron, is a mass spectrometer used to separate uranium isotopes, but was adopted to try and separate zirconium and hafnium from one another. However, this method proved to be very harmful to the environment due to the presence of a combination of reagents like carbon tetrachloride, sulphuric acid, nitric acid, hydrochloric acid and phosgene. The combination of these chemicals and the physical environment corroded the equipment and the health of some of the team members was adversely affected.

Besides hafnium, there are other elements which are detrimental to the performance of the nuclear grade zirconium. These elements (mentioned in section **1.4.2, Table 1.4**) are permissible at thresholds specified to render zirconium viable for nuclear application. Various analytical methods have been developed over the years to quantify the different elements in zirconium. They include, among others, gravimetry, colorimetry and spectrometry. In order to perform these analytical techniques on zirconium, its alloys, ores and their impurities, it is

[89] http://www.y12.doe.gov/library/pdf/about/history/08-11-06.pdf (20 June 2011)

necessary to get these samples into solution. Several digestion techniques have been explored and applied, to varying successes, in dissolving zirconium samples. They include flux fusions involving soda ash, borax, acid digestions as well as bench-top and microwave-assisted digestions with various acids, salts and the combinations of these. The purpose of this chapter is to give a general overview on research done on the dissolution and analysis of zirconium, its alloys, ores and impurities. The discussion will also highlight the most suitable methods to be employed in the pursuit of developing or improving the analytical methods of determining impurities in nuclear grade zirconium.

2.2 METHODS OF DIGESTION

The protective layer of oxide on the surface of zirconium enhances the resistance of the metal from being attacked by most acids.[51] Besides being able to be digested by hydrofluoric acid, zirconium metal has been proven to be dissolved by alkali melts containing the fluoride ion[90], *e.g.* fluoride salts of sodium, potassium, *etc.* Other alternative methods to HF digestion involve the dissolution by mixtures of mineral (perchloric, nitric and hydrochloric) acids, fluxes and microwave-assisted digestion using various reagents.[90]

2.2.1 DIGESTION WITH BORAX

P. Gaines[90] made a number of recommendations for the digestion of zirconium and hafnium when borax (sodium tetraborate, $Na_2B_4O_7$) is used as fluxing agent. These recommendations included the use of platinum crucibles above those made of graphite and silver. He also recommended that the flux be added to the crucible before a sample ore and melted to coat the walls of the crucible by swirling. After cooling, the sample should be added after the lining process and fused at temperatures of 1050 – 2000 °C for 30 minutes or until a clear viscous melt is observed. He also recommends mixing by swirling during and after the heating to make the dissolution of the flux easier. The flux is finally dissolved using a mixture of nitric acid, water and hydrofluoric acid, however the presence of any insoluble fluoride products requires an alternative mixture of water and hydrochloric acid to facilitate complete dissolution.

[90] http://www.inorganicventures.com/tech/sample-preparation/zirconium-hafnium (20 June 2011)

In determining the concentration of zirconium and its impurities in zirconium ores, Lundell and Knowles[91] developed a digestion method for zirconia using borax in the same fashion as advised by Gaines.[90] Their technique involved a gravimetric analysis that made use of cupferron as a precipitant in an acidic medium

$$ZrO_2 + 4cupf^- + 4H^+ \longrightarrow Zr(cupf)_4 + 2H_2O \qquad (2.1)$$

They obtained very accurate recoveries of zirconium, titanium and rare earth metals following their standard additions of zirconia and titanium dioxide to a rock sample under investigation. An excerpt of the results from their publication is shown in **Table 2.1**.

Table 2.1: Analyses of zirconium and titanium in diorite rock

Exp.	Cupferron added (g)	Weight added (g)		Weight recovered (g)	
		ZrO_2	TiO_2	ZrO_2	TiO_2
1	0.2129	0.2096	0.0034	0.2090	0.0039
2	0.2192	0.2151	0.0042	0.2149	0.0043
3	0.2212	0.2151	0.0042	0.2152	0.0044
4	0.2235	0.2151	0.0043	0.2153	0.0043
5	0.2234	0.2151	0.0043	0.2153	0.0043

The above results show that the analysts developed an efficient method for the determination of zirconium and titanium in rocks using borax as a flux reagent. The average percentage recovery for zirconia and titanium dioxide were 99.97 % and 104.2 %, respectively. However, it is a tedious and expensive procedure which takes almost 2 days to complete involving many steps and reagents to separate the elements under investigation.

2.2.2 DIGESTION BY PEROXIDE

Gaines[90] also recommended the use of sodium peroxide as the flux reagent in the zirconium digestion. A portion of the sample ore is mixed with an excess amount of sodium peroxide in

[91] G.E.F. Lundell and H.B. Knowles., *J. Am. Chem. Soc.*, **42** (7), pp. 1439 – 1448 (1920)

a nickel crucible that has been pre-treated with sodium carbonate. The process of lining the walls of the crucible with sodium carbonate is necessary to protect the crucible against attack from the peroxide. The fusion reaction is allowed to take place for about 5 to 10 minutes at dull red heat over a small flame. After the fusion, the reaction mixture is cooled and the crucible is transferred to a large container – either of platinum or porcelain – and immersed under warm water. The container is covered with a watch glass and heated to boil until the carbonate lining has dissolved. After boiling, the crucible is removed, cooled and the fusion melt is acidified by adding 10 % or more concentrated hydrochloric acid. The resulting solution is boiled to expel carbon dioxide and the consequent products are analysed for the content of constituents, including zirconium.

The method for the hydrogen peroxide digestion of different zirconium-containing alloy steels was developed by Cunningham and Price[92] to quantify zirconium. The samples were first treated with concentrated hydrochloric acid. Zirconium was precipitated out of the digested material as a phosphate, $Zr(HPO_4)_2$, by using diammonium phosphate, weighed off and the mass divided by the weight of the sample taken. **Table 2.2** shows the results obtained by these analysts.

Table 2.2: Determination of zirconium in steel

Exp	Kind of Steel	Mass Steel Taken (g)	Zirconium Added (g)	Zirconium Found (g)	Error (g)
1	Plain C	10	0.00047	0.00045	-0.00002
2	Plain C	10	0.00094	0.00093	-0.00001
3	Plain C	5	0.00450	0.00455	+0.00005
4	CrWV[a]	5	0.00235	0.00234	-0.00001
5	CrWV[a]	10[b]	0.00094	0.00090	-0.00004

[a] – Standard sample 50 A from the Bureau of Standards

[b] – Two 5 gram portions were taken and the precipitate combined after using sodium carbonate fusion to separate the tungsten

This digestion technique proved to be efficient in quantifying zirconium in various zirconium-containing alloy steels. The procedure spans about 30 – 45 minutes to complete depending

[92] T.R. Cunningham and R.J. Price., *Ind. Eng. Chem. Anal. Ed.*, **5** (5), pp 334–335 (1933)

on the time taken to eliminate carbon from the filter paper at red heat. It involves the reduction of iron with sodium sulphite so as to be soluble while the zirconium phosphate precipitates from the reacting mixture. Further success of this method lies in determining the titanium content by colorimetry before determining the content of zirconium without interference.

2.2.3 DIGESTION BY CARBONATES

In their preparations and study of zirconates, Venable and Clarke[93] used sodium and potassium carbonate salts to fuse zirconia. The alkali metals were then leached with water and the remaining fused zirconium was dissolved with dilute hydrochloric acid and heated to precipitate as an hydroxide. Quantification results from this study indicates that the fusion of the zirconium with varying amounts of sodium carbonate for long periods were less satisfactory as indicated in **Table 2.3**.

Table 2.3: Fusions of zirconia using sodium carbonate flux

Amount of ZrO_2 added (g)	Amount of Na_2CO_3 added (g)	Amount of fused ZrO_2 (g)	ZrO_2 Recovery (%)	Fusion Time (hrs)
2.000	8	0.1588	7.94	3
2.000	16	0.3042	15.21	4
2.000	16	0.1220	6.1	8

The above results show that time and the increasing amounts of sodium carbonate flux do not improve the digestion of zirconia. They reported that the amount of unfused zirconia ranged from 85 – 94 %. Thus this method cannot be deemed efficient to use in quantifying zirconia. The fusion of zirconia with potassium carbonate was even worse than that of sodium carbonate in that no significant amounts of fused product were recovered from the reaction mixture for analysis.

Okai[94] compared the efficiency of acid digestion to alkali fusion in determining the zirconium content in six carbonate rocks by spectrophotometric analysis using xylenol orange. For the

[93] F. P. Venable and T. Clarke., *J. Am. Chem. Soc.*, *18* (5), pp. 434–444 (1896)

[94] T. Okai., *J. Geostand. Geoanal.*, **21** (1), pp. 97 – 99 (1997)

acid digestion method he employed the acid combination ($HNO_3/HClO_4/HF$) while he employed sodium carbonate to fuse the rock samples and digested them with the acid combination. To minimize the interference of calcium in the quantification of zirconium Okai added calcium in the blank solution. Both the acid digestion and sodium carbonate fusion were performed on 0.3 g of powdered samples and the results obtained for the zirconium determinations are shown on **Table 2.4**.

Table 2.4: Comparison of results for zirconium in six carbonate rock reference materials by different dissolution methods

Sample	Acid digestion (µg/g)[a]	Alkali fusion followed by acid digestion (µg/g)
JDo-1 (dolomite)	3.5 ± 0.4	3.7 ± 0.2
JLs-1 (limestone)	2.4 ± 0.3	2.3 ± 0.5
SRM-1c (argillaceous limestone)	11.0 ± 0.7	23.6 ± 3.0
SRM-88a (dolomitic limestone)	2.7 ± 0.7	3.0 ± 0.6
BCS-368 (dolomite)	4.1 ± 0.6	4.4 ± 0.2
BCS-393 (limestone)	2.4 ± 0.3	2.5 ± 0.5

[a] – average value (n = 5 or 6)

The digestion of the rock samples by carbonate fusion gave higher results for SRM-1c as compared to the digestion by acid combination. However, the results obtained for the rest of the samples were approximately similar. The high content of non-carbonate material in the rock SRM-1c, as compared to other rock materials, renders it relatively less digestible using the acid combination of choice.[94] Without specifying the zirconium content in the carbonate rocks or making a reference of the metal content as probably provided by their respective suppliers (GSJ, NIST and BAS), Okai proceeds to compare his work with the results obtained by other researchers who had previously investigated zirconium content in these carbonate rock materials. For the comparison of the quantification of zirconium content in different carbonate rocks using various digestion methods, refer to **Table 2.5**. Not much conclusions can be drawn as to the efficiency of the alkali method employed in digesting zirconium-containing rock materials due to i) no prior known quantity of zirconium is noted in these rock materials by the researcher and ii) the alkali digestion method seems not to be any better than using the acid combination on its own, except in digesting only one rock material with

high concentrations of non-carbonate material. The sodium carbonate method would probably be useful in digesting the material which possesses non-carbonate material in substantial amounts.

Table 2.5: Comparison of results for zirconium in six carbonate rock reference materials by different analytical techniques

Sample	Okai's Zirconium content (μg/g)[a]	Method	Other Zirconium contents (μg/g)	Method
Geological Survey of Japan (GSJ)				
JDo-1	3.5 ± 0.4	Acid digestion	6.21	Not specified
JLs-1	2.3 ± 0.3		4.19	
National Institute of Standards and Technology (NIST)				
SRM 1c	23 ± 3	Alkali fusion	40	INAA + XRF
SRM 88a	2.7 ± 0.7	Acid digestion	6.6	XRF
			< 1	ICP-OES
Bureau of Analysed Samples (BAS)				
BCS 368	4.1 ± 0.6	Acid digestion	2.7	ICP-OES
BCS393	2.4 ± 0.3			

[a] – average value (n = 5 or 6) with standard deviation

Mihaljevič *et al.*[95] quantified both the boron and zirconium contents in ceramic materials by fusing them with a mixture of $NaKCO_3$ and boric acid, and then treat the fused material with an acid combination consisting of HF and $HClO_4$. Ten replications were performed by flame atomic absorption spectrometry (FAAS) on the ceramics GBW 07708 and NIM L to determine boron and zirconium content, respectively. See **Table 2.6** for the results they obtained.

[95] M. Mihaljevič, O. Šebek, E. Lukešová and A. Bouzková., *Fres. J. Anal. Chem.*, **371**, pp. 1158 – 1160 (2001)

Table 2.6: Results of boron and zirconium determinations in ceramic materials

	Reported (µg/g)	Found (µg/g)	n	LOD (mg/kg)
Boron (GBW 07708)	500 ± 12	507 ± 16	10	450
Zirconium (NIM L)	11400 ± 100	11500 ± 80	10	1750

Some advantages of using the sodium carbonate as a flux agent were listed by Mihaljevič *et al.* It is important in that it decreases the precipitation and subsequent deposition of salts in the burner slot by keeping the analytes in solution so that there is little or no effect on the spectrometric determinations of boron and zirconium and it minimizes corrosion of the digestion vessel, among others. The results show that the method used was efficient in determining both the boron and zirconium content in their respective ceramic materials.

2.2.4 DIGESTION BY HYDROXIDES

Venable and Clarke[93] fused zirconia with sodium and potassium hydroxides following the same methods they used for the carbonate fluxing. Quantitative results obtained from these fusions were much better than digesting it with the carbonates. Their research gave no indication of time duration of the flux but only the increasing mass of flux in the case of sodium hydroxide. Dilute hydrochloric acid was used to dissolve the zirconium from the flux mixture. The same procedure as in the carbonate fusion was followed where the mixture was heated to obtain zirconium hydroxide precipitate. The results compared between sodium and potassium hydroxides are shown in **Tables 2.7** and **2.8**.

Table 2.7: Results of sodium hydroxide fusions of zirconia

Amount of ZrO_2 added (g)	Amount of NaOH added (g)	Amount of fused ZrO_2 (g)	ZrO_2 Recovery (%)
2.000	8	1.1855	59.28
2.000	8	0.7655	38.28
2.000	16	0.8004	40.02

Table 2.8: Results of potassium hydroxide fusions of zirconia

Amount of ZrO_2 added (g)	Amount of KOH added (g)	Amount of fused ZrO_2 (g)	ZrO_2 Recovery (%)
2.000	16	0.8850	44.25
2.000	16	1.5241	76.21
2.000	16	1.2078	60.39
2.000	16	0.9297	46.49

Increasing amounts of sodium hydroxide flux did not improve the digestion of zirconia. Fusion with potassium hydroxide seemed to be better than sodium hydroxide but both fusions did not yield total recovery. The average amount of fused zirconia by sodium hydroxide flux was 0.9171 g (45.86 %) with the standard deviation of ± 0.23 while the average amount of fused zirconia by potassium hydroxide flux was 1.137 g (56.84 %) with the standard deviation of ± 0.3.

2.2.5 MICROWAVE-ASSISTED DIGESTION OF ZIRCONIUM-CONTAINING SAMPLES

The use of microwave-assisted digestion technique is relatively new.The first reports of zirconium digestion were published in the late 1990's. Chakraborty *et al.*[96] mentioned that the use of microwave digestion became a popular digestion of choice for trace elements analysis found in biological specimens after a review by Matusiewicz and Sturgeon[97] in 1989. In this article Matusiewicz and Sturgeon emphasized the most important aspects of open and closed digestion systems with major focus on the efficiency of microwave instrumentation and its applications. The use of microwave digestion has since been extended to include the digestion of numerous kinds of inorganic samples, including different zirconium containing chemicals.

Merten *et al.*[98] investigated microwave-assisted digestion of zirconium based ceramic powders using a combination of mineral acids, and compared it with conventional digestion

[96] R. Chakraborty, A.K. Das, M.L. Cervera and M. de la Guardia., *Fres. J. Anal. Chem.* **355**, pp. 99 – 111 (1996)

[97] H. Matusiewicz and R.E. Sturgeon., *Prog. Anal. Spectrosc.*, **12**, p. 21 (1989)

[98] D. Merten, J.A.C. Broekaert, R. Brandt and N. Jakubowski., *J. Anal. At. Spectrom.*, **14**, pp. 1093 – 1098 (1999)

of the same samples at high pressures and power settings as well as temperature settings of 625 ± 4 W and 220 °C using various mineral acids and decomposition by fusion with ammonium acid sulphate (NH_4HSO_4). ICP-OES was used as the analytical technique to quantify the elements. They studied the presence of different elements in nine ceramic powders, with sample masses ranging from 200 – 600 mg. Standard impurity elements were added to these ceramic powders. An amount of 40 µg of each of these elements – Al, B, Ca, Cr, Cu, Fe, Mg, Mn, Na, Ni, Si, Ti, V and Zn as well as 1 mg of Hf and 5 mg of Y were added to the ceramic samples. Recoveries of 100 %, within the experimental error of 3 – 8 %, were obtained for elements Al, Ca, Cr, Cu, Fe, Hf, Mg, Mn, Na, Ni, Si, Ti, V, Y and Zn. However, positive errors of 200 and 300 % were obtained for B and Si respectively when microwave-assisted digestion was applied at high temperature using a combination of nitric and sulphuric acid. However, losses of up to 40 % were obtained for Si when they used combination of HF and H_2SO_4 during the microwave digestion.

Conventional digestions of ceramic powders were repeated on samples with masses ranging from 200 – 1000 mg and with the similar quantities and type of elements mentioned for the microwave-digested method. Whereas the complete digestion of ceramic powder samples was achieved within 1 hour using microwave digestion, it took 10 – 20 hours to completely digest the samples in the conventional digestion. All the investigated elements, except boron and silicon, were recovered at 100 % within the experimental error of 3 – 8 %. The recovery of boron was about 80 % and that of silicon was between 30 and 50 %.

The fusion method using ammonium acid sulphate (NH_4HSO_4) that Merten *et al.*,[98] studied during their comparative study only managed to completely digest five of the zirconia ceramic powders while the remaining four ceramic samples were digested with differing degrees of success. It took 5 hours to complete the fusion process and only the recoveries of elements found in the 5 digestible ceramic samples were reported. As in the previous methods of microwave-assisted and conventional digestions, quantitative results obtained from this digestion indicated that all the elements, except for B and Si, were recovered at 100 % with the experimental error of 5 – 13 %. However, positive errors of up to 50 % were reported for Si, possibly as a result of contamination from the crucibles and losses by up to 80 % were reported for B as a result of the high temperatures that were applied.

Ma and Li[99] developed a rapid, accurate and precise method for the quantification of trace impurities in high-purity zircon by employing a microwave-assisted digestion of the ore with ammonium sulphate-sulphuric acid mixture and analyzing with ICP-OES. They reported that the time taken to digest the ore using this method was 30 minutes which, according to their observation, is significantly shorter than that required for the open system. Results obtained from this digestion method are reported in **Table 2.9**.

Table 2.9: Analytical results of microwave-assisted digestion of zircon samples

Element	Spiked (µg)	Recovery (mean ± SD) (%)	
		Wavelet transform correction	Off-peak correction
Fe	2	93.6 ± 2.2	68.7 ± 4.5
	5	96.3 ± 1.8	77.2 ± 3.6
	20	102.8 ± 1.1	89.3 ± 3.4
Hf	50	112.0 ± 2.5	86.0 ± 6.2
	125	106.2 ± 2.4	92.1 ± 5.9
	500	104.5 ± 2.0	97.5 ± 4.1
Mn	2	107.0 ± 2.7	128.3 ± 6.4
	5	104.2 ± 2.5	117.4 ± 6.3
	20	99.3 ± 1.4	106.5 ± 5.0
Na	10	105.6 ± 3.3	91.3 ± 4.7
	25	103.3 ± 2.8	102.6 ± 4.2
	100	104.4 ± 1.5	98.1 ± 3.2
Si	10	87.3 ± 2.1	72.2 ± 4.9
	25	96.5 ± 1.5	84.3 ± 3.7
	100	94.1 ± 1.8	95.3 ± 3.3
Ti	2	88.4 ± 1.2	131.3 ± 2.8
	5	96.9 ± 0.8	122.9 ± 2.4
	20	98.2 ± 0.8	104.4 ± 1.9

[99] X. Ma and Y. Li. *Anal. Chim. Acta.*, **579**, pp. 47 – 52 (2006)

Ma and Li[99] used two different techniques to quantify the impurities in these samples, namely wavelet transform and off-peak corrections. Both the wavelet transform and off-peak corrections are mathematical methods that were applied by these researchers to eliminate spectral interferences. They compared the results obtained using both these mathematical methods on an ICPS-1000 spectrometer and preferred the wavelet transform over off-peak correction. The results in **Table 2.9** for the wavelet transform correction indicated excellent recovery with reduced standard deviations compared to the off-peak correction with large standard deviations. These results clearly indicated the success of microwave-assisted digestion method in quantifying trace impurity elements in zircon.

However, Lötter[100] went on to show that the microwave-assisted acid digestion of different zircon materials using $(NH_4)_2SO_4$ – H_2SO_4 mixture was a less viable digestion method of choice. Quantification of the major constituents in zircon and plasma dissociated zircon (PDZ) yielded recoveries of zirconium and hafnium at below 20 % while a higher recovery was obtained for iron. The results obtained are reported in **Table 2.10**.

Table 2.10: Table showing microwave-assisted digestion experiment results using various reagents

No	Sample	Reagents	Max Temperature Reached	Zr Recovery (%)	Hf Recovery (%)	Al Recovery (%)	Fe Recovery (%)
1	SARM62	4 g $(NH_4)_2SO_4$, 10 ml H_2SO_4	240 °C	4.58	4.01	51.05	73.14
2	SARM62	4 g $(NH_4)_2SO_4$, 10 ml H_2SO_4, 10 ml H_2O	140 °C	2.43	2.20	49.81	90.00
3	SARM62	10 ml H_2SO_4	240 °C	6.41	7.17	72.53	68.86
4	SARM62	10 ml H_2SO_4	240 °C	14.58	18.31	7.18	15.14
5	PDZ	4 g $(NH_4)_2SO_4$, 10 ml H_2SO_4	240 °C	1.53	1.63	2.89	8.43
6	PDZ	4 g $(NH_4)_2SO_4$, 10 ml H_2SO_4, 10 ml H_2O	140 °C	0.13	0.12	3.08	8.00
7	PDZ	2 ml HNO_3, 8ml HCl	140 °C	0.03	0.26	2.82	8.14
8	PDZ	10 ml 8M NaOH	140 °C	0.20	0.24	18.82	17.00

[100] S.J. Lötter., *Identification and Quantification of Impurities in Zircon, PDZ and Other Relevant Zirconium Products.*, M.Sc. Dissertation at the Department of Chemistry, University of the Free State, UFS, RSA (2008)

Lötter proceeded to modify his experiment by varying the quantities of ammonium sulphate while keeping the volume of sulphuric acid (10 ml), the power (1200 W), the temperature (~240 °C), and the pressure (60 bar) constant for 30 minutes and still did not manage to recover the elements at satisfactory values as reported in **Table 2.11**.

Table 2.11: Table showing the effect of varying amounts of ammonium sulphate on the % recovery of different elements

No.	Sample	Mass $(NH_4)_2SO_4$ (g)	Zr Recovery (%)	Hf Recovery (%)	Al Recovery (%)	Fe Recovery (%)
1	SARM62	0	10.44	10.51	94.19	99.52
2	SARM62	1.0596	9.57	10.23	145.58	140.94
3	SARM62	2.0449	12.21	12.88	158.20	149.26
4	SARM62	3.0507	10.64	10.71	140.33	142.69
5	SARM62	3.9895	11.30	11.94	130.20	140.47
6	SARM62	5.0484	14.31	15.36	145.03	153.57
7	SARM62	6.0737	17.36	19.88	141.81	138.73
8	PDZ	0	57.79	83.77	28.17	46.74

Addition of ammonium sulphate seemingly has adverse effects on recoveries of all the elements under study, probably due to spectral interference. In the absence of this reagent, both recoveries for aluminium and iron were satisfactory but when added in increasing amounts, they are consistently recovered at higher values. Quantification of both zirconium and hafnium still yielded undesired recoveries with or without the addition of ammonium sulphate. Thus, according to this study, microwave-assisted digestion of zircon and PDZ with ammonium sulphate-sulphuric acid is not efficient for the purpose of quantifying elements in these samples.

2.3 METHODS OF ANALYSIS

Digestion is mainly aimed at total destruction of the original sample with the purpose of getting it into solution for quantification analytical purposes. Numerous different analytical

methods can then be employed to quantify the zirconium or any impurity associated with the sample. These methods include gravimetry, potentiometry, volumetry, spectroscopy, *etc.*

2.3.1 PRECIPITATION AND TITRATION TECHNIQUES

These techniques include, among others, analytical procedures such as gravimetry, volumetry, *etc.* Hill and Miles[101] developed a method for the gravimetric determination of zirconium in titanium alloys using mandelic acid. Zirconium tetramandelate can be quantitatively precipitated from hydrochloric acid and perchloric acid solutions. They reported that the presence of trace impurities, *e.g.* iron, aluminium, vanadium, tin, copper, chromium, cobalt, magnesium, manganese, molybdenum and nickel, above the quantities that are normally associated with alloys interfere with zirconium determination. The results they obtained from their research are shown in **Tables 2.12**, **2.13** and **2.14**.

Table 2.12: Effect of common alloying elements on the analysis of zirconium

Zr added (%)	Zr found (%)	Recovery (%)	Zr added (%)	Zr found (%)	Recovery (%)
Synthetic 1: Ti (92 %)			Synthetic 2: Ti (70 %), V (5 %), Mo (5 %), Mn (10 %), Mg (0.5 %)		
7.98	7.95	99.6	9.98	9.94	99.6
	7.99	100.1		9.99	100.1
	8.00	100.2		9.99	100.1
Average	7.97	100.0	Average	9.97	99.9
Synthetic 3: Ti (76 %), V (5 %), Mo (5 %), Mn (10 %), Mg (0.5 %)			Synthetic 4: Ti (78 %), V (5 %), Mo (5 %), Mn (10 %), Mg (0.5 %)		
3.99	4.04	101.2	1.995	1.985	99.5
	4.06	101.7		2.015	101.0
	4.03	101.0		2.020	101.3
Average	4.04	101.3	Average	2.005	100.5
Synthetic 5: Ti (79 %), V (5 %), Mo (5 %), Mn (10 %), Mg (0.5 %)					
1.000	1.010	101.0			
	1.010	101.0			
	1.005	100.5			
Average	1.008	100.8			

[101] J.H. Hill and M.J. Miles., *Anal. Chem.*, **31** (2), pp. 252 – 254 (1959)

Table 2.13: Analysis of zirconium in synthetic metallic standards

Composition (%)	Zr Recovered (%)	Recovery (%)
1.00 Zr, 1.00 Mo, 98 Ti	1.02	102
	1.02	102
	0.99	99
Average	1.01	101
3.00 Zr, 1.00 Mo, 96 Ti	3.07	102
	3.10	103
	3.14	105
Average	3.10	103
2.00 Zr, 98 Ti	2.05	102
	2.03	101
	2.03	101
Average	2.04	102

Table 2.14: Analysis of zirconium in the presence of titanium

Sample	Ti present (g)	Zr (g)		Recovery (%)	Sample	Ti present (g)	Zr (g)		Recovery (%)
		Added	Recovered				Added	Recovered	
1	1.00	0.0894	0.0897	100.3	2	2.00	0.0447	0.0446	99.8
			0.0894	100.0				0.0446	99.8
			0.0899	100.6				0.0448	100.2
			0.0899	100.6				0.0443	99.1
		Average	0.0897	100.3			Average	0.0446	99.8
3	2.00	0.0224	0.0221	98.7	4	1.00	0.0954	0.0948	99.4
			0.0214	95.5				0.0950	99.6
			0.0224	100.0				0.0951	99.7
			0.0212	94.6				0.0946	99.2
		Average	0.0218	97.3			Average	0.0949	99.5

The quantification of zirconium by gravimetric analysis using mandelic acid proved to be an efficient method. However, due to a minute presence of hafnium in zirconium metal, the total mass recovery for zirconium is considered as the combination of both these elements. Zirconium was recovered accurately in the presence of other elements of titanium alloys, therefore it can be concluded that these elements did not interfere with the analysis.

Mukherji[102] developed a gravimetric analytical method to quantify zirconium and hafnium by using various carboxylic acids, namely trimesic, trimellitic and pyromellitic acids. Standard zirconium and hafnium nitrate solutions were acidified with concentrated nitric acid, warmed and followed by the carboxylic acid addition. The solutions were heated at 80 – 90 °C and the metals are precipitated as carboxylates. The results obtained are shown on **Tables 2.15** and **2.16**.

Table 2.15 Determination of zirconium in zirconia

Zirconium added (g)	Zirconium found (g)	Recovery (%)
Precipitation with Trimesic Acid		
0.0062	0.0060	96.77
0.0124	0.0124	100.0
0.0197	0.0195	98.98
0.0394	0.0400	101.5
0.0788	0.0790	100.3
Average		99.51
Precipitation with Trimellitic Acid		
0.0197	0.0196	99.49
0.0394	0.0396	100.5
0.0591	0.0591	100.0
0.0788	0.0790	100.3
0.0986	0.0985	99.90
Average		100.04
Precipitation with Pyromellitic Acid		
0.0024	0.0024	100.0
0.0036	0.0038	105.6
0.0048	0.0049	102.1
0.0072	0.0070	97.22
0.0096	0.0093	96.88
Average		100.4

[102] A.K. Mukherji., *Anal. Chem.*,**36** (6), pp. 1064 – 1066 (1964)

Table 2.16 Determination of hafnium in hafnia

Hafnium added (g)	Hafnium found (g)	Recovery (%)
Precipitation with Trimesic Acid		
0.0171	0.0173	101.2
0.0342	0.0343	100.3
0.0513	0.0509	99.22
0.0684	0.0692	101.2
0.1368	0.1372	100.3
Average		100.4
Precipitation with Trimellitic Acid		
0.0171	0.0170	99.42
0.0342	0.0344	100.6
0.0513	0.0510	99.42
0.0684	0.0680	99.42
0.1368	0.1375	100.5
Average		99.87
Precipitation with Pyromellitic Acid		
0.0171	0.0169	98.83
0.0342	0.0345	100.9
0.0513	0.0508	99.03
0.0684	0.0688	100.6
0.1368	0.1372	100.3
Average		99.93

The precision in the quantification of zirconium in zirconia is lower as compared to that in the method applied in quantifying hafnium in hafnia . These results, however, show very good

accuracy (about 100 %) for both elements indicating their success in quantifying both the elements. In quantifying zirconium in the presence of other elements, the researchers reported that bismuth(III) and cerium(IV) had adverse interference effects due to their relative affinities to the precipitants. Elements were added in their chloride or nitrate salts in amounts of 100 mg and 0.0394 g of zirconium was used. The results obtained are given in **Table 2.17**.

Table 2.17 Determination of zirconium with trimesic acid in the presence of diverse ions

Ion added	Zirconium found (g)	Recovery (%)
Cu^{2+}	0.0392	99.49
Ba^{2+}	0.0396	100.5
Ca^{2+}	0.0397	100.8
Mg^{2+}	0.0391	99.24
Be^{2+}	0.0392	99.49
Zn^{2+}	0.0391	99.24
Cd^{2+}	0.0395	100.3
Hg^{+}	0.0390	98.98
Hg^{2+}	0.0393	99.75
Pb^{2+}	0.0396	100.5
Bi^{3+}	0.0504	**127.9**
Mn^{2+}	0.0393	99.75
Co^{2+}	0.0393	99.75
Ni^{2+}	0.0392	99.49
Fe^{3+}	0.0395	100.3
Al^{3+}	0.0394	100.0
Cr^{3+}	0.0396	100.5
Ce^{3+}	0.0391	99.24
Ce^{4+}	0.0453	**115.0**
Th^{4+}	0.0397	100.8
VO^{2+}	0.0390	98.98
UO^{+}	0.0396	100.5

A detailed step-by-step analysis of contaminants determination in zirconium was discussed by Elwell and Wood.[80] These procedures are tedious and environmentally harmful to carry out due to the time consumed and the acid combinations (including hydrofluoric acid) involved in achieving the desired outcomes.

2.3.2 SPECTROMETRIC TECHNIQUES

Spectral measurements including spectrophotometry, plasma spectrometry, *etc.*, have been applied in determining the quantities of elements in different zirconium samples.

2.3.2.1 SPECTROPHOTOMETRY AND SPECTROGRAPHY

Spectrophotometric, also known as absorptiometric, analyses of zirconium found favour with the analysts in the 1930's. Liebhafsky and Winslow[103] developed a method of determining zirconium at 10 ppm to 100 ppm range after obtaining stable coloured solutions using hydroxyanthraquinones, namely alizarin, quinalizarin and purpurin, as analytical reagents. However the success of this method depends heavily on the presence of other cations at lower concentrations so as not to interfere with the quantification of zirconium. No definite quantification results were reported in this study except for the qualitative information provided by the researchers in advocating for the usage of these colouring reagents.

Horton[104] re-developed a modified technique of Liebhafsky and Winslow by using thorin [1-(o-arsonophenylazo)-2-naphthol-3,6-disulfonic acid] in place of hydroxyanthraquinones moieties to analyze zirconium in the same range with a standard deviation of 5.7 % for the 10 ppm range and 2.9 % for the 100 ppm range. Pure zirconium metal (99.8 %) was digested with the combination of sodium fluoride and diluted hydrochloric acid. The effects of interference in determining zirconium are shown in **Table 2.18** below.

[103] H.A. Liebhafsky and E.H. Winslow., *J. Am. Chem. Soc.*, **60**, pp. 1776 – 1784 (1938)

[104] A.D. Horton., *Anal. Chem.*, **25** (9), pp. 1331 – 1333 (1953)

Table 2.18: Effect of known interferences on zirconium determination

Sample No.	Ion	Interference (ppm)	Zirconium (ppm)		
			Known	Found	Deviation from known
1	Cr (VI)	100	10	11.1	+1.1
		100	100	100.6	+0.6
		1000	100	110.7	+10.7
2	Fe (III)	100	10	10.8	+0.8
		100	100	101.8	+1.8
		1000	100	107.4	+7.4
3	Molybdate	100	10	12.3	+2.3
		100	100	100.9	+0.9
		1000	100	103.6	+3.6
4	Sn (IV)	100	10	10.5	+0.5
		100	100	97.0	-3.0
		1000	100	precipitate	-
5	Sn (II)	100	10	10.8	+0.8
		100	100	100.0	0.0
		1000	100	92.9	-7.1
6	Ti (IV)	100	10	9.6	-0.4
		100	100	98.2	-1.8
		1000	100	precipitate	-
7	Ti (II)	100	10	8.1	-1.9
		100	100	95.5	-4.5
		1000	100	56.5	-43.5
8	U (VI)	100	10	11.2	+1.2
		100	100	99.4	-0.6
		1000	100	103.3	+3.3

Judging from the above table, it can be deduced that the quantification of zirconium in the presence of increasing amounts of trace impurities using spectrophotometry analysis is

relatively an efficient method. While the highest amount of tin(IV) results in the precipitation of the reaction mixture making it difficult to quantify zirconium using spectrophotometric analysis, the highest amount of titanium(II) leads to the under-recovery of zirconium. As long as the reaction mixture remains in solution and some impurities are kept at a minimum content, this method is relatively efficient to quantify zirconium in the presence of its associated impurities. However, those elements [*e.g.* Ti(II) and Ti(IV)] which interfere with the quantification of zirconium at higher concentrations should be determined prior to carrying out the analysis, thus making this analytical method a time-consuming procedure to use in quantifying zirconium.

Spectrographic determinations have been applied, with good level of satisfaction, in quantifying zirconium and its impurities. Hettel and Fassel[105] developed an analytical method to quantify rare earth elements in zirconium samples by using ion exchange separation of zirconium and the rare earth impurities. Two reactor grade zirconium metals (labelled 1 and 2) of 100 mg each were digested with 48 % hydrofluoric acid. Three yttrium oxide (99.5 %) samples (labelled A, B and C) of 20 mg each, which possessed rare elements at known concentrations as specified in **Table 2.19**, were added to the zirconium as internal standards with average experimental errors of approximately 10 %. As observed in **Table 2.19**, terbium, holmium and samarium could not be detected at concentrations lower than 0.04 ppm for terbium, 0.01 ppm for holmium and 0.1 ppm for samarium. The researchers noted that it was not easy to detect these elements at concentrations lower than these values by using spectrographic technique.

This study was aimed at quantifying only the rare elements but there are steps within the procedure they used which render other impurity elements soluble so as to selectively separate and remove them from those of interest. No quantification of zirconium was done to determine the effect of the rare elements on its analysis. In general spectrographic analysis seems to be efficient in quantifying contaminantsin zirconium metal but it involves long procedures to get impurity elements into solution.

[105] H.J. Hettel and V.A. Fassel., *Anal. Chem.*, **27** (8), pp. 1311 – 1314 (1955)

Table 2.19: Analysis of zirconium samples after addition of known amounts of rare earths

Impurity	Zirconium Sample	Y_2O_3 standard	Impurity in Zirconium (ppm)		Normal Error
			Conc. before addition	Conc. after addition	
Gd	1	A	0.043	0.046	± 0.004
	1	B	0.13	0.14	± 0.015
	2	B	0.13	0.14	± 0.015
	1	C	0.30	0.27	± 0.03
	2	C	0.30	0.29	± 0.03
Tb	1	A	n.d.[a]	n.d.	-
	2	A	n.d.	n.d.	-
	1	B	0.51	0.51	± 0.05
	2	B	0.51	0.51	± 0.05
	1	C	1.07	1.00	± 0.10
	2	C	1.07	1.07	± 0.10
Ho	1	A	n.d.[b]	n.d.	-
	2	A	n.d.	n.d.	-
	1	B	0.36	0.36	± 0.035
	2	B	0.36	0.39	± 0.035
	1	C	1.20	1.05	± 0.11
	2	C	1.20	1.16	0.12
Sm	1	A	n.d.[c]	n.d.	-
	2	A	n.d.	n.d.	-
	1	B	0.16	0.16	± 0.15
	2	B	0.16	0.16	± 0.15
	1	C	0.74	0.66	± 0.07
	2	C	0.74	0.70	± 0.07
Dy	1	A	0.13	0.12	± 0.001
	2	A	0.13	0.17	± 0.001
	1	B	0.42	0.44	± 0.04
	2	B	0.42	0.44	± 0.04
	1	C	0.71	0.63	± 0.07
	2	C	0.71	0.73	± 0.07

[a] – not detectable if less than 0.04 ppm

[b] – not detectable if less than 0.01 ppm

[c] – not detectable if less than 0.1 ppm

Farrell *et al.*[106] developed a reproducible point-to-plane spectrochemical determination of trace impurities in solid zirconium in the parts per million ranges with coefficient of variance of ~5 %. Samples and standards were prepared by melting in a graphite furnace and analyzed spectrochemically. The results of their project are shown in **Table 2.20**.

Table 2.20 Statistical study of reproducibility in solid zirconium day-to-day analyses

Element	C_{max} (ppm)	C_{min} (ppm)	$C_{average}$ (ppm)	Coefficient of Variance (%)
ZAS – 3				
Al	83	78	80	2
Cr	80	74	77	3
Cu	245	190	220	7
Fe	540	450	500	5
Mn	24	21	23	4
Si	125	100	110	7
Sample 2				
Al	60	52	56	4
Cr	140	125	131	5
Cu	26	20	23	10
Fe	880	810	843	4
Mn	28	24	26	7
Pb	46	37	40	10
Si	45	37	40	8
Ti	26	20	22	10

Although the data above is less informing regarding the accurate quantification of these elements in zirconium metal, the spectrographic analysis of zirconium for these impurities can be deemed efficient due to the lower values observed for the coefficient of variance. Thus the method is reproducible and fit for the purpose of analyzing the impurities in solid zirconium.

[106] R.F. Farrell, G.J. Harter and R.M. Jacobs., *Anal. Chem.*, **31** (9), pp. 1550 – 1554 (1959)

2.3.2.2 INDUCTIVELY COUPLED PLASMA (ICP) SPECTROSCOPIC TECHNIQUE

The inductively coupled plasma (ICP) method is currently the technique mostly employed in analyses of zirconium metal, its mineral ores and alloys. This is mainly due to the rapid sample analysis by identifying and quantifying many elements simultaneously. It comprises of two most commonly used analytical instruments, namely inductively coupled plasma – optical emission spectroscopy (ICP-OES) and inductively coupled plasma – mass spectroscopy (ICP-MS).

Stefan and Vujicic[107] employed ICP-OES to analyze trace elements in zirconium alloys (SRM 360a, SRM 1238, and SRM 1239) after digesting them with an acid combination of hydrofluoric, nitric and hydrochloric acids. While considering the spectral interferences in their analyses, they compared their results to that of the certified samples with the confidence interval of 95 % probability in the error level range of 2 – 12 % depending on the element and concentration. Their results are shown in **Table 2.21**.

Table 2.21: Trace elements determined in the Zr SRMs from NIST

Element	LOD (µg/g)	SRM 360a		SRM 1238		SRM 1239	
		Certified (µg/g)	Found (µg/g)	Certified (µg/g)	Found (µg/g)	Certified (µg/g)	Found (µg/g)
Cu	2.1	140	138 ± 6	60	62 ± 4	130	129 ± 8
Cr	3.3	1060	1048 ± 44	580	592 ± 30	1055	1050 ± 42
Fe	1.4	1441	1450 ± 30	2500	2420 ± 100	2300	2180 ± 80
Hf	5.5	-	-	178	180 ± 6	77	74 ± 4
Mn	1.5	3	2.8 ± 0.1	60	58 ± 2	50	48 ± 2
Mo	13	-	-	120	124 ± 5	45	40 ± 4
Ni	1.6	554	538 ± 18	100	110 ± 5	45	40 ± 5
Sn (%)	6.2	1.42	1.4 ± 0.15	-	-	-	-
Ti	4.2	27	24.0 ± 2	100	95 ± 5	40	38 ± 3
U	5.6	0.15	< LOD	-	-	-	-
W	37	-	-	90	95 ± 4	45	44 ± 3

[107] I. Steffan and G.Vujicic, *J. Anal. Atom. Spec.*, **9**, pp. 785 – 789 (1994)

All the impurity elements were accurately quantified by the researchers based on their certified content in zirconium alloys. The results for tin varied from the rest of the elements under investigation as they were given in percentage units. These results clearly indicate the efficiency of ICP for quantification of trace elements in zirconium alloys.

McKelvey and Orians[108] developed an analytical technique which uses isotope dilution and ICP-MS to quantify dissolved zirconium and hafnium at ultra low concentrations found in seawater. Extractions of zirconium and hafnium were done by making use of a chelating ion-exchange resin, Chelex-100, employing isotope dilution analysis. They reported the zirconium content at the range 25 – 366 pmol/kg and that of hafnium at 0.20 – 1.02 pmol/kg. They also noted that concentrations increased relatively with the depth of the sea.

Merten *et al.*,[98] analyzed for the trace elements in zircon powders using ICP-OES and ICP-MS after digesting the samples in a microwave system. Refer to **Section 2.2.5** for the results obtained. Notwithstanding the positive errors they observed for boron and silicon, their method proved to be efficient in precisely quantifying trace elements in zirconium-containing ceramic samples.

Agrawal and Sudhakar[43] developed and compared the techniques of spectrophotometry (absorptiometry) and ICP-OES in determining the zirconium content of samples in the presence of hafnium. Zirconium oxychloride was dissolved with hydrochloric acid and extracted with dibenzo-18-crown-6 (DB18C6) in dichloromethane (DCM). To carry out the ICP-OES analysis, the extract was further diluted with DCM. For the spectrophotometric analysis, the extract was treated with KSCN solution, separated and the organic (DCM) layer measured at a wavelength of 450 nm and analyzed with a spectrophotometer. The results of their study are shown in **Table 2.22**.

[108] B.A. McKelvey and K.J. Orians., *Mar. Chem.*, **60**, pp. 245 – 255 (1998)

Table 2.22: Determination of zirconium in the presence of hafnium

Zirconium (ppm)	Hafnium added (ppm)	Zirconium Found (ppm)	
		Spectrophotometry	ICP-OES
3	10	2.98 ± 0.05	3.001 ± 0.002
3	15	2.99 ± 0.03	2.997 ± 0.005
5	10	4.97 ± 0.04	5.000 ± 0.002
5	20	4.99 ± 0.02	5.003 ± 0.005
5	25	5.02 ± 0.02	4.995 ± 0.005
5	30	4.98 ± 0.03	4.998 ± 0.006
5	40	5.00 ± 0.02	5.000 ± 0.002

The researchers further applied their developed method in analyzing for the zirconium content in seawater but no results were published. Quantification of zirconium in the presence of hafnium by both ICP-OES and absorptiometry indicated excellent recovery and precision. However, ICP-OES was more accurate as compared to spectrophotometry (absorptiometry) as the standard deviations were about an order of magnitude lower. Therefore, ICP-OES was proved to be the most efficient analytical method in quantifying zirconium in the presence of hafnium.

After microwave-assisted digestion of zircon, Ma and Li[99] did their analysis using ICP-OES for the quantification of trace elements. Refer to **Table 2.9** in **Section 2.2.5** for the results obtained by these analysts. This analytical method was more efficient after the recovery was corrected by wavelet transform as compared to off-peak correction.

2.3.3 ATOMIC ABSORPTION SPECTROSCOPY (AAS) TECHNIQUES

These techniques include flame or graphite flame atomic absorption spectrometry (FAAS or GFAAS) and neutron activation analysis spectrometry (NAAS). Unlike the use of an inert gas to produce a plasma, flame atomic absorption uses combination of air and acetylene whereas GFAAS, known also as electrothermal atomic absorption spectrometry (ETAAS), uses graphite-coated furnace where the sample is electrically heated and vaporized. Some of

the disadvantages of FAAS are the short-lived time of atoms generated in the flame making it possible to measure only those atoms concentrated in the steady state and the limitation in the poor efficiency of the nebulizer or burner system, where not more than 10 % of the nebulized sample solution reaches the flame.[109] These factors render the FAAS to be less sensitive in analyzing materials at lower concentrations. The electrothermal (ETAAS) system has been applied to determine zirconium at trace levels in standard samples due to its sensitive nature.[110] However, the disadvantages of ETAAS are associated with low sample throughput, low precision and it requires high level of operator skill to be run.[111] Both FAAS and ETAAS have a similar limitation in being able to analyze a limited number of elements at a given time.

Neutron activation analysis spectroscopy (NAAS) is the method that simultaneously determines many elements at trace amounts. It is very sensitive, accurate, precise and determines up to 74 (including zirconium) elements at concentrations of parts per billion or trillion (ppb or pptr) depending on the element under investigation, with or without chemical separation.[112,113] Many samples, ranging from 50 to 100, can be analyzed in one batch. However, due to the slow rate at which elements can be analyzed due to their long half-lives, it can be time-consuming.

Bond[114] reported the enhancement of determining zirconium and other elements in flame atomic absorption spectrometry by using ammonium fluoride as the digesting material. However, only the spectral interferences by other elements were reported and not the recovery results of zirconium. Taddia[115] determined the copper impurities in zirconium(IV) salts using FAAS. He initially studied the effects of both zirconium(IV) ion and hydrofluoric acid on the copper absorbance, and then continued to analyze the samples from different manufacturers of zirconium salts. Zirconium matrix proved to have a depressing effect on the copper signal with the increasing concentration of zirconium. This is depicted in **Figure 2.1**.

[109] H. Matusiewicz., *Spectrochim. Acta Part B.*, **52**, pp. 1711 – 1736 (1997)

[110] Y.K. Agrawal, M. Sanyal, P. Shrivastav, S.K. Menon., *Talanta*, **46**, pp. 1041 – 1049 (1998)

[111] http://www.nuigalway.ie/chemistry/level2/courses/CH205_atomic_absorption_spectroscopy.pdf (22 June 2011)

[112] http://en.wikipedia.org/wiki/Neutron_activation_analysis#Analytical_capabilities (22 June 2011)

[113] http://www.reak.bme.hu/Wigner_Course/WignerManuals/Budapest/NEUTRON_ACTIVATION_ANALYSIS.htm#_Toc38122506 (22 June 2011)

[114] A.M. Bond., *Anal. Chem.*, **42** (8), pp. 932 – 935 (1970)

[115] M. Taddia., Fresenius Z. *Anal. Chem.*, **299**, pp. 261 – 263 (1979)

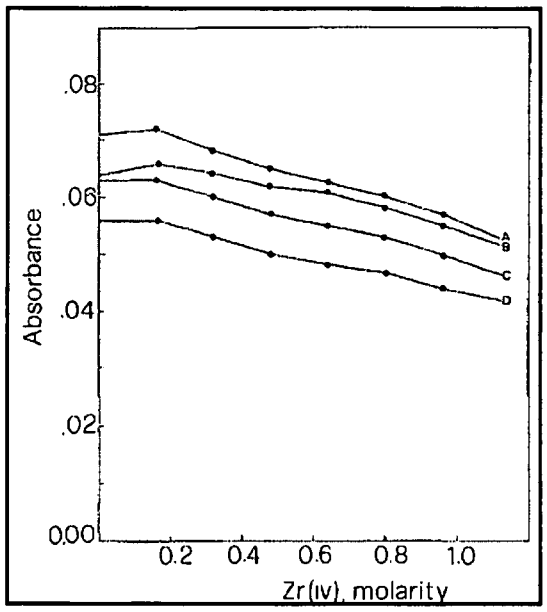

Figure 2.1: A graph depicting the effect of Zr^{4+} ion on the copper absorbance. [Cu] = 1 ppm[114]

Taddia[115] reported that the extent of interference slightly increased with the age of the zirconium solution. He found hydrofluoric acid to be effective in reducing the interference on the copper signal from the matrix. Zirconium concentration was kept constant while the concentrations of copper and hydrofluoric acid were varied. See **Table 2.23** for the percentage change on the absorbance of copper due to the effect of hydrofluoric acid.

Table 2.23: Effect of hydrofluoric acid on the absorbance (% change) of copper in the presence of 0.62 M $ZrOCl_2$

[Cu] (ppm)	HF (mol.dm^{-3})			
	0.0	1.8	2.4	3.0
0.2	- 6.7	0.0	0.0	+ 6.7
0.4	- 12.9	- 9.7	- 3.2	0.0
0.6	- 12.8	- 10.6	- 4.0	- 4.3
0.8	-11.5	- 9.0	- 3.3	- 3.3
1.0	- 12.0	- 10.2	- 4.1	- 8.3

From **Table 2.23** above, the researcher remarked that the optimum hydrofluoric acid concentration for quantifying copper in a 0.65 M zirconium solution is 2.4 M. Therefore he

proceeded by adopting a molar ratio HF:Zr of about 4 for the analyses of commercial samples. See the results of this research in **Table 2.24**.

Table 2.24: Quantification of copper in commercial zirconium samples

Salt	Supplier	$[Cu]_{mean}$ (ppm)
$Zr(NO_3)_4$	E-ERBA	1.15 ± 0.02
$Zr(NO_3)_4$	BDH	0.57 ± 0.01
$ZrOCl_2$	E-ERBA	0.11 ± 0.002
$ZrOCl_2$	H & W	0.13 ± 0.002

Hauptkorn *et al.*,[116] showed the advantage of using slurry sampling ETAAS over d.c. arc excitation OES and ICP-OES as the better analytical method for quantifying silicon in powdered titanium dioxide (TiO_2) and zirconium dioxide (ZrO_2) samples. Samples were prepared by dissolving them in a calcium nitrate solution and agitated on the ultrasonic bath to have them as slurries. The results as compared to those of other researchers are shown in **Table 2.25**.

Table 2.25: Silicon contents determined in TiO_2 and ZrO_2 by slurry ETAAS and AES (n = 7)

Sample	Slurry ETAAS (ppm)	d.c. OES (ppm)	Slurry ICP-OES (ppm)	Solution ICP-OES (ppm)
TiO_2	76 ± 4	75 ± 5	-	-
ZrO_2 – 1	244 ± 46	314 ± 15	250 ± 10	255 ± 11
ZrO_2 – 2	166 ± 30	90.99	102 ± 7	105 ± 7
ZrO_2 – 3	130 ± 41	81.102	100 ± 7	95 ± 7
ZrO_2 – 4	25 ± 4	-	-	-

Even though Hauptkorn *et al.*,[116] remarked that ETAAS is advantageous in quantifying silicon in titanium dioxide and zirconium dioxide as compared to the others, they did not indicate the certified content of silicon in the titanium oxide and zirconia ore materials under their study.

[116] S. Hauptkorn, G. Schneider and V. Krivan., *J. Anal. Atom. Spectro.*, **9**, pp. 463 – 468 (1993)

Thus, not much can be concluded from these results regarding the efficiency of the analytical method. However, it is worth mentioning that ETAAS can be employed in determining and quantifying impurities in zirconium-containing ores.

A sensitive neutron activation analytical technique was developed by Rebagay and Ehmann[117] to determine and quantify zirconium and hafnium in a variety of standard rocks and meteorites. Rock samples were fluxed with sodium peroxide and dissolved in concentrated hydrochloric acid. Several steps are followed, which involve various reagents where eventually zirconium and hafnium are separated by strongly basic anion-exchange resin before being analyzed. The results of their projects are listed in **Table 2.26**.

Table 2.26: Zirconium and hafnium abundances in some standard rocks and related natural materials

Specimen	Average Zr (ppm)	Average Hf (ppm)	mean $\frac{\text{Zr (ppm)}}{\text{Hf (ppm)}}$ **
A. Standard rocks			
DTS-1, Std. Dunite	1.4	0.01	-
PCC-1, Std. Peridotite	8.1	0.03	-
W-1, Std. Diabase	110	3.0	37
BCR-1, Std. Basalt	184	2.8	66
AGV-1, Std. Andesite	213	4.1	52
GSP-1, Std. Granodiorite	645	17	38
G-1, Std. Granite	219	4.2	52
G-2, Std. Granite	393	5.8	68
GA, Std. Granite	217	4.5	48
B. Tektites			
Mingenew, W.A. Australite	325	4.2	77
Port Campbell, Vic. Australite	306	3.4	90
C. Other terrestrial materials			
Eclogite (Roberts Victor Mine, RSA)	27	0.81	33
Basalt (Mid-Atlantic Ridge, Station 20)	62	1.4	44

** - Not listed where precision is poor, or Hf content is near detection limit

[117] T.V. Rebagay and W.D. Ehmann., *J. Radioanal. Chem.*, **5**, pp. 51 – 60 (1970)

From the above research data, NAAS can be employed in determining and quantifying zirconium and its associated impurities. However, the researchers did not supply the information regarding the certified contents of zirconium and hafnium in the specimen so that any conclusion can be made as to the efficiency of NAAS as the analytical method of choice.

2.4 CONCLUSION

Since the realization of the importance of zirconium in the nuclear reactors in 1947, many analytical methods have been developed and applied in separating and quantifying this metal from the impurities which may render it unusable in cladding of nuclear rods, *etc.* The great necessity was to develop methods that will enable the nuclear industry to determine the level of content of these impurity elements in nuclear grade zirconium metal. With the advance in analytical and technological knowledge most of these methods have been modified to increase sensitivity, accuracy, precision, *etc.* to determine these elements with much confidence. From the preceding paragraphs discussed here, most of the analytical techniques indicated are limitated in their use as preferred methods, such as accuracy, precision, cost, environmental consideration as well as time constraints.

The most promising method for the determination and quantification of zirconium and its impurities appears to be the use of microwave digestion of the sample, followed by ICP-OES analysis. However, besides the success being reported for this method by Ma and Li and the subsequent disputing of a comparative procedure by Lötter, the method pertained to zircon ore has not so far been extended to include the zirconium metal analysis. Both techniques of microwave-assisted digestion and ICP-OES are advantageous in that they are efficient in some cases, environmentally benign and are rapidly carried out. This will be the purpose of this thesis.

3 AN OVERVIEW ON PRINCIPLES AND SELECTION OF ANALYTICAL TECHNIQUES

3.1 INTRODUCTION

A thorough literature review on the possible analytical methods employed for the quantification of zirconium and its associated impurities was embarked upon to determine which would be the most efficient and appropriate technique to accurately analyze for zirconium and its associated impurities. Most of these analytical methods were reported to be capable of completely digesting and subsequently analyzing for zirconium, its alloys and associated impurities with varying extent of efficiency. The advantages and disadvantages of the discussed analytical methods were scrutinized and compared with one another prior to selection of the preferred analytical techniques for this study. However, the concepts behind these analytical techniques need to be understood prior to selecting the most efficient of all. Thus, the purpose of this chapter is to study the theoretical principles and benefits of some of the most promising analytical techniques from **Chapter 2**. Factors such as the availability of equipment, accuracy, time constraints as well as operating and maintenance costs will be considered before the carrying out of this project.

Principles of digestion methods such as open and closed systems, flux as well as the use of hydrofluoric acid in decomposing zirconium metal will be studied. Concepts of analytical techniques such as atomic absorption spectroscopy (AAS), inductively coupled plasma-optical emission spectroscopy (ICP-OES) and inductively coupled plasma-mass spectroscopy (ICP-MS), neutron activation analysis spectrometry (NAAS) as well as X-ray techniques like X-ray fluorescence (XRF) and X-ray diffraction (XRD) will also be studied for the best analysis of zirconium metal. Analytical parameters, including accuracy, precision, linearity, sensitivity, *etc.*, will be discussed for a general overview on method development and its validation.

3.2 METHODS OF DIGESTION

Any method that will render a complete digestion of zirconium metal so as to analyze the metal for its impurity content serves as the ideal and preferred method that is capable of dissolving the sample with minimal or no volatilization and contamination from the environment. An overview on advantages and disadvantages of flux, hydrofluoric acid, closed and open digestion techniques will be done in this section to weigh the benefits of each method.

3.2.1 DIGESTION BY FLUX FUSIONS

Various inorganic samples such as mineral ores, metal oxides and silicates are generally insoluble in strong mineral acids.[90] Flux fusions involving peroxides, carbonates and borates at temperatures higher than the melting point of the flux are then required to render these materials soluble for analytical purposes. Refer to **Section 1.1.1; Paragraph B** for examples of fusions involving zirconium-containing ores. Samples are ground into a fine powder prior to mixing with the flux and fusions are carried out in corrosion-resistant crucibles. Upon heating of the mixtures, the flux melts and acts as a solvent by fusing with the sample. The flux alters the chemical makeup of the sample to a form that is soluble in various solvents. The reaction is left to cool down to room temperature and the formed crystalline product is dissolved in an acid, base or water.

3.2.2 CLOSED DIGESTION TECHNIQUES

Closed digestion systems involve decomposition methods such as conventional pressure-assisted digestions and microwave-assisted digestions. These methods are considered advantageous and ideal for effective and complete decomposition of inorganic materials due to i) the use of high temperatures beyond the boiling point of the solvent, ii) improved dissolution of inorganic samples, iii) expected minimal loss of material, vi) less contamination of material from the surroundings because of the closed system, vii) low reagent consumption, and viii) prevention of the reaction from harming the environment.[118,119]

[118] G. Schwedt., *The Essential Guide to Analytical Chemistry*, John Wiley & Sons, Chichester (1997)

[119] G. Knapp., *Efficient digestion and separation techniques in trace element analysis of difficult sample materials*, Presentation at the European Winter Conference on Plasma Spectrochemistry (2009)

3.2.2.1 CONVENTIONAL PRESSURE-ASSISTED ACID DIGESTIONS

There are several procedures which involve conventional pressure-assisted decomposition techniques to digest samples for analytical purposes. These include using apparatus such as Parr bombs, Tölg containers and Knapp incinerators.[118]

A. Parr bomb

This equipment is operated by pressurising the bomb with about 25 – 30 atmospheric pressure of oxygen then creating a spark by igniting the fused wire and the sample is burned *via* heat that is produced. The produced heat is absorbed by the water in the bucket that houses the bomb and gets distributed evenly by stirring the water to ensure the uniform heating of the sample inside the bomb. The instrument is shown in **Figure 3.1**. Samples must be combustible in order to be digested and analyzed and in the case of wet digestion involving acids, samples must not be too wet as they might be rendered incompletely digested.

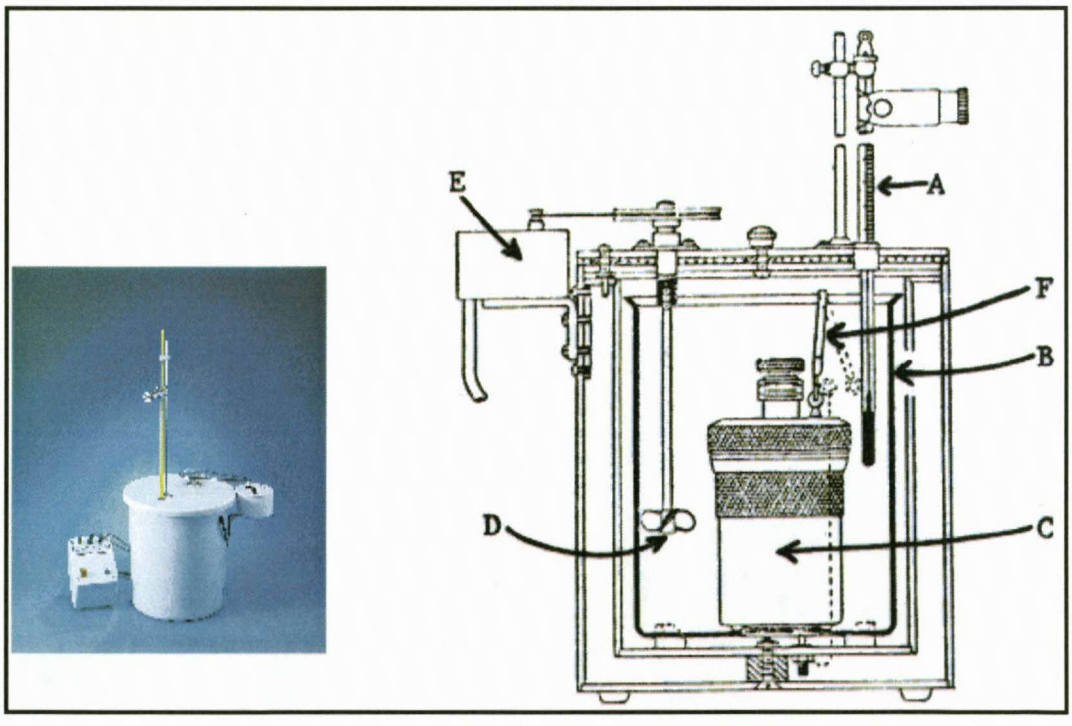

Figure 3.1: Cross section of Parr plain calorimeter[120]; **A** – thermometer, **B** – inner jacket (bucket), **C** – bomb, **D** – stirrer, **E** – stirring motor, **F** – wire to firing mechanism

[120] http://ntweb.deltastate.edu/vp_academic/jbentley/teaching/labman/bomb/bomb1.htm (08 Nov 2011)

B. Tölg container

This instrument is operated up to a maximum pressure of 200 bar and up to a maximum temperature of 260 °C.[121] The instrument is shown in **Figure 3.2**. The sample and the digesting acid or combinations of acids are added to the PTFE (polytetrafluoroethylene) cup enclosed in a steel bomb. No special gas is added but the atmospheric gas is trapped in the bomb when the cup is shut in before the heating of the mixture. The bomb is inserted in the heating blocks and the temperature regulator is turned on to the temperature of choice. Due to high pressures and temperatures employed, this system is capable of completely digesting almost any sample and getting the sample into solution. However, some samples require longer times to be entirely digested depending on the choice of acid combinations and the components of the sample.

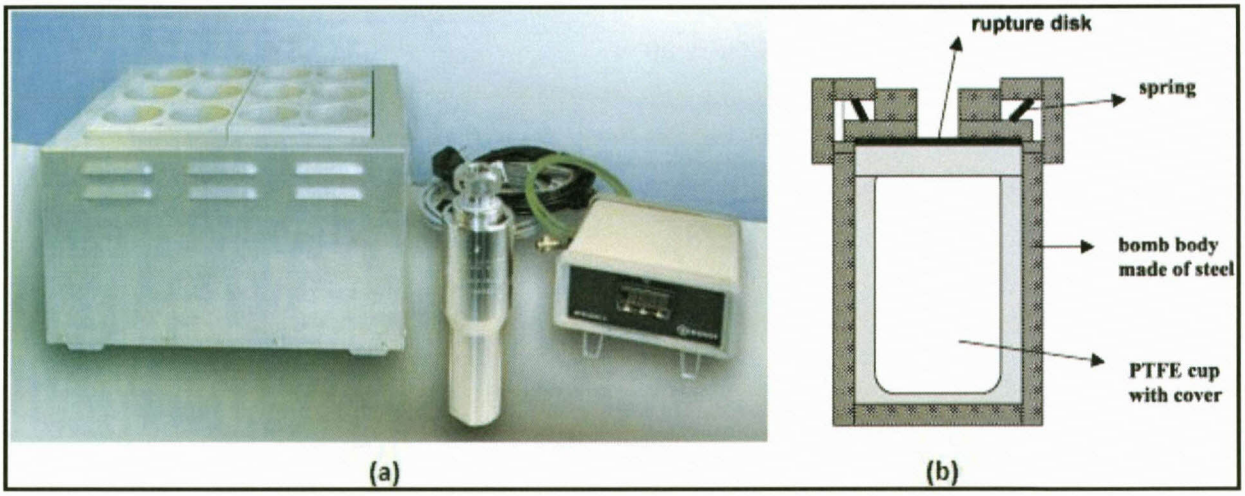

Figure 3.2: (a) Tölg's stainless steel pressure digestion system with a 12-sample heating block and temperature regulator; (b) Scheme of Tölg's PTFE bomb for sample preparation[121]

C. Knapp Asher

A high-pressure Asher similar to the Tölg container, and which enables the decomposition of samples at 180 – 300 °C was developed by Knapp[122] to generate practically carbon-free solutions. The Asher is shown in **Figure 3.3**. The Asher operates with the same principles as the Tölg bomb with minor deviations of instrument components. The sample and the

[121] http://www.chemeurope.com/en/whitepapers/43107/pressure-digestion-for-sample-preparation.htmL (10 Nov 2011)

[122] G. Knapp; *Fresenius Z. Anal. Chem.* **317**, p. 213 (1984)

digesting acid or combinations of acids are added to the quartz vessel, which is then closed with a quartz lid and a PTFE stripe. The vessel is inserted in a steel autoclave coupled to a heating element, which in turn is closed with its steel lid. An external gas, preferably nitrogen, at a pressure of 14 megapascals (MPa) is added to the autoclave so as to compensate for the vapour and reaction gas pressures generated during the decomposition.[118]

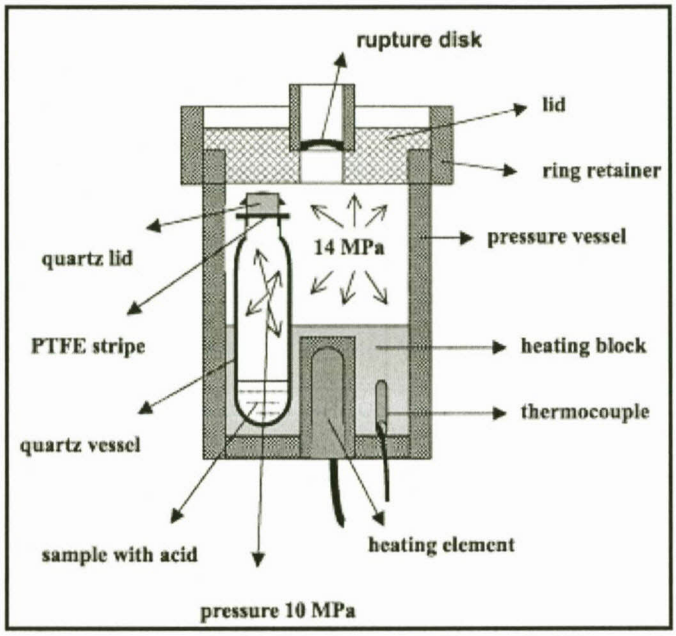

Figure 3.3: Scheme of Knapp's high-pressure Asher for sample preparation[122]

3.2.2.2 MICROWAVE-ASSISTED DIGESTION METHODS[123]

Microwave-assisted digestion has been recently used and is the preferred method instead of thermal-initiated digestions.[96-99,122] However, conflicting evidences were provided for and against this method in the digestion of zircon materials (see **Chapter 2, Section 2.2.5**). Ma and Li[98] reported the success of digesting zircon ore with microwave-assisted ammonium sulphate-sulphuric acid digestion while Lötter[99] disputed this statement by reporting the method as less viable in digesting various zircon materials. Microwave-assisted digestion is also a pressure digestion technique as the sample is directly heated *via* interaction with microwaves and the pressure resulting from the reaction accelerates the decomposition of the sample. However, it is advantageous over thermal-assisted digestion due to shorter times (less than 1 hour) needed to decompose the sample. PTFE pressure vessels that can take up to 700 kPa and up to 200 °C are used for this type of decomposition.[118] Most research

[123] http://hyperphysics.phy-astr.gsu.edu/hbase/ems1.htmL (18 Oct 2011)

and large-scale industrial microwave applications are in the range of 3 – 30 GHz (gigahertz) even though there are some radar bands which fall in the range 1300 – 1600 MHz (megahertz).

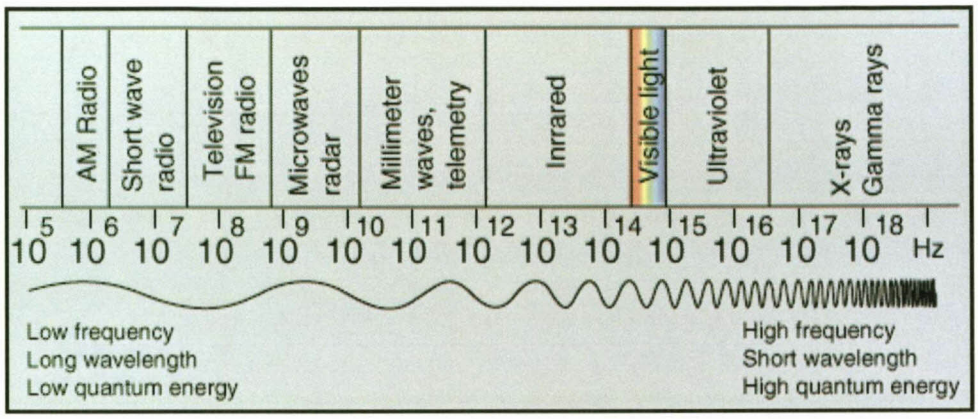

Figure 3.4: The electromagnetic spectrum[123]

Microwaves have wavelengths of 0.1 – 100 cm and are situated in the region between the infrared and radio frequencies in the electromagnetic spectrum (**Figure 3.4**). In a microwave digester the waves are produced by a device called a magnetron based on the phenomenon explained in **Figures 3.5** and **Figures 3.6**.

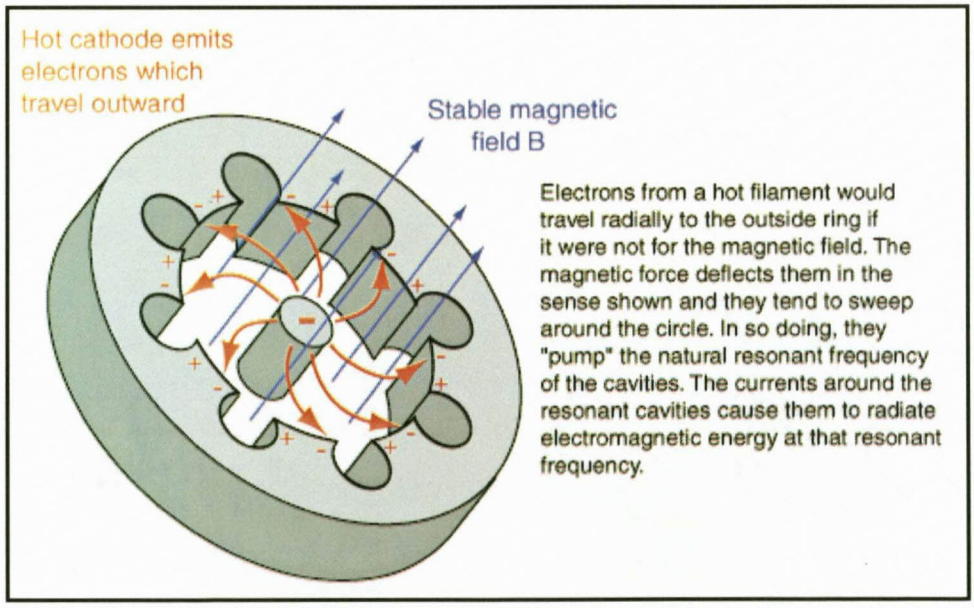

Figure 3.5: The magnetron[123]

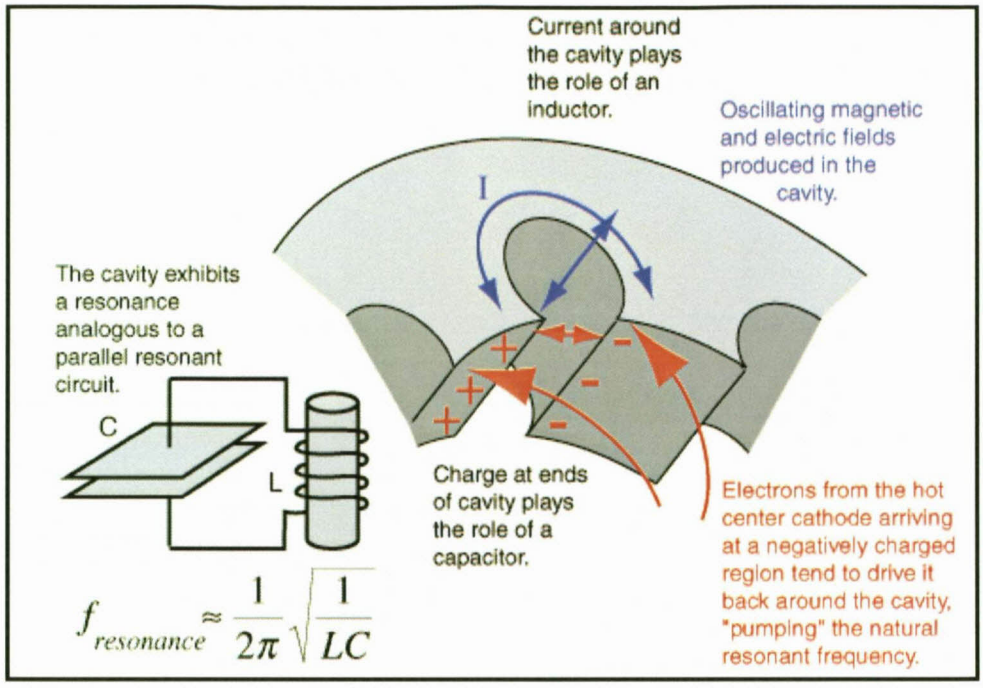

Figure 3.6: The operating concept of a magnetron[123]

In the electromagnetic spectrum, each wave has quantum energies enough to excite various processes of chemical and physical substances (**Figure 3.4**). The higher energy spectra have the strength to displace electrons from an atom and thus produce ionization while the relatively lower quantum energies of microwave photons are capable of interacting with a molecule and course it to rotate or twist. However, metallic samples absorb microwaves to cause electric currents which will in turn heat the material.

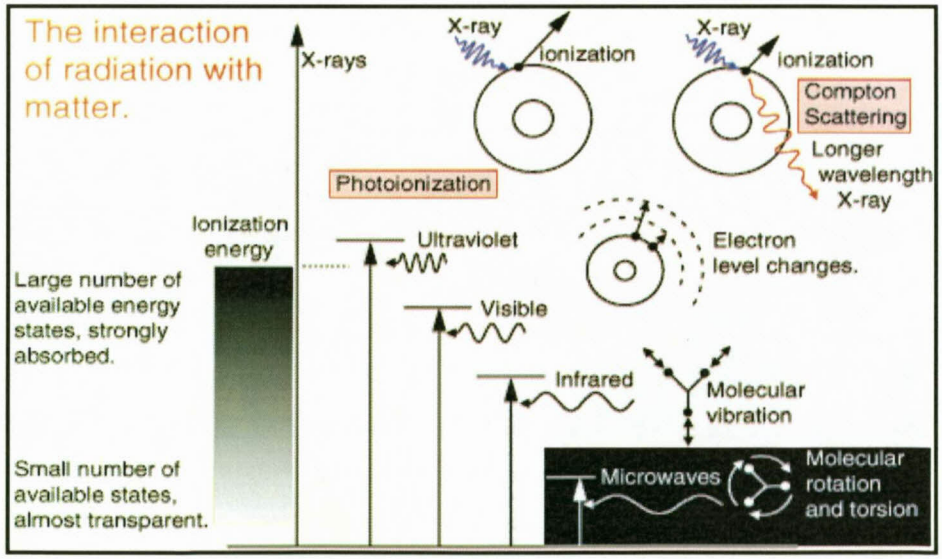

Figure 3.7: The interaction of various electromagnetic radiations with matter[123]

Sun *et al.*,[124] mentioned that microwave heating is advantageous in that i) it can accelerate reaction rates and reduce reaction temperatures by decreasing activation energy and ii) provides a benefit of saving costs in capital investment, labour and energy by reducing reactors and production facilities to smaller quantities than needed for conventional heating.

A report on comparison of sample preparation using different digestion methods such as acid, pressure and microwave decompositions was compiled by Berghof Products and Instruments.[125] While the report advocates for microwave digestion it noted several disadvantages such as i) the dependence of actual heating in the microwave on sample type, quantity and type of digestion medium and ii) the high rate with which the samples are heated can result in exothermic reactions during the digestion process. The summary of comparison of sample preparation by various digestion methods is depicted in **Table 3.1**.

3.2.3 BENCH-TOP DIGESTION

Bench-top digestion is normally the first and easiest method to perform the digestion of inorganic materials and minerals, involving mainly strong acids and alkalis. An open digestion system involving various mineral acids may seem disadvantageous considering the possibility of contamination of the reaction system from the environment. One other disadvantage of an open system is the possible loss of some sample components due to factors like volatility, sputtering and adsorption to the vessel walls, which may lead to the underestimation of elemental contents. The most important acids that are usually used for bench-top or open vessel digestion are HF, H_2SO_4, HCl, HNO_3 and *aqua regia*.

3.2.3.1 HYDROFLUORIC ACID DIGESTION

Hydrofluoric acid is mainly used for the digestion of silicate rocks and minerals and the excess 40 % HF is normally removed by the evaporation with H_2SO_4 or $HClO_4$. However, the use of hydrofluoric acid as a digesting medium has proved to be successful in the complete digestion of zirconium metal (see **Equation 3.1**).

$$Zr_{(s)} + 4HF_{(aq)} \longrightarrow ZrF_4 + 2H_2\uparrow \qquad (3.1)$$

[124] X. Sun, J-Y. Hwang, X. Huang, B. Li and S. Shi., *J. Miner. Mater. Charac. Eng.*, **4** (2), pp. 107 – 112 (2005)

[125] http://www.berghof.com (18 Oct 2011)

Pure zirconium metal is susceptible to oxidation by air, which leads to a small layer of oxide covering the metal. This layer renders zirconium indigestible to many mineral as well as organic acids, bases and salts but is reactive towards HF.[126] The dangers of working with this acid have led to the need for alternative digestion methods in getting zirconium into solution.

3.2.3.2 SULPHURIC ACID DIGESTION

Sulphuric acid (H_2SO_4) is the most versatile acid in the digestion of the majority of inorganic compounds and minerals, mainly due to its high boiling point, which is its major advantage as a reagent. The digestibility of zirconium metal by sulphuric acid leads to the release of molecular hydrogen gas in the same way as the hydrofluoric acid. This gas may in turn be difficult to deal with if necessary caution is not considered (see **Equation 3.2**).

$$Zr_{(s)} + 2H_2SO_4 \xrightarrow{150^{\circ}C} Zr(SO_4)_2 + 2H_2\uparrow \qquad (3.2)$$

Carcassi and Fineschi[127] mentioned that for the hydrogen-air gas mixture to support combustion and the subsequent explosiveness, the volumetric concentration of hydrogen would have to reach the flammability range of 4 – 75 %. Thus, the release of the hydrogen gas from any of the above reactions of sulphuric and hydrofluoric acids with zirconium would, for analytical purposes, be on a small scale; *i.e.* it will not cause any explosion when mixed with the atmosphere. However, the digestion of zirconium metal with sulphuric acid would serve as the preferred method of choice compared to the extremely dangerous hydrofluoric acid.

3.2.3.3 HYDROCHLORIC ACID DIGESTION

Hydrochloric acid is ideally employed in the digestion of many metal oxides and metals that are more easily oxidized than hydrogen.[128] Hydrochloric acid is, however, incapable of digesting zirconium at room temperature and when boiled, it evaporates and its concentration is reduced even further to be able to digest the metal.

---

[126] Kirk-Othmer *Encyclopedia of Chemical Technology*, **3** (24), John Wiley & Sons, pp. 863 – 896 (1984)

[127] M.N. Carcassi and F. Fineschi., *Energy*, **30**, pp. 1439 – 1451 (2005)

[128] D.A. Skoog, D.M. West and F.J. Holler., *Fundametals of Analytical Chemistry*, 6th Ed., Saunders College Publishing, pp. 764 – 774 (1992)

3.2.3.4 NITRIC ACID DIGESTION

Hot nitric acid digests most common metals with the exception of those that form a surface oxide, which renders them unreactive to many mineral acids, *e.g.* zirconium, aluminium and chromium.

3.2.3.5 AQUA REGIA DIGESTION

Aqua regia, a mixture of three volumes of hydrochloric acid to one of nitric acid, acts as the oxidizing reagent in the digestion of metals. A characteristic yellowish-brown chlorine gas is released from the making of this mineral acid mixture (see **Equation 3.3**)

$$HNO_3 + 3HCl \longrightarrow NOCl + 2H_2O + Cl_2\uparrow \qquad (3.3)$$

However, *aqua regia* is as weak in the digestion of zirconium metal as nitric acid or hydrochloric acid.

3.2.4 COMPARISON OF OPEN AND CLOSED DIGESTION METHODS

Table 3.1: A summary of benefits and limitations of open and closed acid digestion systems

Open acid digestion	Closed acid digestion
Maximum temperature limited by the solution's boiling point	Maximum temperature: 260 – 300 °C
Permits large sample mass	Requires small sample quantities
High acid consumption	Reduced acid consumption resulting in reduced blank values
Digestion quality frequently unsatisfactory	High digestion quality
Loss of volatile elements	No loss of volatile elements
Contamination risk	No contamination risk
Digestion period of about 2 – 5 hours	Digestion period of about 20 – 60 min. (microwave digestion)

3.3 ANALYTICAL TECHNIQUES

After digestion and the dissolution of a sample into aqueous solution, several analytical methods may be employed based on the availability, sensitivity and selectivity of equipment to the sample components. The best technique to be employed will be that which enables rapid, accurate and reproducible analysis. An overview of principles on analytical techniques such as AAS, ICP-OES and ICP-MS, NAAS as well as XRD and XRF will be done.

3.3.1 ATOMIC ABSORPTION SPECTROSCOPY (AAS) [129]

The AAS technique operates on the principles of Beer-Lambert law by measuring the absorbance and emission of radiation by atoms. Samples are atomized into their constituents and one element is analyzed per measurement. Most commonly used atomizers are flame (FAAS) and electrothermal or graphite tube atomizers (ETAAS/GFAAS). FAAS is the oldest technique which uses acetylene coupled with either air or nitrous oxide flame to excite elements of interest. The nitrous-acetylene FAAS is ideal for application when analysis is done for analytes with high affinity for oxygen. Flames with temperatures of up to 2500 K are generated for air-acetylene gas and those for nitrous oxide-acetylene gas are generated at 3000 K. Dissolved sample solutions are introduced into a spray chamber by pneumatic nebuliser as aerosol, which then mixes with flame gasses and result in the processes such as desolvation, vaporization, atomization and ionization taking place (see **Figure 3.8**).

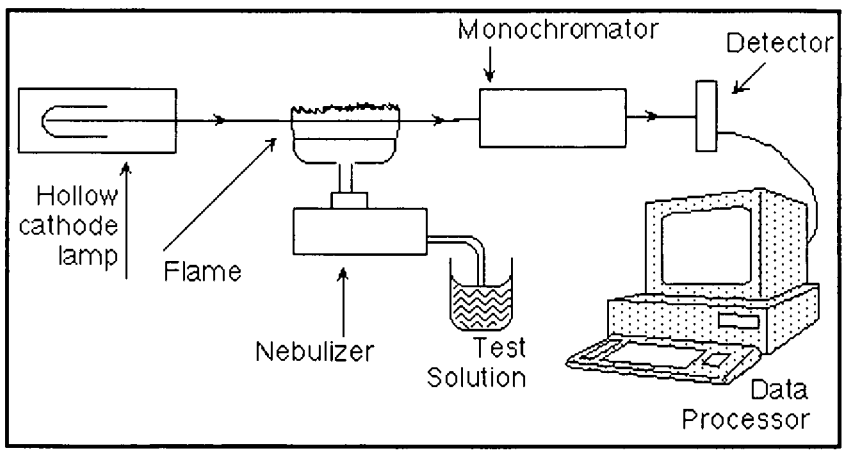

Figure 3.8: Components of AA spectrometer[130]

[129] http://en.wikipedia.org/wiki/Atomic_absorption_spectroscopy (21 Oct 2011)

[130] http://www.chemistry.nmsu.edu/Instrumentation/AAS1.htmL (21 Oct 2011)

During the process of desolvation, the solvent is dried by evaporation and the ultra small particles of the sample remain. The solid particles are vaporized and converted into gaseous molecules, which dissociate into individual atoms. Atoms may be converted to gaseous ions depending on their potential ionization energy or the different energy portions in the flame. During any of these processes, there is a risk of interference and the degree thereof may vary for the element in the calibration solution and in the sample. It is generally undesirable to have the ionization process as the number of atoms being analyzed is reduced, resulting in the underestimation of element content in the sample.

Figure 3.9: Graphite tubes[131]

In electrothermal AAS (ETAAS), also known as graphite furnace AAS (GFAAS), samples can be analyzed directly as solids, liquids or gasses in a graphite tube (see **Figure 3.9**). A sample, in any of the mentioned forms, is introduced into the graphite tube and heated to a programmed and monitored temperature so as to control the processes of desolvation, pyrolysis, atomization and finally cleaning of the tube.

In pyrolysis, the majority of the matrix components are removed so as to minimize interference and this is further improved by delaying atomization until the gas phase in the atomizer has reached a stable temperature. The delay is achieved by atomization of sample from a graphite platform inserted into the graphite tube rather than from the tube wall. Cleaning is lastly done by removing eventual residues in the graphite tube at high temperature. The sensitivity of ETAAS is 2 – 3 orders of magnitude higher than that of FAAS

[131] http://www.world-trades.com/selling/776/802/lab-supplies-7.htmL (30 Nov 2011)

where analyses of samples can be done at parts per billion (ppb) ranges. Both FAAS and ETAAS make use of hollow cathode lamps as sources of radiation (see **Figure 3.10**). The disadvantage of both these atomic absorption spectroscopies is the analysis of one element at a time, which is time consuming and a lot of sample is needed for these types of analyses.

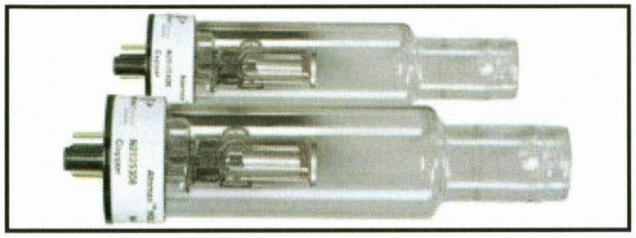

Figure 3.10: Hollow cathode lamps for AAS[132]

3.3.2 INDUCTIVELY COUPLED PLASMA (ICP) TECHNIQUE[133]

There are two types of inductively coupled plasma, namely ICP-OES and ICP-MS. ICP-OES qualitatively and quantitatively analyze the elements by measuring their characteristic wavelengths and the intensity with which they emit such wavelengths respectively. In ICP-MS, the elements are analyzed by measuring the atomic weight to the charge created by ionization (m/z).

Inductively coupled plasma works in a similar manner as the atomic absorption spectroscopy but uses inert gas such as argon, which is converted to a plasma (**Equation 3.4**), to effectively excite any element at temperatures in the 5000 – 10000 K range. A spark from a Tesla coil initiates the plasma.

$$Ar_{(g)} + \text{Energy} \longrightarrow Ar^{+} + e^{-} \qquad (3.4)$$

A plasma is generated when argon gas is supplied to the water-cooled load coil, and the high radio frequency (RF) electric current from RF generator is applied to the work coil at the tip of the torch tube. The electromagnetic field created in the tube from the high frequency current is then used to ionize the argon gas and thus the plasma is generated (see **Figure 3.11**). The

[132] http://www.analytics-shop.com/gb/spectroscopy/atomic-absorption-spectroscopy-aas.htmL (30 Nov 2011)

[133] J.R. Dean., *Practical Inductively Coupled Plasma Spectroscopy*, John Wiley & Sons, Chichester (2005)

ohmic resistance of the charged gas, generated at the end of the torch, occurs when an electrical current is passed through a conductor that in turn creates more heat.

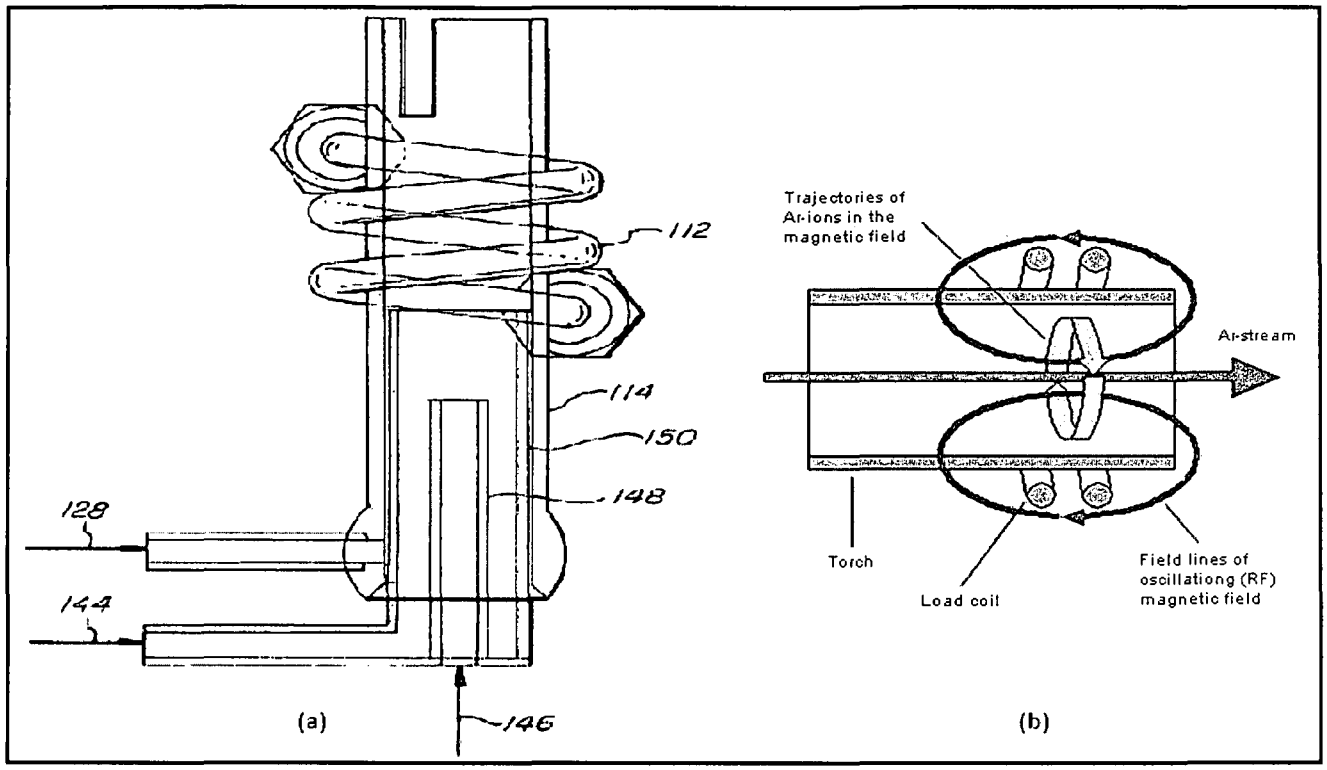

Figure 3.11: (a) Components of an ICP torch; **112** – load coil, **114**, **148**,**150** – concentric tubes, **128** – carrier gas flow, **144** – auxiliary gas flow and **146** – atomized sample flow. (b) Generation of plasma in an ICP torch[134,135]

The advantage of using argon as the plasma is its inhibiting effect towards elements forming oxides and nitrides, which may result in false readings due to elements being rendered unexcitable.[136] When the sample is introduced as a nebulised aerosol into argon plasma, the atomic components are excited from their ground state (low energy level) to an excited state (high energy level). As they return from their excited state to the ground state, these atomic components emit their characteristic radiation (see **Figure 3.12**).

[134] P.J. Morrisroe and T. Myles., U.S. Patent **7106438 B2** (2006)

[135] http://www.msscien.com/aj/Fund_AAS/web/alternate-techniques.129%20m52087573ab0.0.htmL(21Oct2011)

[136] http://www.siint.com/en/products/icp/tec_descriptions/descriptions1_e.htmL (21 Oct 2011)

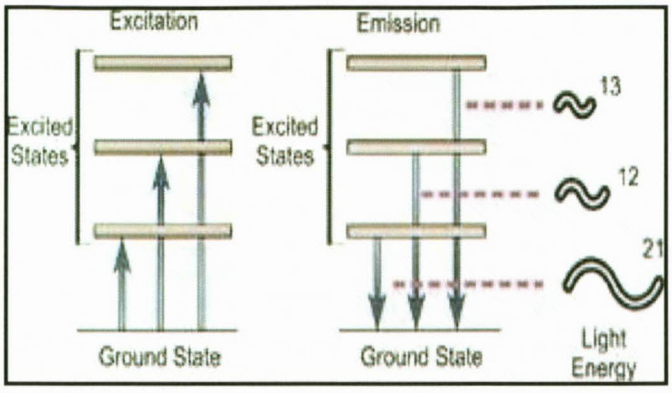

Figure 3.12: Energy transitions of electrons[137]

A sample is introduced into the instrument by means of a peristaltic pump which is connected to the nebuliser. The nebuliser sprays the sample as an aerosol into the spray chamber where the small amount of aerosol enters the gas flow into the plasma (see **Figure 3.13**).

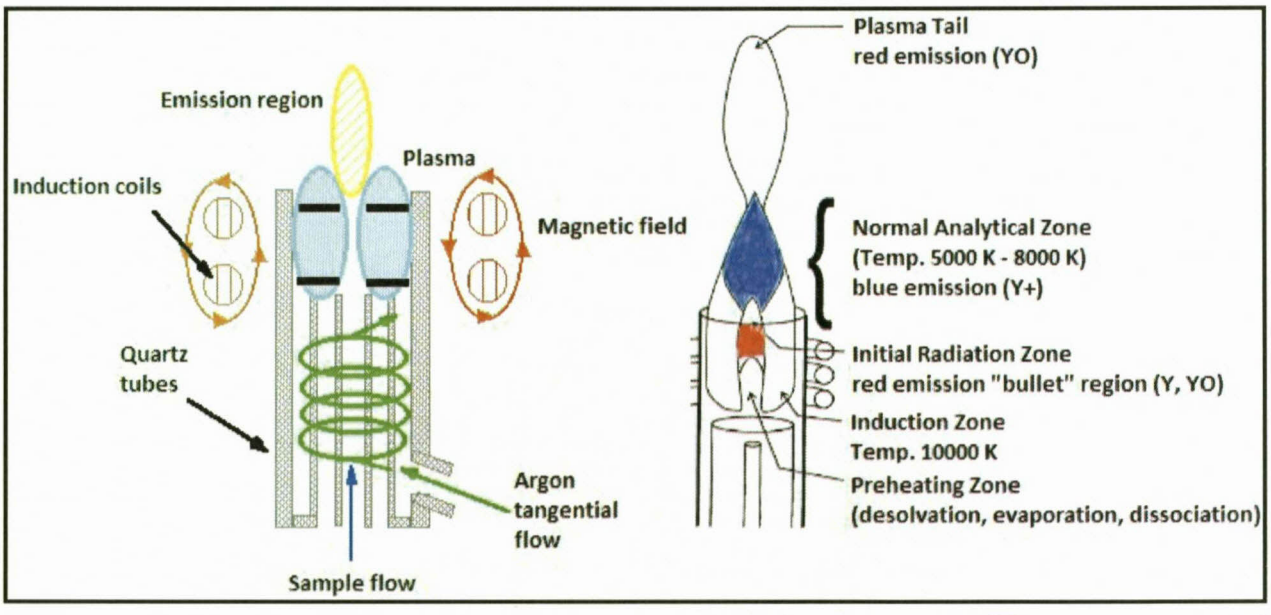

Figure 3.13: Temperature regions of a typical ICP discharge[138]

Three dominant processes in the spray chamber may occur, namely i) collisions of sample droplets with the walls, ii) droplet-droplet collisions due to low sample uptake from the spray chamber to the plasma and iii) evaporation from the walls, which may cause matrix interferences if the walls are not preconditioned with the sample before the analysis.[139] The

[137] http://www.andor.com/learning/applications/Atomic_Spectroscopy/ (21 Oct 2011)

[138] http://www.chemistry.nmsu.edu/Instrumentation/NMSU_Optima2100.htmL (21 Oct 2011)

[139] L.F. Østergaard., *Procedures for the determination of stable elements in construction materials from the nuclear reactors at Risø National Laboratory*, Risø National Laboratory, Roskilde, Denmark (2006)

instrument is insulated by the constant flow of gasses such as the outer gas, intermediate gas and the carrier gas. These gasses prevent the possibility of short-circuiting as well as meltdown as a result of high temperatures of plasma. When the elements emit their unique wavelength radiances, after being excited by the plasma, the ICP-OES detector measure each wavelength to determine which elements are present in the sample and record these on the computer (see **Figure 3.14**).

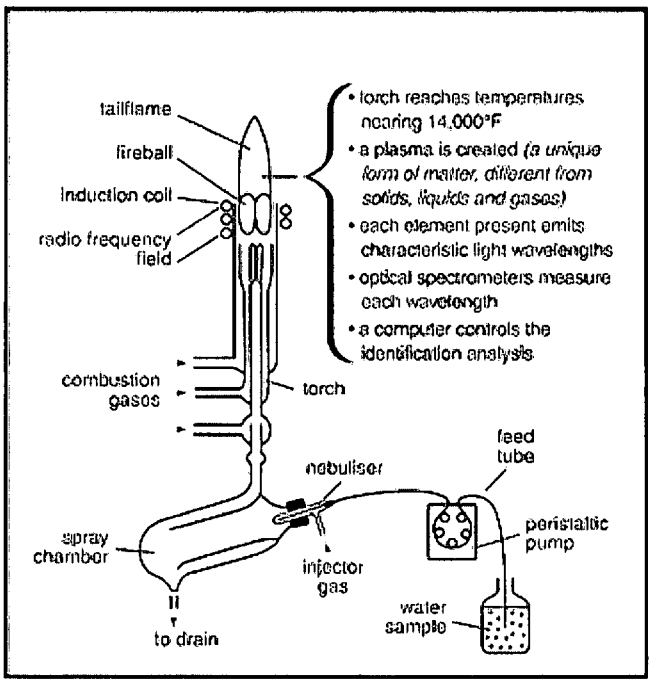

Figure 3.14: Schematic representation of the ICP components and the process of analysis[140]

3.3.2.1 ICP-OES EQUIPMENT[136]

There are two types of ICP-OES instruments based on differences in the spectrometer and the detector, namely sequential and simultaneous equipment.

A. *Sequential ICP-OES*

This type possesses a spectrometer with a Czerny-Turner monochromator, and a most common detector with a photomultiplier tube (PMT). The programmed wavelength of the spectrometer is consecutively varied to measure multiple elements. This is rather time

[140] http://www.cleanwatertesting.com/news_NR149.htm (21 Oct 2011)

consuming, but due to its high resolution spectrometer, it is favourable for the measurement of high-matrix samples (see **Figure 3.15**).

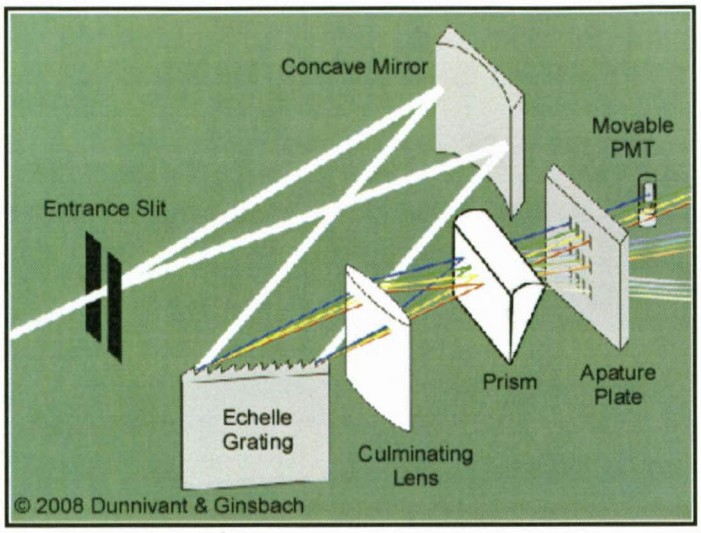

Figure 3.15: A sequential (single detector) type monochromator ICP-OES system[141]

B. *Simultaneous ICP-OES*

Simultaneous ICP-OES systems typically use an echelle cross disperser in spectrometer and semi-conductor detector such as charge couple device (CCD) or charge injection device (CID) for the detector (see **Figure 3.16**). PMT is also used.

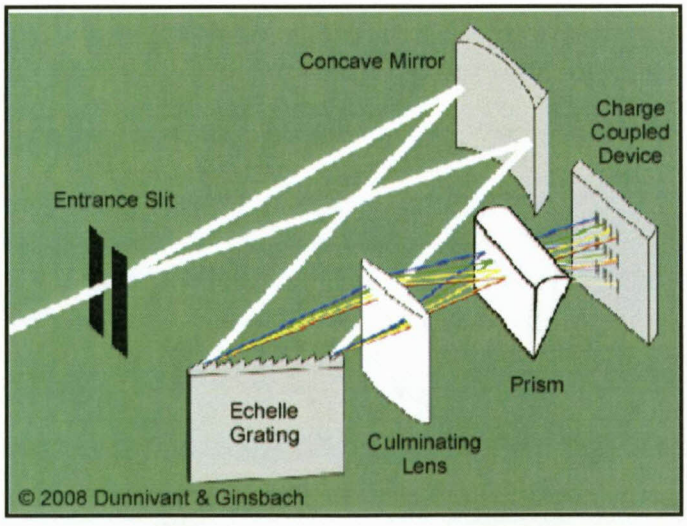

Figure 3.16: A multi-detector type monochromator ICP-OES system[141]

[141] http://people.whitman.edu/~dunnivfm/FAASICPMS_Ebook/CH3/3_3_4.htmL (21 Oct 2011)

A combination of prism and echelle diffraction grating enables the echelle cross disperser to scatter light of measurable wavelength range two-dimensionally and a combination of echelle cross disperser and a CCD detector simplifies the multi-element measurement at any wavelength. This equipment rapidly measures up to 72 elements in about 1 to 2 minutes. Simultaneous multi-channel ICP-OES has rapidly become economical as component production costs decreased and labour costs increased with time.[141]

3.3.2.2 ICP-MS EQUIPMENT

ICP-MS instruments are less susceptible to matrix interferences due to factors such as plasma modelling and shorter times for sample washout. Improvements in practical analysis of semiconductor gases and development of helium plasmas for ICP-MS have been achieved through plasma remodelling.[142] A schematic representation of ICP-MS components and the processes of analysis are shown in **Figure 3.17** below.

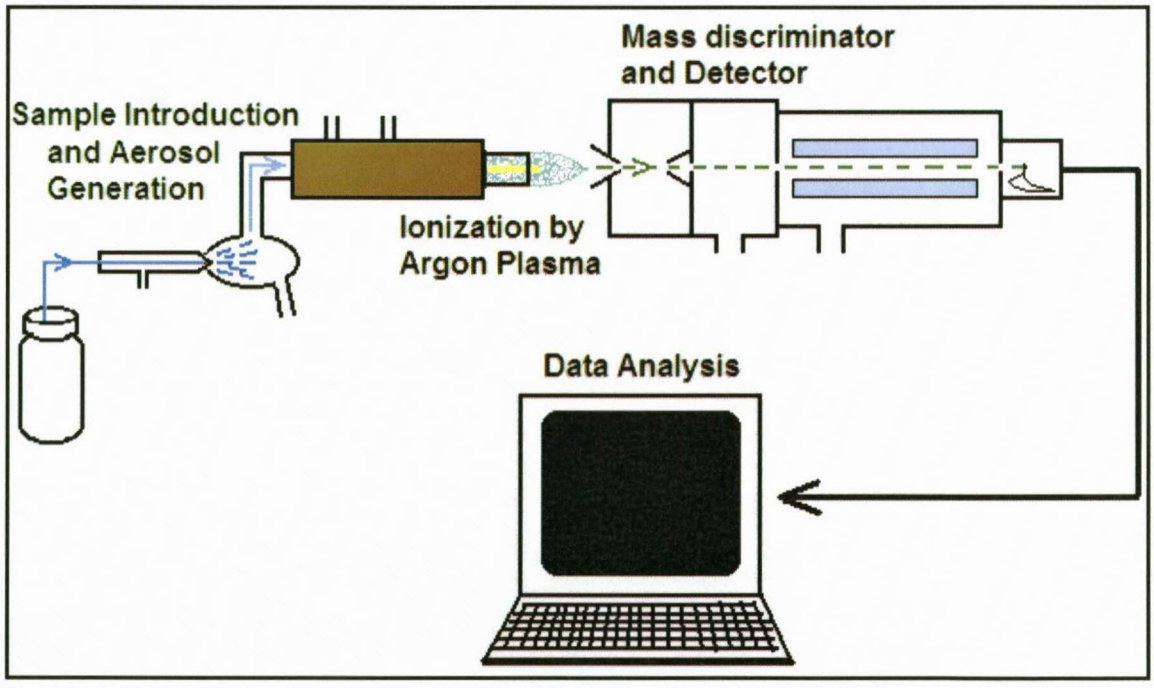

Figure 3.17: Schematic representation of ICP-MS components and processes[143]

Another different aspect of ICP-MS is the ability to analyze solid samples by using laser ablation which can be bought as an accessory.[143] It is vital to have a vacuum environment at

[142] J.W. Olesik., *Anal. Chem.*, **68** (15), pp. 469A – 474A (1996)

[143] http://www.cee.vt.edu/ewr/environmental/teach/smprimer/icpms/icpms.htm (30 Nov 2011)

the interface of ICP and MS systems so that the ions are free to move without collisions with atmospheric molecules. The ions are removed from the plasma by a pumped extraction system and enter the mass spectrometer. A produced ion beam is focussed into a unit where different isotopes are separated based on their mass to charge ratio (m/z) by quadrupole analyzers (see **Figure 3.18**).

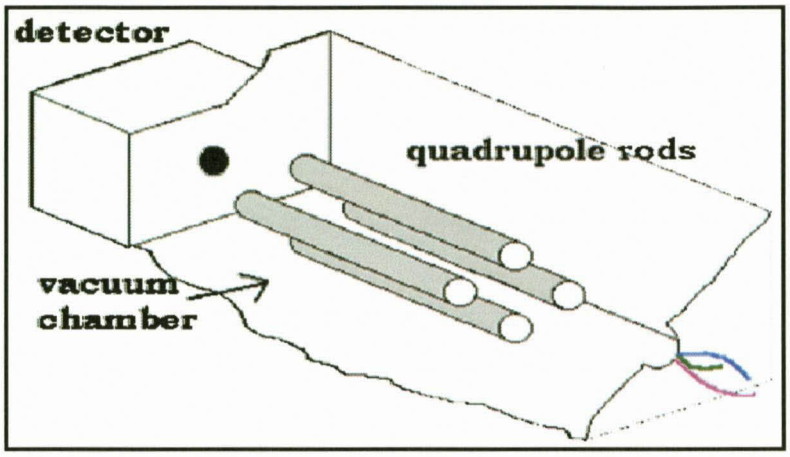

Figure 3.18: ICP-MS quadrupole mass filter separating ions[143]

3.3.3 NEUTRON ACTIVATION ANALYSIS SPECTROMETRY (NAAS)

The neutron activation analysis technique is initiated by placing of a sample in a neutron field that has been produced by a neutron source. The sample is then bombarded with neutrons to convert stable isotopes to radioactive isotopes. The radioisotopes formed due to irradiation decay with time and a portion of energy is released in the form of gamma rays, which then escape from the sample with characteristic radioisotope energies.[144]

A functional illustration of modern inventions for measuring element at trace concentrations is shown in **Figure 3.19**. Moderator assembly (**1**) is made of steel and/or lead shielding that is filled with polyethylene or any hydrocarbon polymer, holds a neutron source (**2**) which may be any substance that produces a predictable flux of neutrons, *e.g.* californium-252, close to an irradiation chamber (**3**). Samples (**4**) with known geometry are placed in irradiation chamber to allow for the absorption of neutrons from the source. During the process these species become activated and radioactively unstable due to the irradiation. The samples are then carefully removed from the moderator assembly and placed close to a radiation detector

[144] E.C. Pearcy, M.S. Jarzemba and J.R.Weldy., U.S. Patent **6577697** (2003)

(**5**) to allow for the measurement of the subsequent radiation from the decay of the unstable elements in the activated sample.

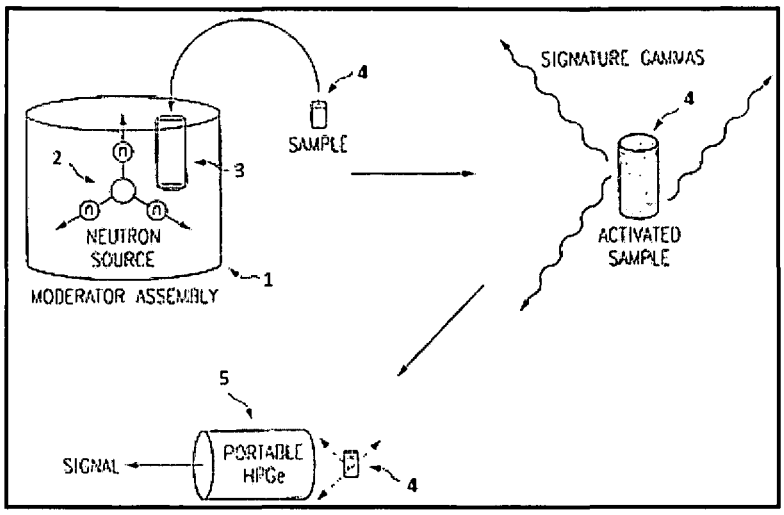

Figure 3.19: Procedure of NAAS in analyzing trace elements; **1** – Moderator assembly, **2** – Neutron source, **3** – Irradiation chamber, **4** – Sample, **5** – Radiation detector [144]

There are 75 elements that may be quantitatively measured using NAAS (see **Table 3.2**).

Table 3.2: Elements that are quantitatively analyzed using NAAS[145]

Aluminium	Gadolinium	Neodymium	Sodium
Antimony	Gallium	Nickel	Strontium
Arsenic	Germanium	Niobium	Tantalum
Barium	Gold	Osmium	Tellurium
Bromine	Hafnium	Palladium	Terbium
Cadmium	Indium	Platinum	Thorium
Cerium	Iodine	Potassium	Thulium
Caesium	Iridium	Praseodymium	Tin
Chlorine	Iron	Rhenium	Titanium
Chromium	Lanthanum	Rubidium	Tungsten
Cobalt	Lutetium	Ruthenium	Uranium
Copper	Magnesium	Samarium	Vanadium
Dysprosium	Manganese	Scandium	Ytterbium
Erbium	Mercury	Selenium	Zinc
Europium	Molybdenum	Silver	Zirconium

[145] http://www.sciner.com/Neutron/naa.htmL (30 Nov 2011)

Most of these elements, except for zirconium, have large cross section for neutron capture and are more likely to be activated. Thus, depending on the element under investigation, NAAS analysis can take a long time to be done due to the stability of some isotopes generated and their subsequent emission of radiation. This leads to the lower accuracy, about 5 %, and relative precision, about 0.1 %, in the analysis of these elements.[146] Other disadvantages of NAAS are that it is expensive to carry out and that the sample becomes very radioactive afterwards, which would need special radiological handling.

3.3.4 X-RAY FLUORESCENCE AND DIFFRACTION (XRF/XRD)[147]

X-ray fluorescence is when the sample absorbs X-rays and generating electronically excited ions which return to their ground state by transitions involving electrons from higher energy levels. An excited ion with a vacant K-shell is produced when the element absorbs radiation of quantum energy exactly equal to the energy required to remove the electron just to the outer part of the atom; after a short period, the ion returns to its ground state following a series of characteristic electronic transitions and emission of fluorescent wavelengths similar to those resulting from excitation by electron bombardment (see **Figure 3.20**).

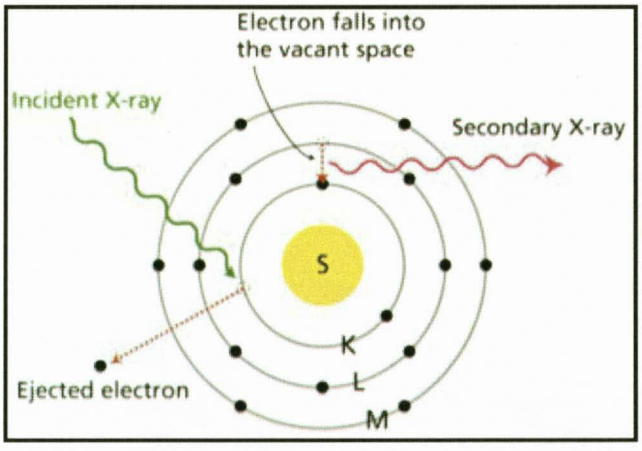

Figure 3.20: Principle of X-ray fluorescence[148]

The advantage of XRF, as compared to AAS, ICP and NAAS, is its general non-destructive and cost effective approach.[149] However, its disadvantage is the inability to generally analyze

[146] A.M. Pollard and C. Heron., *Archaeological Chemistry*, Cambridge Royal Society of Chemistry (1996)

[147] D.A. Skoog, F.J. Holler and T.A. Nieman., *Principles of Instrumental Analysis*, 5th Ed., Brooks/Cole, pp. 272 – 296 (1998)

[148] http://www.oxford-instruments.com (15 Dec 2011)

elements lighter than fluorine. Different XRF equipment manufacturers will have specific arrangements of components and one of XRF instruments is shown in **Figure 3.21**. The components include beam filters located between X-ray source and sample to filter out undesirable and interfering parts of the source radiation for some applications and to improve signal-to-noise ratio. There are collimators consisting of parallel slats which are used to select parallel beam of X-radiations from the sample and focus them onto a crystal changer.

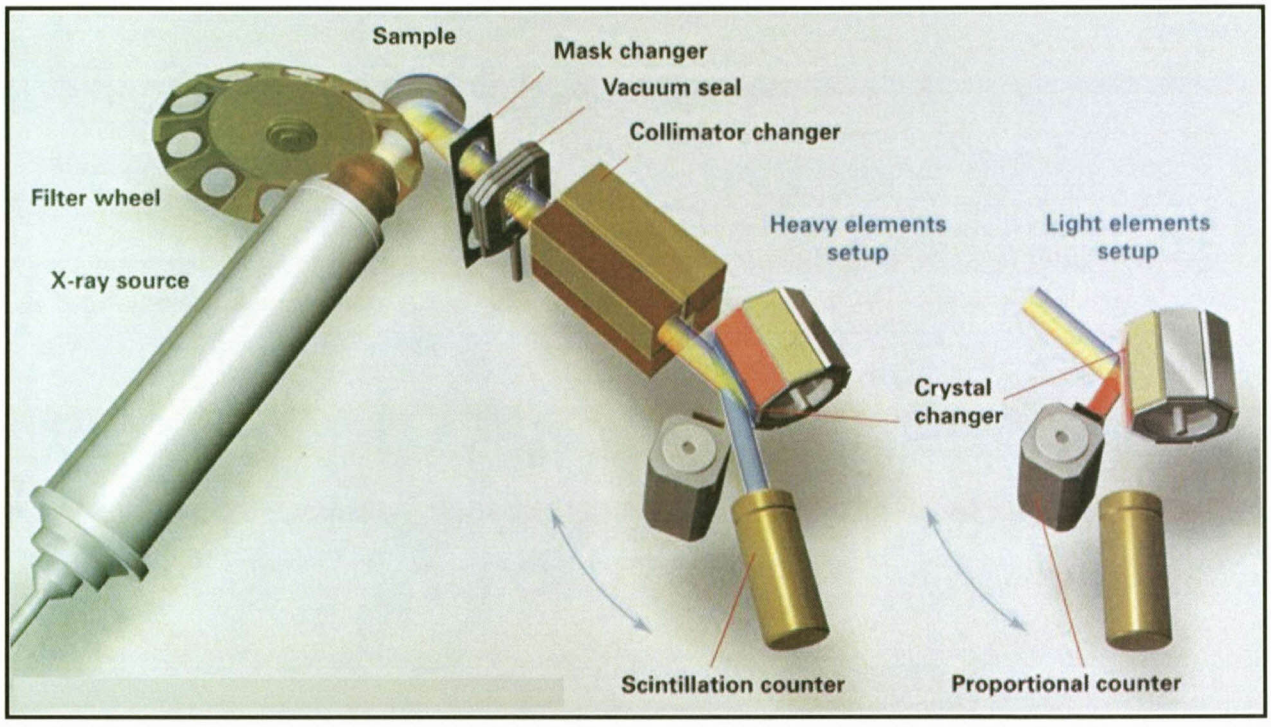

Figure 3.21: XRF component arrangement in a Bruker S8 Tiger WDXRF[150]

Samples can be analyzed in different forms, including solids like metals and powders, fused beads and liquid forms. X-ray diffraction (XRD) is when the X-radiation interacts with electrons in the sample and get scattered by the controlled environment in crystal changer. Scattered rays result in interference among themselves because distances between scattering centres are of similar order of magnitude as the wavelength of the radiation. Every crystalline substance has a characteristic pattern of diffracting the X-rays, and this pattern is the basis for which a particular sample, or substance, can be identified when XRD analysis is done.[151] Thus, during an XRD analysis, the components of a sample can be identified by

[149] http://stephenson-associates-inc.com/XRF%20Basic%20Principles.pdf (15 Dec 2011)

[150] http://naturweb.uit.no/ig/xrf/AboutXRF.htmL (15 Dec 2011)

[151] http://epswww.unm.edu/xrd/xrdbasics.pdf (07 Jan 2012)

their diffraction patterns observed and compared to any of the known and established patterns.

3.4 VALIDATION OF ANALYTICAL METHODS[152]

The objective of validation is to illustrate that a method is suitable for its intended purpose and to ensure that analytical results in all areas of analysis are accurate and reliable. In obtaining the overall knowledge of the capabilities of an analytical procedure, it is best to plan and execute the experimental work such that the appropriate validation aspects and parameters are considered at the same time.

3.4.1 VALIDATION PARAMETERS[153]

Analytical methods may be either qualitative or quantitative/semi-quantitative. Qualitative analyses are only necessary for the determination of the element presence in a particular sample while quantitative methods would extend such an investigation to determine the amount of a particular element or group of elements in a given sample. Methods may be developed and validated by the laboratory for the purpose of its own special needs or they can be developed and validated for global investigations with convergent purposes. Thus the extent of validation of methods may be greatly different. There are factors which are taken into consideration before and when selecting a method. These include limit of detection (LOD), precision, accuracy, and limit of quantification (LOQ), recovery as well as selectivity, to name a few.

3.4.1.1 DETECTION LIMITS (LOD and LOQ)

The limit of detection of any given element is its smallest amount in a sample which can be detected using the chosen analytical procedure. The limit of detection can be expressed by deriving the smallest concentration, x_L, which can be detected with a reasonable certainty for a given procedure. The presence of an analyte at this concentration will be indicated by

[152] C.C. Chan, Y.C. Lee, H. Lam and X-M. Zhang., *Analytical Method Validation and Instrument Performance Verification*, John Wiley & Sons Inc., pp. 11 – 22, 51 – 66 (2004)

[153] E. Prichard and V. Barwick., *Quality Assurance in Analytical Chemistry*, John Wiley and Sons Ltd., pp. 51 – 93 (2007)

the procedure, at the stated level of significance, but without specifying the amount. The value x_L is given by **Equation 3.3**

$$x_L = \bar{x}_{bl} + ks_{bl} \quad (3.3)$$

where $\bar{x}_{bl}$ is the average of the obtained results from the measurement of blank solutions, s_{bl} is the standard deviation of blank solutions measurements and k is a numerical factor chosen according to the confidence level required for the method. However, in many instances an approximate value of LOD is necessary and this is calculated as in **Equation 3.4**

$$LOD = 3 \times s_{bl} \quad (3.4)$$

or if the signal-to-noise (S/N) ratio, due to response of the instrument to the analyte, is opted for use in the determination of LOD, then it may be calculated according to **Equation 3.5**

$$LOD = 3 \times S/N \quad (3.5)$$

Equations 3.4 and **3.5** are approximations which are probably adequate during method validation as they provide an indication of the concentration below when detection becomes difficult. A solution containing a low level concentration of analyte may be used in substitution of the blank solution. It is advisable that LOD of the chosen method be at a minimum of one-tenth of the concentration set as a legal threshold.

Limit of quantification (LOQ) is defined as the lowest amount of analyte in a sample that can be determined with acceptable precision and accuracy.[152] An approximate value of LOQ is calculated as in **Equation 3.6**

$$LOQ = 10 \times s_{bl} \quad (3.6)$$

or if the instrument signal-to-noise (S/N) ratio is obtained due to response, LOQ may be calculated according to **Equation 3.7**

$$LOQ = 10 \times \frac{x}{S/N} \quad (3.7)$$

where x is the concentration of an analyte expressed as percentage (%). The relationship between the blank, LOD and LOQ is depicted in **Figure 3.22** by illustrating the probability density function for normally distributed measurements at the blank, LOD and LOQ levels. The alpha error, defined as the probability of false positive, is small (about 1 %) for a signal at the LOD while the beta error, defined as the probability of false negative, is about half for a sample with a concentration at the LOD.[154] This means an impurity in a sample may be at the LOD with a 50 % probability that the measurement would give a value less than the LOD. However, there is a minimal chance of a false negative at the LOQ.

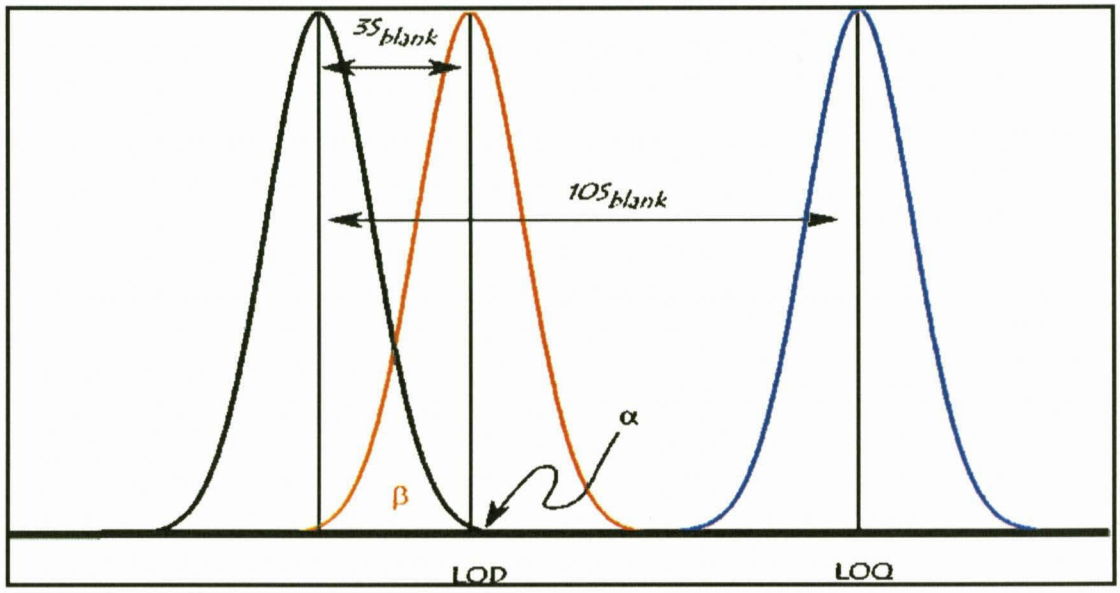

Figure 3.22: Illustration of the concept of LOD and LOQ by showing the theoretical normal distributions associated with blank, LOD and LOQ level samples[154]

For experimental purposes, LOD and LOQ are calculated by respectively rearranging **Equations 3.6** and **3.7** to **Equations 3.8** and **3.9** as well as making use of the slope from the equation $y = mx + e_y$ as described in **Section 3.4.1.6**.

$$LOD = 3 \times \frac{s_{bl}}{m} \qquad (3.8)$$

$$LOQ = 10 \times LOD \qquad (3.9)$$

The extrapolation of LOD and LOQ are shown in **Figure 3.23**.

[154] http://en.wikipedia.org/wiki/Detection_limit#Limit_of_quantification (15 Dec 2011)

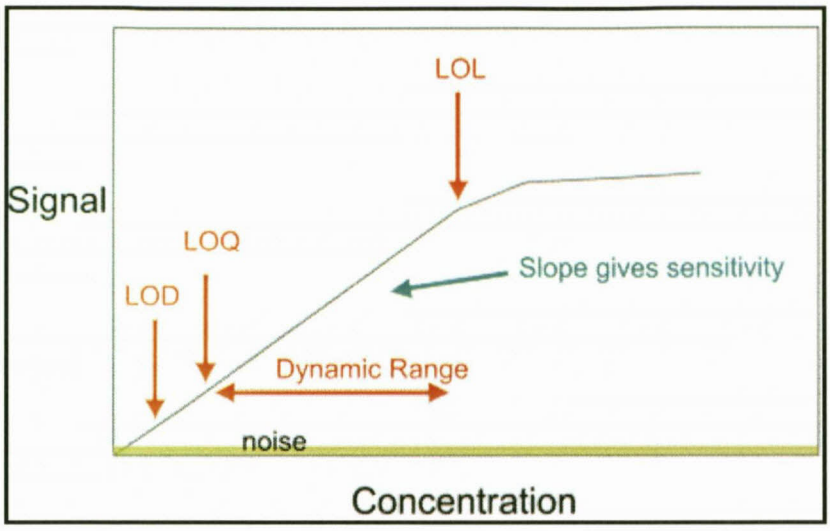

Figure 3.23: A plot depicting different positions of validation parameters, such as LOD, LOQ and LOL (limit of linearity) on a calibration curve[155]

3.4.1.2 ACCURACY

Accuracy of an analytical procedure is the closeness of agreement between the values that are accepted either as conventional true values or an accepted reference value and the value found.[152] By using the selected analytical method, accuracy is usually reported as percentage recovery of a known amount of analyte added to the sample by assay. Accuracy may be determined from a set of data collected from an experiment by considering the absolute and relative errors, as accuracy can never be exactly determined because the true value of a quantity can never be known exactly.[128] The absolute error (E) in measuring the amount x_i is given by **Equation 3.10**

$$E = x_i - x_t \tag{3.10}$$

where x_t is the true, or accepted, value of the given amount. The relative error (E_r) is a more frequently used parameter than the absolute error and is given by **Equation 3.11**

$$E_r = \frac{x_i - x_t}{x_t} \tag{3.11}$$

Relative error can also be expressed either in percentage or parts per thousand as in **Equation 3.12**, respectively

[155] http://en.wikipedia.org/wiki/Calibration_curve (15 Mar 2012)

$$E_r = \frac{x_i - x_t}{x_t} \times 100\% \text{ or } E_r = \frac{x_i - x_t}{x_t} \times 1000 \quad (3.12)$$

Certain statistical factors, such as linearity and hypothesis testing, may aid in achieving the accuracy of an experimental measurement. The sensitivity of a method in analyzing for the amount of a substance within a sample can be determined from the linearity of the calibration curve (see **Figure 3.23**). It often occurs that all the data points of the calibration curve do not lie exactly in a straight line and the acceptable extent of such deviations from linearity may be determined by the analyst.

a) Linearity

Linearity of an analytical method is the ability, within a given range, to obtain test results proportional to the concentration (amount) of a measurand in a sample. Linearity is demonstrated by preparing dilute stock solutions (may be solids or gasses) of varying, but consistently increasing, concentrations from a single known standard solution so as to minimize experimental errors. Linearity is evaluated by inspection of a plot of signals (absorbance) as a function of measurand concentration. The data from the standard calibration curve is used to determine a regression coefficient (r) – see **Equation 3.13** -, slope and intercept. Refer to **Figure 3.26** for a good calibration curve.

$$r = \frac{n(\sum xy) - (\sum x)(\sum y)}{\sqrt{n(\sum x^2) - (\sum x)^2} \bullet \sqrt{n(\sum y^2) - (\sum y)^2}} \quad (3.13)$$

b) Hypothesis Testing

Regression analysis is normally applied to measure the uncertainties associated with the data points of the calibration curve. Such uncertainties can be evaluated by considering the percentage confidence level (commonly 95 %) under specified degrees of freedom to which an outcome can be accepted or rejected using the hypothesis test.[128] There are two contradictory hypothesis tests, which influence the decision on whether to accept or reject an experimental outcome. One hypothesis testing, known as the null hypothesis (H_o), postulates that a quantity μ from an analysis is equal to a known or acceptable value μ_o (i.e. $\mu = \mu_o$). The other hypothesis testing, known as alternative hypothesis (H_a), can be explained in several

ways that deviate from the null hypothesis. Thus H_a can be used instead of the null hypothesis when the quantity μ varies from the acceptable μ_o (i.e. $\mu \neq \mu_o$). The critical value for the rejection of the null hypothesis is calculated as in **Equation 3.14**

$$\bar{x} - \mu = \pm \frac{ts}{\sqrt{N}} \tag{3.14}$$

where $\bar{x}$ is the mean value, s the standard deviation, t the t-statistic value that depends on the desired confidence level and N the number of replicate measurements used in an experimental test. When an analysis test is carried out on a large number of experimental replicates (≥ 20) such that the sample standard deviation (s) is a good estimate of the population standard deviation (σ), a z-statistic is employed. In the case where s is not a good estimate of σ, a t-statistic is employed. The z values, which depend on the desired confidence level as the t values are calculated as shown in **Equation 3.15**

$$z = \frac{\bar{x} - \mu}{\left(\frac{\sigma}{\sqrt{N}}\right)} \tag{3.15}$$

There is a possibility that an unbiased estimation of a population mean may fall far away from the true or expected value. Thus, the probability with which this estimated mean value may be established will be to construct a desired confidence interval within which it will fall. Supposing that a confidence interval of 95 % is desired, any value outside the region of mean distribution and lesser than z-value of – 1.96 or greater than z-value of + 1.96 will be rejected (see **Figure 3.24**).

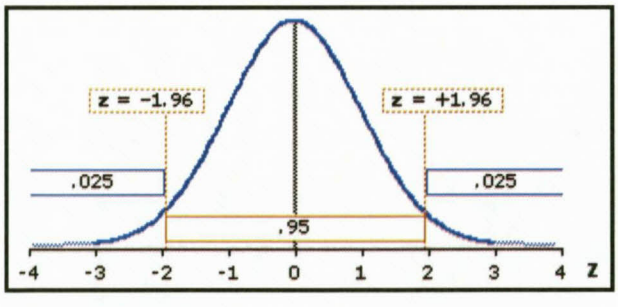

Figure 3.24: The normal distribution for the z-statistic at 95 % confidence interval[156]

[156] http://faculty.vassar.edu/lowry/ch10pt1.htmL (29 Feb 2012)

3.4.1.3 PRECISION

The precision of an analytical procedure expresses the closeness of agreement between a series of measurements obtained from many assays of the same homogeneous sample under recommended conditions.[152,153] Precision is reported as the coefficient of variance, also known as relative standard deviation (CV or RSD), expressed as a percentage or in parts per thousand as shown in **Equations 3.16** to **3.18**

$$\text{Standard deviation } (s) = \sqrt{\frac{\sum (x_i - \bar{x})^2}{N-1}} \tag{3.16}$$

$$\text{Mean } (\bar{x}) = \frac{\sum_{i=1}^{N} x_i}{N} \tag{3.17}$$

$$\text{CV} = \frac{s}{\bar{x}} \text{ x } 100 \text{ (\%) or RSD} = \frac{s}{\bar{x}} \text{x } 1000 \text{ (ppt)} \tag{3.18}$$

Precision and accuracy are differentiated from one another in the sense that accuracy is based on the degree of trueness while precision focuses on the degree of reproducibility. Quantitative measures of precision are critically investigated at the repeatability, reproducibility and intermediate precision levels.

a) Repeatability

Repeatability (r) is the measurement of precision value that is expected to lie below the absolute difference of two single test results obtained by using a similar method on identical material, under similar conditions. Repeatability is given by **Equation 3.19**

$$r = t_{\upsilon,\alpha} \text{ x } s_r\sqrt{2} \tag{3.19}$$

where $t_{\upsilon,\alpha}$ is the *t*-value for υ degrees of freedom and α corresponds to any given probability and s_r is the repeatability standard deviation.

Also referred to as intra-assay precision, repeatability is carried out on experiment done in pre-determined replicates within the same laboratory by one analyst. In addition to the standard deviation, experimental parameters such as coefficient of variance or relative standard deviation (CV/RSD) and confidence interval (CI) are also reported.

b) Reproducibility

Reproducibility (R) is the measurement of precision value that is expected to lie below the absolute difference of two single test results obtained by using a similar method on identical material, under different conditions. Reproducibility is given by **Equation 3.20**

$$R = t_{v,\alpha} \times s_R\sqrt{2} \qquad (3.20)$$

where $t_{\upsilon,\alpha}$ is the *t*-value for υ degrees of freedom and α corresponds to any given probability and s_R is the reproducibility standard deviation.

This parameter is measured between laboratories such as collaborative projects where similar homogeneous material make up and the same experimental design are performed. It is considered to be the method standardization parameter.

c) Intermediate Precision

Intermediate precision is defined as the intra-laboratory variation where similar experimental parameters are investigated by different analysts on a day-to-day basis using varying equipments.

The illustration of accuracy as the closeness of data to the true value and precision as the repeatability and/or reproducibility of measurement in reference to the true value are depicted in **Figure 3.25**.

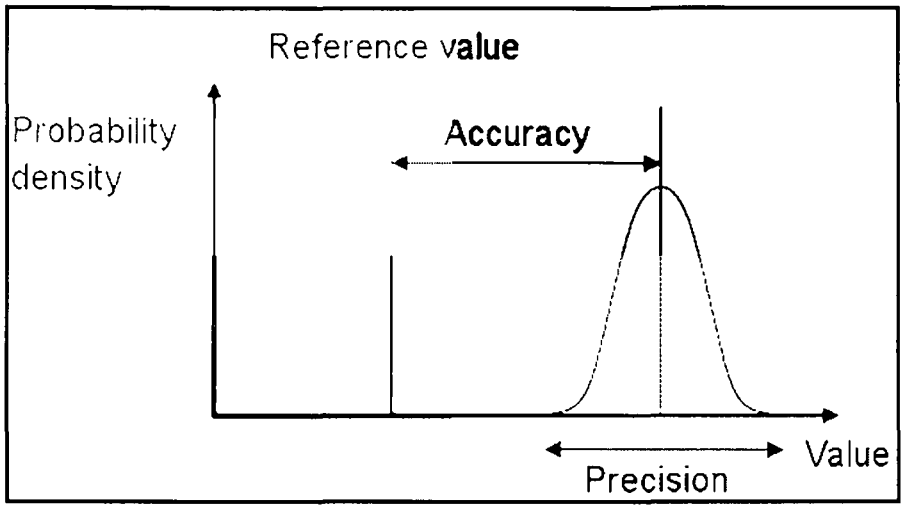

Figure 3.25: Illustration of accuracy and precision in relation to the reference value[157]

3.4.1.4 ROBUSTNESS

Robustness is the measure of the capacity for an analytical procedure to remain unaffected by small but deliberate variations in its parameters, such as varying the temperature, solvent volume and amount of a sample. It thus provides an indication of the method to be reliable under the normal use and should be evaluated during the development of the method. Should the measurements be susceptible to any variation in experimental conditions, a remedial action must be taken to control the analytical conditions or a statement should be included in the procedure to caution of any modification.

3.4.1.5 SPECIFICITY

Specificity, also referred to as selectivity, is the ability of an experimental method to unambiguously analyze for a measurand in the presence of other components in a given sample. The specificity of an experimental procedure can be determined by various methods, such as to add a reagent that will only react specifically with an analyte under investigation or selecting wavelength intensity in a machine that will only be characteristic of an analyte and will have little or no interference from wavelengths emitted by other components of a sample. To minimize any interference, specificity can be determined by also simultaneously analyzing the experimental sample with a blank sample that has a similar matrix. Thus the blank sample must possess all the matrix components as the sample except the analyte of interest.

[157] https://wiki.caudit.edu.au/confluence/display/CTSCIdMWG/V1+Risk+assessment+and+risk+management (15 Nov 2011)

3.4.1.6 MINIMIZATION OR ELIMINATION OF MATRIX INTERFERENCES

Sample matrix effects, which may arise from spectral interferences, acid as well as reagent interferences, may lead to significant systematic errors in accurately determining the measurement of results. There are several methods that can be employed to reduce such errors and improve the accurate determination of measurands. These include direct calibration curve, standard and internal standard additions methods.

a) Direct calibration method[158]

Direct calibration method is the operation that determines the functional relationships between measured values (*i.e.* signal intensities) and analytical quantities characterising types of analytes and their amount (*i.e.* concentration). A good calibration curve, without matrix effects, exhibits a linear regression coefficient (r^2) that is approximately one (1) over a wide concentration. Since the calibration curve serves as the reference from which the analytical measurements are read, the concentration of an analyte can thus be determined by extrapolation of the corresponding emission intensity (y) against the calibration curve (see **Figure 3.26**).

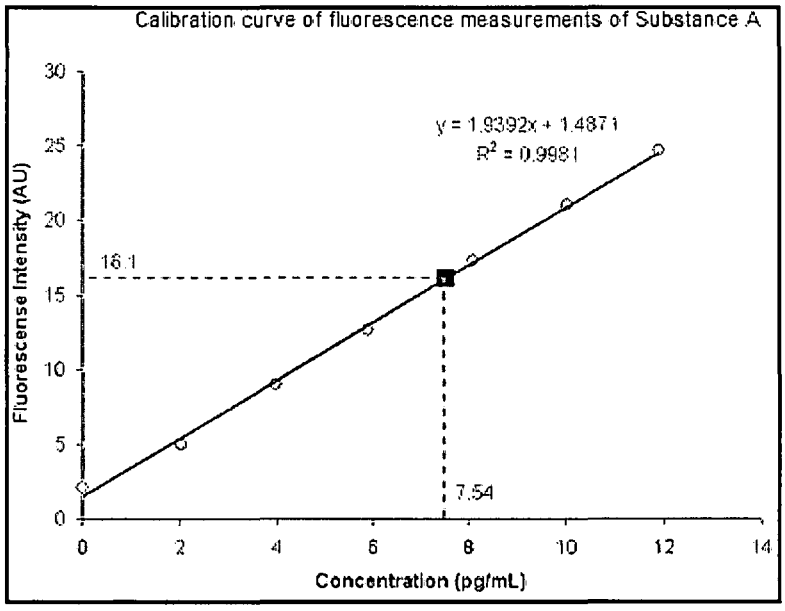

Figure 3.26: Direct calibration method[159]

[158] K. Danzer and L.A. Currie., *Pure & Appl. Chem.*, **70** (4), pp. 993 – 1014 (1998)

[159] http://www.chem.utoronto.ca/coursenotes/analsci/StatsTutorial/ProperGraph.htmL (13 Feb 2012)

The response of an instrument to the analyte content in each standard can yield a straight line from which a linear regression analysis may be applied to calculate the concentration of an analyte in an unknown sample using the equation $y = mx + e_y$; where y is the matrix measured values or the instrument response, m is the sensitivity of the instrument to the matrix, x is the analyte concentration and e_y is an error of the matrix or a constant that describes the background.

b) Standard addition method

The standard additions method (often referred to as "spiking" the sample) is commonly used to determine the concentration of an analyte that is in a complex matrix. The reason for using the standard additions method is that the matrix may contain other components that interfere with the analyte signal causing inaccuracy in the determined concentration. The idea is to add analyte to the sample ("spike" the sample) and monitor the change in instrument response. The change in instrument response between the sample and the spiked samples is assumed to be due only to change in analyte concentration.

The procedure for standard additions is to split the sample into several even aliquots in separate volumetric flasks of the same volume. The first flask is then diluted to volume with the selected solvent. A standard containing the analyte is then added in increasing volumes to the subsequent flasks and each flask is then diluted to volume with the selected solvent. The instrument response is then measured for all of the diluted solutions and the data is plotted with volume standard added in the x-axis and instrument response in the y-axis. Linear regression is performed and the slope (m) and y-intercept (c) of the calibration curve are used to calculate the concentration of analyte in the sample (see **Figure 3.27**).

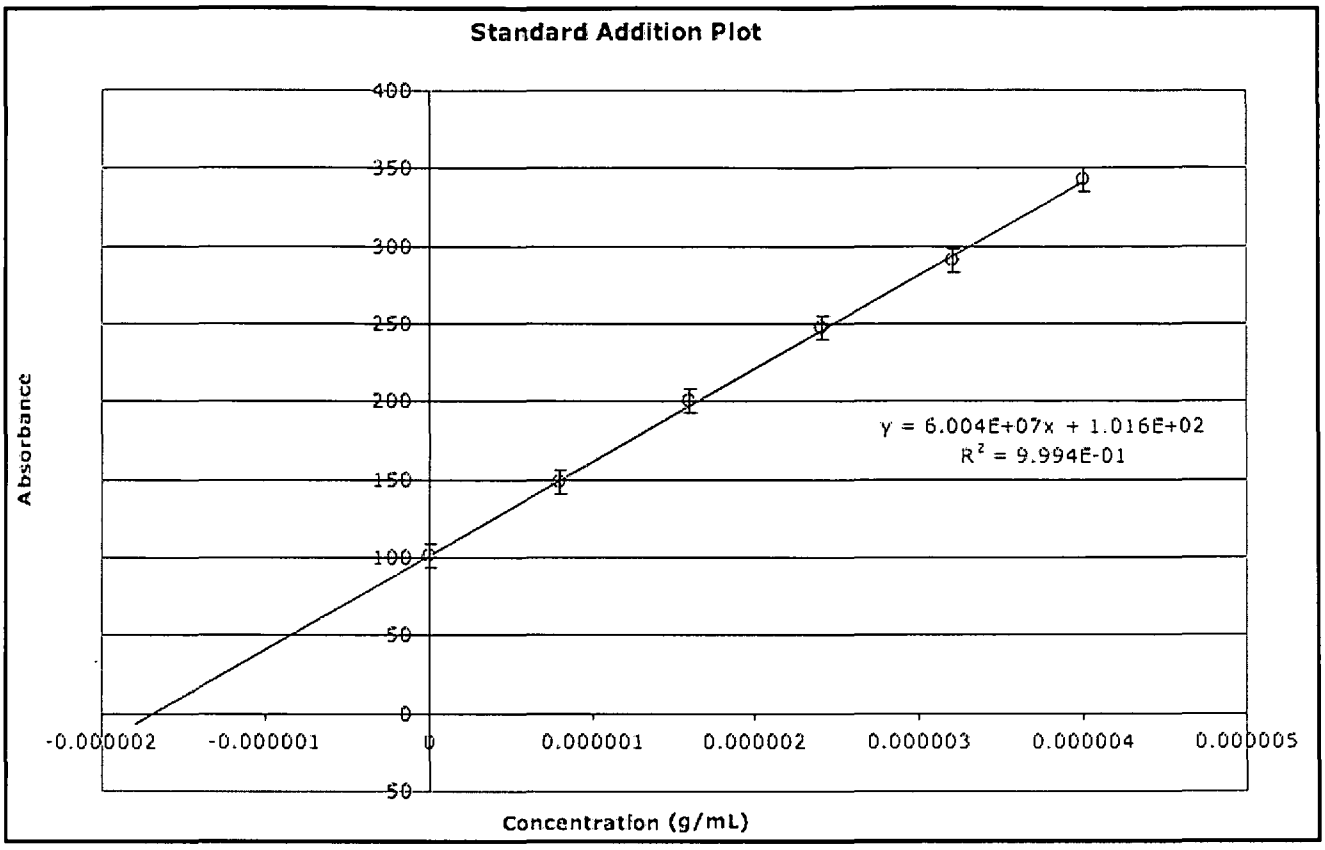

Figure 3.27: Standard addition calibration curve[160]

The advantage of this method is the ability to counteract the spectral interferences from other sample components and enhancing the signal of the analyte. However, the disadvantage of this method is the requirement of relatively large volumes of analyte sample (>100 mL) for analysis and the changes in the temperature of the nebuliser can easily affect its accuracy.

c) Internal standard addition method

Similar to the standard addition method, this method is used as an attempt to make corrections for the uncontrollable random errors caused by other components in the system or the instrument itself. An internal standard is any chemical substance or element added in a constant amount to samples, the blank and calibration standards in a chemical analysis. This substance can then be used for calibration by plotting the ratio of the signal to the internal standard signal as a function of the analyte concentration of the standards (see **Equation 3.21**).[161] This is done to correct for the loss of analyte during sample preparation.

[160] http://en.wikipedia.org/wiki/File:StandardAddition.png (13 Feb 2012)

[161] http://paws.wcu.edu/bacon/SAandIS.pdf (13 Feb 2012)

$$\frac{A_x}{[X]} = F\left(\frac{A_s}{[S]}\right) \quad (3.21)$$

where F is the response factor of the instrument, A_x and A_s are the absorbance of the analyte and standard, respectively, [X] is the concentration of the analyte solution and [S] is the concentration of the standard solution.

3.5 CONCLUSION

Gathering from the principles of all the dissolution techniques in this chapter, microwave-assisted digestion method is arguably the best method to get most inorganic samples into solution for the purpose of analysis. As summarised in **Table 3.1**, it is ideal to be employed in this study due to a smaller risk of contamination of the reaction from environment, high pressure and temperature, little or no loss of material and the speed with which samples are degraded. Due to the availability of equipment, ICP-OES and ICP-MS will be the analytical methods to be employed. The disadvantage of using AAS is the slow through-put rate of samples, while for NAAS one has to be close to a neutron source and the high probability of radioactivity of the sample after analysis as well as the cost of carrying it out act are the deterring factors in its application. Some disadvantages of using ICP spectroscopy include i) requirement for the sample to be completely dissolved in aqueous solution, ii) matrix effects and line rich emissions from most elements may cause spectral interferences, *etc*. However, following a proper digestion and dissolution protocol as well as the purification of the sample can ensure minimum matrix effects. The use of dilute solutions may also help in reducing matrix effects. Other ways of minimizing the matrix effect are internal standard additions and matching the matrix of the blank and standard calibration solutions with that of the sample as discussed in this chapter.

4 METHOD VALIDATION FOR THE ACCURATE DETERMINATION OF ZIRCONIUM IN HIGH PURITY PRODUCTS

4.1 INTRODUCTION

Since the discovery of zirconium in 1789, several methods have been developed and applied in producing the metal in its purest form employing different industrial purposes. By far the most successful methods for the synthesis of pure zirconium were developed by van Arkel and de Boer[23] and Kroll and his co-workers[28] in the early 20th century. The ultimate phase in pursuit of obtaining zirconium metal of ultra purity from its mineral ores is the production of the metal to be used for nuclear purposes, as discussed in **Section 1.4.3**. The purpose of this study (see **Paragraph 1.5**) is to develop and validate the analytical methods for the accurate analysis of zirconium and its permissible impurities at their specified threshold for its viability and usage in nuclear reactors.

Most methods developed and discussed in **Chapter 2** were argued for by their respective researchers to be efficient in analyzing zirconium and its impurities, but some showed to be time-consuming, element-specific and seemed consistent in using hydrofluoric acid as the digestive medium. Few of these methods focussed on the digestion and analysis of zirconium as a pure metal while most were based on zirconium as a component of its mineral ores and alloys. The principles of those analytical methods which were deemed to be of interest for the purpose of this study were discussed in **Chapter 3** with the view of having an in-depth understanding of how they may help in developing and validating alternative methods suitable for the dissolution and accurate determination of zirconium and its associated impurities specified for the nuclear grade zirconium metal.

From the results and discussion in **Chapter 3**, it appeared that microwave-assisted digestion and ICP analytical methods may be the most suitable procedures, in principle, for their

outstanding advantages, such as rapid dissolution of the sample, speed and range of analysis. Microwave-assisted digestions are also less susceptible to environmental contamination, loss of components due to volatilization and the application of high pressure and temperature for the complete separation of the sample into its simplest components, while ICP is advantageous in identifying and analyzing many elements in a short time.

This study involves the development of appropriate and efficient methods for the accurate quantification of zirconium in different samples, such as zirconium metal, ZrF_4 and K_2ZrF_6, using external calibration standards. Different acid mediums will also be used in the microwave digestion and open vessel dissolution to determine their suitability for zirconium metal dissolution. The unavailability of zirconium CRM's as well as nuclear grade zirconium metal in the open market necessitated that pure metal samples (99.9+ %) from chemical suppliers be investigated in the zirconium dissolution and quantification. The study also involved the development of in-house reference materials for method validation. All the validation parameters as discussed in **Chapter 3** will also be evaluated to determine the suitability of the developed methods for the digestion and analysis of zirconium.

4.2 EQUIPMENTS AND REAGENTS

4.2.1 BENCH-TOP MAGNETIC STIRRER EQUIPMENT

A Heidolph MR Hei-Tec magnetic stirrer/hotplate from Labotec was used to assist with the open vessel digestion of the pure zirconium metal sample at temperatures ranging between 90°C and 150 °C.

4.2.2 MICROWAVE EQUIPMENT

An Anton Paar Perkin-Elmer Multiwave 3000 microwave instrument, equipped with an 8SXF 100 rotor and eight PTFE reaction vessels, was used for digestion of the pure zirconium metal samples (see **Figure 4.1**).

Figure 4.1: Anton Paar Perkin-Elmer Multiwave 3000 microwave equipment

An internal program for the digestion of zirconium metal was selected with conditions set in **Table 4.1**.

Table 4.1: Microwave digestion conditions for the high purity zirconium metal

Parameter	Condition
Power	1400 Watts
Ramp	15 min
Hold	15, 45 and 60 min
Fan	1,1 and 3 min
Pressure rate	0.5 bar/sec
Temperature	240 °C
Pressure	60 bar
Weight	about 100 mg
Volume of acid	10.0 mL
Possible reagents	H_2SO_4 (98 %), H_3PO_4 (80 %), *Aqua regia* [3:1 (55 % HNO_3:32 % HCl)]

4.2.3 ICP-OES SPECTROMETER

A Shimadzu ICPS-7510 ICP-OES instrument equipped with a radial-sequential plasma spectrometer was used to analyze the water-based solutions of different zirconium samples and their associated impurities (see **Figure 4.2**).

Figure 4.2: Shimadzu ICPS-7510 radial-sequential plasma spectrometer

The emission intensity measurements were done by using the default conditions as shown in **Table 4.2**.

Table 4.2: Operating conditions of the ICP-OES analysis of zirconium content

Parameter	Condition
RF Power	1200 Watts
Coolant gas flow rate	14.0 L/min
Plasma gas flow rate	45 L/min
Auxiliary gas flow rate	0.5 L/min
Carrier gas flow rate	0.7 L/min
Sample introduction method	Peristaltic pump
Type of spray chamber	Glass cyclonic
Type of nebuliser	Concentric
Injector tube diameter	3.0 mm

4.2.4 ATOMIC ABSORPTION (AA) SPECTROPHOTOMETER

A Shimadzu Atomic Absorption spectrophotometer, using a flame photometric optical double beam method, was used to analyze the water-based solutions of potassium hexafluorozirconate samples (see **Figure 4.3**).

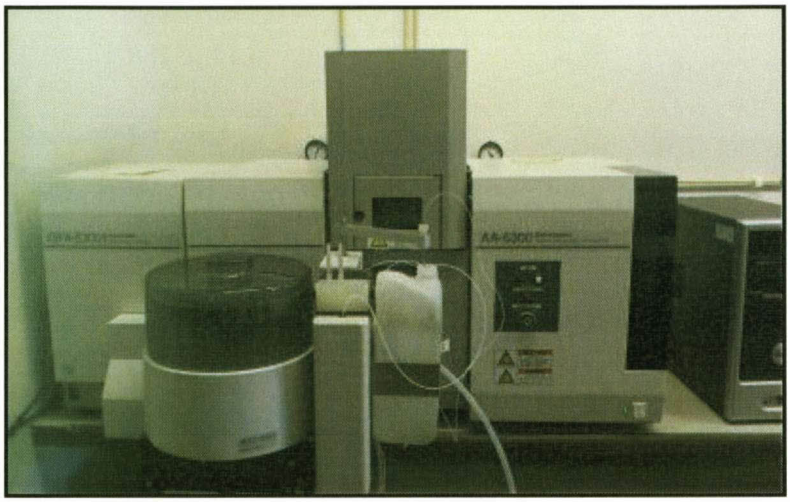

Figure 4.3: Shimadzu AA-6300 atomic absorption spectrophotometer

Table 4.3: Operating conditions of the AA analysis of zirconium content

Parameter	Condition
Air gas flow rate	17.5 L/min
Acetylene gas flow rate	4.0 L/min
Sample introduction method	Automatic pump suction
Type of spray chamber	Polypropylene
Type of nebuliser	Pt-Ir capillary with PTFE orifice

4.2.5 WATER DISTILLATION EQUIPMENT

Double distilled water was prepared in the laboratory with an electronic distillatory vessel (Fisons w/FF9/4) which consists of a round bottom flask (20 litres) equipped with a heating element, a condenser and an outlet and inlet pipes. All the experimental solutions were prepared by using the double distilled water.

4.2.6 WEIGHING EQUIPMENT

All the samples were weighed accurately to 0.1 mg at room temperature using a Scaltec (SBA 33) electronic balance scale certified under an ISO 9001 quality assurance system. All experimental samples and reagents used in this study were weighed by adding a sample in a glass vial that was zeroed on the balance scale. The weighed masses were recorded to 4 decimal places.

4.2.7 GLASSWARE

Two kinds of volumetric flasks, namely Blau brand grade (A) glass type (25, 50, 100, 250 and 500 mL) and Kartell HDPE type (25, 50, 100, 250 and 500 mL) were used for sample dilutions and the beakers (50 and 250 mL) were of the Schott Duran glass type used for the digestion of the zirconium samples.

4.2.8 PIPETTES

The solutions were dispensed into volumetric flasks at room temperature using semi-automatic Brand Transferpette-S type (1000 µL and 10 mL) pipettes.

4.2.9 REAGENTS

Zirconium foil (99.98 %, cat. no. 419141-4.6G), zirconium metal rod (99+ %; cat. no. 267724-20G) and zirconium(IV) tetrafluoride (99.9 % ZrF_4, cat. no. 311464-100G) were purchased from Sigma-Aldrich. Hydrochloric (32 %, cat. no. 7647-01-0) and phosphoric (80 %, 7664-38-2) acids were purchased from Associated Chemicals Enterprises. Nitric acid (55 %, SAAR4465080LP) and sulphuric acid (98 %; Cat. nr 5885060LC; Batch nr 1015597) were purchased from Merck. Zirconium ICP standard (1000 ppm Zr, cat. no. 1.70370.0100), multi-element ICP standard (1000 ppm, cat. no. 1.11355.0100) and Silicon ICP standard (1000 ppm Si, cat. no. CGSI 1-1) were purchased from Inorganic Ventures.

4.3 QUANTIFICATION OF ZIRCONIUM IN HIGH PURITY PRODUCTS BY ICP-OES

4.3.1 GENERAL EXPERIMENTAL PROCEDURE

All the experimental samples were diluted with double distilled water after digestion and each analytical run was carried out in triplicate, unless stated otherwise. The zirconium analyses by ICP-OES were carried out at the selected wavelengths of 343.823 nm and 339.198 nm. These are the most sensitive wavelengths in the analysis of zirconium.[162] The elements which mainly interfere at these wavelengths are calcium, chromium, iron, manganese and titanium. The calibration standard solutions were prepared to resemble the matrix of the zirconium samples.

4.3.2 PREPARATION OF ICP CALIBRATION STANDARDS

Three sets of the zirconium calibration standard solutions were prepared from aliquots (0.2, 0.4, 0.6, 0.8 and 1.0 mL) of the zirconium ICP standard into 100 mL Blau brand grade (A) glass volumetric flasks. To the first set of zirconium standard solutions was added diluted *aqua regia* (3.5 %, 2.5 mL), while diluted sulphuric acid (3.5 %, 2.5 mL) was added to the second set and diluted phosphoric acid (3.5 %, 2.5 mL) was added to the third set. All the flasks were filled to the mark with double distilled water to achieve final concentrations of 2, 4, 6, 8 and 10 ppm, respectively.

4.3.3 DETECTION LIMITS

In order to ensure that the correct analytical conditions are selected for the accurate determination of zirconium, the limit of detection (LOD) and limit of quantification (LOQ) for the ICP-OES instrument were determined applying the prevailing experimental conditions. In this study the limit of detection (LOD) and limit of quantification (LOQ) were determined by the measurement of the intensities of the blank solution (10 replicates) at wavelengths 343.823 nm and 339.198 nm and calculated according to **Equations 3.8** and **3.9** in **Chapter**

[162] R.K. Winge, V.A. Fassel, V.J. Peterson and M.A. Floyd., *Inductively Coupled Plasma-Atomic Emission Spectroscopy: An Atlas of Spectral Information*, Amsterdam; New York, Elsevier., pp. 262 – 286 (1985)

3. The calculation of the standard deviation (*s*) was done as shown in **Chapter 3**, **Equation 3.15**. The LOD's and LOQ's of zirconium are shown in **Table 4.4**.

A set of standard solutions between 2 and 10 ppm zirconium were prepared from the ICP standard as discussed in **Section 4.3.2** and obtained the calibration curves as shown in **Figures 4.4** and **4.5** while the intensity measurements for the blank solution are reported in **Table 4.4**.

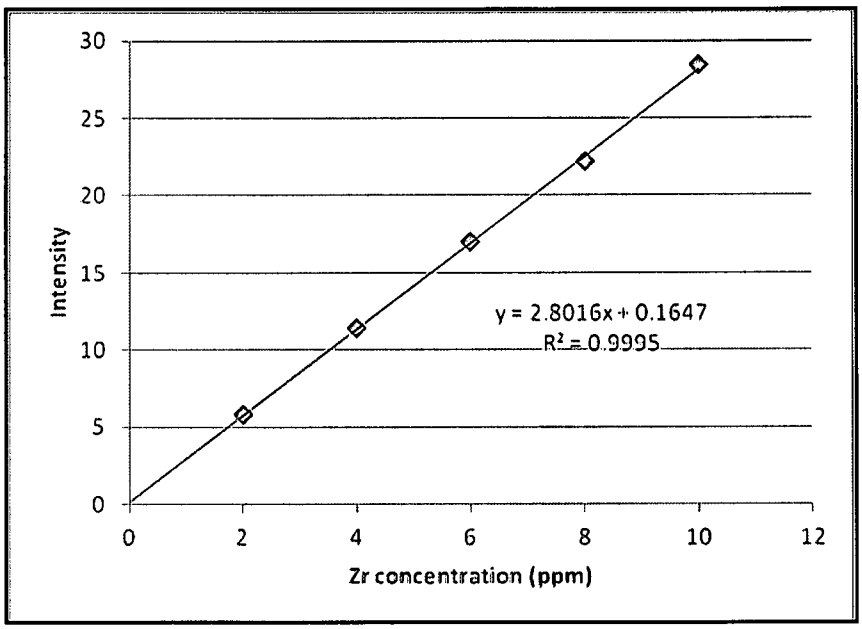

Figure 4.4: Calibration curve of zirconium at wavelength 339.198 nm

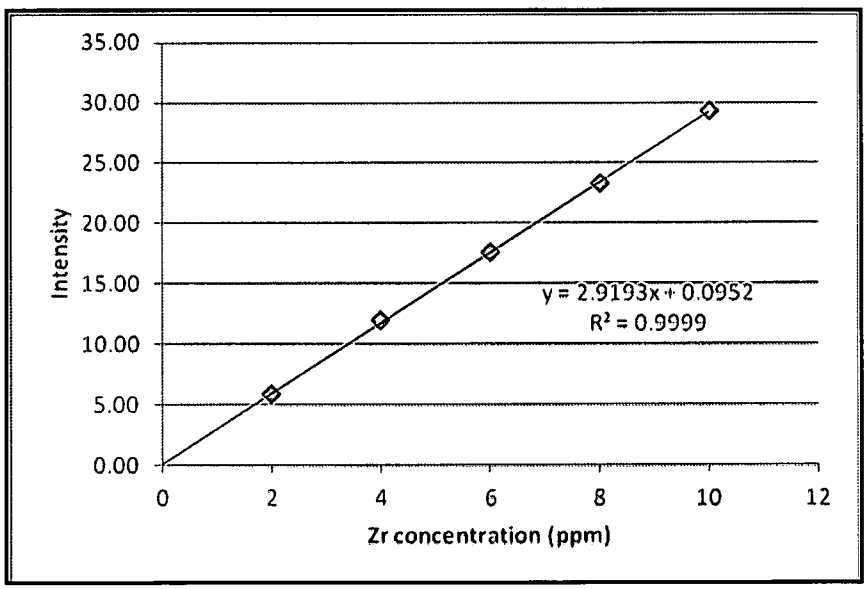

Figure 4.5: Calibration curve of zirconium at wavelength 343.823 nm

The standard deviations in the following tables are reported to single significant figures rather than the calculated value as a whole, which indicate the uncertainty in the last figure of the mean values.

Table 4.4: Determination of the LOD and LOQ for zirconium

Measurement number	Intensity of the blank solution @ 339.198 nm	Intensity of the blank solution @ 343.823 nm
1	0.7485	0.5923
2	0.7485	0.5942
3	0.7568	0.6059
4	0.7576	0.5998
5	0.7555	0.5931
6	0.7546	0.6013
7	0.7559	0.5982
8	0.7555	0.5989
9	0.7594	0.5994
10	0.7576	0.6006
Mean (SD)	**0.755 (4)**	**0.598 (4)**
LOD (ppm)	**0.003922**	**0.004289**
LOQ (ppm)	**0.03922**	**0.04289**

4.3.4 DISSOLUTION OF THE ZIRCONIUM ROD

4.3.4.1 DISSOLUTION BY BENCH-TOP DIGESTION

Zirconium rod (20 g) was mechanically cut into small discs for zirconium determination. Nine different pieces of zirconium rod sample were accurately weighed (~100 mg) and each transferred into 50.0 mL Schott Duran glass beaker. Different concentrated acids (15 mL of H_2SO_4, H_3PO_4 and *aqua regia*) were added to the rods and digested in fumehood at 150 °C

on a hot-plate while constantly stirring for 2 hours. Visual inspection indicated that the zirconium rods in the sulphuric acid solutions were completely dissolved after this period of digestion while metal pieces were still visible in the other acid solutions. After cooling to room temperature, the sulphuric acid reaction mixtures were quantitatively transferred to 500.0 mL Kartell HDPE volumetric flasks and filled to the mark with double distilled water. The zirconium discs in the phosphoric acid digestions were digested for another 48 hours after which partial dissolution took place with only small pieces of metal still visible in the acid. After this digestion period, the reaction mixtures were cooled to room temperature, diluted with double distilled water (50 mL) and filtered with a Whattman filter paper. The undigested metal was weighed and the filtrates were quantitatively transferred into 100.0 mL Blau brand volumetric flasks and filled to the mark with double distilled water.

The *aqua regia* had evaporated under the given experimental conditions but no visual evidence of zirconium rod digestion was observed. A further volume of *aqua regia* (15 mL) was added and the solutions left at room temperature (to reduce evaporation) for a further 48 hours to continue with the digestion process. After this period, the zirconium rods were, again, partially digested and the reaction mixtures were cooled to room temperature, diluted with double distilled water (50 mL) and filtered with a Whattman filter paper. The undigested metal was weighed and the filtrates were quantitatively transferred into 100.0 mL Blau brand volumetric flasks and filled to the mark with double distilled water.

For the quantification of zirconium in these samples, three aliquots of each reaction mixture (~3 mL for sulphuric acid, ~1 mL for phosphoric acid and ~5 mL for *aqua regia*) were transferred to the respective 100.0 mL Blau brand volumetric flasks and filled to the mark with double distilled water to achieve the final concentrations of ~5 ppm in zirconium. The results for the analyses of digested zirconium rods are shown in **Tables 4.5** and **4.6**.

Table 4.5: ICP-OES analyses results for bench-top digestions of zirconium rods with different mineral acids (λ = 343.823 nm)

	Phosphoric acid			Sulphuric acid			*Aqua regia*		
	Sample 1	Sample 2	Sample 3	Sample 1	Sample 2	Sample 3	Sample 1	Sample 2	Sample 3
Mean % (SD)	55.4 (8)	68 (2)	56 (2)	97 (1)	101.3 (8)	103 (1)	93 (2)	95.1 (6)	90.7 (3)
RSD (ppt)	14	29	36	10	8	10	22	6	3

Table 4.6: ICP-OES analyses results for bench-top digestions of zirconium rods with different mineral acids (λ = 339.198 nm)

	Phosphoric acid			Sulphuric acid			*Aqua regia*		
	Sample 1	Sample 2	Sample 3	Sample 1	Sample 2	Sample 3	Sample 1	Sample 2	Sample 3
Mean % (SD)	53 (2)	61 (2)	52 (2)	103.7 (6)	101 (1)	101.6 (8)	87 (2)	81.0 (5)	91 (1)
RSD (ppt)	38	33	39	6	10	8	23	6	11

4.3.4.2 DISSOLUTION BY MICROWAVE-ASSISTED DIGESTION

The next step in this study was to investigate the microwave digestion of the zirconium metal rod. Nine different pieces of a zirconium rod sample were accurately weighed (~100 mg) and placed into the microwave PTFE vessels. The samples were digested in two separate runs since the microwave setup can only digest eight samples at a given time. Nitric acid (10 mL) was added to the empty PTFE vessels to prevent any damage during the digestion period. Different acids (10 mL) were added to the zirconium samples and they were digested employing the microwave conditions as specified in **Section 4.2.1**, **Table 4.1**. The reaction mixtures were allowed to cool to room temperature, then diluted with double distilled water (50 mL) and filtered with a Whattman filter paper. The undigested metal was weighed and the filtrates were transferred into 100.0 mL Blau brand volumetric flasks and filled to the mark with double distilled water.

For the quantification of zirconium in these samples, three aliquots of each reaction mixture (~1 mL for sulphuric acid, ~4 mL for phosphoric acid and ~1 mL for *aqua regia*) were transferred to the respective 100.0 mL Blau brand volumetric flasks and filled to the mark

with double distilled water to achieve the final concentrations of ~5 ppm in zirconium. The results for the analyses of the microwave-assisted digestion of the zirconium rods are shown in **Tables 4.7** and **4.8**.

Table 4.7: ICP-OES analyses results for microwave-assisted digestions of zirconium rods with different mineral acids (λ = 343.823 nm)

	Phosphoric acid			Sulphuric acid			*Aqua regia*		
	Sample 1	Sample 2	Sample 3	Sample 1	Sample 2	Sample 3	Sample 1	Sample 2	Sample 3
Mean % (SD)	88.0 (3)	94 (2)	89 (1)	103 (1)	98 (1)	101 (3)	100 (1)	100.9 (5)	102.9 (2)
RSD (ppt)	3	21	11	10	10	30	10	5	2

Table 4.8: ICP-OES analyses results for microwave-assisted digestions of zirconium rods with different mineral acids (λ = 339.198 nm)

	Phosphoric acid			Sulphuric acid			*Aqua regia*		
	Sample 1	Sample 2	Sample 3	Sample 1	Sample 2	Sample 3	Sample 1	Sample 2	Sample 3
Mean % (SD)	87 (1)	86 (1)	85 (1)	101.4 (8)	101.0 (6)	96.9 (4)	99 (2)	102 (2)	96.9 (2)
RSD (ppt)	12	12	12	8	6	4	20	20	2

4.3.5 DISSOLUTION OF THE ZIRCONIUM FOIL

4.3.5.1 DISSOLUTION BY BENCH-TOP DIGESTION

The dissolution and quantification of zirconium was repeated on a high purity metal foil, mainly to try and decrease the duration of the digestion period. Nine different masses of zirconium foil sample were accurately weighed (~100 mg) and respectively transferred into 50.0 mL Schott Duran glass beakers. Different acids (15 mL) were added to the foils and digested in fumehood for 1 hour at 150 °C on a hot-plate with constant stirring. Visual inspection indicated that zirconium foil samples in the sulphuric acid were completely dissolved as no visible metal was observed. These solutions were cooled to room

temperature and the reaction mixtures were transferred to 500.0 mL Kartell HDPE volumetric flasks and finally filled to the mark with double distilled water.

The samples in the phosphoric acid were digested for another 48 hours while more *aqua regia* (15 mL) was added to the zirconium samples that were initially digested with this acid combination. The reaction mixture was left at room temperature for a further 48 hours. During this time period, a significant amount of digestion of the foils in both acids was observed and the reaction mixtures were transferred to 100.0 mL Blau brand volumetric flasks without filtering and filled to the mark with double distilled water.

As was described for the metal rod analysis, three aliquots of each reaction mixture (~3 mL for sulphuric acid, ~0.5 mL for phosphoric acid and ~0.5 mL for *aqua regia*) were transferred to the respective 100.0 mL Blau brand volumetric flasks and filled to the mark with double distilled water to achieve the final concentrations of ~5 ppm in zirconium. The results for the analyses of the bench-top digestion of the zirconium foils are shown in **Tables 4.9** and **4.10**.

Table 4.9: ICP-OES analyses results for bench-top digestions of zirconium foils with different mineral acids (λ = 343.823 nm)

	Phosphoric acid			Sulphuric acid			*Aqua regia*		
	Sample 1	Sample 2	Sample 3	Sample 1	Sample 2	Sample 3	Sample 1	Sample 2	Sample 3
Mean % (SD)	99 (2)	102 (1)	101 (1)	101.9 (7)	102 (1)	102 (2)	89 (1)	92.4 (2)	72.2 (2)
RSD (ppt)	20	10	10	7	10	20	11	2	3

Table 4.10: ICP-OES analyses results for bench-top digestions of zirconium foils with different mineral acids (λ = 339.198 nm)

	Phosphoric acid			Sulphuric acid			*Aqua regia*		
	Sample 1	Sample 2	Sample 3	Sample 1	Sample 2	Sample 3	Sample 1	Sample 2	Sample 3
Mean % (SD)	102 (1)	101 (2)	100 (1)	103 (2)	101 (2)	102 (2)	93 (2)	90 (2)	74 (2)
RSD (ppt)	10	20	10	19	20	20	22	22	27

4.3.5.2 DISSOLUTION BY MICROWAVE-ASSISTED DIGESTION

The dissolution of the zirconium metal foil was continued with the microwave digestion technique. Nine different masses of a zirconium foil sample were accurately weighed (~100 mg) and respectively transferred into the microwave PTFE vessels. The samples were digested in two separate runs since the microwave setup can only digest eight samples at a given time. Nitric acid (10 mL) was added to the empty PTFE vessels to prevent any damage during the digestion period. Different acids (10 mL) were added to the zirconium samples and they were digested employing the microwave conditions as specified in **Section 4.2.1**, **Table 4.1**. The reaction mixtures were allowed to cool to room temperature, then diluted with double distilled water (50 mL) and filtered with a Whattman filter paper. The undigested metal was weighed and the filtrates were transferred into 100.0 mL Blau brand volumetric flasks and filled to the mark with double distilled water.

As was described for the metal rod analysis, three aliquots of each reaction mixture (~2 mL for sulphuric acid, ~2 mL for phosphoric acid and ~2 mL for *aqua regia*) were transferred to the respective 100.0 mL Blau brand volumetric flasks and filled to the mark with double distilled water to achieve the final concentrations of ~5 ppm in zirconium. The results for the analyses of digested zirconium foils are shown in **Tables 4.11** and **4.12**.

Table 4.11: ICP-OES analyses results for microwave-assisted digestions of zirconium foils with different mineral acids (λ = 343.823 nm)

	Phosphoric acid			Sulphuric acid			*Aqua regia*		
	Sample 1	Sample 2	Sample 3	Sample 1	Sample 2	Sample 3	Sample 1	Sample 2	Sample 3
Mean % (SD)	34 (2)	39.2 (9)	37.3 (3)	94 (1)	95 (1)	99 (4)	3.8 (3)	8.4 (8)	3.4 (1)
RSD (ppt)	59	23	8	11	11	40	79	95	29

Table 4.12: ICP-OES analyses results for microwave-assisted digestions of zirconium foils with different mineral acids (λ = 339.198 nm)

	Phosphoric acid			Sulphuric acid			*Aqua regia*		
	Sample 1	Sample 2	Sample 3	Sample 1	Sample 2	Sample 3	Sample 1	Sample 2	Sample 3
Mean % (SD)	24.9 (4)	32 (1)	29 (3)	97.5 (2)	103.7 (2)	95.2 (4)	3.3 (3)	7.7 (3)	6.8 (9)
RSD (ppt)	16	31	103	2	2	4	91	39	132

4.3.6 PREPARATION AND QUANTIFICATION OF ZIRCONIUM REFERENCE MATERIALS (RM)

The difficulty with which zirconium metal samples were digested, associated with the uncertainty of total dissolution, the subsequent accuracy of the recovery and, therefore, the whole method, prompted the search for the readily soluble, very pure zirconium samples which can be used as reference materials (RM). Such a compound turned out to be ZrF_4, which can be obtained from the market in an ultra? pure form, but can also be used as the starting material for the synthesis of the very soluble K_2ZrF_6 salt. The analysis of the RM was done in two ways by i) directly dissolving the zirconium(IV) tetrafluoride salt in diluted sulphuric acid and ii) the quantification of zirconium in alkali metal fluorozirconate salts, *e.g.* potassium hexafluorozirconate.

4.3.6.1 PREPARATION OF RM BY THE DISSOLUTION OF ZrF_4 IN DILUTED H_2SO_4

Three samples of zirconium(IV) tetrafluoride were accurately weighed (~100 mg) and transferred into respective 50.0 mL Schott Duran glass beakers containing 3.5% diluted sulphuric acid (10 mL). The mixtures were heated and stirred at 70 °C for 20 minutes. After cooling to room temperature, the reaction mixtures were quantitatively transferred to 500.0 mL Kartell HDPE volumetric flasks and diluted to the mark with double distilled water. For ICP-OES analysis, three equal aliquots (~3.0 mL) of each zirconium(IV) tetrafluoride sample solutions were transferred into 100.0 mL Blau brand volumetric flasks and filled to the mark with double distilled water. The results for the analyses of digested zirconium(IV) tetrafluoride are shown in **Tables 4.13** and **4.14**. Qualitative ICP-OES analyses were also carried out on the diluted zirconium(IV) tetrafluoride and it was discovered that three impurity elements,

namely silicon, aluminium and chromium were present. The LOD and LOQ of these elements are shown in **Chapter 5, Section 5.4.3**. These samples were quantified and the results thereof are shown in **Table 4.15**.

Table 4.13: ICP-OES analysis for bench-top diluted sulphuric acid digestion of ZrF_4 (λ = 343.823 nm)

	Sample 1	Sample 2	Sample 3
Mean % (SD)	100.7 (7)	98.6 (1)	99.3 (9)
RSD (ppt)	7	1	9

Table 4.14: ICP-OES analysis for bench-top diluted sulphuric acid digestion of ZrF_4 (λ = 339.198 nm)

	Sample 1	Sample 2	Sample 3
Mean % (SD)	103 (2)	100.3 (5)	101.6 (8)
RSD (ppt)	19	5	8

Table 4.15: Quantitative ICP-OES analyses of the impurities present in the bench-top diluted sulphuric acid digestion of ZrF_4

	Aluminium	Chromium	Silicon
Concentration (ppm)	1.9	0.9	0.7
R^2	1	1	0.9995
Slope	0.26	0.31	0.21
Intercept	-0.9	-0.2	-0.3

4.3.6.2 PREPARATION OF POTASSIUM HEXAFLUOROZIRCONATE (K_2ZrF_6) AS THE RM

Potassium fluoride (~6.0 g, 0.11 moles) was accurately weighed and transferred into a 250.0 mL Schott Duran glass beaker containing double distilled water (150 mL). Zirconium(IV) tetrafluoride (~9.0 g, 0.06 moles) was accurately weighed and transferred in portions into the beaker containing potassium fluoride solution while stirring at a temperature of 70 °C. All the zirconium(IV) tetrafluoride salt was completely dissolved after about 1 hour. The mixture was

left to cool down to room temperature while the recrystallization of potassium hexafluorozirconate was allowed to take place.

a) Analysis of the prepared K_2ZrF_6 by infrared (IR) spectrometer

The clear glassy rod-like shaped crystals of the expected product and that of the ZrF_4 were dried in an open atmosphere at 120 °C. The two zirconium complexes were subsequently analyzed by IR and their spectrums were compared to confirm the production of the new zirconium product as shown in **Figures 4.6** to **4.11**.

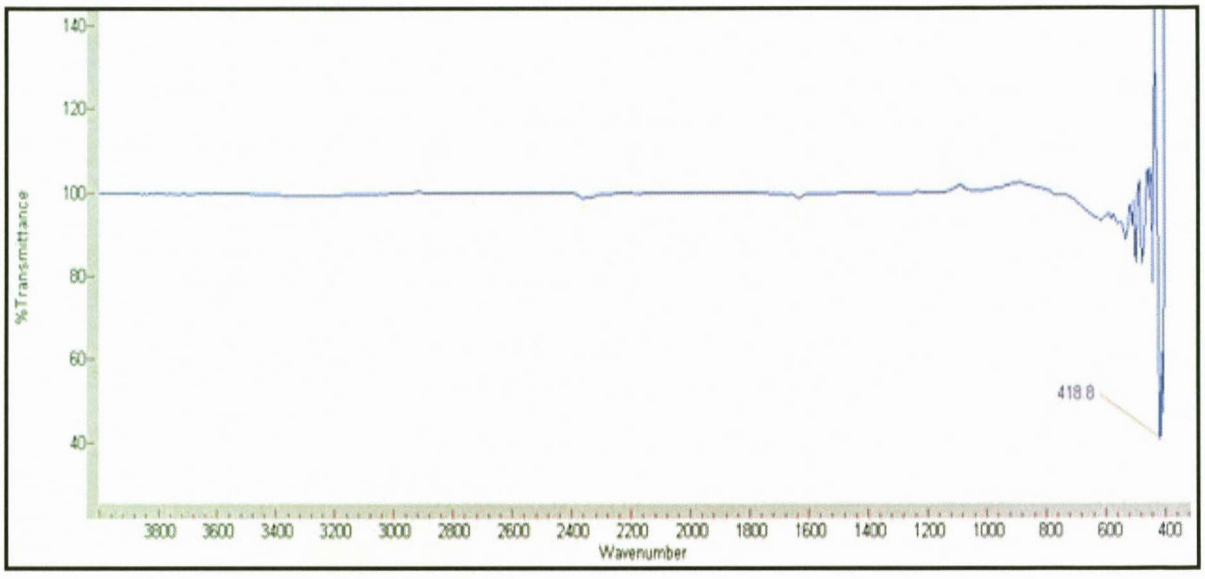

Figure 4.6: Full infrared (IR) spectrum of ZrF_4

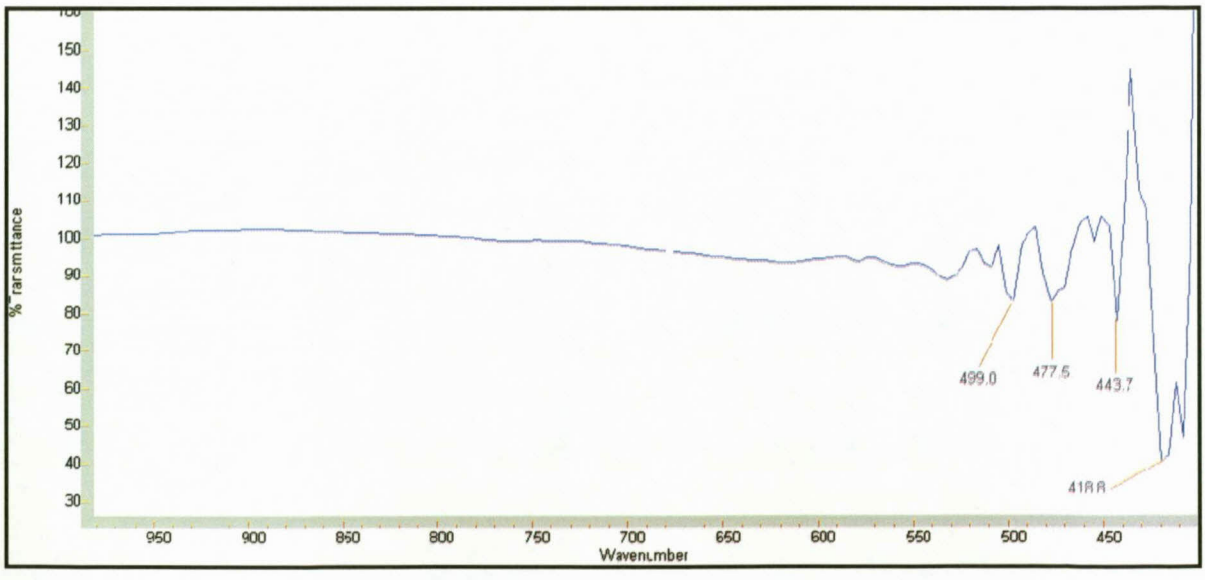

Figure 4.7: Spectrum of ZrF_4 magnified on the far IR

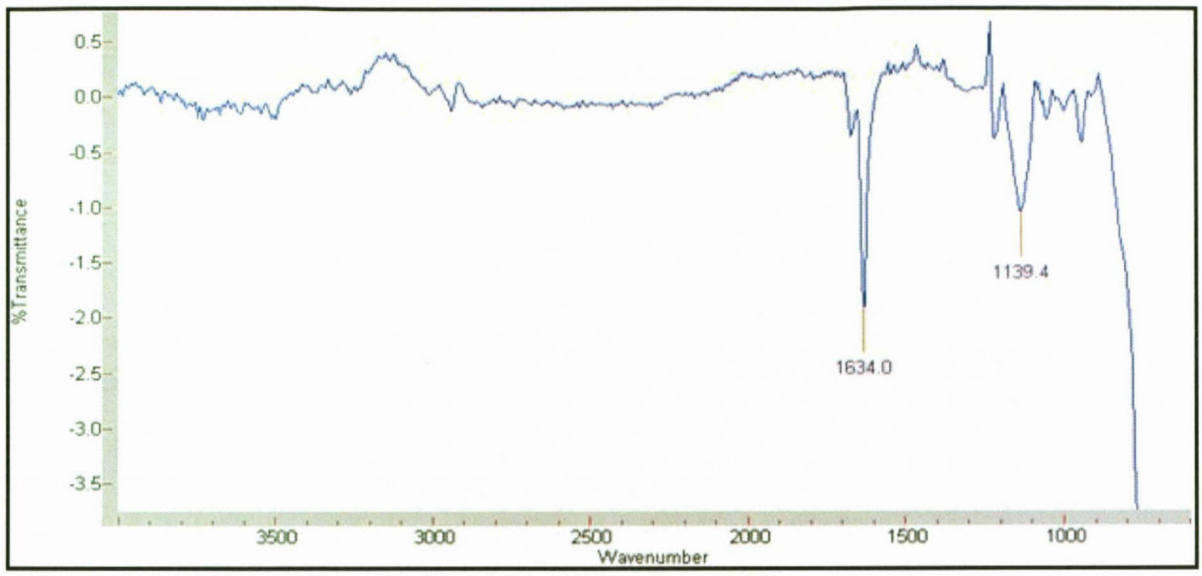

Figure 4.8: Spectrum of ZrF_4 magnified and stretched on the near IR

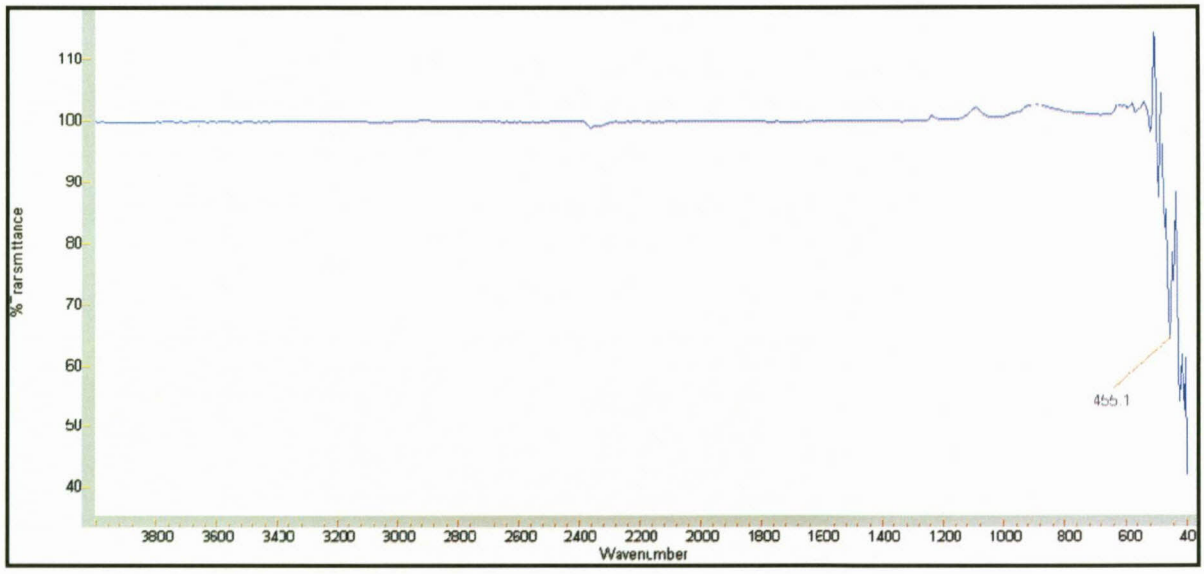

Figure 4.9: Full infrared (IR) spectrum of K_2ZrF_6

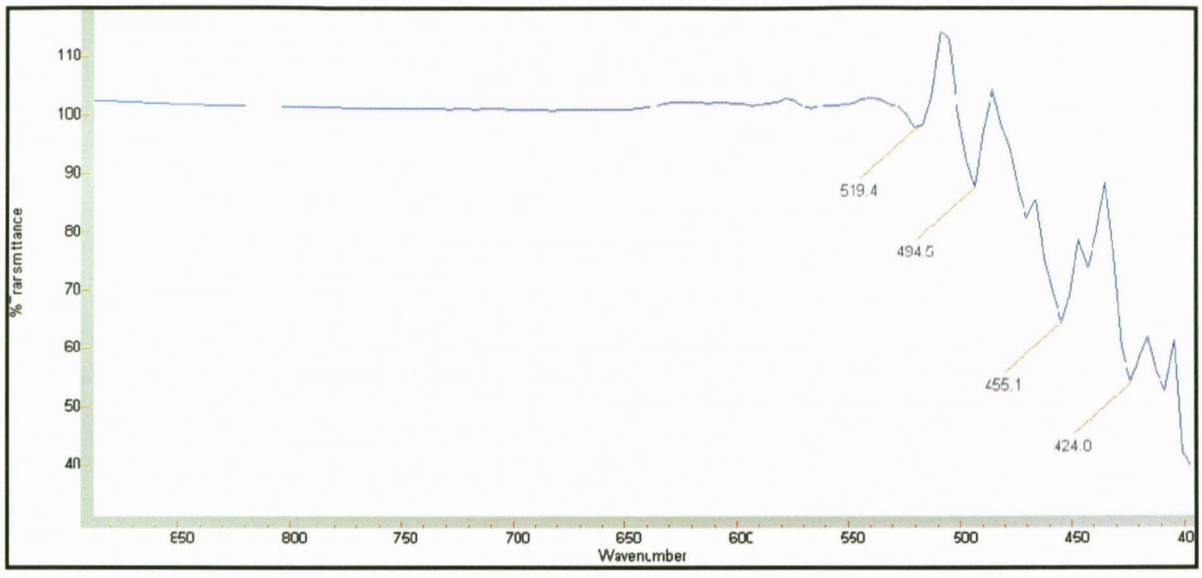

Figure 4.10: Spectrum of K_2ZrF_6 magnified on the far IR

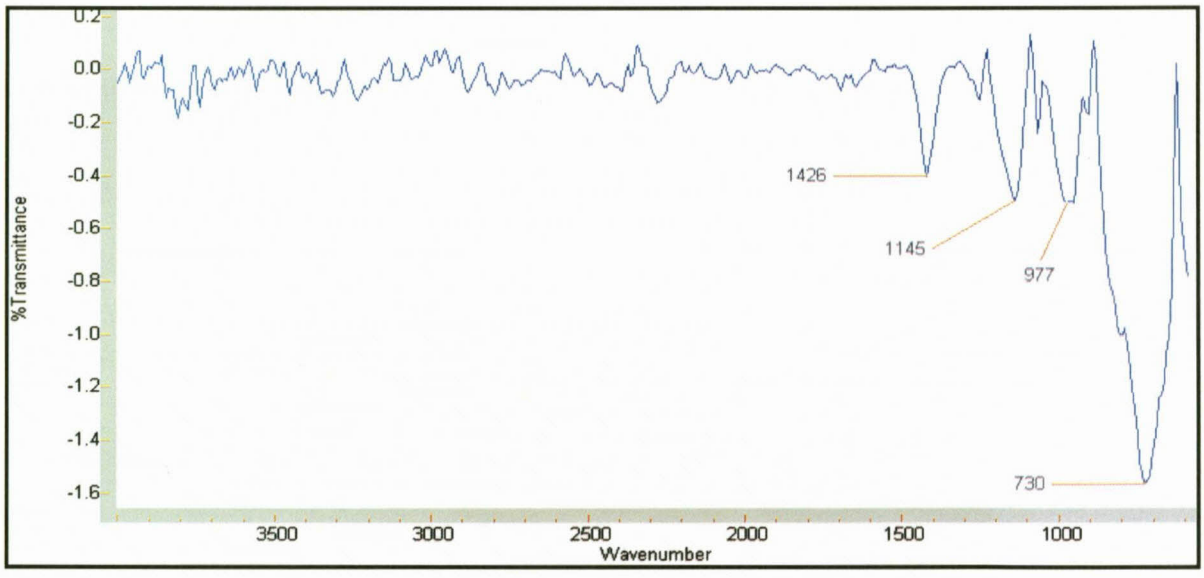

Figure 4.11: Spectrum of K_2ZrF_6 magnified and stretched on the near IR

A comparison of the IR spectrums (**Figures 4.6 – 4.8**) of the starting material, ZrF_4, and those of the expected product (**Figures 4.9 – 4.11**) K_2ZrF_6 show some difference in the far infrared region to suggest the successful preparation of the new zirconium reference material. The chemical formation of the product was subsequently verified with the zirconium and potassium analysis.

b) Analysis of the prepared K_2ZrF_6

Three portions of potassium hexafluorozirconate were accurately weighed (~100 mg) and transferred into 100.0 mL Blau brand volumetric flasks followed by the addition of 3.5 % sulphuric acid to the mark. For ICP-OES analysis, three equal aliquots (~2.0 mL) of each potassium hexafluorozirconate sample solution were transferred to 100.0 mL Blau brand volumetric flasks and filled to the mark with double distilled water. The results for the analysis of dissolved potassium hexafluorozirconate are shown in **Tables 4.16** and **4.17**. Qualitative ICP-OES analysis was also carried out on the diluted potassium hexafluorozirconate samples and they were found to contain no trace element. This can be attributed to the purification of the product by the precipitation and crystallization step, which could have resulted in the trace elements being left in the solution.

Table 4.16: ICP-OES analyses of K (λ = 766.491 nm) and Zr (λ = 343.823 nm) in K_2ZrF_6

	Potassium Recovery			Zirconium Recovery		
	Sample 1	Sample 2	Sample 3	Sample 1	Sample 2	Sample 3
Mean % (SD)	100 (65)	137 (30)	199 (93)	97.8 (8)	100 (1)	105 (2)
RSD (ppt)	650	219	467	8	10	19

Table 4.17: ICP-OES analyses of K (λ = 769.898 nm) and Zr (λ = 339.198 nm) in K_2ZrF_6

	Potassium Recovery			Zirconium Recovery		
	Sample 1	Sample 2	Sample 3	Sample 1	Sample 2	Sample 3
Mean % (SD)	226 (258)	124 (92)	146 (167)	102 (1)	100 (2)	99.6 (8)
RSD (ppt)	1142	742	1144	10	20	8

The extremely poor potassium results obtained from the ICP analysis prompted the use of AA to analyze for the potassium in K_2ZrF_6. It is a well-known fact that AA is an excellent technique to quantify metals – such as Na, K, Rb and Cs – that are easily excited to higher energy levels at relatively lower flame temperatures. In order to ensure that the correct

analytical conditions are selected for the accurate determination of potassium, the limits of detection (LOD) and quantification (LOQ) by the AA instrument were determined by applying the prevailing experimental conditions as discussed in **Table 4.3**. The LOD and LOQ were determined by the measurement of the intensities of the blank solution (10 replicates) at wavelengths 766.491 nm and 769.898 nm and calculated according to **Equations 3.8** and **3.9** in **Chapter 3**. The LOD's and LOQ's of potassium are shown in **Table 4.18**.

Table 4.18: AA determinations of the LOD and LOQ for potassium

Measurement number	Intensity of the blank solution @ 766.491 nm	Intensity of the blank solution @ 769.898 nm
1	0.02948	0.02752
2	0.02952	0.02745
3	0.02968	0.02774
4	0.02932	0.02746
5	0.02944	0.02736
6	0.02956	0.02732
7	0.02935	0.02735
8	0.02931	0.02735
9	0.02946	0.02721
10	0.02932	0.02756
Mean (SD)	**0.02944 (1)**	**0.02743 (1)**
Gradient	**0.1257**	**0.1300**
LOD (ppm)	**0.002901**	**0.003445**
LOQ (ppm)	**0.02901**	**0.03445**

For AA analysis, three equal aliquots (~2.0 mL) of each potassium hexafluorozirconate sample solution were transferred to 100.0 mL Blau brand volumetric flasks and filled to the mark with double distilled water. The results for the analysis of potassium are shown in **Tables 4.19** and **4.20**.

Table 4.19: AA analyses of K (λ = 766.491 nm) in K_2ZrF_6

	Potassium Recovery		
	Sample 1	Sample 2	Sample 3
Mean % (SD)	98.6 (8)	99.4 (3)	98.7 (4)
RSD (ppt)	8	3	4

Table 4.20: AA analyses of K (λ = 769.898 nm) in K_2ZrF_6

	Potassium Recovery		
	Sample 1	Sample 2	Sample 3
Mean % (SD)	100 (1)	101 (1)	98.6 (5)
RSD (ppt)	10	10	5

4.4 DISCUSSION, VALIDATION AND CONCLUSION

4.4.1 DISCUSSION OF RESULTS

The decomposition of zirconium samples were carried out in closed (microwave) and open digestion (bench-top) systems with different mineral acids so as to identify which method is the best for the complete dissolution of pure zirconium metal samples. The methods developed in this study for the digestion of zirconium-containing samples with various acids and at different experimental conditions were validated using ICP-OES. The analyses of zirconium samples were carried out at its most sensitive wavelengths of 343.823 nm and 339.198 nm. This was done to compare the two wavelengths to identify which would be the best for the accurate analysis of zirconium in various samples. An overview of all the results obtained at these wavelengths showed no significant difference of accuracy in the analysis of zirconium.

i. Limits of detection (LOD) and quantification (LOQ)

The first step in this study was the determination for the minimum detectible (LOD) and quantified (LOQ) amounts of zirconium on the ICP-OES instrument before any analysis was done on the samples as discussed in **Section 4.3.3**. Detection limits for zirconium have been reported to be between 0.5 – 5 ppm (mg/L)[163] while detection limits as low as 0.21 and 0.5 ppb (µg/L) have been recorded.[164,165,166] These zirconium detection limits were obtained under conditions specified for the simultaneous multi-element analysis with similar ICP-OES instrument components as those discussed in **Section 4.2.3**. In this study, the LOD was determined to be ~4 ppb, which is well within the acceptable range for the zirconium detection limit (see **Table 4.4**). Experimental conditions, such as viewing direction (axial or radial), flow gas rate as well as solution matrix, all play an important role in the detection limit. The limit of quantification was calculated as ~40 ppb or 0.04 mg/L, which is well below the zirconium concentrations that were used in this study. Therefore, this gives credibility to the zirconium recoveries that were obtained.

ii. Bench-top dissolution of zirconium rod and foil

The bench-top digestions of both the zirconium rod and the foil by sulphuric acid (see **Tables 4.5**, **4.6**, **4.9** and **4.10**) indicate that the zirconium recovery was the highest under the initial experimental conditions with an average of 101.3 % (combined at both wavelengths) and 102.0 % (combined at both wavelengths) for the rod and foil, respectively. The bench-top digestions of both the zirconium rod and the foil by phosphoric acid and *aqua regia* on the other hand were not that effective to completely dissolve the metal samples employing the initial experimental conditions. The samples were allowed to digest for a total of three days in order to improve dissolution. At the end of this period, the rod was partially digested, while visual inspection indicated that the foil was significantly digested by both acids. The quantification results in **Tables 4.5**, **4.6**, **4.9** and **4.10** confirm the partial dissolution of the rod with the lowest recovery obtained for phosphoric acid, with average recovery of 57.6 % (combined at both wavelengths). The additional time and acid improved the *aqua regia*

[163] http://www.appliedgeochemists.org /ChemElements/zr.html (29 Aug 2012)

[164] http://www.perkinelmer.com/PDFs/Downloads/BRO_WorldLeaderAAICPMSICPMS.pdf (08 Aug 2012)

[165] http://www.cetac.com/pdfs/AP_U5001.pdf (29 Aug 2012)

[166] http://www.eaglabs.com/documents/icp-oes-ms-detection-limit-guidance-BR023.pdf (29 Aug 2012)

dissolution of the rod to yield the average recovery of 89.6 % (combined at both wavelengths). It is clear from these quantitative results that sulphuric acid is by far the superior dissolution medium in terms of dissolution time and metal recovery. However, the time taken to digest the zirconium rod was twice that required to digest the zirconium foil with sulphuric acid in an open system. This is mainly attributed to the large surface area of the foil as compared to that of the rod. It is also evident that improved zirconium foil recovery was observed for phosphoric acid and *aqua regia* with average quantitative recovery of 100.8 % (at both wavelengths) for phosphoric acid and between 72 and 93 % (at both wavelengths) for *aqua regia*. It is therefore concluded that digestion of the zirconium foil by sulphuric acid is the most efficient for the purpose of developing a method for the rapid dissolution and analysis of zirconium metal samples.

iii. Microwave-assisted dissolution of zirconium rod and foil

Interesting results were obtained for the microwave digestions of the zirconium rod and foil as indicated in **Tables 4.6**, **4.7**, **4.11** and **4.12**. The zirconium recovery for the metal rod dissolution in the microwave yielded excellent results for both the sulphuric acid and *aqua regia* dissolutions (averages of 100.2 and 100.3 % for sulphuric acid and *aqua regia*, respectively), while phosphoric acid only yielded an average recovery of 88.2 %. The zirconium recovery from the metal foil on the other hand was substantially lower for all the acids with average recoveries of 32.7, 5.6 and 97.4 % for phosphoric acid, *aqua regia* and sulphuric acid, respectively. Thus the high pressure and high temperature settings employed in the microwave-assisted digestion are insignificant in digesting the zirconium metal samples.

iv. Analysis of zirconium(IV) tetrafluoride (ZrF_4)

The zirconium recovery in the water soluble ZrF_4 (1.5 g/100 mL H_2O at 25 ^{o}C) yielded excellent recoveries of 99.5 % at 343.823 nm and 101.7 % at 339.198 nm with relatively small standard deviations, reflecting the effectiveness and simplicity of the zirconium analysis. A qualitative analysis indicated the presence of small quantities of aluminium, chromium and silicon in the sample. Quantification of these impurities yielded 1.9, 0.1 and 0.5 ppm of the aluminium, chromium and silicon, respectively.

v. Analysis of potassium hexafluorozirconate (K_2ZrF_6)

The frequencies of the asymmetrical valence vibrations of fluorozirconates of the alkali metals and diammonium salts have been reported to be in the far infrared region of 455 – 575 cm^{-1}.[167,168,169] The spectrums above were found to be consistent with the frequencies as reported in the literature. There is some shift in peak frequencies as depicted from the spectrum of ZrF_4 to that of K_2ZrF_6 suggesting that the addition of two fluorine atoms to the zirconium metal have an influence in the IR absorption of the formed compound. However, this shift is negligible even though the difference seems to occur between the starting material and the product.

This prompted a further investigation in the near infrared region of both the spectrums. Since the frequencies were not that elaborate to make an informed deduction, the spectrums were then stretched and magnified to have a clearer view. The two absorption peaks with frequencies of 1139 and 1634 cm^{-1}, have significantly shifted in the potassium hexafluorozirconate spectrum to frequencies 1145 and 1426 cm^{-1}. This can be concluded that a product different from the starting material, ZrF_4, was formed in the reaction with potassium fluoride.

The quantitative analysis of the zirconium recovery for K_2ZrF_6 (see **Tables 4.16** and **4.17**) yielded excellent zirconium results of 100.9 and 100.5 % at the two different wavelengths. The potassium recovery, in terms of precision, using the ICP was extremely poor with values in excess of 200 % and high relative standard deviation. The potassium analysis with the AA yielded the expected recovery of 99.4 % (see **Tables 4.19** and **4.20**), confirming the chemical formula of the product for the reaction as K_2ZrF_6.

$$ZrF_4 + 2KF \longrightarrow K_2ZrF_6 \qquad (4.1)$$

It is clear from the preparation method that the potassium salt, K_2ZrF_6, is much more soluble than the starting material, ZrF_4, which simplifies the zirconium analysis and may prove to be a more suitable reference material for future zirconium analyses. Another interesting fact

[167] K. Nakamoto., *Infrared spectra of Inorganic and Coordination Compounds*, 2nd Ed., p. 166 (1970)

[168] V.I. Sergienko, R.L. Davidovich, T.F. Levchishina and Yu.N. Sklyadnev, *Russian Chemical Bulletin,* **19** (5), pp. 966 – 968 (1970)

[169] A. Kruger and A.M. Heyns, *Vibrational Spectroscopy*, **14**, pp. 171 – 181 (1997)

obtained from this analysis is that the dissolution of ZrF_4 with KF was extremely effective yielding a very pure product, K_2ZrF_6, without aluminium, chromium and silicon impurities as indicated by the absence of these metals in the qualitative analysis. The purification of the product from these trace elements was probably obtained by the crystallization process.

4.4.2 VALIDATION OF RESULTS

The validation of the analytical method for the zirconium quantification in the selective high purity samples, after their digestions with various acids, was carried out at the confidence level of 95 % for the first and second order wavelengths of 343.823 nm and 339.198 nm. The pooled standard deviations as well as RSD's calculated were from nine (9) experimental replicates in each acid digestion. Relative standard deviations (RSD) with values less than or equal to 20 parts per thousand (ppt) were regarded as good or acceptable.[170] The selectivity indicated that the method for the analysis of zirconium was not affected by the acid matrix. The digestion technique was considered to be robust where the results were shown to be highly reproducible.

The *t*-statistic values were also calculated at 95 % confidence level for 9 experimental replicates. The region of acceptance or rejection, as indicated by *t*-values was calculated according to **Equation 3.13** in **Chapter 3**. Rejection was indicated when the result was higher or lower than the t_{crit} (±2.31), depending on the number of replicates. All the validation parameters evaluated on the ICP-OES for the zirconium analysis in the various samples are summarized in **Table 4.21**.

[170] Aus. Pest. & Vet. Authority (APMVA), *GUIDELINES FOR THE VALIDATION OF ANALYTICAL METHODS FOR ACTIVE CONSTITUENT, AGRICULTURAL AND VETERINARY CHEMICAL PRODUCTS.* (2004)

Table 4.21: Validation criteria of the ICP-OES method for the analysis of zirconium in various materials

Validation Criteria	Parameter Tested	Calibration or Real sample
Linearity, sensitivity, and uncertainty	• Linearity of calibration (r,r^2) • Accuracy of calibration (b) • Precision of calibration (n) • Sensitivity of calibration (m) – method/instrument	Calibration
Working range of standards, number of standards, blanks and type of product tested	Working range	Calibration
Precision with acceptable RSD	Precision	Real sample
LOD and LOQ	LOD and LOQ	Calibration
Traceability of all reagents	Traceability	-
Accuracy of the method	Selectivity, specificity (s_c and s_m)	Real sample
Competency of analyst, instrument	Ruggedness	Real sample
Real sample analysis (workability)	Robustness	Real sample
Stability of reagents	Stability	-
Total uncertainty of method	Accuracy	Calibration and Real sample

S_m = standard deviation of the slope (also as S_a)

S_c = standard deviation of the intercept (also as S_b)

4.4.2.1 VALIDATION OF THE ZIRCONIUM ROD RESULTS

The validation of the results from the ICP-OES analyses for the partial digestions of the zirconium rod or foil was only considered for the dissolved portion. The validation parameters for the zirconium rod are reported as shown in **Tables 4.22** to **4.27**.

Table 4.22: Validation of ICP-OES analyses for sulphuric acid digestions of zirconium rod (λ = 343.823 nm)

Validation Criteria	Parameter	Bench-top	Microwave
Recovery	**$Mean_{pooled}$ % (SD)**	100 (3)	101 (3)
Precision	**RSD_{pooled} (ppt)**	30	30
Robustness		Results reproducible	Results reproducible
Working Range	**Calibration Curve**	2 – 10 ppm	
Linearity	**R^2**	1	
Sensitivity	**Slope**	2.4936	
Selectivity	**s_m**	0.0072	
Error of the Slope	**Intercept**	-0.5894	
Specificity	**S_c**	0.0206	
***t*-value**		0.2	0.7
Decision		Accepted	Accepted

Table 4.23: Validation of ICP-OES analyses for sulphuric acid digestions of zirconium rod (λ = 339.198 nm)

Validation Criteria	Parameter	Bench-top	Microwave
Recovery	**$Mean_{pooled}$ % (SD)**	102 (1)	100 (2)
Precision	**RSD_{pooled} (ppt)**	10	20
Robustness		Results reproducible	Results reproducible
Working Range	**Calibration Curve**	2 – 10 ppm	
Linearity	**R^2**	0.9998	
Sensitivity	**Slope**	2.8456	
Selectivity	**s_m**	0.0226	
Error of the Slope	**Intercept**	-1.2705	
Specificity	**S_c**	0.0649	
***t*-value**		4.5	- 0.3
Decision		Rejected	Accepted

Table 4.24: Validation of ICP-OES analyses for phosphoric acid digestions of zirconium rod (λ = 343.823 nm)

Validation Criteria	Parameter	Bench-top	Microwave
Recovery	**$Mean_{pooled}$ % (SD)**	60 (6)	90 (3)
Precision	**RSD_{pooled} (ppt)**	100	33
Robustness		Results reproducible	Results reproducible
Working Range	**Calibration Curve**	2 – 10 ppm	
Linearity	**R^2**	0.9999	
Sensitivity	**Slope**	2.6903	
Selectivity	**s_m**	0.0186	
Error of the Slope	**Intercept**	-0.0548	
Specificity	**S_c**	0.0534	
***t*-value**		- 11.3	- 9.2
Decision		Rejected	Rejected

Table 4.25: Validation of ICP-OES analyses for phosphoric acid digestions of zirconium rod (λ = 339.198 nm)

Validation Criteria	Parameter	Bench-top	Microwave
Recovery	**$Mean_{pooled}$ % (SD)**	55 (4)	86 (1)
Precision	**RSD_{pooled} (ppt)**	73	12
Robustness		Results reproducible	Results reproducible
Working Range	**Calibration Curve**	2 – 10 ppm	
Linearity	**R^2**	0.9996	
Sensitivity	**Slope**	3.3989	
Selectivity	**s_m**	0.0402	
Error of the Slope	**Intercept**	0.2581	
Specificity	**S_c**	0.1153	
***t*-value**		- 16.8	- 33.0
Decision		Rejected	Rejected

Table 4.26: Validation of ICP-OES analyses for *aqua regia* digestions of zirconium rod (λ = 343.823 nm)

Validation Criteria	Parameter	Bench-top	Microwave
Recovery	**$Mean_{pooled}$ % (SD)**	93 (2)	101 (1)
Precision	**RSD_{pooled} (ppt)**	22	10
Robustness		Results reproducible	Results reproducible
Working Range	**Calibration Curve**	2 – 10 ppm	
Linearity	**R^2**	0.9999	
Sensitivity	**Slope**	2.6903	
Selectivity	**s_m**	0.0186	
Error of the Slope	**Intercept**	-0.0548	
Specificity	**S_c**	0.0534	
***t*-value**		- 9.8	2.8
Decision		Rejected	Rejected

Table 4.27: Validation of ICP-OES analyses for *aqua regia* digestions of zirconium rod (λ = 339.198 nm)

Validation Criteria	Parameter	Bench-top	Microwave
Recovery	**$Mean_{pooled}$ % (SD)**	86 (4)	100 (3)
Precision	**RSD_{pooled} (ppt)**	47	30
Robustness		Results reproducible	Results reproducible
Working Range	**Calibration Curve**	2 – 10 ppm	
Linearity	**R^2**	0.9996	
Sensitivity	**Slope**	3.3989	
Selectivity	**s_m**	0.0402	
Error of the Slope	**Intercept**	0.2581	
Specificity	**S_c**	0.1153	
***t*-value**		- 9.4	- 0.5
Decision		Rejected	Accepted

4.4.2.2 VALIDATION OF THE ZIRCONIUM FOIL RESULTS

The validation of the method for the zirconium determination in the masses of the foil sample after their digestions in various acids was carried out in the similar fashion as in **Section 4.4.2.1**. The validation parameters for the zirconium foil are reported as shown in **Tables 4.28** to **4.33**.

Table 4.28: Validation of ICP-OES analyses for sulphuric acid digestions of zirconium foil (λ = 343.823 nm)

Validation Criteria	Parameter	Bench-top	Microwave
Recovery	**$Mean_{pooled}$ % (SD)**	102 (1)	97 (4)
Precision	**RSD_{pooled} (ppt)**	10	41
Robustness		Results reproducible	Results reproducible
Working Range	**Calibration Curve**	2 – 10 ppm	
Linearity	**R^2**	0.9998	0.9998
Sensitivity	**Slope**	2.9453	2.4523
Selectivity	**s_m**	0.0215	0.0193
Error of the Slope	**Intercept**	-0.7925	-0.2694
Specificity	**S_c**	0.0618	0.0553
***t*-value**		5.4	- 1.9
Decision		Rejected	Accepted

Table 4.29: Validation of ICP-OES analyses for sulphuric acid digestions of zirconium foil (λ = 339.198 nm)

Validation Criteria	Parameter	Bench-top	Microwave
Recovery	**$Mean_{pooled}$ % (SD)**	102 (2)	102 (4)
Precision	**RSD_{pooled} (ppt)**	20	39
Robustness		Results reproducible	Results reproducible
Working Range	**Calibration Curve**	2 – 10 ppm	
Linearity	**R^2**	0.9996	0.9998
Sensitivity	**Slope**	4.0170	2.3086
Selectivity	**s_m**	0.0436	0.0169
Error of the Slope	**Intercept**	-3.1857	-0.3597
Specificity	**S_c**	0.1251	0.0486
***t*-value**		3.4	1.9
Decision		Rejected	Accepted

Table 4.30: Validation of ICP-OES analyses for phosphoric acid digestions of zirconium foil (λ = 343.823 nm)

Validation Criteria	Parameter	Bench-top	Microwave
Recovery	**$Mean_{pooled}$ % (SD)**	101 (2)	37 (3)
Precision	**RSD_{pooled} (ppt)**	20	81
Robustness		Results reproducible	Results reproducible
Working Range	**Calibration Curve**	2 – 10 ppm	
Linearity	**R^2**	0.9996	0.9998
Sensitivity	**Slope**	2.6902	2.4523
Selectivity	**s_m**	0.0307	0.0193
Error of the Slope	**Intercept**	-0.1181	-0.2694
Specificity	**S_c**	0.0881	0.0553
***t*-value**		1.1	- 26.0
Decision		Accepted	Rejected

Table 4.31: Validation of ICP-OES analyses for phosphoric acid digestions of zirconium foil (λ = 339.198 nm)

Validation Criteria	Parameter	Bench-top	Microwave
Recovery	**$Mean_{pooled}$ % (SD)**	101 (2)	29 (3)
Precision	**RSD_{pooled} (ppt)**	20	103
Robustness		Results reproducible	Results reproducible
Working Range	**Calibration Curve**	2 – 10 ppm	
Linearity	**R^2**	1	0.9998
Sensitivity	**Slope**	3.6115	2.3086
Selectivity	**s_m**	0.0051	0.0169
Error of the Slope	**Intercept**	-0.9622	-0.3597
Specificity	**S_c**	0.0146	0.0486
***t*-value**		1.8	- 62.9
Decision		Accepted	Rejected

Table 4.32: Validation of ICP-OES analyses for *aqua regia* digestions of zirconium foil (λ = 343.823 nm)

Validation Criteria	Parameter	Bench-top	Microwave
Recovery	**$Mean_{pooled}$ % (SD)**	85 (9)	5 (2)
Precision	**RSD_{pooled} (ppt)**	106	400
Robustness		Results reproducible	Results reproducible
Working Range	**Calibration Curve**	2 – 10 ppm	
Linearity	**R^2**	0.9996	0.9998
Sensitivity	**Slope**	2.6902	2.4523
Selectivity	**s_m**	0.0307	0.0193
Error of the Slope	**Intercept**	-0.1181	-0.2694
Specificity	**S_c**	0.0881	0.0553
***t*-value**		- 4.9	- 118.5
Decision		Rejected	Rejected

Table 4.33: Validation of ICP-OES analyses for *aqua regia* digestions of zirconium foil (λ = 339.198 nm)

Validation Criteria	Parameter	Bench-top	Microwave
Recovery	**$Mean_{pooled}$ % (SD)**	86 (9)	6 (2)
Precision	**RSD_{pooled} (ppt)**	105	333
Robustness		Results reproducible	Results reproducible
Working Range	**Calibration Curve**	2 – 10 ppm	
Linearity	**R^2**	1	0.9998
Sensitivity	**Slope**	3.6115	2.3086
Selectivity	**s_m**	0.0051	0.0169
Error of the Slope	**Intercept**	-0.9622	-0.3597
Specificity	**S_c**	0.0146	0.0486
***t*-value**		- 4.8	- 141.2
Decision		Rejected	Rejected

4.4.2.3 VALIDATION OF THE ZIRCONIUM(IV) TETRAFLUORIDE (ZrF_4) RESULTS

The validation parameters for the ZrF_4 are reported as shown in **Table 4.34**.

Table 4.34: Validation of ICP-OES analyses for sulphuric acid digestions of ZrF_4

Validation Criteria	Parameter	343.823 nm	339.198 nm
Recovery	**$Mean_{pooled}$ % (SD)**	100 (1)	102 (2)
Precision	**RSD_{pooled} (ppt)**	10	20
Robustness		Results reproducible	Results reproducible
Working Range	**Calibration Curve**	2 – 10 ppm	
Linearity	**R^2**	0.9996	0.9998
Sensitivity	**Slope**	4.0373	4.0431
Selectivity	**s_m**	0.0468	0.0364
Error of the Slope	**Intercept**	-3.3685	-1.5867
Specificity	**S_c**	0.1342	0.1043
***t*-value**		- 1.4	3.0
Decision		Accepted	Rejected

4.4.2.4 VALIDATION OF THE POTASSIUM HEXAFLUOROZIRCONATE (K_2ZrF_6) RESULTS

The validation parameters for the K_2ZrF_6 are reported as shown in **Table 4.35**.

Table 4.35: Validation of ICP-OES analyses for sulphuric acid digestions of K_2ZrF_6 at both wavelengths

Validation Criteria	Parameter	343.823 nm	339.198 nm
Recovery	**$Mean_{pooled}$ % (SD)**	101 (3)	100 (2)
Precision	**RSD_{pooled} (ppt)**	30	20
Robustness		Results reproducible	Results reproducible
Working Range	**Calibration Curve**	2 – 10 ppm	
Linearity	**R^2**	0.9999	0.9997
Sensitivity	**Slope**	1.9380	2.7495
Selectivity	**s_m**	0.0108	0.0291
Error of the Slope	**Intercept**	-0.2862	-0.8090
Specificity	**S_c**	0.0309	0.0833
***t*-value**		0.6	0.5
Decision		Accepted	Accepted

4.4.3 CONCLUSION

The aim of this study was to develop appropriate and efficient methods to dissolve and quantify zirconium in different metallic and inorganic samples, such as zirconium metal foil, ZrF_4 and K_2ZrF_6, using external calibration standards. Microwave digestion and open vessel in the presence of different acid mediums were evaluated for their effectiveness to dissolve metallic zirconium samples.

The results obtained from the study clearly identified concentrated sulphuric acid applied in an open vessel digestion step, as the most efficient dissolution agent with zirconium recoveries of 100 ± 2 % in most of the cases. Zirconium quantification with ICP-OES also indicated excellent recoveries for pure ZrF_4, as well as the newly prepared K_2ZrF_6 complex. Satisfactory validation parameters were obtained for all the validation criteria. However, the relatively small standard deviation obtained for some of these analytical results led to negative validation acceptance criteria (rejection of null hypothesis).

5 QUANTITATIVE DETERMINATIONS OF IMPURITIES IN ULTRA PURE ZIRCONIUM METAL SAMPLES

5.1 INTRODUCTION

The development and validation of the method for the complete digestion and accurate determination of the zirconium in high purity samples was successfully validated at 95 % confidence level in **Chapter 4**. Other validation parameters, such as the standard deviation, working range, selectivity and LOD/LOQ, were also determined as part of the validation process. The successful development and validation of the analytical method has been an important prerequisite for the continuation of the study, which requires the stepwise addition of the impurities associated with nuclear grade zirconium metal as indicated in **Section 1.4.2**, **Table 1.4** and aim of the study in **Section 1.5**. Ultra-pure or nuclear grade zirconium metal samples are however not commercially available and it was decided to add the identified impurities, firstly in a stepwise fashion (tenth and threshold permissible content), and then as combinations to solutions of pure zirconium ions (same metal foil of 99.98 % purity that was studied in **Chapter 4**) to determine the success of the recovery of these elements. The non-metals carbon, nitrogen, chlorine and oxygen, that were also identified as possible impurities were not included in this study, mainly due to the inability of ICP-OES spectroscopy to quantitatively identify these elements. The aim of the study was to determine the recovery of these impurities as well as the effects these impurity elements might have on the recoveries of the other elements and that of the zirconium.

Table 5.1: Selection and experimental grouping of the permissible impurities in zirconium in this study

Element	Threshold (ppm)	10^{th} of Threshold (ppm)
Group 1		
Aluminium (Al)	75	7.5
Chromium (Cr)	200	20
Hafnium (Hf)	100	10
Iron (Fe)	1500	150
Group 2		
Boron (B)	0.5	0.05
Cadmium (Cd)	0.5	0.05
Cobalt (Co)	20	2
Copper (Cu)	30	3
Manganese (Mn)	50	5
Group 3		
Molybdenum (Mo)	15	1.5
Nickel (Ni)	70	7
Silicon (Si)	120	12
Titanium (Ti)	50	5
Tungsten (W)	50	5
Uranium (U)	3	0.3

5.2 EQUIPMENT, REAGENTS AND GENERAL EXPERIMENTAL PROCEDURE

5.2.1 ICP-OES SPECTROMETER AND OTHER EQUIPMENT

The ICP-OES spectrometer described in **Section 4.2.3** was used in the analysis of all the added impurities discussed in **Table 5.1**, as well as the zirconium ions, which were obtained from the metal foil dissolution. All the other equipment used in this study were those that were described in **Sections 4.2.5 – 4.2.8**.

5.2.2 REAGENTS

Zirconium foil (99.98 %, cat. no. 419141-4.6G), zirconium ICP standard (10000 ppm Zr, cat. no. 356751) and hafnium tetrachloride (98 % $HfCl_4$, cat. no. 25820-2) were purchased from Sigma-Aldrich. Aluminium chloride (99 % $AlCl_3 \cdot 6H_2O$, cat. no. 1116040) and cobaltous nitrate [99 % $Co(NO_3)_2 \cdot 6H_2O$, cat. no. 166120] were purchased from Saarchem. Sodium borate ($Na_2B_2O_7 \cdot 10H_2O$, cat. no. R3790/500G) and copper chloride (99 % $CuCl_2 \cdot 2H_2O$, cat. no. R0758/500G) were purchased from NT Laboratory Supplies. Sodium silicate ($Na_2SiO_3 \cdot 5H_2O$, cat. no. 24347/8477), hydrochloric (32 %, cat. no. 7647-01-0) and phosphoric (80 %, 7664-38-2) acids were purchased from Associated Chemicals Enterprises. Sodium molybdate (98 – 104 % $Na_2MoO_4 \cdot 2H_2O$, cat. no. 30185) was purchased from BDH Chemicals, nickel sulphate (> 97 % $NiSO_4 \cdot 6H_2O$, cat. no. 62608) from M&B Laboratory Chemicals.

Acetyl uranate (99 % $(CH_3COO)_2UO_2 \cdot 2H_2O$, cat. no. 8473), tungsten ICP standard (1000 ppm W, cat. no. 1.70364.0100), titanium ICP standard (1000 ppm Ti, cat. no. 1.70243.0500), zirconium ICP standard (1000 ppm Zr, cat. no. 1.70370.0100), multi-element ICP standard (1000 ppm, cat. no. 1.11355.0100), hafnium ICP standard (1000 ppm Hf, cat. no. 1.70322.0100), molybdenum ICP standard (1000 Mo, cat. no. 1.70334.0100) and iron ICP standard (10000 ppm Fe, cat. no. 1.70243.0100), nitric acid (55 %, SAAR4465080LP) and sulphuric acid (98 %; Cat. nr 5885060LC; Batch nr 1015597) were purchased from Merck. Uranium ICP standard (1000 ppm U, cat. no. 992R83) was purchased from Ultraspec. Silicon ICP standard (1000 ppm Si, cat. no. CGSI 1-1) and chromium ICP standard (1000 ppm Cr, cat. no. CGCR(3)1-1) was purchased from Inorganic Ventures. Potassium permanganate ($KMnO_4$), sodium dichromate ($Na_2Cr_2O_7$), cadmium chloride ($CdCl_2 \cdot H_2O$) and iron chloride ($FeCl_3$) were supplied by the Chemistry Department of the University of the Free State.

5.3 PREPARATION OF THE ZIRCONIUM AND THE IMPURITY STOCK SOLUTIONS

5.3.1 PREPRATION OF THE ALUMINIUM STOCK SOLUTION

A mass of $AlCl_3 \cdot 6H_2O$ (~900 mg) was accurately weighed to 0.1 mg and quantitatively transferred to a 100.0 mL Blau brand volumetric flask. The solid was dissolved in double distilled water and filled to the mark to give a final aluminium concentration of 1000 ppm.

5.3.2 PREPARATION OF THE BORON STOCK SOLUTION

A mass of $Na_2B_4O_7 \cdot 10H_2O$ (~1000 mg) was accurately weighed to 0.1 mg and quantitatively transferred to a 100.0 mL Kartell HDPE volumetric flask. Concentrated hydrochloric acid (10 mL) was added to assist with the dissolution and the flask was filled to the mark with double distilled water to give a final boron concentration of 1000 ppm.

5.3.3 PREPARATION OF THE CADMIUM STOCK SOLUTION

A mass of $CdCl_2 \cdot H_2O$ (~190 mg) was accurately weighed to 0.1 mg and quantitatively transferred to a 100.0 mL Blau brand volumetric flask. The solid was dissolved in double distilled water and filled to the mark to give a final cadmium concentration of 1000 ppm.

5.3.4 PREPARATION OF THE CHROMIUM STOCK SOLUTION

A mass of $Na_2Cr_2O_7$ (~3600 mg) was accurately weighed to 0.1 mg and quantitatively transferred to a 250.0 mL Kartell HDPE volumetric flask. The solid was dissolved in double distilled water and filled to the mark to give a final chromium concentration of 5000 ppm.

5.3.5 PREPARATION OF THE COBALT STOCK SOLUTION

A mass of $Co(NO_3)_2 \cdot 6H_2O$ (~500 mg) was accurately weighed to 0.1 mg and quantitatively transferred to a 100.0 mL Blau brand volumetric flask. The solid was dissolved in double distilled water and filled to the mark to give a final cobalt concentration of 1000 ppm.

5.3.6 PREPARATION OF THE COPPER STOCK SOLUTION

A mass of $CuCl_2 \cdot 2H_2O$ (~270 mg) was accurately weighed to 0.1 mg and quantitatively transferred to a 100.0 mL Blau brand volumetric flask. The solid was dissolved in double distilled water and filled to the mark to give a final copper concentration of 1000 ppm.

5.3.7 PREPARATION OF THE IRON STOCK SOLUTION

A mass of $FeCl_3$ (~7600 mg) was accurately weighed to 0.1 mg and quantitatively transferred to a 250.0 mL Kartell HDPE volumetric flask. Concentrated hydrochloric acid (10 mL) was added to assist with the dissolution and the flask was filled to the mark with double distilled water to give a final iron concentration of 10000 ppm.

5.3.8 PREPARATION OF THE HAFNIUM STOCK SOLUTION

A mass of $HfCl_4$ (~350 mg) was accurately weighed to 0.1 mg and quantitatively transferred to a 100.0 mL Blau brand volumetric flask. The solid was dissolved in double distilled water and filled to the mark to give a final hafnium concentration of 2000 ppm.

5.3.9 PREPARATION OF THE MANGANESE STOCK SOLUTION

A mass of $KMnO_4$ (~300 mg) was accurately weighed to 0.1 mg and quantitatively transferred to a 100.0 mL Blau brand volumetric flask. The solid was dissolved in double distilled water and filled to the mark to give a final manganese concentration of 1000 ppm.

5.3.10 PREPARATION OF THE MOLYBDENUM STOCK SOLUTION

A mass of $Na_2MoO_4 \cdot 2H_2O$ (~130 mg) was accurately weighed to 0.1 mg and quantitatively transferred to a 100.0 mL Blau brand volumetric flask. The solid was dissolved in double distilled water and filled to the mark to give a final molybdenum concentration of 500 ppm.

5.3.11 PREPARATION OF THE NICKEL STOCK SOLUTION

A mass of $NiSO_4 \cdot 6H_2O$ (~460 mg) was accurately weighed to 0.1 mg and quantitatively transferred to a 100.0 mL Blau brand volumetric flask. The solid was dissolved in double distilled water and filled to the mark to give a final nickel concentration of 1000 ppm.

5.3.12 PREPARATION OF THE SILICON STOCK SOLUTION

A mass of $Na_2SiO_3 \cdot 5H_2O$ (~1500 mg) was accurately weighed to 0.1 mg and quantitatively transferred to a 100.0 mL Kartell HDPE volumetric flask. The solid was dissolved in double distilled water and filled to the mark to give a final silicon concentration of 2000 ppm.

5.3.13 PREPARATION OF THE TITANIUM STOCK SOLUTION

No titanium solution was prepared. However, in the quantitative analyses of this impurity, titanium ICP standard mentioned in **Section 5.2.2** was used.

5.3.14 PREPARATION OF THE TUNGSTEN STOCK SOLUTION

The tungsten ICP standard mentioned in **Section 5.2.2** was used for the quantitative analyses of tungsten as an impurity in this study.

5.3.15 PREPARATION OF THE URANIUM STOCK SOLUTION

A mass of $(CH_3COO)_2UO_2 \cdot 2H_2O$ (~200 mg) was accurately weighed to 0.1 mg and quantitatively transferred to a 100.0 mL Blau brand volumetric flask. The solid was dissolved in double distilled water and filled to the mark to give a final uranium concentration of 1000 ppm.

5.3.16 PREPARATION OF THE ZIRCONIUM STOCK SOLUTION

A mass of zirconium foil (~2 g) was accurately weighed to 0.1 g and quantitatively transferred to 250.0 mL Schott Duran glass beaker. Concentrated sulphuric acid (100 mL) was added to the beaker and the foil was digested in a fumehood at 150 °C on a hot-plate while constantly stirring for 75 minutes. After cooling to room temperature, the reaction mixture was

quantitatively transferred to 500.0 mL Kartell HDPE volumetric flask and filled to the mark with double distilled water to give a final zirconium concentration of 4600 ppm.

5.4 QUANTIFICATION OF THE SPECIFIED IMPURITIES IN THE ZIRCONIUM FOIL BY ICP-OES

5.4.1 GENERAL EXPERIMENTAL PROCEDURE

All the experimental samples were diluted with double distilled water after their mixing and each analytical analysis was carried out in triplicate, unless stated otherwise. The calibration standard solutions were prepared in such a way that their matrices closely resemble those of the analyzed samples. Standard ICP solutions of some of the elements with similar matrices, such as those for molybdenum, titanium and tungsten, were mixed to make laboratorial multi-element standard solutions. This was done to ensure compatibility between different standard ICP solutions. The ICP-OES analyses for all the elements were carried out at selected wavelengths which ensured no interferences from other elements present in the solution.[161]

Zirconium was added to obtain a concentration in the mixtures at ~500 ppm for the analyses of the impurities at the tenth of their permitted content and at ~1000 ppm for the analyses of the impurities at the threshold of their permitted content. This was done to ensure that the zirconium concentration remains the highest of its associated impurities for nuclear viability. The samples were analyzed first by quantifying the zirconium in all samples using the same calibration curve, and then followed by the quantification of the individual impurities. This procedure was repeated also for the quantification of impurities in their respective groups as well as their combinations.

5.4.2 PREPARATION OF THE ICP CALIBRATION STANDARDS

Multi-element calibration standard solutions (containing Al, B, Cd, Co, Cu, Cr, Fe, Mn and Ni) were prepared from aliquots (2, 4, 6, 8 and 10 mL) of the multi-element ICP standard into 100.0 mL Kartell HDPE volumetric flasks. Mineral acids (1 mL), *viz.* sulphuric, hydrochloric and nitric acids, were combined and added to the multi-element standard aliquots and subsequently filled with double distilled water to the mark to obtain final concentrations of 20,

40, 60, 80 and 100 ppm, respectively, in each element. Due to insufficient working range for both chromium and iron impurities (highest permissible levels) in the above multi-element standards, the calibration standard solutions of these elements were prepared by mixing their ICP standards in 100.0 mL Blau brand volumetric flasks. Iron ICP standard aliquots (5, 10, 15, 20 and 25 mL) were respectively added to the flasks containing the chromium ICP standard aliquots (5, 10, 15, 20 and 25 mL). Mineral acids (1 mL), *viz.* sulphuric, hydrochloric and nitric acids, were combined and added to the standard aliquots and the flasks were filled with double distilled water to the mark to obtain final concentrations of 500, 1000, 1500, 2000 and 2500 ppm in iron and 50, 100, 150, 200 and 250 ppm in chromium.

Molybdenum, titanium and tungsten were prepared by mixing their aliquots (2, 4, 6, 8 and 10 mL) from their respective ICP standards in 100.0 mL Blau brand volumetric flasks. Mineral acids (1 mL), *viz.* sulphuric, hydrochloric and nitric acids, were combined and added to the standard aliquots and subsequently filled with double distilled water to the mark to obtain final concentrations of 20, 40, 60, 80 and 100 ppm, respectively, in each element.

Due to the small volumes needed to prepare and the subsequent lower calibration range, the uranium ICP calibration standards were prepared separately from any combination. Uranium aliquots (0.2, 0.4, 0.6, 0.8 and 1.0 mL) were transferred to 100.0 mL Blau brand volumetric flasks. Mineral acids (1 mL), *viz.* sulphuric, hydrochloric and nitric acids were combined and added to the standard aliquots and subsequently filled with double distilled water to the mark to obtain final concentrations of 2, 4, 6, 8 and 10 ppm in uranium.

Zirconium, hafnium and silicon were prepared by mixing their aliquots (3, 6, 9, 12 and 15 mL) from their respective ICP standards in 100.0 mL Kartell HDPE volumetric flasks. Diluted mineral acids (0.01 %, 10 mL), *viz.* sulphuric, hydrochloric and nitric acids, were added to the standard aliquots and subsequently filled with double distilled water to the mark to obtain final concentrations of 30, 60, 90, 120 and 150 ppm, respectively, for hafnium and silicon. The final concentrations obtained for zirconium were 300, 600, 900, 1200 and 1500 ppm.

5.4.3 DETECTION AND QUANTIFICATION LIMITS OF THE IMPURITIES ASSOCIATED WITH THE NUCLEAR GRADE ZIRCONIUM

The limits of detection (LOD's) and limits of quantification (LOQ's) of the impurities associated with the nuclear grade zirconium were determined in a similar way as discussed in **Chapter 3**, **Equations 3.8** and **3.9,** in order to ensure that the correct analytical conditions were selected for their accurate determination in zirconium. The LOD's and LOQ's of all the impurity elements are shown in **Tables 5.2** and **5.3**.

Table 5.2: Determination of the LOD and LOQ from their blank intensities for impurities associated with nuclear grade zirconium

Replicate Nr	Al	B	Cd	Co	Cu	Cr	Fe
1	0.2897	0.1334	0.0676	0.0557	0.3370	0.1119	0.0642
2	0.2908	0.1327	0.0690	0.0562	0.3356	0.1109	0.0677
3	0.2930	0.1346	0.0685	0.0562	0.3396	0.1133	0.0745
4	0.2892	0.1320	0.0675	0.0556	0.3345	0.1117	0.0813
5	0.2899	0.1333	0.0679	0.0559	0.3357	0.1135	0.0852
6	0.2902	0.1351	0.0700	0.0557	0.3361	0.1117	0.0871
7	0.2907	0.1352	0.0683	0.0554	0.3364	0.1117	0.0872
8	0.2919	0.1333	0.0690	0.0562	0.3342	0.1117	0.0870
9	0.2880	0.1333	0.0697	0.0555	0.3350	0.1111	0.0864
10	0.2872	0.1312	0.0698	0.0564	0.3350	0.1112	0.0882
Mean (SD)	**0.290 (2)**	**0.133 (1)**	**0.069 (1)**	**0.0559 (4)**	**0.336 (2)**	**0.112 (1)**	**0.081 (9)**
Gradient	**0.1966**	**0.2575**	**0.7737**	**0.2924**	**0.5408**	**0.3122**	**0.3230**
LOD (ppm)	**0.02637**	**0.01517**	**0.00346**	**0.00388**	**0.00860**	**0.00823**	**0.08258**
LOQ (ppm)	**0.2637**	**0.1517**	**0.03458**	**0.03880**	**0.08598**	**0.08231**	**0.8258**

Table 5.3: Determination of the LOD and LOQ from their blank intensities for impurities associated with nuclear grade zirconium

Replicate Nr	Hf	Mn	Mo	Ni	Si	Ti	W	U
1	0.0354	0.0808	0.0217	0.0709	0.0691	0.3604	0.0309	0.2487
2	0.0360	0.0809	0.0220	0.0710	0.0697	0.3568	0.0311	0.2490
3	0.0355	0.0806	0.0219	0.0708	0.0687	0.3597	0.0312	0.2505
4	0.0364	0.0818	0.0216	0.0701	0.0694	0.3620	0.0311	0.2523
5	0.0372	0.0822	0.0227	0.0704	0.0695	0.3606	0.0309	0.2463
6	0.0372	0.0818	0.0227	0.0708	0.0686	0.3578	0.0315	0.2479
7	0.0366	0.0824	0.0224	0.0714	0.0656	0.3615	0.0311	0.2485
8	0.0364	0.0827	0.0231	0.0701	0.0680	0.3618	0.0306	0.2523
9	0.0370	0.0830	0.0240	0.0699	0.0666	0.3636	0.0318	0.2476
10	0.0368	0.0837	0.0231	0.0712	0.0646	0.3620	0.0316	0.2473
Mean (SD)	**0.0364 (7)**	**0.082 (1)**	**0.0225 (7)**	**0.0707 (5)**	**0.068 (2)**	**0.361 (2)**	**0.0312 (4)**	**0.249 (2)**
Gradient	**0.1069**	**2.297**	**0.1268**	**0.3433**	**0.1896**	**3.283**	**0.0388**	**0.0651**
LOD (ppm)	**0.01825**	**0.00134**	**0.01771**	**0.00439**	**0.02791**	**0.00189**	**0.02796**	**0.09355**
LOQ (ppm)	**0.1825**	**0.01343**	**0.1771**	**0.04388**	**0.2791**	**0.01893**	**0.2796**	**0.9355**

5.4.4 QUANTIFICATION OF INDIVIDUALLY ADDED IMPURITIES IN THE ULTRA PURE ZIRCONIUM FOIL

5.4.4.1 QUANTIFICATION ZIRCONIUM IN THE DIGESTED ZIRCONIUM FOIL

The zirconium in the digested zirconium foil was quantified to verify its dissolution in the digestion process by sulphuric acid. First, the set of calibration standard solutions used to quantify the zirconium foil was prepared in a similar way as discussed in **Section 4.3.2**. Three aliquots (~0.1 mL) of this zirconium stock solution were transferred to different 100.0 mL Blau brand volumetric flasks and filled to the mark with double distilled water to achieve

the final concentrations of 5 ppm in zirconium. The quantitative results of zirconium, measured at the wavelength 339.198 nm, are shown in **Tables 5.4**.

Table 5.4: ICP-OES analysis for the sulphuric acid digestion of zirconium foil (λ = 339.198 nm)

	Zirconium foil		
	Solution 1	Solution 2	Solution 3
% Recovery	101	103	101
Mean % Recovery (SD)	102 (1)		
RSD (ppt)	10		

5.4.4.2 QUANTIFICATION OF ALUMINIUM AS IMPURITY

For the quantification of aluminium as impurity within the pure zirconium solution, the three aliquots (3.0 mL) of zirconium stock solution were transferred to different 25.0 mL Blau brand volumetric flasks. Three aliquots (~0.2 mL) of the aluminium stock solution were added to each zirconium aliquot and the flasks were filled to the mark with double distilled water to obtain the final concentrations of 500 ppm zirconium and 8 ppm aluminium.

Another set of the zirconium foil solution was prepared by transferring three aliquots (6.0 mL) of the stock solution to different 25.0 mL Blau brand volumetric flasks. Three aliquots (~2.0 mL) of the aluminium stock solution were added to each zirconium aliquot and the flasks were filled to the mark with double distilled water to obtain the final concentrations of 1000 ppm zirconium and 80 ppm aluminium. Zirconium and the aluminium in these samples were quantified against their respective calibration curves using ICP-OES analysis. The results for these analyses are shown in **Table 5.5**.

5.4.4.3 QUANTIFICATION OF CHROMIUM AS IMPURITY

For the quantification of chromium as impurity in the pure zirconium solution, three aliquots (3.0 mL) of the zirconium stock solution were transferred to different 25.0 mL Blau brand volumetric flasks. Three aliquots (0.1 mL) of the chromium stock solution were added to the

zirconium aliquots and the flasks were filled to the mark with double distilled water to obtain the final concentrations of 500 ppm zirconium and 20 ppm chromium.

Another set of the zirconium solutions was prepared by transferring three aliquots (6.0 mL) of the stock solution to different 25.0 mL Blau brand volumetric flasks. Three aliquots (1.0 mL) of the chromium stock solution were then added to each of these flasks and then filled to the mark with double distilled water to yield final concentrations of 1000 ppm zirconium and 200 ppm chromium. Zirconium and the chromium content in these samples were then quantified against their respective calibration curves by using ICP-OES analysis. The results for these analyses are shown in **Table 5.5**.

5.4.4.4 QUANTIFICATION OF HAFNIUM AS IMPURITY

For the quantification of hafnium as impurity in the pure zirconium solution, three aliquots (3.0 mL) of the zirconium stock solution were transferred to different 25.0 mL Blau brand volumetric flasks. Three aliquots (~0.1 mL) of the hafnium stock solution were added to each of the flasks containing zirconium aliquots and the flasks were then filled to the mark with double distilled water to give final concentrations of 500 ppm zirconium and 10 ppm hafnium.

The next set of solutions was prepared by transferring three aliquots (6.0 mL) of the zirconium stock solution to different 25.0 mL Blau brand volumetric flasks. Three aliquots (~1.0 mL) of the hafnium stock solution were added to each flask containing zirconium aliquot and the flasks were subsequently filled to the mark with double distilled water to give final concentrations of 1000 ppm zirconium and 100 ppm hafnium. Zirconium and the hafnium contents in these samples were then quantified against their respective calibration curves by using ICP-OES analysis. The results for these analyses are shown in **Table 5.5**.

5.4.4.5 QUANTIFICATION OF IRON AS IMPURITY

For the quantification of iron as impurity in the pure zirconium solution, three aliquots (3.0 mL) of the zirconium stock solution were transferred to different 25.0 mL Blau brand volumetric flasks. Three aliquots (~0.4 mL) of the iron stock solution were added to each of the flasks containing zirconium aliquots and the flasks were filled to the mark with double distilled water to yield final concentrations of 500 ppm zirconium and 150 ppm iron.

The other set of the zirconium solutions was prepared by transferring three aliquots (6.0 mL) of the stock solution to different 25.0 mL Blau brand volumetric flasks. Three aliquots (~4.0 mL) of the iron stock solution were then added to each of the flasks containing zirconium aliquots and subsequently filled to the mark with double distilled water to yield final concentrations of 1000 ppm zirconium and 1500 ppm iron. The zirconium and the iron contents in these samples were then quantified against their respective calibration curves by using ICP-OES analysis. The results for these analyses are shown in **Table 5.5**.

5.4.4.6 QUANTIFICATION OF BORON AS IMPURITY

For the quantification of boron as impurity in the pure zirconium solution, a new boron stock solution was prepared by transferring an aliquot (0.215 mL) to a 50.0 mL Kartell HDPE volumetric flask and then diluted with double distilled water to obtain the final concentration of 5 ppm boron. The zirconium solutions were prepared by transferring three aliquots (3.0 mL) of the stock solution to different 25.0 mL Kartell HDPE volumetric flasks. Three aliquots (~0.25 mL) of the diluted boron stock solution were added to each flask containing the zirconium aliquots and the flasks were filled to the mark with double distilled water to yield final concentrations of 500 ppm zirconium and 0.05 ppm boron.

Another set of the zirconium foil solutions were prepared by transferring three aliquots (6.0 mL) of the stock solution to different 25.0 mL Blau brand volumetric flasks. Three aliquots (~2.5 mL) of the diluted boron stock solution were added to each flask containing the zirconium aliquots and the flasks were filled to the mark with double distilled water to obtain the final concentrations of 1000 ppm zirconium and 0.5 ppm boron. Zirconium and the boron in these samples were quantified against their respective calibration curves by using ICP-OES analysis. The results for these analyses are shown in **Table 5.5**.

5.4.4.7 QUANTIFICATION OF CADMIUM AS IMPURITY

For the quantification of cadmium as impurity in the pure zirconium solution, a new cadmium stock solution was prepared by transferring an aliquot (0.24 mL) to a 50.0 mL Blau brand volumetric flask and then diluted with double distilled water to obtain the final concentration of 5 ppm cadmium. The zirconium solutions were prepared by transferring three aliquots (3.0 mL) of the stock solution to different 25.0 mL Blau brand volumetric flasks. Three aliquots (~0.25 mL) of the diluted cadmium stock solution were added to each flask containing the

zirconium aliquots. The flasks were filled to the mark with double distilled water to yield final concentrations of 500 ppm zirconium and 0.05 ppm cadmium.

The second set of the zirconium solutions were prepared by transferring three aliquots (6.0 mL) of the stock solution to different 25.0 mL Blau brand volumetric flasks. Three aliquots (~2.5 mL) of the diluted cadmium stock solution were added to these flasks and then filled to the mark with double distilled water to obtain the final concentrations of 1000 ppm zirconium and 0.5 ppm cadmium. Zirconium and the cadmium in these samples were then quantified against their respective calibration curves by using ICP-OES analysis. The results for these analyses are shown in **Table 5.5**.

5.4.4.8 QUANTIFICATION OF COBALT AS IMPURITY

In the quantification of cobalt as impurity in the pure zirconium solution, three aliquots (3.0 mL) of the stock solution were transferred to different 25.0 mL Blau brand volumetric flasks. Three aliquots (~0.05 mL) of the cobalt stock solution were added to these flasks and filled to the mark with double distilled water to obtain the final concentrations of 500 ppm zirconium and 2 ppm cobalt.

Another set of the zirconium foil solutions were prepared by transferring three aliquots (6.0 mL) of the stock solution to different 25.0 mL Blau brand volumetric flasks. Three aliquots (~0.5 mL) of the cobalt stock solution were added to these zirconium aliquots and the flasks were filled to the mark with double distilled water to obtain final concentrations of 1000 ppm zirconium and 20 ppm cobalt. The zirconium and the cobalt content in these samples were quantified against their respective calibration curves by using ICP-OES analysis. The results for these analyses are shown in **Table 5.5**.

5.4.4.9 QUANTIFICATION OF COPPER AS IMPURITY

For the quantification of copper as impurity in the pure zirconium solution, three aliquots (3.0 mL) of the zirconium stock solution were transferred to different 25.0 mL Blau brand volumetric flasks. Three aliquots (~0.07 mL) of the copper stock solution were then added to these zirconium aliquots and the flasks were filled to the mark with double distilled water to obtain final concentrations of 500 ppm zirconium and 3 ppm copper.

The next set of the zirconium solutions was prepared by transferring three aliquots (6.0 mL) of the stock solution to different 25.0 mL Blau brand volumetric flasks. Three aliquots (~0.7 mL) of the copper stock solution were added to each of the volumetric flasks containing zirconium aliquots and were then filled to the mark with double distilled water to obtain the final concentrations of 1000 ppm zirconium and 30 ppm copper. Zirconium and the copper content in these samples were then quantified against their respective calibration curves by using ICP-OES analysis. The results for these analyses are shown in **Table 5.5**.

5.4.4.10 QUANTIFICATION OF MANGANESE AS IMPURITY

For the quantification of manganese as impurity in the pure zirconium, three aliquots (3.0 mL) of the zirconium stock solution were transferred to different 25.0 mL Blau brand volumetric flasks. Three aliquots (~0.1 mL) of the manganese stock solution were added to each flask containing zirconium aliquots and the flasks were then filled to the mark with double distilled water to yield final concentrations of 500 ppm zirconium and 5 ppm manganese.

Another set of the zirconium solution was prepared by transferring three aliquots (6.0 mL) of the stock solution to different 25.0 mL Blau brand volumetric flasks. Three aliquots (~1.0 mL) of the manganese stock solution were added to each of the flasks containing zirconium aliquots and filled to the mark with double distilled water to yield final concentrations of 1000 ppm zirconium and 50 ppm manganese. Zirconium and the manganese contents in these samples were subsequently quantified against their respective calibration curves by using ICP-OES analysis. The results for these analyses are shown in **Table 5.5**.

5.4.4.11 QUANTIFICATION OF MOLYBDENUM AS IMPURITY

For the quantification of molybdenum as impurity in the pure zirconium, three aliquots (3.0 mL) of the zirconium stock solution were transferred to different 25.0 mL Blau brand volumetric flasks. Three aliquots (~0.07 mL) of the molybdenum stock solution were added to each of the flasks containing zirconium aliquots and the flasks were subsequently filled to the mark with double distilled water to obtain final concentrations of 500 ppm zirconium and 1.5 ppm molybdenum.

The next set of the zirconium solutions was prepared by transferring three aliquots (6.0 mL) of the stock solution to different 25.0 mL Blau brand volumetric flasks. Three aliquots (~0.7

mL) of the molybdenum stock solution were then added to each flask containing zirconium aliquots and the flasks were filled to the mark with double distilled water to obtain the final concentrations of 1000 ppm zirconium and 15 ppm molybdenum. Zirconium and the molybdenum contents in these samples were quantified against their respective calibration curves by using ICP-OES analysis. The results for these analyses are shown in **Table 5.5**.

5.4.4.12 QUANTIFICATION OF NICKEL AS IMPURITY

For the quantification of nickel as impurity in the pure zirconium, three aliquots (3.0 mL) of the zirconium stock solution were transferred to different 25.0 mL Blau brand volumetric flasks. Three aliquots (~0.2 mL) of the nickel stock solution were added to each of the flasks which contain zirconium aliquots and the flasks were filled to the mark with double distilled water to give final concentrations of 500 ppm zirconium and 7 ppm nickel.

The following set of the zirconium solutions was prepared by transferring three aliquots (6.0 mL) of the stock solution to different 25.0 mL Blau brand volumetric flasks. Three aliquots (~2.0 mL) of the nickel stock solution were added to each of the flasks containing zirconium aliquots and these were then filled to the mark with double distilled water to give final concentrations of 1000 ppm zirconium and 70 ppm nickel. The zirconium and the nickel contents in these samples were then quantified against their respective calibration curves by using ICP-OES analysis. The results for these analyses are shown in **Table 5.5**.

5.4.4.13 QUANTIFICATION OF SILICON AS IMPURITY

For the quantification of silicon as impurity in the pure zirconium, three aliquots (3.0 mL) of the zirconium stock solution were transferred to different 25.0 mL Kartell HDPE volumetric flasks. Three aliquots (0.15 mL) of the silicon stock solution were added to each flask containing zirconium aliquots and the flasks were then filled to the mark with double distilled water to obtain final concentrations of 500 ppm zirconium and 12 ppm silicon.

Another set of the zirconium solutions was prepared by transferring three aliquots (6.0 mL) of the stock solution to different 25.0 mL Kartell HDPE volumetric flasks. Three aliquots (1.5 mL) of the silicon stock solution were added to each flask containing zirconium aliquot and the flasks were then filled to the mark with double distilled water to obtain final concentrations of 1000 ppm zirconium and 120 ppm silicon. Zirconium and the silicon contents in these

samples were subsequently quantified against their respective calibration curves by using ICP-OES analysis. The results for these analyses are shown in **Table 5.5**.

5.4.4.14 QUANTIFICATION OF TITANIUM AS IMPURITY

For the quantification of titanium as impurity in the pure zirconium, three aliquots (3.0 mL) of the zirconium stock solution were transferred to different 25.0 mL Blau brand volumetric flasks. Three aliquots (0.125 mL) of the titanium stock solution were added to each flask containing zirconium aliquots and the flasks were then filled to the mark with double distilled water to yield final concentrations of 500 ppm zirconium and 5 ppm titanium.

The other set of zirconium solutions was prepared by transferring three aliquots (6.0 mL) of the stock solution to different 25.0 mL Blau brand volumetric flasks. Three aliquots (1.25 mL) of the titanium stock solution were added to each flask containing zirconium aliquots and the flasks were then filled to the mark with double distilled water to yield final concentrations of 1000 ppm zirconium and 50 ppm titanium. Zirconium and the titanium contents in these samples were subsequently quantified against their respective calibration curves by using ICP-OES analysis. The results for these analyses are shown in **Table 5.5**.

5.4.4.15 QUANTIFICATION OF TUNGSTEN AS IMPURITY

For the quantification of tungsten as impurity in the pure zirconium, three aliquots (3.0 mL) of the zirconium stock solution were transferred to different 25.0 mL Blau brand volumetric flasks. Three aliquots (0.125 mL) of the tungsten stock solution were added to each of the flasks which contained zirconium aliquots and the flasks were then filled to the mark with double distilled water to obtain final concentrations of 500 ppm zirconium and 5 ppm tungsten.

Another set of the zirconium solutions was prepared by transferring three aliquots (6.0 mL) of the stock solution to different 25.0 mL Blau brand volumetric flasks. Three aliquots (1.25 mL) of the tungsten stock solution were added to each of the flasks which contained zirconium aliquots and the flasks were then filled to the mark with double distilled water to obtain final concentrations of 1000 ppm zirconium and 50 ppm tungsten. Zirconium and the tungsten contents in these samples were then quantified against their respective calibration curves by using ICP-OES analysis. The results for these analyses are shown in **Table 5.5**.

5.4.4.16 QUANTIFICATION OF URANIUM AS IMPURITY

For the quantification of uranium as impurity in the pure zirconium solution, a new uranium stock solution was prepared by transferring an aliquot (~0.2 mL) to a 50.0 mL Blau brand volumetric flask and then diluted with double distilled water to obtain the final concentration of 50 ppm uranium. The zirconium solutions were prepared by transferring three aliquots (3.0 mL) of the stock solution to different 25.0 mL Blau brand volumetric flasks. Three aliquots (~0.15 mL) of the diluted uranium stock solution were added to each flask containing the zirconium aliquots. The flasks were filled to the mark with double distilled water to yield final concentrations of 500 ppm zirconium and 0.3 ppm uranium.

The second set of the zirconium solutions were prepared by transferring three aliquots (6.0 mL) of the stock solution to different 25.0 mL Blau brand volumetric flasks. Three aliquots (~1.5 mL) of the diluted uranium stock solution were added to these flasks and then filled to the mark with double distilled water to yield final concentrations of 1000 ppm zirconium and 0.5 ppm uranium. Zirconium and the uranium contents in these samples were then quantified against their respective calibration curves by using ICP-OES analysis. The results for these analyses are shown in **Table 5.5**.

Table 5.5: ICP-OES analyses of individual impurities at their most sensitive wavelengths in Zr-solution (λ = 339.198 nm)

Impurity	λ/nm	Content (ppm)		Impurity Recovery/% ± SD (RSD (ppt))		Zirconium Recovery/% ± SD (RSD (ppt))	
		Tenth	Threshold	Tenth	Threshold	500 ppm	1000 ppm
Al	309.271	8	80	100.9 ± 7 (7)	99.6 ± 2 (2)	103 ± 1 (10)	101.4 ± 9 (9)
Cr	283.563	20	200	101 ± 1 (10)	101.6 ± 9 (9)	100 ± 1 (10)	101 ± 2 (20)
Hf	277.336	10	100	101 ± 3 (30)	102 ± 4 (39)	102 ± 3 (29)	101 ± 2 (20)
Fe	238.204	150	1500	101.3 ± 9 (9)	100 ± 3 (30)	102 ± 4 (39)	99 ± 3 (30)
B	249.773	0.05	0.5	102 ± 4 (39)	101 ± 3 (30)	98 ± 2 (20)	99 ± 2 (20)
Cd	214.438	0.05	0.5	101 ± 2 (20)	100 ± 1 (10)	101.5 ± 8 (8)	98 ± 2 (20)
Co	238.892	2	20	98.3 ± 3 (3)	100.7 ± 7 (7)	100 ± 3 (30)	102 ± 2 (20)
Cu	324.754	3	30	101 ± 4 (40)	100.6 ± 4 (4)	102 ± 4 (39)	101 ± 2 (20)
Mn	257.610	5	50	100 ± 2 (20)	99 ± 1 (10)	102 ± 2 (20)	102 ± 2 (20)
Mo	202.030	1.5	15	101 ± 1 (10)	102 ± 4 (39)	102.5 ± 5 (5)	101.1 ± 8 (8)
Ni	231.604	7	70	102 ± 1 (10)	100.3 ± 2 (2)	100 ± 1 (10)	102 ± 1 (10)
Si	212.415	12	120	99 ± 2 (20)	100 ± 1 (10)	98.3 ± 1 (1)	98 ± 1 (10)
Ti	337.280	5	50	100.1 ± 2 (2)	102.0 ± 2 (2)	100 ± 3 (30)	100 ± 3 (30)
W	220.448	5	50	102 ± 2 (20)	99 ± 2 (20)	101 ± 2 (20)	102 ± 2 (20)
U	393.203	0.3	3	102 ± 4 (39)	102 ± 3 (29)	100.4 ± 2 (2)	102 ± 1 (10)

5.4.5 QUANTIFICATION OF GROUPS OF IMPURITIES ADDED IN THE ULTRA PURE ZIRCONIUM FOIL

5.4.5.1 QUANTIFICATION OF THE GROUP 1 IMPURITIES

The first set of solutions was prepared by transferring three aliquots of **Group 1** impurities (aluminium, chromium, iron and hafnium – see **Table 5.1**), with the same volumes specified in **Paragraphs 5.4.4.2** to **5.4.4.5** to three different 25.0 mL Blau brand volumetric flasks.

Three aliquots (3.0 mL) of the zirconium stock solution were added to the different flasks containing **Group 1** impurities then filled to the mark with double distilled water to yield final concentrations of 500 ppm zirconium, 8 ppm aluminium, 20 ppm chromium, 10 ppm hafnium and 150 ppm iron.

The second set of solutions was prepared by transferring three aliquots (6.0 mL) of the zirconium stock solution to three different 25.0 mL Blau brand volumetric flasks. Three aliquots of **Group 1** impurities, with the same volumes specified for their individual additions in **Paragraphs 5.4.4.2** to **5.4.4.5**, were added to each flask containing zirconium aliquots and the flasks were then filled to the mark with double distilled water to yield final concentrations of 1000 ppm zirconium, 80 ppm aluminium, 200 ppm chromium, 100 ppm hafnium and 1500 ppm iron. The zirconium and the **Group 1** contents in these samples were then quantified against their respective calibration curves by using ICP-OES analysis. The results for these analyses are shown in **Tables 5.6** and **5.7**.

Table 5.6: ICP-OES analyses of Group 1 (Tenth of the threshold) in Zr-solution (500 ppm)

Element (λ/nm)	Zr (357.247)	Al (309.271)	Cr (283.563)	Hf (282.023)	Fe (238.204)
Mean % Recovery (SD)	100.8 (2)	102 (3)	98 (7)	99.9 (8)	103 (2)
RSD (ppt)	2	294	71	8	19

Table 5.7: ICP-OES analyses of Group 1 (Threshold) in Zr-solution (1000 ppm)

Element (λ/nm)	Zr (357.247)	Al (309.271)	Cr (283.563)	Hf (282.023)	Fe (238.204)
Mean % Recovery (SD)	99 (3)	100.2 (1)	102 (2)	101 (4)	100.9 (4)
RSD (ppt)	30	1	20	40	4

5.4.5.2 QUANTIFICATION OF THE GROUP 2 IMPURITIES

The first set of solutions in this part of the study was prepared by transferring three aliquots of **Group 2** impurities (boron, cadmium, cobalt, copper and manganese – see **Table 5.1**), with the same amount of volumes specified for their individual additions (see **Paragraphs**

5.4.4.6 to **5.4.4.10**) to three different 25.0 mL Kartell HDPE volumetric flasks, each containing zirconium stock solution (3.0 mL). The flasks were then filled to the mark with double distilled water to yield final concentrations of 500 ppm zirconium, 0.05 ppm boron, 0.05 ppm cadmium, 2 ppm cobalt, 3 ppm copper and 5 ppm manganese.

The second set of solutions was prepared by transferring three aliquots (6.0 mL) of the zirconium stock solution to three different 25.0 mL Blau brand volumetric flasks. Three aliquots of **Group 2** impurities, with the same volumes specified for their individual additions in **Paragraphs 5.4.4.6** to **5.4.4.10**, were added to each flask containing zirconium aliquots and the flasks were then filled to the mark with double distilled water to yield final concentrations of 1000 ppm zirconium, 0.5 ppm boron, 0.5 ppm cadmium, 20 ppm cobalt, 30 ppm copper and 50 ppm manganese. The zirconium and the **Group 2** contents in these samples were then quantified against their respective calibration curves by using ICP-OES analysis. The results for these analyses are shown in **Tables 5.8** and **5.9**.

Table 5.8: ICP-OES analyses of Group 2 (Tenth of the threshold) in Zr-solution (500 ppm)

Element (λ/nm)	Zr (339.198)	B (249.773)	Cd (214.438)	Co (238.892)	Cu (324.754)	Mn (257.610)
Mean % Recovery (SD)	100 (1)	N.D	N.D	99.9 (7)	101 (3)	100 (5)
RSD (ppt)	10	-	-	7	30	50

ND: Not Detectable

Table 5.9: ICP-OES analyses of Group 2 (Threshold) in Zr-solution (1000 ppm)

Element (λ/nm)	Zr (339.198)	B (249.773)	Cd (214.438)	Co (238.892)	Cu (324.754)	Mn (257.610)
Mean % Recovery (SD)	100 (3)	100 (2)	101 (2)	98 (2)	102 (3)	102 (2)
RSD (ppt)	30	20	20	20	29	20

5.4.5.3 QUANTIFICATION OF THE GROUP 3 IMPURITIES

The first set solutions for the quantification of the **Group 3** impurities (molybdenum, nickel, silicon, titanium, tungsten and uranium) were prepared by transferring to three 25.0 mL

Kartell HDPE volumetric flasks the same amount of the first volumes specified for their individual additions above (see **Paragraphs 5.4.4.11 – 5.4.4.16**. Three zirconium stock solution aliquots (3.0 mL) were added to the flasks containing **Group 3** impurities and these were filled to the mark with double distilled water to yield final concentrations of 500 ppm zirconium, 1.5 ppm molybdenum, 5 ppm nickel, 12 ppm silicon, 5 ppm titanium, 5 ppm tungsten and 0.3 ppm uranium.

The second set of solutions was prepared by transferring three aliquots (6.0 mL) of the zirconium stock solution to three different 25.0 mL Blau brand volumetric flasks. Three aliquots of **Group 3** impurities, with the same volumes specified for their individual additions in **Paragraphs 5.4.4.11 – 5.4.4.16**, were added to each flask containing zirconium aliquots and the flasks were then filled to the mark with double distilled water to yield final concentrations of 1000 ppm zirconium, 15 ppm molybdenum, 50 ppm nickel, 120 ppm silicon, 50 ppm titanium, 50 ppm tungsten and 3 ppm uranium. The zirconium and the **Group 3** contents in these samples were then quantified against their respective calibration curves by using ICP-OES analysis. The results for these analyses are shown in **Tables 5.10** and **5.11**.

Table 5.10: ICP-OES analyses of Group 3 (Tenth of the threshold) in Zr-solution (500 ppm)

Element (λ/nm)	Zr (339.198)	Mo (202.030)	Ni (231.604)	Si (212.415)	Ti (337.280)	W (220.448)	U (393.203)
Mean % Recovery (SD)	100 (4)	99 (3)	99.3 (6)	101 (1)	99 (2)	102 (1)	N.D
RSD (ppt)	40	30	6	10	20	10	-

ND: Not Detectable

Table 5.11: ICP-OES analyses of Group 3 (Threshold) in Zr-solution (1000 ppm)

Element (λ/nm)	Zr (339.198)	Mo (202.030)	Ni (231.604)	Si (212.415)	Ti (337.280)	W (220.448)	U (393.203)
Mean % Recovery (SD)	102 (1)	101 (2)	102 (2)	102 (2)	100 (2)	101.8 (9)	101 (5)
RSD (ppt)	10	20	20	20	20	9	50

5.4.6 QUANTIFICATION OF COMBINED GROUPS OF IMPURITIES ADDED TO THE PURE ZIRCONIUM FOIL

5.4.6.1 QUANTIFICATION OF THE COMBINED GROUPS 1 AND 2 IMPURITIES

The first set of solutions for this part of study was prepared by the addition of three aliquots (similar amount of volumes specified for their individual additions above) of **Groups 1 and 2** impurities to the three aliquots of the zirconium stock solution (3.0 mL) in the 25.0 mL Kartell HDPE volumetric flasks. The flasks were filled to the mark with double distilled water to obtain the final concentrations of 500 ppm zirconium, 8 ppm aluminium, 20 ppm chromium, 10 ppm hafnium, 150 ppm iron, 0.05 ppm boron, 0.05 ppm cadmium, 2 ppm cobalt, 3 ppm copper and 5 ppm manganese.

The second set of solutions was prepared by transferring three aliquots (6.0 mL) of the zirconium stock solution to three different 25.0 mL Kartell HDPE volumetric flasks. Three aliquots of **Groups 1 and 2** impurities (similar amount of volumes specified for their individual additions above) were added to each flask containing zirconium aliquots and the flasks were then filled to the mark with double distilled water to yield final concentrations of 1000 ppm zirconium, 80 ppm aluminium, 200 ppm chromium, 100 ppm hafnium, 1500 ppm iron, 0.5 ppm boron, 0.5 ppm cadmium, 20 ppm cobalt, 30 ppm copper and 50 ppm manganese. The zirconium and the impurities in these samples were then quantified against their respective calibration curves by using ICP-OES analysis. The results for these analyses are shown in **Tables 5.12** and **5.13**.

Table 5.12: ICP-OES analyses of Group 1 and 2 (Tenth of the threshold) in Zr-solution (500 ppm)

Element (λ/nm)	Zr (357.247)	Al (309.271)	Cr (283.563)	Fe (238.204)	Hf (282.023)
Mean % Recovery (SD)	98.7 (8)	98 (2)	102.1 (4)	101.7 (9)	99 (2)
RSD (ppt)	8	20	4	9	20
Element (λ/nm)	**B (249.773)**	**Cd (361.051)**	**Co (238.892)**	**Cu (213.598)**	**Mn (259.373)**
Mean % Recovery (SD)	N.D	N.D	102 (1)	101.0 (6)	98.2 (9)
RSD (ppt)	-	-	10	6	9

ND: Not Detectable

Table 5.13: ICP-OES analyses of Group 1 and 2 (Threshold) in Zr-solution (1000 ppm)

Element (λ/nm)	Zr (357.247)	Al (309.271)	Cr (283.563)	Fe (238.204)	Hf (282.023)
Mean % Recovery (SD)	99.9 (3)	101 (1)	100.5 (8)	102 (1)	100 (5)
RSD (ppt)	3	10	8	10	50
Element (λ/nm)	B (249.773)	Cd (361.051)	Co (238.892)	Cu (213.598)	Mn (259.373)
Mean % Recovery (SD)	101 (1)	102 (5)	100 (1)	99.9 (5)	99 (1)
RSD (ppt)	10	49	10	5	10

5.4.6.2 QUANTIFICATION OF THE COMBINED GROUPS 1 AND 3 IMPURITIES

The first set of solutions for the **Groups 1 and 3** impurities was prepared by the addition of three aliquots (similar amount of volumes specified for their individual additions above) to the different 25.0 mL Kartell HDPE volumetric flasks. Three aliquots of the zirconium stock solution (3.0 mL) were added to the volumetric flasks containing the impurities. The flasks were filled to the mark with double distilled water to obtain final concentrations of 500 ppm zirconium, 8 ppm aluminium, 20 ppm chromium, 10 ppm hafnium, 150 ppm iron, 1.5 ppm molybdenum, 5 ppm nickel, 12 ppm silicon, 5 ppm titanium, 5 ppm tungsten and 0.3 ppm uranium.

The second set of solutions was prepared by transferring three aliquots (6.0 mL) of the zirconium stock solution to three different 25.0 mL Kartell HDPE volumetric flasks. Three aliquots of **Groups 1 and 3** impurities (similar amount of volumes specified for their individual additions above) were added to each flask containing zirconium aliquots and the flasks were then filled to the mark with double distilled water to yield final concentrations of 1000 ppm zirconium, 80 ppm aluminium, 200 ppm chromium, 100 ppm hafnium, 1500 ppm iron, 15 ppm molybdenum, 50 ppm nickel, 120 ppm silicon, 50 ppm titanium, 50 ppm tungsten and 3 ppm uranium. The zirconium and the impurities in these samples were then quantified against their respective calibration curves by using ICP-OES analysis. The results for these analyses are shown in **Tables 5.14** and **5.15**.

Table 5.14: ICP-OES analyses of Group 1 and 3 (Tenth of the threshold) in Zr-solution (500 ppm)

Element (λ/nm)	Zr (357.247)	Al (309.271)	Cr (283.563)	Fe (238.204)	Hf (282.023)	Mo (203.844)
Mean % Recovery (SD)	102 (3)	101 (3)	100.9 (5)	103.5 (3)	102 (3)	99 (4)
RSD (ppt)	29	30	5	3	29	40
Element (λ/nm)	Ni (231.604)	Si (212.415)	Ti (337.280)	W (220.448)	U (393.203)	
Mean % Recovery (SD)	98 (2)	103.5 (8)	102.7 (3)	100.4 (9)	70 (2)	
RSD (ppt)	20	8	3	9	29	

Table 5.15: ICP-OES analyses of Group 1 and 3 (Threshold) in Zr-solution (1000 ppm)

Element (λ/nm)	Zr (357.247)	Al (309.271)	Cr (283.563)	Fe (238.204)	Hf (282.023)	Mo (203.844)
Mean % Recovery (SD)	100 (2)	101.1 (1)	102.0 (3)	100.2 (5)	99.8 (6)	99 (2)
RSD (ppt)	20	1	3	5	6	20
Element (λ/nm)	Ni (231.604)	Si (212.415)	Ti (337.280)	W (220.448)	U (393.203)	
Mean % Recovery (SD)	100.5 (2)	102 (1)	100.8 (3)	99 (3)	100 (2)	
RSD (ppt)	2	10	3	30	20	

5.4.6.3 QUANTIFICATION OF THE COMBINED GROUPS 2 AND 3 IMPURITIES

The first set of solutions for this part of study was prepared by transferring three aliquots of the zirconium stock solution (3.0 mL) to the different 25.0 mL Kartell HDPE volumetric flasks. Three aliquots of the **Groups 2 and 3** impurities, corresponding to the volumes indicated in **Paragraphs 5.4.4.6 – 5.4.4.16**, were added to these flasks. The flasks were filled to the mark with double distilled water to obtain the final concentrations of 500 ppm zirconium, 8 ppm aluminium, 20 ppm chromium, 10 ppm hafnium, 150 ppm iron, 0.05 ppm boron, 0.05 ppm cadmium, 2 ppm cobalt, 3 ppm copper, 5 ppm manganese, 1.5 ppm molybdenum, 5 ppm nickel, 12 ppm silicon, 5 ppm titanium, 5 ppm tungsten and 0.3 ppm uranium.

The second set of solutions was prepared by transferring three aliquots (6.0 mL) of the zirconium stock solution to three different 25.0 mL Kartell HDPE volumetric flasks. Three aliquots of **Groups 2 and 3** impurities (similar amount of volumes specified for their individual additions above) were added to each flask containing zirconium aliquots and the flasks were then filled to the mark with double distilled water to yield final concentrations of 1000 ppm zirconium, 0.5 ppm boron, 0.5 ppm cadmium, 20 ppm cobalt, 30 ppm copper, 50 ppm manganese, 15 ppm molybdenum, 50 ppm nickel, 120 ppm silicon, 50 ppm titanium, 50 ppm tungsten and 3 ppm uranium. The zirconium and the impurities in these samples were then quantified against their respective calibration curves by using ICP-OES analysis. The results for these analyses are shown in **Tables 5.16** and **5.17**.

Table 5.16: ICP-OES analyses of Group 2 and 3 (Tenth of the threshold) in Zr-solution (500 ppm)

Element (λ/nm)	Zr (357.247)	B (249.773)	Cd (361.051)	Co (238.892)	Cu (213.598)	Mn (259.373)
Mean % Recovery (SD)	102.1 (2)	N.D	N.D	102 (2)	101.8 (9)	101.0 (9)
RSD (ppt)	2	-	-	20	9	9
Element (λ/nm)	Mo (203.844)	Ni (231.604)	Si (212.415)	Ti (337.280)	W (220.448)	U (393.203)
Mean % Recovery (SD)	100 (3)	100 (6)	101 (1)	99.1 (1)	100 (3)	4 (3)
RSD (ppt)	30	60	10	1	30	750

ND: Not Detectable

Table 5.17: ICP-OES analyses of Group 2 and 3 (Threshold) in Zr-solution (1000 ppm)

Element (λ/nm)	Zr (357.247)	B (249.773)	Cd (361.051)	Co (238.892)	Cu (213.598)	Mn (259.373)
Mean % Recovery (SD)	98.8 (3)	102 (2)	100 (3)	99 (3)	103 (1)	101 (2)
RSD (ppt)	30	20	30	30	10	20
Element (λ/nm)	Mo (203.844)	Ni (231.604)	Si (212.415)	Ti (337.280)	W (220.448)	U (393.203)
Mean % Recovery (SD)	99.5 (6)	103.5 (1)	100 (2)	102 (3)	100 (1)	99 (2)
RSD (ppt)	6	1	20	29	10	20

5.4.7 QUANTIFICATION OF ALL IMPURITIES ADDED TO PURE ZIRCONIUM SOLUTION

In the quantitative analysis of all the impurities associated with the nuclear grade zirconium, the first set of solutions for all the impurities was prepared by the addition of three aliquots (similar amount of volumes specified for their individual additions above) to the different 25.0 mL Kartell HDPE volumetric flasks. Three aliquots of the zirconium stock solution (3.0 mL) were added to the volumetric flasks containing the impurities. The flasks were filled to the mark with double distilled water to yield final concentrations of 500 ppm zirconium, 8 ppm aluminium, 20 ppm chromium, 10 ppm hafnium, 150 ppm iron, 0.05 ppm boron, 0.05 ppm cadmium, 2 ppm cobalt, 3 ppm copper, 5 ppm manganese, 1.5 ppm molybdenum, 5 ppm nickel, 12 ppm silicon, 5 ppm titanium, 5 ppm tungsten and 0.3 ppm uranium.

Due to the maximum volume of the volumetric flasks used in this study, the volumes of some of the impurities were reduced and 100.0 mL Kartell HDPE volumetric flasks were used instead of smaller volume of 25.0 mL. Thus, the second set of solutions was prepared by transferring three aliquots (20 mL) of the zirconium stock solution to three different 100.0 mL Kartell HDPE volumetric flasks. Three aliquots of each impurity (reduced volumes for some impurities) were added to each flask containing zirconium aliquots and the flasks were then filled to the mark with double distilled water to yield final concentrations of 900 ppm zirconium, 60 ppm aluminium, 200 ppm chromium, 80 ppm hafnium, 1250 ppm iron, 0.4 ppm boron, 0.4 ppm cadmium, 20 ppm cobalt, 28 ppm copper, 42 ppm manganese, 15 ppm molybdenum, 60 ppm nickel, 120 ppm silicon, 40 ppm titanium, 40 ppm tungsten and 2 ppm uranium. The zirconium and the impurities in these samples were then quantified against their respective calibration curves by using ICP-OES analysis. The results for these analyses are shown in **Tables 5.18** and **5.19**.

Table 5.18: ICP-OES analyses of all impurities (Tenth of the threshold) in Zr-solution (500 ppm)

Element (λ/nm)	Zr (357.247)	Al (309.271)	Cr (283.563)	Fe (238.204)	Hf (282.023)	B (249.773)	Cd (361.051)	Co (238.892)
Mean % Recovery (SD)	100 (1)	101 (2)	100 (1)	100.6 (7)	100 (1)	N.D	N.D	97.8 (2)
RSD (ppt)	10	20	10	7	10	-	-	2
Element (λ/nm)	Cu (213.598)	Mn (259.373)	Mo (203.844)	Ni (231.604)	Si (212.415)	Ti (337.280)	W (220.448)	U (393.203)
Mean % Recovery (SD)	101 (2)	102 (1)	101 (2)	102 (2)	100 (1)	101 (1)	101 (2)	N.D
RSD (ppt)	20	10	20	20	10	10	20	-

ND: Not Detectable

Table 5.19: ICP-OES analyses of all impurities (Threshold) in Zr-solution (900 ppm)

Element (λ/nm)	Zr (357.247)	Al (309.271)	Cr (283.563)	Fe (238.204)	Hf (282.023)	B (249.773)	Cd (361.051)	Co (238.892)
Mean % Recovery (SD)	101 (1)	98.2 (2)	101 (1)	102.0 (3)	102 (1)	101.2 (8)	99 (2)	99.9 (1)
RSD (ppt)	10	2	10	3	10	8	20	10
Element (λ/nm)	Cu (213.598)	Mn (259.373)	Mo (203.844)	Ni (231.604)	Si (212.415)	Ti (337.280)	W (220.448)	U (393.203)
Mean % Recovery (SD)	101 (3)	102.3 (3)	99.2 (7)	99 (2)	100 (4)	102.0 (3)	99.7 (6)	101 (4)
RSD (ppt)	30	3	7	20	40	3	6	40

5.5 DISCUSSION, VALIDATION AND CONCLUSION

5.5.1 DISCUSSION OF RESULTS

The quantitative analyses of all the impurities associated with the pure zirconium foil sample were investigated with the systematic addition of these impurities to the zirconium stock solution and their subsequent quantification by using ICP-OES as discussed in **Chapter 4, Section 4.2.3, Table 4.2**. The zirconium foil used in this study was first digested by the method developed in **Chapter 4, Section 4.3.5.1**, which entailed the sulphuric acid-assisted benchtop technique that yielded 100 % recovery of zirconium. The quantitative analyses of

the zirconium and all the impurities in this part of the study were carried out at the most appropriate wavelengths which were selected to have less or no interference from the other elements present in solution, which proved to be a vital step in the successful analyses of the impurities. Throughout the entire study, the amounts of the impurities were kept constant at a tenth and permissible threshold concentrations (see **Table 5.1**) as specified for their contents in nuclear grade zirconium.

Zirconium was added to the mixtures to achieve its concentration at ~500 ppm for the analyses of the impurities at the tenth of their permitted content and at ~1000 ppm for the analyses of the impurities at the threshold of their permitted content. This was done so in an attempt to keep the concentration of zirconium higher than its associated impurities for nuclear viability with the exception of iron. The concentration of all the different stock solutions were prepared in such a way that the total volume of all the impurity and zirconium additions do not exceed the volume of the volumetric flasks used in the study.

The Kartell HDPE-type of volumetric flasks were used in the quantifications of boron and silicon to prevent the additions of these elements as dissolution products from Blau brand glass volumetric flasks. Some ICP standards, including that of silicon, contained hydrofluoric acid which might have dissolved some of the glass volumetric flask that may have attributed to huge experimental errors in the quantitative analyses of these two impurities. The quantitative analyses of zirconium were done first for all sets of samples, followed by the quantification of individual impurities in their groups. This was done to save time and materials by using the same calibration curve in the quantification of the zirconium.

5.5.1.1 LIMITS OF DETECTION (LOD) AND QUANTIFICATION (LOQ)

The first step in this study was the determination for the minimum detectible (LOD) and quantified (LOQ) amounts of all impurities on the ICP-OES instrument before any analysis was done on the samples as discussed in **Section 5.4.3**. Detection limits for all the impurity elements have been reported.[163-165] In this study, the LOD's of all impurities were determined to be well below the acceptable amounts specified for their quantifications in an ultra pure or nuclear grade zirconium metal. However, the LOQ's for boron, cadmium and uranium (of 0.1517, 0.03458 and 0.9355 ppm respectively), were close to the concentration of these elements at a tenth of the permissible concentrations, namely 0.05, 0.05 and 0.3 ppm

respctively. This may explain the poor recoveries that were obtained in the next part of the study (see **Tables 5.5**, **5.10**, **5.12**, **5.14**, **5.16** and **5.18**).

5.5.1.2 QUANTIFICATION OF THE INDIVIDUAL IMPURITITES IN THE PURE ZIRCONIUM SOLUTION

It has been reported that the analytical wavelength (339.198 nm) for zirconium is susceptible to interference by some elements, such as chromium, iron and titanium.[161] In this part of the study, this wavelength was used for the individual quantitative analyses of impurities, and the quantification results clearly indicate that none of the mentioned elements seemed to have interfered with the quantification of zirconium as observed in the obtained results (see **Tables 5.5**). All the individual impurities were quantified at their most sensitive wavelengths and the results obtained are shown in **Tables 5.5**. The overall average recovery of zirconium and its impurities are summarized in **Table 5.20**.

Table 5.20: The overall average recovery of individual impurities in their respective zirconium solution

Element	Zr	Al	Cr	Fe	Hf	B	Cd	Co
Mean % Recovery (SD)	101 (1)	100 (1)	101.3 (4)	101 (1)	101.5 (7)	102 (1)	101 (1)	100 (2)
Element	Cu	Mn	Mo	Ni	Si	Ti	W	U
Mean % Recovery (SD)	100.8 (3)	100 (1)	102 (1)	101 (1)	100 (1)	101 (1)	101 (2)	102

5.5.1.3 QUANTIFICATION OF THE GROUPS OF IMPURITIES IN THE PURE ZIRCONIUM SOLUTION

Since the analytical wavelength (339.198 nm) used in the quantification of zirconium is prone to being interfered with by the mentioned elements above, another analytical wavelength (357.247 nm) reported to have no interference from any element[161], was used to quantify zirconium in the quantification of the **Group 1** elements only. However, since none of the **Group 2** elements interfered with the analytical wavelength 339.198 nm and titanium being the only element in **Group 3** reported to interfere with this wavelength, zirconium was successfully quantified for both these groups using 339.198 nm as the wavelength. The analytical wavelengths of some of the impurities were reported to be susceptible to the

interference by other elements. Therefore, those impurities whose wavelengths were interfered by more than one element were replaced by others which were less susceptible to interference by one or none of the elements specified for the nuclear grade zirconium. These substituted wavelengths successfully assisted in quantitatively analyzing for those impurities. The results obtained for the lower amounts of boron, cadmium and uranium yielded insufficient recoveries or no recoveries at all. This could be attributed to the quantitative analyses of these impurities at the ranges lower or near their limits of quantification. The results for all the group impurities are shown in **Tables 5.6** to **5.11**. The results indicated that the element recovery between 99 and 102 % were obtained for **Group 1**, 98 and 102 % for **Group 2** and 100 and 102 % for **Group 3** at threshold recovery. Recoveries between 98 and 103 % for **Group 1**, 99 and 101 % for **Group 2** and 99 and 102 % for **Group 3** elements were obtained at a tenth of the threshold. Poor recoveries for boron, cadmium and uranium at a tenth of the threshiold were obtained for the individual groups. These elements were not detected in their respective groups.

5.5.1.4 QUANTIFICATION OF THE COMBINED GROUPS OF IMPURITIES IN THE PURE ZIRCONIUM SOLUTION

The wavelength of 357.247 nm was used in the quantification of zirconium for the various combinations of impurity groups. The wavelengths used for the quantifications of the impurities were chosen in the same way as it was done for their quantitative analyses in their respective groups. All the impurities were successfully quantified at their tenth and permissible threshold contents, except for the lower amounts of boron, cadmium and uranium. The results for all the group impurities are shown in **Tables 5.12** to **5.17**. The quantification results indicated that recoveries for element combinations of **Groups 1** and **2** between 99 and 102 %, which were similar also for **Groups 1** and **3** combinations while 98 and 103.5 % were obtained for the **Groups 2** and **3** combinations. At a tenth of the threshold the recoveries were obtained between 98 and 102 % for **Groups 1** and **2**, 70 and 103.5 % for **Groups 1** and **3** while 4 and 102 % were achieved for **Groups 2** and **3**. Poor recoveries for boron, cadmium and uranium were obtained for their respective group combinations at a tenth of the threshold. Boron and cadmium were not detectable for **Groups 1** and **2** combinations as well as for element combinations of **Groups 2** and **3**, while uranium was recovered at 70 % for **Groups 1** and **3** combination and at 4 % for element combinations of **Groups 2** and **3**.

5.5.1.5 QUANTIFICATION OF ALL THE IMPURITITES IN THE PURE ZIRCONIUM SOLUTION

Due to the maximum volume regarding the volumetric flasks used in this study, the volumes used for some of the impurities in their quantitative analyses at the permissible threshold contents were reduced. A small amount of the concentrated hydrochloric acid was added to assist with keeping the components of the experimental samples in the solution. These alterations proved not to drastically influence the quantifications of all the impurities, except that the recoveries of boron, cadmium and uranium were again not sufficiently quantified at the lower range (see **Tables 5.18** and **5.19**). Recoveries between 98.8 and 102.3 % were obtained at threshold recovery while 97.8 and 102 % were obtained at a tenth of the threshold concentrations. Thus, the method for quantifying the impurities associated with nuclear grade zirconium was successfully developed. Poor recoveries at a tenth of the threshold for boron, cadmium and uranium were obtained for the mixture containing all the impurities. These elements were not detectable, which could be due to the matrix intereferences from other elements.

5.5.2 VALIDATION OF RESULTS

The validation of the analytical method for the quantification of impurities in the pure zirconium was carried out at the confidence level of 95 %. The standard deviations as well as RSD's calculated were from three (3) experimental replicates for each quantitative analysis. Since about 16 elements were analyzed in this study, the component ratio of each element is 6.25 %. Therefore, the relative standard deviations (RSD) with values less than or equal to 50 ppt were regarded as good or acceptable.[169] The wavelength selections indicated that the method for the analysis of the impurities in the pure zirconium was not affected by the sample matrix. The digestion technique was considered to be robust where the results were shown to be reproducible.

The *t*-statistic values were also calculated at 95 % confidence level for 3 experimental replicates. The region of acceptance or rejection, as indicated by *t*-values was calculated according to **Equation 3.13** in **Chapter 3**. Rejection was indicated when the result was higher or lower than the t_{crit} (±4.30), depending on the number of replicates. All the validation parameters evaluated on the ICP-OES for the zirconium analysis in the various samples are similar as those summarized in **Chapter 4**, **Table 4.20**. The validation of the results from the

ICP-OES analyses for the additions of all the impurities to the pure zirconium solution were reported as shown in **Tables 5.21** to **5.49**.

Table 5.21: Validation of ICP-OES analyses for aluminium in the pure zirconium solution

Validation Criteria	Parameter	Aluminium		Zirconium	
		Tenth	Threshold	500	1000
Recovery	**Mean % (SD)**	100.9 (7)	99.6 (2)	103 (1)	101.4 (9)
Precision	**RSD (ppt)**	7	2	10	9
Robustness		Results reproducible	Results reproducible	Results reproducible	Results reproducible
Working Range	**Calibration Curve**	20 – 100 ppm		300 – 1500 ppm	
Linearity	**R^2**	0.9998		0.9997	
Sensitivity	**Slope**	0.1966		1.5492	
Selectivity	**s_m**	0.0016		0.0148	
Error of the Slope	**Intercept**	-0.1198		-3.4884	
Specificity	**S_c**	0.0463		6.2807	
***t*-value**		2.2	-3.5	5.2	2.7
Decision		Accepted	Accepted	Rejected	Accepted

Table 5.22: Validation of ICP-OES analyses for chromium in the pure zirconium solution

Validation Criteria	Parameter	Chromium		Zirconium	
		Tenth	Threshold	500	1000
Recovery	Mean % (SD)	101 (1)	101.6 (9)	100 (1)	101 (2)
Precision	RSD (ppt)	10	9	10	20
Robustness		Results reproducible	Results reproducible	Results reproducible	Results reproducible
Working Range	Calibration Curve	50 – 250 ppm		300 – 1500 ppm	
Linearity	R^2	0.9999		0.9997	
Sensitivity	Slope	0.3122		1.5492	
Selectivity	s_m	0.0014		0.0148	
Error of the Slope	Intercept	0.4258		-3.4884	
Specificity	S_c	0.0978		6.2807	
t-value		1.7	3.1	0	0.9
Decision		Accepted	Accepted	Accepted	Accepted

Table 5.23: Validation of ICP-OES analyses for hafnium in the pure zirconium solution

Validation Criteria	Parameter	Hafnium		Zirconium	
		Tenth	Threshold	500	1000
Recovery	Mean % (SD)	101 (3)	102 (4)	102 (3)	101 (2)
Precision	RSD (ppt)	30	39	29	20
Robustness		Results reproducible	Results reproducible	Results reproducible	Results reproducible
Working Range	Calibration Curve	30 – 150 ppm		300 – 1500 ppm	
Linearity	R^2	0.9997		0.9997	
Sensitivity	Slope	0.1069		1.5492	
Selectivity	s_m	0.0011		0.0148	
Error of the Slope	Intercept	0.1490		-3.4884	
Specificity	S_c	0.0456		6.2807	
t-value		0.6	0.9	1.2	0.9
Decision		Accepted	Accepted	Accepted	Accepted

Table 5.24: Validation of ICP-OES analyses for iron in the pure zirconium solution

Validation Criteria	Parameter	Iron		Zirconium	
		Tenth	Threshold	500	1000
Recovery	Mean % (SD)	101.3 (9)	100 (3)	102 (4)	99 (3)
Precision	RSD (ppt)	9	30	39	30
Robustness		Results reproducible	Results reproducible	Results reproducible	Results reproducible
Working Range	Calibration Curve	500 – 2500 ppm		300 – 1500 ppm	
Linearity	R^2	0.9999		0.9997	
Sensitivity	Slope	0.3230		1.5492	
Selectivity	s_m	0.0018		0.0148	
Error of the Slope	Intercept	0.1971		-3.4884	
Specificity	S_c	1.2419		6.2807	
t-value		2.5	0	0.9	-0.6
Decision		Accepted	Accepted	Accepted	Accepted

Table 5.25: Validation of ICP-OES analyses for boron in the pure zirconium solution

Validation Criteria	Parameter	Boron		Zirconium	
		Tenth	Threshold	500	1000
Recovery	Mean % (SD)	102 (4)	101 (3)	98 (2)	99 (2)
Precision	RSD (ppt)	39	30	20	20
Robustness		Results reproducible	Results reproducible	Results reproducible	Results reproducible
Working Range	Calibration Curve	20 – 100 ppm		300 – 1500 ppm	
Linearity	R^2	0.9993		0.9992	
Sensitivity	Slope	0.2575		2.4329	
Selectivity	s_m	0.0040		0.0387	
Error of the Slope	Intercept	0.3329		-2.5460	
Specificity	S_c	0.1129		16.4139	
t-value		0.9	0.6	-1.7	-0.9
Decision		Accepted	Accepted	Accepted	Accepted

Table 5.26: Validation of ICP-OES analyses for cadmium in the pure zirconium solution

Validation Criteria	Parameter	Cadmium		Zirconium	
		Tenth	Threshold	500	1000
Recovery	Mean % (SD)	101 (2)	100 (1)	101.5 (8)	98 (2)
Precision	RSD (ppt)	20	10	8	20
Robustness		Results reproducible	Results reproducible	Results reproducible	Results reproducible
Working Range	Calibration Curve	20 – 100 ppm		300 – 1500 ppm	
Linearity	R^2	0.9993		0.9992	
Sensitivity	Slope	0.7737		2.4329	
Selectivity	s_m	0.0121		0.0387	
Error of the Slope	Intercept	0.8343		-2.5460	
Specificity	S_c	0.3426		16.4139	
t-value		0.9	0	3.2	-1.7
Decision		Accepted	Accepted	Accepted	Accepted

Table 5.27: Validation of ICP-OES analyses for cobalt in the pure zirconium solution

Validation Criteria	Parameter	Cobalt		Zirconium	
		Tenth	Threshold	500	1000
Recovery	Mean % (SD)	98.3 (3)	100.7 (7)	100 (3)	102 (2)
Precision	RSD (ppt)	3	7	30	20
Robustness		Results reproducible	Results reproducible	Results reproducible	Results reproducible
Working Range	Calibration Curve	20 – 100 ppm		300 – 1500 ppm	
Linearity	R^2	0.9979		0.9992	
Sensitivity	Slope	0.2924		2.4329	
Selectivity	s_m	0.0077		0.0387	
Error of the Slope	Intercept	0.3720		-2.5460	
Specificity	S_c	0.2195		16.4139	
t-value		-9.8	1.7	0	1.7
Decision		Rejected	Accepted	Accepted	Accepted

Table 5.28: Validation of ICP-OES analyses for copper in the pure zirconium solution

Validation Criteria	Parameter	Copper		Zirconium	
		Tenth	Threshold	500	1000
Recovery	Mean % (SD)	101 (4)	100.6 (4)	102 (4)	101 (2)
Precision	RSD (ppt)	40	4	39	20
Robustness		Results reproducible	Results reproducible	Results reproducible	Results reproducible
Working Range	Calibration Curve	20 – 100 ppm		300 – 1500 ppm	
Linearity	R^2	0.9999		0.9992	
Sensitivity	Slope	0.5408		2.4329	
Selectivity	s_m	0.0035		0.0387	
Error of the Slope	Intercept	0.4264		-2.5460	
Specificity	S_c	0.1002		16.4139	
t-value		0.4	2.6	0.9	0.9
Decision		Accepted	Accepted	Accepted	Accepted

Table 5.29: Validation of ICP-OES analyses for manganese in the pure zirconium solution

Validation Criteria	Parameter	Manganese		Zirconium	
		Tenth	Threshold	500	1000
Recovery	Mean % (SD)	100 (2)	99 (1)	102 (2)	102 (2)
Precision	RSD (ppt)	20	10	20	20
Robustness		Results reproducible	Results reproducible	Results reproducible	Results reproducible
Working Range	Calibration Curve	20 – 100 ppm		300 – 1500 ppm	
Linearity	R^2	0.9995		0.9992	
Sensitivity	Slope	2.2973		2.4329	
Selectivity	s_m	0.0282		0.0387	
Error of the Slope	Intercept	0.2231		-2.5460	
Specificity	S_c	0.7975		16.4139	
t-value		0	-1.7	1.7	1.7
Decision		Accepted	Accepted	Accepted	Accepted

Table 5.30: Validation of ICP-OES analyses for molybdenum in the pure zirconium solution

Validation Criteria	Parameter	Molybdenum		Zirconium	
		Tenth	Threshold	500	1000
Recovery	Mean % (SD)	101 (1)	102 (4)	102.5 (5)	101.1 (8)
Precision	RSD (ppt)	10	39	5	8
Robustness		Results reproducible	Results reproducible	Results reproducible	Results reproducible
Working Range	Calibration Curve	20 – 100 ppm		300 – 1500 ppm	
Linearity	R^2	0.9995		0.9998	
Sensitivity	Slope	0.1268		3.8331	
Selectivity	s_m	0.0017		0.0344	
Error of the Slope	Intercept	0.2058		-3.3170	
Specificity	S_c	0.0476		14.5923	
t-value		1.7	0.9	8.7	2.4
Decision		Accepted	Accepted	Rejected	Accepted

Table 5.31: Validation of ICP-OES analyses for nickel in the pure zirconium solution

Validation Criteria	Parameter	Nickel		Zirconium	
		Tenth	Threshold	500	1000
Recovery	Mean % (SD)	102 (1)	100.3 (2)	100 (1)	102 (1)
Precision	RSD (ppt)	10	2	10	10
Robustness		Results reproducible	Results reproducible	Results reproducible	Results reproducible
Working Range	Calibration Curve	20 – 100 ppm		300 – 1500 ppm	
Linearity	R^2	0.9994		0.9998	
Sensitivity	Slope	0.3433		3.8331	
Selectivity	s_m	0.0049		0.0344	
Error of the Slope	Intercept	-0.1732		-3.3170	
Specificity	S_c	0.1400		14.5923	
t-value		3.5	2.6	0	3.5
Decision		Accepted	Accepted	Accepted	Accepted

Table 5.32: Validation of ICP-OES analyses for silicon in the pure zirconium solution

Validation Criteria	Parameter	Silicon		Zirconium	
		Tenth	Threshold	500	1000
Recovery	Mean % (SD)	99 (2)	100 (1)	98.3 (1)	98 (1)
Precision	RSD (ppt)	20	10	1	10
Robustness		Results reproducible	Results reproducible	Results reproducible	Results reproducible
Working Range	Calibration Curve	30 – 150 ppm		300 – 1500 ppm	
Linearity	R^2	0.9991		0.9998	
Sensitivity	Slope	0.1896		3.8331	
Selectivity	s_m	0.0033		0.0344	
Error of the Slope	Intercept	-0.0077		-3.3170	
Specificity	S_c	0.1382		14.5923	
t-value		-0.9	0	-29.4	-3.5
Decision		Accepted	Accepted	Rejected	Accepted

Table 5.33: Validation of ICP-OES analyses for titanium in the pure zirconium solution

Validation Criteria	Parameter	Titanium		Zirconium	
		Tenth	Threshold	500	1000
Recovery	Mean % (SD)	100.1 (2)	102.0 (2)	100 (3)	100 (3)
Precision	RSD (ppt)	2	2	30	30
Robustness		Results reproducible	Results reproducible	Results reproducible	Results reproducible
Working Range	Calibration Curve	20 – 100 ppm		300 – 1500 ppm	
Linearity	R^2	0.9997		0.9998	
Sensitivity	Slope	3.2831		3.8331	
Selectivity	s_m	0.0344		0.0344	
Error of the Slope	Intercept	0.4344		-3.3170	
Specificity	S_c	0.9739		14.5923	
t-value		0.9	17.3	0	0
Decision		Accepted	Rejected	Accepted	Accepted

Table 5.34: Validation of ICP-OES analyses for tungsten in the pure zirconium solution

Validation Criteria	Parameter	Tungsten		Zirconium	
		Tenth	Threshold	500	1000
Recovery	Mean % (SD)	102 (2)	99 (2)	101 (2)	102 (2)
Precision	RSD (ppt)	20	20	20	20
Robustness		Results reproducible	Results reproducible	Results reproducible	Results reproducible
Working Range	Calibration Curve	20 – 100 ppm		300 – 1500 ppm	
Linearity	R^2	0.9999		0.9998	
Sensitivity	Slope	0.0388		3.8331	
Selectivity	s_m	0.0002		0.0344	
Error of the Slope	Intercept	-0.0275		-3.3170	
Specificity	S_c	0.0068		14.5923	
t-value		1.7	-0.9	0.9	1.7
Decision		Accepted	Accepted	Accepted	Accepted

Table 5.35: Validation of ICP-OES analyses for uranium in the pure zirconium solution

Validation Criteria	Parameter	Uranium		Zirconium	
		Tenth	Threshold	500	1000
Recovery	Mean % (SD)	102 (4)	102 (3)	100.4 (2)	102 (1)
Precision	RSD (ppt)	39	29	2	10
Robustness		Results reproducible	Results reproducible	Results reproducible	Results reproducible
Working Range	Calibration Curve	2 – 10 ppm		300 – 1500 ppm	
Linearity	R^2	0.9993		0.9998	
Sensitivity	Slope	0.0651		3.8331	
Selectivity	s_m	0.0010		0.0344	
Error of the Slope	Intercept	0.0151		-3.3170	
Specificity	S_c	0.0028		14.5923	
t-value		0.9	1.2	3.5	3.5
Decision		Accepted	Accepted	Accepted	Accepted

Table 5.36: Validation of ICP-OES analyses for group 1 impurities (Tenth of the threshold) in the pure zirconium solution

Validation Criteria	Parameter	Zr	Al	Cr	Fe	Hf
Recovery	**Mean % (SD)**	100.8 (2)	102 (3)	98 (7)	103 (2)	99.9 (8)
Precision	**RSD (ppt)**	2	29	70	19	8
Robustness		R.R	R.R	R.R	R.R	R.R
Working Range	**Calibration Curve**	300 – 1500 ppm	20 – 100 ppm	50 – 250 ppm	500 – 2500 ppm	30 – 150 ppm
Linearity	**R^2**	0.9998	0.9997	1.0000	1.0000	0.9996
Sensitivity	**Slope**	1.85	0.1189	0.2007	0.2752	0.0757
Selectivity	**s_m**	0.0152	0.0012	0.0003	0.0007	0.0009
Error of the Slope	**Intercept**	0.6150	0.0396	0.2647	-0.1877	-0.0303
Specificity	**S_c**	6.4542	0.0349	0.0235	0.5047	0.0379
***t*-value**		6.9	1.2	-0.5	2.6	-0.2
Decision		Rejected	Accepted	Accepted	Accepted	Accepted

R.R: Results reproducible

Table 5.37: Validation of ICP-OES analyses for group 1 impurities (Threshold) in the pure zirconium solution

Validation Criteria	Parameter	Zr	Al	Cr	Fe	Hf
Recovery	**Mean % (SD)**	99 (3)	100.2 (1)	102 (2)	100.9 (4)	101 (4)
Precision	**RSD (ppt)**	30	1	20	4	40
Robustness		R.R	R.R	R.R	R.R	R.R
Working Range	**Calibration Curve**	300 – 1500 ppm	20 – 100 ppm	50 – 250 ppm	500 – 2500 ppm	30 – 150 ppm
Linearity	**R^2**	0.9998	0.9997	1.0000	1.0000	0.9996
Sensitivity	**Slope**	1.85	0.1189	0.2007	0.2752	0.0757
Selectivity	**s_m**	0.0152	0.0012	0.0003	0.0007	0.0009
Error of the Slope	**Intercept**	0.6150	0.0396	0.2647	-0.1877	-0.0303
Specificity	**S_c**	6.4542	0.0349	0.0235	0.5047	0.0379
***t*-value**		-0.6	3.5	1.7	3.9	0.4
Decision		Accepted	Accepted	Accepted	Accepted	Accepted

R.R: Results reproducible

Table 5.38: Validation of ICP-OES analyses for group 2 impurities (Tenth of the threshold) in the pure zirconium solution

Validation Criteria	Parameter	Zr	B	Cd	Co	Cu	Mn
Recovery	**Mean % (SD)**	100 (1)	N.D	N.D	99.9 (7)	101 (3)	100 (5)
Precision	**RSD (ppt)**	10	-	-	7	30	50
Robustness		R.R	-	-	R.R	R.R	R.R
Working Range	**Calibration Curve**	300 – 1500 ppm	20 – 100 ppm	20 – 100 ppm	20 – 100 ppm	20 – 100 ppm	20 – 100 ppm
Linearity	**R^2**	0.9998	1.0000	0.9995	0.9991	0.9996	0.9996
Sensitivity	**Slope**	1.85	0.1483	0.9828	0.1855	0.7418	2.9355
Selectivity	**s_m**	0.0152	0.0004	0.0121	0.0032	0.0086	0.0323
Error of the Slope	**Intercept**	0.6150	-0.0214	0.3480	-0.1685	0.9187	-2.8583
Specificity	**S_c**	6.4542	0.0115	0.3438	0.0916	0.2436	0.9158
***t*-value**		0	-	-	-0.2	0.6	0
Decision		Accepted	Rejected	Rejected	Accepted	Accepted	Accepted

ND: Not Detectable

R.R: Results reproducible

Table 5.39: Validation of ICP-OES analyses for group 2 impurities (Threshold) in the pure zirconium solution

Validation Criteria	Parameter	Zr	B	Cd	Co	Cu	Mn
Recovery	**Mean % (SD)**	100 (3)	100 (2)	101 (2)	98 (2)	102 (3)	102 (2)
Precision	**RSD (ppt)**	30	20	20	20	29	20
Robustness		R.R	R.R	R.R	R.R	R.R	R.R
Working Range	**Calibration Curve**	300 – 1500 ppm	20 – 100 ppm	20 – 100 ppm	20 – 100 ppm	20 – 100 ppm	20 – 100 ppm
Linearity	**R^2**	0.9998	1.0000	0.9995	0.9991	0.9996	0.9996
Sensitivity	**Slope**	1.85	0.1483	0.9828	0.1855	0.7418	2.9355
Selectivity	**s_m**	0.0152	0.0004	0.0121	0.0032	0.0086	0.0323
Error of the Slope	**Intercept**	0.6150	-0.0214	0.3480	-0.1685	0.9187	-2.8583
Specificity	**S_c**	6.4542	0.0115	0.3438	0.0916	0.2436	0.9158
***t*-value**		0	0	0.9	-1.7	1.2	1.7
Decision		Accepted	Accepted	Accepted	Accepted	Accepted	Accepted

R.R: Results reproducible

Table 5.40: Validation of ICP-OES analyses for group 3 impurities (Tenth of the threshold) in the pure zirconium solution

Validation Criteria	Parameter	Zr	Mo	Ni	Si	Ti	W	U
Recovery	**Mean % (SD)**	100 (4)	99 (3)	99.3 (6)	101 (1)	99 (2)	102 (1)	N.D
Precision	**RSD (ppt)**	40	30	6	10	20	10	-
Robustness		R.R	R.R	R.R	R.R	R.R	R.R	-
Working Range	**Calibration Curve**	300 – 1500 ppm	20 – 100 ppm	20 – 100 ppm	30 – 150 ppm	20 – 100 ppm	20 – 100 ppm	2 – 10 ppm
Linearity	**R^2**	0.9998	0.9999	0.9999	1.0000	0.9997	0.9995	0.9999
Sensitivity	**Slope**	1.85	0.0742	0.4009	0.1997	3.1299	0.0263	0.0375
Selectivity	**s_m**	0.0152	0.0005	0.0025	0.0005	0.0335	0.0003	0.0002
Error of the Slope	**Intercept**	0.6150	-0.0132	-0.0966	-1.2929	1.3026	-0.0685	0.0134
Specificity	**S_c**	6.4542	0.0138	0.0703	0.0207	0.9485	0.0098	0.0005
***t*-value**		0	-0.6	-2.0	1.7	-0.9	3.5	-
Decision		Accepted	Accepted	Accepted	Accepted	Accepted	Accepted	Rejected

ND: Not Detectable

R.R: Results reproducible

Table 5.41: Validation of ICP-OES analyses for group 3 impurities (Threshold) in the pure zirconium solution

Validation Criteria	Parameter	Zr	Mo	Ni	Si	Ti	W	U
Recovery	**Mean % (SD)**	102 (1)	101 (2)	102 (2)	102 (2)	100 (2)	101.8 (9)	101 (5)
Precision	**RSD (ppt)**	10	20	20	20	20	9	50
Robustness		R.R	R.R	R.R	R.R	R.R	R.R	R.R
Working Range	**Calibration Curve**	300 – 1500 ppm	20 – 100 ppm	20 – 100 ppm	30 – 150 ppm	20 – 100 ppm	20 – 100 ppm	2 – 10 ppm
Linearity	**R^2**	0.9998	0.9999	0.9999	1.0000	0.9997	0.9995	0.9999
Sensitivity	**Slope**	1.85	0.0742	0.4009	0.1997	3.1299	0.0263	0.0375
Selectivity	**s_m**	0.0152	0.0005	0.0025	0.0005	0.0335	0.0003	0.0002
Error of the Slope	**Intercept**	0.6150	-0.0132	-0.0966	-1.2929	1.3026	-0.0685	0.0134
Specificity	**S_c**	6.4542	0.0138	0.0703	0.0207	0.9485	0.0098	0.0005
***t*-value**		3.5	0.9	1.7	1.7	0	3.5	0.3
Decision		Accepted	Accepted	Accepted	Accepted	Accepted	Accepted	Accepted

R.R: Results reproducible

Table 5.42: Validation of ICP-OES analyses for groups 1 and 2 impurities (Tenth of the threshold) in the pure zirconium solution

Validation Criteria	Parameter	Zr	Al	Cr	Fe	Hf	B	Cd	Co	Cu	Mn
Recovery	**Mean % (SD)**	98.7 (8)	98 (2)	102.1 (4)	101.7 (9)	99 (2)	N.D	N.D	102 (1)	101.0 (6)	98.2 (9)
Precision	**RSD (ppt)**	8	20	4	9	20	-	-	10	6	9
Robustness		R.R	R.R	R.R	R.R	R.R	-	-	R.R	R.R	R.R
Working Range	**Calibration Curve**	300 – 1500 ppm	20 – 100 ppm	50 – 250 ppm	500 – 2500 ppm	30 – 150 ppm	20 – 100 ppm	20 – 100 ppm	20 – 100 ppm	20 – 100 ppm	20 – 100 ppm
Linearity	**R^2**	0.9992	1.0000	0.9999	0.9998	0.9995	0.9991	0.9994	0.9991	1.0000	0.9999
Sensitivity	**Slope**	1.7999	0.2347	0.2091	0.2998	0.0713	0.2795	0.6210	0.3050	0.6495	2.4385
Selectivity	**s_m**	0.0298	0.0007	0.0010	0.0024	0.0009	0.0047	0.0091	0.0053	0.0015	0.0169
Error of the Slope	**Intercept**	0.4550	-0.7321	0.0798	0.0346	-0.0526	0.0653	0.0101	0.2770	-1.9203	-0.9629
Specificity	**S_c**	12.7	0.0200	0.0730	1.7216	0.0381	0.1343	0.2582	0.1508	0.0427	0.4783
***t*-value**		-2.8	-1.7	9.1	3.3	-0.9	-	-	3.5	2.9	-3.5
Decision		Accepted	Accepted	Rejected	Accepted	Accepted	Rejected	Rejected	Accepted	Accepted	Accepted

ND: Not Detectable

R.R: Results reproducible

Table 5.43: Validation of ICP-OES analyses for groups 1 and 2 impurities (Threshold) in the pure zirconium solution

Validation Criteria	Parameter	Zr	Al	Cr	Fe	Hf	B	Cd	Co	Cu	Mn
Recovery	Mean % (SD)	99.9 (3)	101 (1)	100.5 (8)	102 (1)	100 (5)	101 (1)	102 (5)	100 (1)	99.9 (5)	99 (1)
Precision	RSD (ppt)	3	10	8	10	50	10	49	10	5	10
Robustness		R.R	R.R	R.R	R.R	R.R	R.R	R.R	R.R	R.R	R.R
Working Range	Calibration Curve	300 – 1500 ppm	20 – 100 ppm	50 – 250 ppm	500 – 2500 ppm	30 – 150 ppm	20 – 100 ppm	20 – 100 ppm	20 – 100 ppm	20 – 100 ppm	20 – 100 ppm
Linearity	R^2	0.9992	1.0000	0.9999	0.9998	0.9995	0.9991	0.9994	0.9991	1.0000	0.9999
Sensitivity	Slope	1.7999	0.2347	0.2091	0.2998	0.0713	0.2795	0.6210	0.3050	0.6495	2.4385
Selectivity	s_m	0.0298	0.0007	0.0010	0.0024	0.0009	0.0047	0.0091	0.0053	0.0015	0.0169
Error of the Slope	Intercept	0.4550	-0.7321	0.0798	0.0346	-0.0526	0.0653	0.0101	0.2770	-1.9203	-0.9629
Specificity	S_c	12.7	0.0200	0.0730	1.7216	0.0381	0.1343	0.2582	0.1508	0.0427	0.4783
t-value		-0.6	1.7	1.1	3.5	0	1.7	0.7	0	-0.3	-1.7
Decision		Accepted	Accepted	Accepted	Accepted	Accepted	Accepted	Accepted	Accepted	Accepted	Accepted

R.R: Results reproducible

Table 5.44: Validation of ICP-OES analyses for groups 1 and 3 impurities (Tenth of the threshold) in the pure zirconium solution

Validation Criteria	Parameter	Zr	Al	Cr	Fe	Hf	Mo	Ni	Si	Ti	W	U
Recovery	**Mean % (SD)**	102 (3)	101 (3)	100.9 (5)	103.5 (3)	102 (3)	99 (4)	98 (2)	103.5 (8)	102.7 (3)	100.4 (9)	70 (2)
Precision	**RSD (ppt)**	29	30	5	3	29	40	20	8	3	9	29
Robustness		R.R	R.R	R.R	R.R	R.R	R.R	R.R	R.R	R.R	R.R	R.R
Working Range	**Calibration Curve**	300 – 1500 ppm	20–100 ppm	50–250 ppm	500 – 2500 ppm	30–150 ppm	20–100 ppm	20–100 ppm	30–150 ppm	20–100 ppm	20–100 ppm	2 – 10 ppm
Linearity	**R^2**	0.9992	0.9993	0.9999	0.9992	0.9998	0.9998	0.9994	0.9990	0.9999	0.9997	0.9999
Sensitivity	**Slope**	1.7999	0.3898	0.2035	0.2974	0.0452	0.0472	0.3832	0.0981	1.9634	0.0115	0.0386
Selectivity	**s_m**	0.0298	0.0058	0.0013	0.0049	0.0004	0.0004	0.0055	0.0018	0.0096	0.0001	0.0002
Error of the Slope	**Intercept**	0.4550	0.0017	0.2798	0.8346	0.0667	0.0986	0.3619	0.0583	2.9014	0.0074	-0.0099
Specificity	**S_c**	12.7	0.1634	0.0934	3.4938	0.0151	0.0117	0.1551	0.0756	0.2729	0.0032	0.0007
***t*-value**		1.2	0.6	3.1	20.2	1.2	0.4	-1.7	7.6	15.6	0.8	-26.0
Decision		Accepted	Accepted	Accepted	Rejected	Accepted	Accepted	Accepted	Rejected	Rejected	Accepted	Rejected

R.R: Results reproducible

Table 5.45: Validation of ICP-OES analyses for groups 1 and 3 impurities (Threshold) in the pure zirconium solution

Validation Criteria	Parameter	Zr	Al	Cr	Fe	Hf	Mo	Ni	Si	Ti	W	U
Recovery	Mean % (SD)	100 (2)	101.1 (1)	102.0 (3)	100.2 (5)	99.8 (6)	99 (2)	100.5 (2)	102 (1)	100.8 (3)	99 (3)	100 (2)
Precision	RSD (ppt)	20	1	3	5	6	20	2	10	3	30	20
Robustness		R.R	R.R	R.R	R.R	R.R	R.R	R.R	R.R	R.R	R.R	R.R
Working Range	Calibration Curve	300 – 1500 ppm	20–100 ppm	50–250 ppm	500 – 2500 ppm	30–150 ppm	20–100 ppm	20–100 ppm	30–150 ppm	20–100 ppm	20–100 ppm	2 – 10 ppm
Linearity	R^2	0.9992	0.9992	0.9993	0.9999	0.9992	0.9998	0.9998	0.9994	0.9990	0.9999	0.9997
Sensitivity	Slope	1.7999	1.7999	0.3898	0.2035	0.2974	0.0452	0.0472	0.3832	0.0981	1.9634	0.0115
Selectivity	s_m	0.0298	0.0298	0.0058	0.0013	0.0049	0.0004	0.0004	0.0055	0.0018	0.0096	0.0001
Error of the Slope	Intercept	0.4550	0.4550	0.0017	0.2798	0.8346	0.0667	0.0986	0.3619	0.0583	2.9014	0.0074
Specificity	S_c	12.7	12.7	0.1634	0.0934	3.4938	0.0151	0.0117	0.1551	0.0756	0.2729	0.0032
t-value		0	19.1	11.5	0.7	-0.6	-0.9	4.3	3.5	4.6	-0.6	0
Decision		Accepted	Rejected	Rejected	Accepted	Accepted	Accepted	Accepted	Accepted	Rejected	Accepted	Accepted

R.R: Results reproducible

Table 5.46: Validation of ICP-OES analyses for groups 2 and 3 impurities (Tenth of the threshold) in the pure zirconium solution

Validation Criteria	Parameter	Zr	B	Cd	Co	Cu	Mn	Mo	Ni	Si	Ti	W	U
Recovery	Mean % (SD)	102.1 (2)	N.D	N.D	102 (2)	101.8 (9)	101.0 (9)	100 (3)	100 (6)	101 (1)	99.1 (1)	100 (3)	4 (3)
Precision	RSD (ppt)	20	-	-	20	9	9	30	60	10	1	30	750
Robustness		R.R	R.R	R.R	R.R	R.R	R.R	R.R	R.R	R.R	R.R	R.R	R.R
Working Range	Calibration Curve	300–1500 ppm	20 – 100 ppm	20 – 100 ppm	20 – 100 ppm	20 – 100 ppm	20 – 100 ppm	20 – 100 ppm	20 – 100 ppm	30 – 150 ppm	20 – 100 ppm	20 – 100 ppm	2 – 10 ppm
Linearity	R^2	0.9992	0.9999	0.9996	0.9995	0.9998	0.9986	0.9996	0.9994	0.9982	0.9997	0.9995	0.9999
Sensitivity	Slope	1.7999	0.3043	0.1350	0.5591	0.6105	0.4232	0.0644	0.0212	0.1633	3.1399	0.0263	0.0469
Selectivity	s_m	0.0298	0.0015	0.0015	0.0075	0.0052	0.0092	0.0007	0.0003	0.0040	0.0337	0.0003	0.0003
Error of the Slope	Intercept	0.4550	0.1307	0.0951	0.8194	-0.8311	0.4854	0.2854	0.0004	-0.5110	0.5026	-0.0685	-0.0075
Specificity	S_c	12.7	0.0418	0.0429	0.2110	0.1466	0.2608	0.0200	0.0083	0.1706	0.9538	0.0098	0.0008
t-value		1.8	-	-	1.7	3.5	1.9	0	0	1.7	-15.6	0	-55.4
Decision		Accepted	Rejected	Rejected	Accepted	Accepted	Accepted	Accepted	Accepted	Accepted	Rejected	Accepted	Rejected

R.R: Results reproducible

Table 5.47: Validation of ICP-OES analyses for groups 2 and 3 impurities (Threshold) in the pure zirconium solution

Validation Criteria	Parameter	Zr	B	Cd	Co	Cu	Mn	Mo	Ni	Si	Ti	W	U
Recovery	**Mean % (SD)**	98.8 (3)	102 (2)	100 (3)	99 (3)	103 (1)	101 (2)	99.5 (6)	103.5 (1)	100 (2)	102 (3)	100 (1)	99 (2)
Precision	**RSD (ppt)**	3	20	30	30	10	20	6	1	20	29	10	20
Robustness		R.R	R.R	R.R	R.R	R.R	R.R	R.R	R.R	R.R	R.R	R.R	R.R
Working Range	**Calibration Curve**	300–1500 ppm	20 – 100 ppm	20 – 100 ppm	20 – 100 ppm	20 – 100 ppm	20 – 100 ppm	20 – 100 ppm	20 – 100 ppm	30 – 150 ppm	20 – 100 ppm	20 – 100 ppm	2 – 10 ppm
Linearity	**R^2**	0.9992	0.9992	0.9999	0.9996	0.9995	0.9998	0.9986	0.9996	0.9994	0.9982	0.9997	0.9995
Sensitivity	**Slope**	1.7999	1.7999	0.3043	0.1350	0.5591	0.6105	0.4232	0.0644	0.0212	0.1633	3.1399	0.0263
Selectivity	**s_m**	0.0298	0.0298	0.0015	0.0015	0.0075	0.0052	0.0092	0.0007	0.0003	0.0040	0.0337	0.0003
Error of the Slope	**Intercept**	0.4550	0.4550	0.1307	0.0951	0.8194	-0.8311	0.4854	0.2854	0.0004	-0.5110	0.5026	-0.0685
Specificity	**S_c**	12.7	12.7	0.0418	0.0429	0.2110	0.1466	0.2608	0.0200	0.0083	0.1706	0.9538	0.0098
***t*-value**		-6.9	3.5	0	-0.6	5.2	0.9	-2.9	60.6	0	1.2	0	-0.9
Decision		Rejected	Accepted	Accepted	Accepted	Rejected	Accepted	Accepted	Rejected	Accepted	Accepted	Accepted	Accepted

R.R: Results reproducible

Table 5.48: Validation of ICP-OES analyses for all the impurities (Tenth of the threshold) in the pure zirconium solution

Validation Criteria	Parameter	Zr	Al	Cr	Fe	Hf	B	Cd	Co	Cu	Mn
Recovery	**Mean % (SD)**	100 (1)	101 (2)	100 (1)	100.6 (7)	100 (1)	N.D	N.D	97.8 (2)	101 (2)	102 (1)
Precision	**RSD (ppt)**	10	20	10	7	10	-	-	2	20	10
Robustness		R.R	R.R	R.R	R.R	R.R	-	-	R.R	R.R	R.R
Working Range	**Calibration Curve**	300 – 1500 ppm	20 – 100 ppm	50 – 250 ppm	500 – 2500 ppm	30 – 150 ppm	20 – 100 ppm	20 – 100 ppm	20 – 100 ppm	20 – 100 ppm	20 – 100 ppm
Linearity	**R^2**	0.9995	0.9998	0.9999	0.9997	0.9998	0.9997	0.9998	0.9996	0.9996	0.9997
Sensitivity	**Slope**	1.0786	0.4280	0.2094	0.3894	0.0421	0.6045	0.1832	0.7080	0.7003	2.3525
Selectivity	**s_m**	0.0142	0.0033	0.0010	0.0040	0.0003	0.0056	0.0014	0.0079	0.0081	0.0251
Error of the Slope	**Intercept**	0.2704	0.3912	0.7611	0.2156	0.0512	0.0799	0.2599	-0.6849	-0.4938	-0.4784
Specificity	**S_c**	6.0074	0.0939	0.0727	2.8058	0.0140	0.1578	0.0407	0.2224	0.2307	0.7109
***t*-value**		0	0.9	0	1.5	0	-	-	-19.1	0.9	3.5
Decision		Accepted	Accepted	Accepted	Accepted	Accepted	Rejected	Rejected	Rejected	Accepted	Accepted

ND: Not Detectable

R.R: Results reproducible

Table 5.48 (continuation): Validation of ICP-OES analyses for all the impurities (Tenth of the threshold) in the pure zirconium solution

Validation Criteria	Parameter	Mo	Ni	Si	Ti	W	U
Recovery	**Mean % (SD)**	101 (2)	102 (2)	100 (1)	101 (1)	101 (2)	N.D
Precision	**RSD (ppt)**	20	20	10	10	20	-
Robustness		R.R	R.R	R.R	R.R	R.R	-
Working Range	**Calibration Curve**	20 – 100 ppm	20 – 100 ppm	30 – 150 ppm	20 – 100 ppm	20 – 100 ppm	2 – 10 ppm
Linearity	**R^2**	0.9997	0.9990	1.0000	0.9998	0.9997	0.9991
Sensitivity	**Slope**	0.0470	0.4483	0.0740	1.8771	0.0115	0.0564
Selectivity	**s_m**	0.0005	0.0082	0.0002	0.0143	0.0001	0.0010
Error of the Slope	**Intercept**	0.0246	-0.0531	1.5363	1.5316	0.0074	0.0035
Specificity	**S_c**	0.0128	0.2323	0.0083	0.4048	0.0032	0.0028
***t*-value**		0.9	1.7	0	1.7	0.9	-
Decision		Accepted	Accepted	Accepted	Accepted	Accepted	Rejected

ND: Not Detectable

R.R: Results reproducible

Table 5.49: Validation of ICP-OES analyses for all the impurities (Threshold) in the pure zirconium solution

Validation Criteria	Parameter	Zr	Al	Cr	Fe	Hf	B	Cd	Co	Cu	Mn
Recovery	**Mean % (SD)**	101 (1)	98.2 (2)	101 (1)	102.0 (3)	102 (1)	101.2 (8)	99 (2)	99.9 (1)	101 (3)	102.3 (3)
Precision	**RSD (ppt)**	10	2	10	3	10	8	20	1	30	3
Robustness		R.R	R.R	R.R	R.R	R.R	R.R	R.R	R.R	R.R	R.R
Working Range	**Calibration Curve**	300 – 1500 ppm	20 – 100 ppm	50 – 250 ppm	500 – 2500 ppm	30 – 150 ppm	20 – 100 ppm	20 – 100 ppm	20 – 100 ppm	20 – 100 ppm	20 – 100 ppm
Linearity	**R^2**	0.9995	0.9998	0.9999	0.9997	0.9998	0.9997	0.9998	0.9996	0.9996	0.9997
Sensitivity	**Slope**	1.0786	0.4280	0.2094	0.3894	0.0421	0.6045	0.1832	0.7080	0.7003	2.3525
Selectivity	**s_m**	0.0142	0.0033	0.0010	0.0040	0.0003	0.0056	0.0014	0.0079	0.0081	0.0251
Error of the Slope	**Intercept**	0.2704	0.3912	0.7611	0.2156	0.0512	0.0799	0.2599	-0.6849	-0.4938	-0.4784
Specificity	**S_c**	6.0074	0.0939	0.0727	2.8058	0.0140	0.1578	0.0407	0.2224	0.2307	0.7109
***t*-value**		1.7	-15.6	1.7	11.5	3.5	2.6	-0.9	-1.7	0.6	13.3
Decision		Accepted	Rejected	Accepted	Rejected	Accepted	Accepted	Accepted	Accepted	Accepted	Rejected

R.R: Results reproducible

Table 5.49 (continuation): Validation of ICP-OES analyses for all the impurities (Threshold) in the pure zirconium solution

Validation Criteria	Parameter	Mo	Ni	Si	Ti	W	U
Recovery	**Mean % (SD)**	99.2 (7)	99 (2)	100 (4)	102.0 (3)	99.7 (6)	101 (4)
Precision	**RSD (ppt)**	7	20	40	3	6	40
Robustness		R.R	R.R	R.R	R.R	R.R	R.R
Working Range	**Calibration Curve**	20 – 100 ppm	20 – 100 ppm	30 – 150 ppm	20 – 100 ppm	20 – 100 ppm	2 – 10 ppm
Linearity	**R^2**	0.9997	0.9990	1.0000	0.9998	0.9997	0.9991
Sensitivity	**Slope**	0.0470	0.4483	0.0740	1.8771	0.0115	0.0564
Selectivity	**s_m**	0.0005	0.0082	0.0002	0.0143	0.0001	0.0010
Error of the Slope	**Intercept**	0.0246	-0.0531	1.5363	1.5316	0.0074	0.0035
Specificity	**S_c**	0.0128	0.2323	0.0083	0.4048	0.0032	0.0028
***t*-value**		-2.0	-0.9	0	11.5	-0.9	0.4
Decision		Accepted	Accepted	Accepted	Rejected	Accepted	Accepted

R.R: Results reproducible

5.5.3 CONCLUSION

The objective of developing a method fit for the purpose of enabling the quantitative analyses of impurities in the zirconium solution was achieved. The wavelength selection in the analysis of all the elements that were investigated in this study played a crucial role in the quantification of all the impurities to ensure that none of the elements in solution interfered with each other in their analysis. This is indicated in the quantitative analyses of, among others, cadmium (214.438 and 361.051 nm), hafnium (277.336 and 282.023 nm) and copper (324.754 and 213.598 nm). The matrices of the samples and the calibration standards were matched and this proved to have eliminated any errors in the analysis of all the elements in this study. All the elements were recovered with an overall average of 100 ± 2 %, with the exception of boron, cadmium and uranium when analyzed at a tenth of their permissible threshold.

The validations of the results obtained for most elements were acceptable at a 95 % confidence interval. The relatively large standard deviations obtained for the analytical results led to the positive validation acceptance criteria. Thus this led to the rejection of the null hypothesis. The acceptable precision for an analyte composition of between 1 and 10 % in a given sample is that with a relative standard deviation (RSD) of up to 50 ppt.[169] Thus, since the composition of all the elements investigated in this study was 6.25 %, considered only in the sample containing all of the impurities at the threshold, each was precisely recovered with RSD values below 50 ppt.

6 EVALUATION OF THE STUDY AND FUTURE RESEARCH

6.1 INTRODUCTION

The purpose of this chapter is firstly to evaluate the success of the study as measured against the objectives set at the beginning of the study in Chapter 1 and secondly it identifies possible future projects which may supplement/compliment the current study.

6.2 DEGREE OF SUCCESS OF STUDY WITH REGARD TO THE SET OBJECTIVES

The main objectives of this study as outlined in **Chapter 1**, **Section 1.5** were as follows:

a) To develop an alternative digestion method for zirconium metal and zirconium tetrafluoride samples for the analysis of their impurity elements; zirconium tetrafluoride is used as is or converted to zirconium hexafluoride to develop as the RM

b) To develop effective and efficient analytical method for the multi-element quantification of zirconium and its impurities in ultra-pure of nuclear grade metal samples at different levels of concentration (at threshold and a 1/10 of threshold) by using commercially available equipment such as ICP-OES

c) To identify and compare the different analytical techniques, with much emphasis on the recent and modern technique such as ICP-OES

d) To determine LOD/LOQ for zirconium and its associated impurities for nuclear purposes

e) To perform method validation on these analytical methods

f) To perform a physical evaluation of the most relevant and promising analytical methods using pure standards in the mentioned technique.

This study is been regarded as highly successful if the results obtained, are measured against the set objectives. Firstly, the digestion of the pure zirconium metal discs and foil (>99.98 %) was successfully accomplished with H_2SO_4 at high temperatures compared to acids such as H_3PO_4 and *aqua regia*. The zirconium was accurately quantified using ICP-OES at 339.198 and 343.823 nm. Secondly, the zirconium in a newly prepared K_2ZrF_6 reference material was also accurately quantified at the above-mentioned wavelengths. The LOD and LOQ for zirconium were determined to be within the limits of those reported in literature while all the other validation parameters were acceptable within the required specifications to render this method highly effective for the dissolution and quantification of zirconium in different samples.

The quantification of the artificially added impurities in the presence of zirconium, single and multi-element matrices, as specified for ultra-pure or nuclear grade zirconium, also proved to be extremely successful, especially at threshold quantities. Recoveries between 97 and 103 % were obtained for the zirconium and all 15 added impurities. It was only at a tenth of the threshold that three elements, namely cadmium, boron and uranium were not quantitatively recovered which was attributed to their concentration being very close or below the LOD.

The successful recovery of the elements are mainly attributed to careful wavelength selection which minimized or prevented any spectral overlap with that of the other elements and secondly to acid matrix matching. The limits of detection (LOD) and quantification (LOQ) for all the impurities were determined at levels which were comparable/compatible with those reported in the literature, while most of the other validation parameters were acceptable within the required specifications to render this method highly effective for the quantification of zirconium and all its permissible impurities in different samples. It was only the accuracy of some of the impurities that were rejected at the 95 % confidence level due to the small standard deviations obtained during the statistical evaluation of the results (high degree of precision).

It is therefore concluded that all the goals as set out in Chapter 1, namely an alternative dissolution method to hydrofluoric acid (bench dissolution with H_2SO_4 at elevated temperatures), the establishment (method development and validation) for the accurate

determination of zirconium as well as its permissible levels impurities, using ICP-OES as analytical method were successfully achieved during this study.

6.3 FUTURE RESEARCH

An outstanding issue from the current study is the quantification of the non-metals, namely nitrogen, oxygen, chlorine and carbon at their permissible levels which could not be done using the method of choice for the metals, namely ICP-OES. A possible future study which will address the quantification of these elements in pure zirconium metal samples, using micro-element analysis such as combustion techniques at extremely high temperatures will complete the study on the quantification of all the possible impurities specified for nuclear grade zirconium production.

The establishment of new dissolution methods of different zirconium-alloys and the quantification of all the impurities in these metals samples are also possible research projects which may extent the knowledge and skill basis for the analysis of these notoriously inert metal compounds.

A comparative study on the use of non-destructive analytical techniques such as glow-discharge (GD) and laser ablation (LA) to analyze the presence of impurities in all these metal samples may also prove to save time as well highlight any limitations compared to the wet techniques.